

THE DEVELOPMENT OF A HUMAN-RELEVANT PRE-CLINICAL MOUSE MODEL OF
DISSEMINATED CEREBRAL ASPERGILLOSIS AND DEFINING THE SUBSEQUENT
NEUROIMMUNE RESPONSE

AN ABSTRACT

SUBMITTED ON THE FIFTH DAY OF AUGUST 2022

TO THE NEUROSCIENCE PROGRAM

IN PARTIAL FULFILLMENT OF THE REQUIREMENTS

OF THE SCHOOL OF SCIENCE AND ENGINEERING

OF TULANE UNIVERSITY

FOR THE DEGREE

OF

DOCTOR OF PHILOSOPHY

BY

Brianne Sullivan

Brianne N. Sullivan

APPROVED: _____

Chad Steele

Dr. Chad Steele, Ph.D.

Prasad Katakam

Dr. Prasad Katakam, M.D., Ph.D.

Tracy Fischer

Dr. Tracy Fischer, Ph.D.

Andrew MacLean

Dr. Andrew MacLean, Ph.D.

Sean Lee

Dr. Sean Lee, Ph.D.

ABSTRACT

Exposure of immunosuppressed individuals to the opportunistic fungal pathogen *Aspergillus (A.) fumigatus* may result in invasive pulmonary aspergillosis (IPA), which could lead to the development of cerebral aspergillosis (CA), a highly lethal infection localized in the central nervous system. Disseminated CA following IPA contributes significantly to mortality amongst patients with hematologic malignancies (HMs). *However, little is known about the risk factors for disease amongst HM patients.* A systematic review using PRISMA guidelines was undertaken to define HM patient subgroups, preventative measures, therapeutic interventions, and outcomes of patients with disseminated CA. The systematic review identified the following patient populations as the highest risk for disseminated CA: patients with acute myeloid leukemia and patients receiving corticosteroids as a part of their HM therapeutic regimen.

Currently, there are no experimental models of CA that effectively mimic human disease, resulting in a considerable knowledge gap regarding mechanisms of neurological pathogenicity and neuroimmune responses during infection. In the current report, the information derived from the systematic review was utilized to develop a novel, human-relevant model of disseminated CA. Specifically, mice were immunosuppressed via acute, high-dose corticosteroid administration, challenged with *A. fumigatus* resting conidia intranasally, followed by a 70-fold

lower inoculum of pre-swollen conidia intravenously (IN+IV+steroid). Increased weight loss, clinical severity, fungal burden in the brain, and lethality compared to immunosuppressed mice challenged intranasally only (IN+steroid), or non-immunosuppressed mice challenged intranasally and intravenously (IN+IV) was observed. The IN+IV+steroid group demonstrated significant decreases in monocytes, eosinophils, dendritic cells, and invariant natural killer T-cells, but not neutrophils, macrophages, or $\gamma\delta$ T-cells, in the brain when compared to the IN+IV group. Likewise, the IN+IV+steroid group had significantly lower levels of IL-1 β , IL-6, IL-17A, CCL3, CXCL10, and VEGF in the brain when compared to the IN+IV group. Notably, IN+IV+steroid was superior to both IN+IV+chemotherapy (cytarabine + daunorubicin) and IN+IV+neutropenia for the development of CA. In conclusion, we developed a well-defined, physiologically relevant model of disseminated CA in corticosteroid-induced immunosuppressed mice with a primary pulmonary infection and are the first to define the corresponding inflammatory and immune responses within the brain. This model will serve to advance understanding of disease mechanisms, identify immunopathogenic processes, and aid in defining the neuroinflammatory response to CA.

THE DEVELOPMENT OF A HUMAN-RELEVANT PRE-CLINICAL MOUSE MODEL OF
DISSEMINATED CEREBRAL ASPERGILLOSIS AND DEFINING THE SUBSEQUENT
NEUROIMMUNE RESPONSE

A DISSERTATION

SUBMITTED ON THE FIFTH DAY OF AUGUST 2022

TO THE NEUROSCIENCE PROGRAM

IN PARTIAL FULFILLMENT OF THE REQUIREMENTS

OF THE SCHOOL OF SCIENCE AND ENGINEERING

OF TULANE UNIVERSITY

FOR THE DEGREE

OF

DOCTOR OF PHILOSOPHY

BY

Brianne Sullivan
Brianne N. Sullivan

APPROVED:

Chad Steele

Dr. Chad Steele, Ph.D.

Prasad Katakam

Dr. Prasad Katakam, M.D., Ph.D.

Tracy Fischer

Dr. Tracy Fischer, Ph.D.

Andrew MacLean

Dr. Andrew MacLean, Ph.D. Dr.

Sean Lee

Sean Lee, Ph.D.

TABLE OF CONTENTS

ACKNOWLEDGEMENTS.....	ii
LIST OF TABLES.....	vi
LIST OF FIGURES.....	viii
CHAPTERS	
1. BACKGROUND.....	1
1.1. <i>Aspergillus fumigatus</i>	1
1.2. Invasive pulmonary aspergillosis.....	2
1.3. Disseminated aspergillosis to the CNS.....	4
1.4. Current models of cerebral aspergillosis.....	5
1.5. Immunosuppression and aspergillosis.....	7
1.6. Neuroimmune response to aspergillosis.....	11
1.7. Systemic immune response to infection in the brain.....	12
2. A SYSTEMATIC REVIEW TO ASSESS THE RELATIONSHIP BETWEEN DISSEMINATED CEREBRAL ASPERGILLOSIS, LEUKEMIAS AND LYMPHOMAS, AND THEIR RESPECTIVE THERAPEUTICS.....	15
2.1. Introduction.....	15
2.2. Materials and methods.....	18
2.3. Results.....	22
2.3.1. Search results.....	22
2.3.2. Quality appraisal.....	22
2.3.3. Demographic characteristics.....	28
2.3.4. Underlying disease.....	30
2.3.5. Prevalence of known risk factors for IPA in the IPA + CA population.....	32
2.3.6. Prophylactic anti-fungal treatment.....	36
2.3.7. Treatment.....	38
2.3.8. Species.....	39
2.3.9. Mortality.....	41
2.4. Discussion.....	44

2.5. Limitations.....	49
2.6. Conclusion.....	51
3. DEVELOPMENT OF A PRECLINICAL MOUSE MODEL OF DISSEMINATED CEREBRAL ASPERGILLOSIS IN AN IMMUNOSUPPRESSED HOST	52
3.1. Introduction.....	52
3.2. Materials and methods.....	55
3.3. Results.....	60
3.3.1. Induction of IPA in immunosuppressed mice dose not result in cerebral dissemination.....	60
3.3.2. Successful induction of disseminated CA via IV inoculation.....	62
3.3.3. Development of an immunosuppression-based “two-hit” disseminated cerebral aspergillosis model.....	64
3.3.4. Disease severity in an immunosuppression-based “two-hit” disseminated cerebral aspergillosis model.....	67
3.3.5. The fungal burden is greater in lungs and brain of disseminated CA model mice.....	69
3.3.6. Severe pathology in the brain of disseminated CA model mice.....	71
3.3.7. The primary pulmonary infection decreases dissemination and prevents rapid mortality in CA model mice.....	73
3.4. Discussion.....	76
3.5. Limitations.....	80
3.6. Conclusion.....	81
4. NEUROIMMUNE RESPONSE IS SIGNIFICANTLY IMPACTED BY CORTICOSTEROID IMMUNOSUPPRESSION IN AN EXPERIMENTAL MODEL OF CEREBRAL ASPERGILLOSIS.....	82
4.1. Introduction.....	82
4.2. Materials and methods.....	85
4.3. Results.....	89
4.3.1. Immune cell infiltration into the brain in an immunosuppression-based “two-hit” disseminated cerebral aspergillosis model.....	89
4.3.2. Inflammatory cytokine and chemokine responses in an immunosuppression-based “two-hit” disseminated cerebral aspergillosis model.....	92

4.3.3. VEGF is not therapeutic in the “two-hit” model of disseminated cerebral aspergillosis.....	96
4.4. Discussion.....	99
4.5. Limitations.....	105
4.6. Conclusion.....	106
5. NEUTROPENIA IS LESS EFFECTIVE FOR INDUCING EXPERIMENTAL DISSEMINATED CEREBRAL ASPERGILLOSIS THAN CORTICOSTEROIDS....	107
5.1. Introduction.....	107
5.2. Materials and methods.....	109
5.3. Results.....	113
5.3.1. Comparison between corticosteroid-mediated immunosuppression and chemotherapy-mediated immunosuppression in the “two-hit” disseminated cerebral aspergillosis model.....	113
5.3.2. Evaluation of neutropenia in the “two-hit” disseminated cerebral aspergillosis model.....	117
5.4. Discussion.....	120
5.5. Limitations.....	123
5.6. Conclusion.....	124
6. CONCLUSIONS AND FUTURE DIRECTIONS.....	125
6.1. Conclusions.....	125
6.2. Future direction 1: Define the systemic and local immune and inflammatory responses in the brain of chemotherapy-induced immunosuppressed mice with and without fungal burden.....	127
6.3. Future direction 2: Investigating the relationship between primary pulmonary infection and secondary hematogenic infection.....	128
6.4. Future direction 3: Susceptibility for disseminated CA in mice exposed to common targeted therapies in AML patients.....	129
6.5. Applications.....	130
6.6. Final thoughts.....	131
7. APPENDIX A.....	132
7.1. Supplemental information for Chapter 2.....	132
8. APPENDIX B.....	139
8.1. Supplemental information for Chapter 4.....	139

9. APPENDIX C: AGE-ASSOCIATED NEUROLOGICAL COMPLICATIONS OF COVID-19: A SYSTEMATIC REVIEW AND META-ANALYSIS.....	146
9.1. Introduction.....	146
9.2. Materials and methods.....	148
9.3. Results.....	153
9.3.1. Search results and population characteristics.....	153
9.3.2. Summary of individual patient data for meta-analyses.....	156
9.3.3. Age-associated neurological complications of COVID-19.....	161
9.3.4. Relationship of age, COVID-19 severity, and comorbidities on neurological manifestations of COVID-19.....	165
9.3.5. Effect of COVID-19 severity and comorbidities on neurological disease outcome.....	168
9.4. Discussion.....	171
9.5. Conclusions.....	180
10. LIST OF REFERENCES.....	181
11. BIOGRAPHY.....	220

ACKNOWLEDGEMENTS

First, thank you to my advisor, Dr. Chad Steele. Thank you for taking me in when I found myself in need of a lab at the end of the third year of my Ph.D. Thank you for your enthusiasm and support, for allowing me the freedom to design my own project, and for always being willing to drop whatever you're doing to answer my questions and help me work out details. Even though we didn't begin this journey together, I count myself very fortunate to end it with you. Your trust, support, and mentorship have propelled my growth as a scientist, researcher, mentor, and colleague.

Thank you to my committee members Dr. Prasad Katakam, Dr. Sean Lee, and Dr. Andrew MacLean, who stuck with me when transitioned labs and began working in a completely different field from what they originally signed up for. I am so fortunate to have had such supportive, intelligent, and kind people in my corner throughout my Ph.D. Thank you to Dr. Tracey Fischer, a late addition to my committee but no less appreciated. Thank you, Dr. Fischer for her continued support, for always being willing to talk neuroimmune with me, you have been an invaluable teacher, and for being so kind and patient.

Thank you to the Steele lab members, past and present, who welcomed this neuroscientist so kindly into their invasive aspergillosis and fungal asthma lab. We might not always have understood what each other was doing, but your support has meant so much to me. Thank you to the following Ph.D. students for making the Steele Lab such a joyous place to join: Dr. Matthew Godwin, Dr. Joesph Mackel, Diandra Ellis, and Mgayya Makullah. To Diandra and Mgayya, thank you for being such trusted, enthusiastic, and intelligent editors, sounding boards, and cheerleaders. To Pari, Thomas, and Folasade, even though we didn't get many years together, it has been a pleasure working with you

and watching you grow and flourish into wonderful scientists as you begin your Ph.D. journeys. A very special thank you to Folasade for taking over the cerebral aspergillosis project, I can walk away knowing it is in capable hands. To Macy Boten for being such a joy to work with and always willing to jump in and help; I would have been underwater without you when I joined the Steele Lab. And to Mary Jane, there are a million things to say, and a million thank-yous that I owe you, but truly I don't know if I could have gotten here without you. You are so much more than the glue that holds us all together, you are the bright light in the lab, an invaluable friend, and the best office mate anyone could ask for.

Thank you to the Bunnell lab members. Even though many of us didn't get to finish together, working with all of you for those few years was one of the highlights of my Ph.D. experience. Thank you to fellow Ph.D. students Dr. Omair Mohiuddin, Dr. Rachel Sabol, and Katelynn Montgomery. A very special thank you to Ph.D. students Dr. Rachel Wise and Mark Harrison, the Glia Squad, without whom I might have sunk when we had to make that tough transition in 2020, but because of the two of you, I was able to swim. Thank you to Rachel Wise, a truly incredible scientist, for being my guidepost, role model, pillar of support, and fierce and loyal friend. I am so honored to have you in my life. To Mark Harrison, my dear friend, who has been by my side since day one as master's students. Thank you for being my best teammate and greatest competition; there is no one whose opinion I value more or who pushes me harder. There will never be enough words to tell you how glad I am that you agreed to be my friend.

Thank you to the following undergraduate research assistants: Ashley Nave, Christa Guillory, and Mia Baggett, who generously gave their time to my research over the years. I would especially like to thank Mia, for her invaluable support and her assistance during my time in the Steele lab.

Thank you to all the amazing fellow Ph.D. students I have met during my time at Tulane. Thank you, especially to all of the fellow women in STEM I have met. To my friends Drs. Amy Goodson, Lydia Crawford, Leila Pashazanusi, and Claire McGraw, you have all been the greatest friends, have shown me New Orleans, and made life infinitely more fun, and for that, I am so grateful. Thank you to the women of the LLLC: Drs. Amy Feehan, Annie Welch, Tiffany Kaul, Bonita Hartono, Rachel Sabol, Rachel Wise, and Sonia Rao, for providing such exemplary examples of women thriving in science. You have all been the best role models and cheerleaders. What an honor it has been to be surrounded by so many amazing women in science.

A big thank you to all of my friends outside of Tulane as well. To my friends all over the world, from the West to the East Coast, from the USA to the EU, thank you for your constant and unwavering support, there are too many to name here, but I am so lucky to have each of you in my life. To my friends in NOLA, my Honey Island Swamp Monsters, my Alley Cats – thank you to every single one of you for adding so much fun, joy, and laughter into my life; I am so thankful to know you all. To my best girls, Julie, Kelsey, and Shenea – I am a better person for knowing each of you. Thank you for your unwavering support and loyalty, for being the best hype girls in town, and for bringing so much love and light into my life.

Thank you to my family, immediate and extended, for their constant love and support. To my dad for always being there to lend an ear, provide advice (solicited or not), and lift my spirits. To my mom, whose love and guidance have carried me through everything I've done. To my brother, the greatest friend, for always being a shoulder to cry on and a pal to laugh with. To my sister, the sweetest soul, thank you for driving me to always be the best version of myself that I can be.

To Sam – I don't know where I would be without you. Thank you for being the best friend, sounding board, support system, voice of reason, role model, dog dad, and partner anyone could ask for. Beauregard and I will forever be lucky to call you ours.

Thank you, all. None of this would have been possible without the support and guidance I have received from so many. I am forever grateful for each and every person in my life who has helped get me to this point, I only hope I can return the favor someday.

LIST OF TABLES

Table 2.1: Characteristics of studies included in the systematic review.....	25
Table 2.2: Demographic characteristics of studies included in the systematic review.....	29
Table 2.3: Patient characteristics.	31
Table 2.4: Risk factors for disease per HM patient subgroup.	33
Table 2.5: Multiple risk factors for dissemination.....	35
Table 2.6: Traditional risk factors with or without antifungal prophylaxis.....	37
Table 2.7: Antifungal therapy.....	40
Table 2.8: <i>Aspergillus</i> species identity and related mortality.....	42
Table 2.9: Potential factors associated with mortality.....	43
Table A1: Literature search results.....	133
Table A2: Quality assessment for each article used in the systematic review and overall level of bias.	135
Table A3: Data for HM, neutropenia status, inclusion of chemotherapy, and outcome of individual patients from included studies.	137
Table B1: Antibodies for flow cytometry.....	139
Table B2: Bioplex Mouse Cytokine/Chemokine Magnetic Bead Panel - Premixed 32 Plex - Immunology Multiplex Assay.....	140
Table B3: Additional bioplex data.....	141
Table C1: Total number (n=584) and percent of each neurological condition reported in patients diagnosed with COVID-19 per decade of age.....	151
Table C2: Summary statistics for age of patients in toto and by sex.....	158

Table C3: Frequencies and percentages of neurological disease, COVID-19 severity, comorbidities, and detectable virus in CSF by sex.....	159
Table C4: Frequencies and percentages of observed neurological disease split by COVID-19 severity.....	160
Supplemental Table C1: Frequencies and percentages of specific diagnoses included under each category of neurological complications.....	181
Supplemental Table C2: Frequencies and percentages of all reported comorbidities..	185

LIST OF FIGURES

Figure 2.1: Prisma flow chart.....	24
Figure 3.1: Induction of IPA does not result in cerebral dissemination, regardless of the conidial dose.	61
Figure 3.2: Successful induction of disseminated CA via IV inoculation.	62
Figure 3.3: The experimental disseminated CA model results in profound mortality.....	66
Figure 3.4: Disease severity in an immunosuppression-based “two-hit” disseminated cerebral aspergillosis model.	68
Figure 3.5: The disseminated CA model results in significant fungal infection in the lung and brain.	70
Figure 3.6: The disseminated CA model results in distinct pathological in the brain.....	72
Figure 3.7: The primary pulmonary infection decreases dissemination and prevents rapid mortality in CA model mice.	74
Figure 4.1: The disseminated CA model results in a significant impact to the immune cell infiltration into the brain.....	90
Figure 4.2: The disseminated CA model results in a significant impact to the inflammatory cytokine and chemokine population in the brain.	94
Figure 4.3: VEGF is not therapeutic in the “two-hit” model of disseminated cerebral aspergillosis.....	97
Figure 5.1: Comparison between corticosteroid-mediated immunosuppression and chemotherapy-mediated immunosuppression in the “two-hit” disseminated cerebral aspergillosis model.	115

Figure 5.2: Evaluation of neutropenia in the “two-hit” disseminated cerebral aspergillosis model.....	118
Figure A1: Overall synthesis of quality assessment and risk of bias.....	132
Figure B1: Gating strategy for flow cytometry for lymphoid-lineage cells in the brain....	142
Figure B2: Gating strategy for flow cytometry for resident immune cells in the brain and infiltrating macrophages.	143
Figure B3: Gating strategy for flow cytometry for infiltrating myeloid-derived cells in the brain.	144
Figure B4: Certain cell populations were unaffected in the brain of disseminated CA model mice compared to control mice.	145
Figure C1: Flow chart of systematic literature search and screening for studies of COVID-19 patients with neurological conditions.....	154
Figure C2: Total number and percent of reported neurological conditions occurring in patients, regardless of demographics.....	155
Figure C3: Percent of total neurological conditions occurring in children, young adults, and older adults diagnosed with COVID-19.....	162
Figure C4: Total number ($n = 584$) of reported neurological manifestations occurring in patients with COVID-19 per decade ranging from ≤ 9 to ≥ 80 years of age.....	163
Figure C5: Simple linear regressions demonstrating the effect of age on neurological symptoms and their relationships with patients with COVID-19.....	164
Figure C6: Pearson's correlation matrices and heatmaps for patients with COVID-19 and diagnosed with a neurological condition(s).....	167
Figure C7: Pearson correlation matrix for age, neurological disease, COVID-19 symptom severity, and comorbidities of COVID-19 patients.....	169
Figure C8: ANOVA of COVID-19 severity score by neurological disease category.....	170
Figure C9: COVID-19 pathology in the CNS: primary impacts and potential mechanisms...	179

CHAPTER 1

BACKGROUND

Invasive pulmonary aspergillosis (IPA), a leading cause of death in immunosuppressed populations, is an infection most often attributed to the opportunistic fungi *Aspergillus (A.) fumigatus*. Incidences of IPA are rising as the number of patients undergoing immunosuppressive therapies for stem cell and solid-organ transplants, hematologic malignancies (HM), and the use of immunomodulating drugs such as corticosteroids increases. IPA primarily occurs within the lungs; however, hematological dissemination of *A. fumigatus* most commonly leads to a secondary infection in the brain known as cerebral aspergillosis (CA). CA occurs in 10-40% of immunocompromised patients with IPA and is fatal in upwards of 90% of cases [1-3]. The immune response to IPA in the lungs has been well characterized, and models of the disease are well established.

Conversely, the models available for disseminated CA do not represent a natural route of infection and are thus limited in their physiological relevance. Further, very little is known about the neurological pathogenicity of infection, anti-fungal immunity, and host defense response following *A. fumigatus* entering the central nervous system (CNS), contributing to the limited number of therapeutics effective against CA.

1.1 *Aspergillus fumigatus*

Aspergillus species (spp.) are saprotrophic filamentous fungi occurring on decaying organic matter throughout nature. Spreading primarily via asexual sporulation,

species of *Aspergillus* can be found in the air, soil, plants, and on humans and animals alike. Of the over 250 species of *Aspergillus*, *A. fumigatus* is the most pathogenically ubiquitous, accounting for approximately 90% of human *Aspergillus* infections [4, 5]. *A. fumigatus* abundantly sporulates, growing faster than any other airborne fungus under various environmental conditions. It can grow between 12° and 65°C (optimally 37°C) and at pH levels between 2.1–8.8 (optimally 3.7-7.6) [6, 7]. Rapid sporulation leads to the release of vast quantities of the buoyant conidia into the air, and humans inhale at least several hundred of these small spores (2-3 µm) each day. *A. fumigatus* can infiltrate the lower respiratory system and evade clearance by mucociliary forces [8, 9]. High virulence of *A. fumigatus* is due, in part, to the accumulation of melanin within the cell wall of the conidia protecting against phagocytosis and reactive oxygen species (ROS) [10, 11]. Additionally, more than any other *Aspergillus* spp. the conidial surface of *A. fumigatus* contains the most exposed negatively charged sialic acid residues, further contributing to the high virulence of *A. fumigatus* as sialic acid partly mediates binding to basal lamina proteins of the host [12]. Altogether, the physical characteristics of *A. fumigatus* make it well suited for reaching the lower respiratory tract and causing disease.

1.2 Invasive pulmonary aspergillosis

In individuals with a healthy immune system, *A. fumigatus* conidia are readily eliminated from the respiratory system. This is due to the innate capacity of macrophages and neutrophils to prevent germination and kill spores and hyphae and the local adaptive immune response to suppress infection [13-16]. However, exposure in individuals with compromised immune systems can lead to several conditions owing to impaired immune cell response. The most severe is the often life-threatening disease IPA. Overwhelmingly, immunocompromised individuals, such as stem cell and/or solid organ transplant recipients, patients with hematological malignancies (HMs) undergoing chemotherapy,

and patients treated with immunomodulating therapeutics such as corticosteroids, are at the greatest risk for developing IPA [17-20]. The epidemiology of IPA is ever-changing as the number of immunocompromised patients changes with increasing and improved therapeutic interventions; however, prolonged neutropenia and/or corticosteroid use are considered the primary risk factors for developing IPA [21-23]. IPA is a relatively rare disease, impacting an estimated 300,000 people globally annually. Still, it is regarded as one of the most common invasive fungal infections and one of the most expensive to treat [24-28]. IPA is particularly devastating, with an overall fatality rate of up to 50%, depending on host immunity. It is one of the most frequently attributed to causes of infectious death amongst immunocompromised patients [2, 21, 25, 29]. Left untreated, IPA almost always results in fatal pneumonia. Although, increasingly effective antifungal drugs, both prophylactic and therapeutic, have significantly reduced mortality in some high-risk populations [30]. Nevertheless, IPA remains a disease of great interest due to the acutely devastating effects it can have on at-risk populations, particularly in the event of hematogenic dissemination.

Host defense against *A. fumigatus* relies on the ability of the respiratory immune system to inhibit spore germination into invasive hyphae and to thwart fungus-induced or inflammation-induced damage in infected tissues. In the immunocompetent host, *A. fumigatus* inhalation initiates an orchestrated immune response, concluding in fungal clearance from the respiratory system. Phagocytotic cells of the innate immune system serve as the first line of defense, initiating fungal clearance following inhaled conidia. Alveolar macrophages are the first mediators of host defense in the lung, followed by subsequent recruitment of peripheral-blood monocytes and neutrophils [15, 31]. However, following fungal germination, neutrophils dominate the host defense response against the hyphae [15]. In the neutropenic host, which is the presence of abnormally few neutrophils in the blood, the reduction of neutrophils significantly contributes to *A. fumigatus*

angioinvasion, and unresolved neutropenia is associated with poorer outcomes [32, 33]. Eosinophils and natural killer (NK) cells are recruited to the lungs by chemokines during experimental aspergillosis and play important roles in the host defense [34, 35]. Corticosteroid therapy significantly suppresses the accumulation of phagocytes at inflammatory sites, effectively breaking down the initial lines of protection against the fungal defense and leaving patients vulnerable to IPA [15]. During IPA, recruited antigen-presenting dendritic cells (DCs) prompt acquired T-cell mediated immunity, specifically inducing selective T-helper (Th) priming of CD4+ T lymphocytes, including Th-1, Th-2, Th-17, and regulatory T-cells (Tregs) [16, 36]. Protective immunity during IPA is driven by Th-1 and, to a lesser extent, Th-17 and Treg responses, while Th2 is considered to push the disease progression [37-39]. Corticosteroid immunosuppression dampens the proliferative, migratory, and functional capabilities of lymphocytes, significantly weakening their response to *A. fumigatus* infection, resulting in poor disease outcomes [40-42].

1.3 Disseminated aspergillosis to the CNS

During IPA, upon reaching the alveoli, *A. fumigatus* conidia swell and germinate, producing hyphae that invade the pulmonary parenchyma [42, 43]. The hyphae invade the endothelial cell lining of the blood vessels by passing from the abluminal to the luminal surface. At this point, some hyphal fragments can break off and circulate in the bloodstream [42, 43]. In the profoundly immunosuppressed host, invasion of the pulmonary vasculature can result in widespread hematogenous dissemination to organs such as the brain, kidneys, heart, spleen, and liver [44, 45].

The occurrence of CA in the immunocompetent host is exceedingly rare and is typically associated with trauma and surgery [46, 47]. Significantly more notable, frequent, and devastating is CA in immunocompromised patients. Often regarded as the **number one dissemination site**, the brain is infected by disseminated *A. fumigatus* in up to 40%

of certain immunocompromised populations, averaging 10-20% in all patients with IPA [1, 48-51]. In addition to being considered the most frequent site of secondary infection, CA is also deemed the **most fatal**, with mortality rates approaching 90% [2, 52, 53]. Symptoms of CA are wide-ranging and often non-specific. These symptoms include fever resistant to antibacterial treatment, headache, altered mental status, lethargy, nausea/vomiting, focal neurological deficits, and seizures [1, 52, 54-56]. The wide range of symptoms is due greatly to the multiple potential clinical presentations of CA, such as meningitis, encephalitis, mycotic aneurysms, granuloma, cerebral blood vessel invasion with or without infarction, secondary infection, or hemorrhage. Most frequently, single or multiple brain abscesses [48, 52, 54-59]. Death from CA is often rapid, reportedly occurring in as few as 5 days post-infection and is predominately associated with hemorrhagic and/or ischemic events [48, 59]. For the treatment of CA, very few available therapeutics are effective in the CNS. Further, little is known regarding the neuroimmune response during CA. All of these factors contribute to the high mortality associated with CA. Thus, investigating the neuroinflammatory milieu is vital for identifying potential therapeutic targets and diagnostic tools.

1.4 Current models of cerebral aspergillosis

Murine models of IPA are well established and have been used extensively to study various aspects of the disease, including pathogenesis and host response. Unfortunately, the same cannot be said for disseminated CA. Currently, two models are typically used for studying CA *in vivo*. In the most common model for studying CA, developed by Chiller et al., CNS *Aspergillus* infection is established via intracranial injection of the conidia [60]. In developing this model, Chiller et al. infected two strains of inbred and one strain of outbred immunocompetent mice, all of whom were highly resistant to infection. Next, neutropenia was induced using cyclophosphamide to immunosuppress

the mice, who were then infected with *A. fumigatus* intracranially, where significant infection and mortality were observed. Unfortunately, this was only validated in the outbred strain of mice. Following intracranial infection in neutropenic mice, *A. fumigatus* was found to disseminate from the brain to the kidneys and spleen. Altogether, this model has serious limitations for studying disease pathogenesis, as well as innate and acquired host-response during CA, as it does not accurately recapitulate human disease, given that primary cerebral infection by *A. fumigatus* is extremely rare. Further, as this model has only been employed and validated in outbred mice, investigating the pathophysiology through genetic manipulation is impossible. However, this model does highlight the need for immunosuppression for the successful induction of CA infection.

Another common method for investigating CA, via dissemination, is by intravenous (IV) inoculation in the lateral tail vein of mice [61]. IV inoculation leads to rapid fungal dissemination through the bloodstream leading to widespread systemic infection. However, this method is used almost exclusively in immunocompetent subjects [62]. Although this model effectively induces widespread fungal infection in mice of many genetic backgrounds, IV fungal administration alone is not a natural route of infection in humans. So, while this model of systemic aspergillosis in immunocompetent animals allows for investigations of mechanisms of resistance to *Aspergillus* without confounding factors, it lacks relevance to the human population and thus limits the applicability of the results. Current models for studying cerebral aspergillosis do not model dissemination following a primary pulmonary infection, and a significant portion does not utilize an immunosuppressive regimen before infection. Therefore, current models do not accurately reflect the physiology of human disease. To enhance understanding of disease pathogenesis and better define the host immune response, it is vital to develop a model that encompasses these key features of human disease.

1.5 Immunosuppression and aspergillosis

Daily, humans inhale at least several hundred conidia of *A. fumigatus*, which are readily eliminated by the innate immune system [8]. However, the same cannot be said for those humans with compromised/suppressed immunity. The highly opportunistic and invasive *A. fumigatus* can evade detection in the immunosuppressed host, germinating within the lung, causing tissue damage, and resulting in IPA. Several studies have identified patients undergoing hematological stem cell transplantation (HSCT), bone marrow or solid organ transplant recipients, and patients with HMs receiving chemotherapeutic drugs with the greatest morbidity and mortality caused by IPA [2, 21, 25, 29]. Therapeutics used to treat these underlying conditions regularly leave patients in a vulnerable, immunocompromised state most often attributed to prolonged neutropenia and/or corticosteroid use. Neutropenia is widely regarded as the classic underlying risk factor for invasive and disseminated aspergillosis, particularly in the HSCT and HM populations [32, 63-66].

The significant reduction or loss of neutrophils following stem cell transplant (SCT) or chemotherapy puts vulnerable patients at increased risk of developing a serious infection. Incidence of IPA in neutropenic patients ranges from 5-15%, depending on the underlying disease and the studied cohort [67-71]. One study found neutropenia preceded IPA in 45% of patients [72]. Early neutrophil recruitment is critical for pathogen clearance and neutrophil activation promotes conidial and hyphal killing, where delayed neutrophil response confers a worse outcome [73-76]. Indeed, in neutrophil-depleted mice, susceptibility to IPA significantly increases compared to immunocompetent mice [75-78]. In patients with HMs and invasive aspergillosis, disseminated disease occurs in 10-30% of patients [79, 80].

Similarly, in SCT patients, disseminated disease during invasive aspergillosis occurs in 10-15% of patients [2, 81]. Loss of neutrophils or neutrophil dysfunction has

been implicated in increased susceptibility and/or severity of infection in the brain for other IFIs such as systemic infection by *Candida albicans* [82]. High susceptibility for disseminated infection and increased disease severity during other infections due to the loss of neutrophils within the brain suggests neutrophils likely play a vital role in mediating disseminated CA.

Neutropenia is frequently associated with cancer chemotherapies, and patients receiving systemic antineoplastic therapy sufficient to adversely affect myeloid cell development are at risk for invasive infection [83]. Particularly, anticancer drugs disrupt the growth of cells by directly or indirectly inducing DNA damage [84]. This broadly halts cancer cell replication but also, unfortunately, often induces secondary cytotoxic effects such as myelosuppression impacting cells involved in immunity and host defense [85]. As neutrophils are thought to be short-lived in circulation, they are particularly susceptible to cytotoxic chemotherapy drugs [86, 87]. Thus, in the presence of chemotherapy, the production of neutrophils is unable to adequately achieve physiological levels, resulting in neutropenia. Given the risk for infection in neutropenic patients, colony-stimulating factors (CSFs) or white blood cell growth factors are often given to promote the neutrophil recovery [88]. This is particularly true for those with neutropenia accompanied by fever. In addition to neutrophils, other cells of myeloid origin are impacted by chemotherapy, including eosinophils, macrophages, and monocytes, for example, the number of which can either increase or decrease depending upon the type of cell and cytotoxic drug in question [89-91]. Further, nearly all chemotherapy agents result in bone marrow suppression, causing a reduction in red cells as well [92]. Beyond myelosuppression, chemotherapy has been found to impact the levels of lymphocyte-lineage cells, including B, T, and NK cells [93].

Moreover, neutropenia resulting from induction chemotherapy for leukemia and lymphoma, or treatments associated with allogenic SCT is considered a top risk factor for

infection [94, 95]. Whereas patients diagnosed with neutropenia following chemotherapy for solid tumors are generally considered at lower risk for infection [94, 96]. The difference between high- and low-risk underlying diseases is, at least in part, due to the expected severity and duration of the resultant neutropenia. In 1984, Gerson et al. described prolonged neutropenia as a significant risk factor for IPA, a notion that has persisted since [64]. Specifically, in this study, a correlation between the duration of neutropenia and the rate of IPA diagnosis was found. Patients with acute leukemia and neutropenia persisting longer than three weeks were identified as being a high-risk population for IPA. However, only one-third of the patients included in this study were diagnosed with IPA.

Interestingly, a recent and much larger study found that neutropenia of any duration preceding IPA was a greater predictor of infection than prolonged neutropenia [33]. Neutropenia preceding IPA was primarily diagnosed in patients with HMs and/or bone marrow transplants, as opposed to those with solid organ transplants or solid tumor cancers. Further, about two-thirds of patients had corticosteroids in their treatment regimen, whereas less than half were neutropenic and only one-third had prolonged neutropenia. While neutropenia remains a significant risk factor, early studies underestimate the importance of neutropenia in general. Furthermore, recent studies additionally highlight corticosteroid use as a significant risk factor for IPA.

Recently, the use of corticosteroids, alone and in conjunction with neutropenia-causing therapeutics, has been regarded as one of the most notable risk factors, given their frequent use in transplant recipients, patients with various malignancies, and other underlying conditions such as AIDS, vascular-collagen disorders, and chronic pulmonary conditions [21, 59, 97, 98]. For example, in a post-transplant epidemiological study, corticosteroid use was identified as a significant risk factor for IPA as 87.5% of bone marrow transplant (BMT) recipients diagnosed with IPA had been treated with corticosteroids [99]. Indeed, one study found corticosteroids to be more

prevalent than neutropenia in IPA patients with underlying diseases, including HMs, BMTs, diabetes, and HIV [72]. Similarly, a 20-year retrospective study of CA in patients with various underlying conditions found corticosteroid use to be amongst the top risk factors, with more than 50% of patients with CA having undergone steroid treatment [59]. Many other reports have identified corticosteroid use for a wide range of underlying conditions before the development of IPA and subsequent dissemination to the brain [29, 100-106].

Exogenous corticosteroid therapy induces cellular immunodeficiency through quantitative and qualitative mechanisms, affecting practically every cell type implicated in the immune response, leaving patients in an immunosuppressive state and vulnerable to the development of disseminated CA. For example, quantitatively, corticosteroids have been found to decrease the proliferation (and migration) of lymphocytes and monocytes, as well as other immune effector cells such as alveolar DCs and microglia [41, 107-112]. Qualitatively, exogenous corticosteroid therapy has been observed to elicit numerous effects on the functionality of a wide range of immune cells. Exposure to glucocorticoids impaired nitric oxide (NO) formation, pro-inflammatory cytokine production, and phagocytosis in neutrophils, monocytes/macrophages, and microglia [109, 113-115]. Altogether, corticosteroid therapy leaves the host vulnerable to fungal infections as the immune system cannot elicit a proper response to eliminate the fungus. Intriguingly, *A. fumigatus* cultured in the presence of corticosteroids were found to have significantly increased fungal growth [116]. As such, patients treated with high-dose corticosteroids are not only likely to have impaired immune cell response allowing *A. fumigatus* conidia to escape initial phagocytotic killing, but the enhanced growth of *A. fumigatus* in the presence of the steroids further compounds the risk for IPA and thus CA. Additionally, likely to contribute to the dissemination of *A. fumigatus* infection to the CNS, astrocytes exposed to corticosteroids *in vitro* and *in vivo* were found to have reduced proliferation and

activation [117-119]. Suggesting that corticosteroid effects on astrocytes may disrupt blood-brain barrier (BBB) integrity, increasing the potential for *A. fumigatus* to enter the brain and result in CA.

1.6 Neuroimmune response to aspergillosis

Hematologic dissemination of *A. fumigatus* into the brain requires the interaction of the fungus with the BBB. Although several mechanisms have been hypothesized, including physical and/or chemical interactions, the mechanism of entry by *A. fumigatus* into the brain parenchyma is currently unknown [120-123]. Importantly, however, contributing to the virulence of *A. fumigatus* and subsequently the high rate of dissemination to the brain is the ability of *A. fumigatus* to produce secondary metabolites known as mycotoxins. Mycotoxins promote conidial resistance to opsonization and inhibition of phagocytosis. They can damage and kill microglia, astrocytes, and neurons through increased apoptosis, increasing the susceptibility for and contributing to the pathogenesis of severe fungal infection by *A. fumigatus* in the brain [120, 121, 124]. One study sought to assess the indirect effects of *A. fumigatus* in the CNS as the pathogenesis of *A. fumigatus* during CA is partly due to secretion of various mycotoxins [125]. Through the culture of astrocytes, microglia, or neurons with *Aspergillus* culture supernatants, the secretory factors of *A. fumigatus* were found to be cytotoxic to the cells. Mycotoxins were shown to inhibit cell growth and reduce cell viability in a dose-dependent manner that particularly affected neurons. The results of this study indicate that through secreted factors, *A. fumigatus* can induce cellular damage not only at the site of infection but in distant brain regions as well. To date, the effects *A. fumigatus* have after entering the CNS and the direct interaction between *A. fumigatus* and cells of the CNS remains, to our knowledge, unknown.

A subject of great interest is the response of the local immune cells, astrocytes and microglia, as well as the infiltration and response of peripheral immune cells involved in anti-fungal immunity and host defense after *A. fumigatus* crosses the BBB. Microglia and astrocytes are activated by infection, neuronal injury, and inflammation of the CNS. This response can vary depending on the health status of the CNS and the type of insult. As discussed above, therapeutics, such as high-dose corticosteroids, can also impact the activation and response of microglia and astrocytes. Immune response initiation, amplification, or suppression in the CNS, primarily mediated by microglia and astrocytes, depends on several factors, including the level and type of cytokine and cytokine receptor expressed and recruitment of peripheral immune cells (i.e., macrophages, neutrophils, and T-cells) into the CNS. During IPA, studies have shown distinctive cellular recruitment and response patterns and cytokine profiles involved in the innate and adaptive immune response against the *A. fumigatus* infection [13, 37, 126-128]. The same cannot be said for disseminated CA. The response of local and peripheral immune cells, cytokine profile, and their contribution to CA have not been reported. Major gaps in knowledge exist regarding the response of local and peripheral immune cells to *A. fumigatus* in the brain; our goal was to define these interactions.

1.7 Systemic immune response to infection in the brain

Immune cells originating in the periphery are well known to be capable of gaining access to and mounting an immune response within the brain. Although the systemic immune response within the brain during CA has yet to be characterized, the infiltration patterns of peripheral immune cells have been investigated during other infectious and inflammatory events. Generally, following the entry of CNS-invading pathogens such as bacteria, viruses, and fungi, glial cells initiate an immune response, secreting chemokines that recruit peripheral immune cells to the brain. Also involved in chemotaxis during

infection and inflammation are parenchymal macrophages. During this, monocytes, circulating macrophages, neutrophils, DCs, NKs, eosinophils, and T-cells are all recruited at varying levels and states of activation.

For example, in a mouse model of invasive candidiasis using *Candida albicans*, neutrophils and monocytes accumulated within the brain early in infection. This response was transient, however, as these cells were essentially undetectable after a week of infection [129, 130]. By contrast, the number of macrophages and DCs increased steadily over the course of infection [129, 130]. The response and accumulation of lymphocytes was delayed compared to when the infection was initiated. However, invariant natural killer T (iNKT)-, CD4 T-, CD8 T-, and B-cells increased throughout the study, albeit at relatively low levels. The exception was NK cells, which were delayed in their trafficking to the brain and whose response was transient. The most abundant myeloid cell at any time during infection was neutrophils, while NK cells were the most abundant lymphocyte. Both peaked at day 4 of 7 during infection. $\gamma\delta$ -T-cells were undetected [129]. Whereas in an experimental murine model of Cryptococcosis with *Cryptococcus neoformans*, trafficking of monocytes, neutrophils, and T-lymphocytes into the brain was delayed, with significant populations not observed in the brain until day 8 post-infection [131]. While the levels of monocytes and neutrophils declined by day 10, the number of T-lymphocytes increased. The most prominent cell population was monocytes. Further yet, the responses of T- and B-cells in the brain have been found to have specific roles in preventing and eliminating fungal infection within the brain [132, 133].

As *Candida albicans*, *Cryptococcus neoformans*, and *A. fumigatus* are known to have differential immune responses to and requirements for resolution within the lung, the same is expected within the brain [134, 135]. Further, the immune status of the host critically influences the immune cell populations and functions. Thus, it is critically important to understand the differential responses to pathogens under normal and

immunosuppressive states. Altogether, cells of the peripheral immune system seem to have unique responses and roles within the brain during infection and inflammation, posing as potential therapeutic targets. Thus, our goal was to define the infiltration patterns of peripheral immune cells within the brain during disseminated CA.

Most frequently caused by inhalation of *A. fumigatus* conidia, aspergillosis poses a significant threat to life in immunocompromised individuals. Thought to be at particularly high risk for developing disseminated CA subsequent to IPA are HM patients. However, the risk factors of disseminated CA related to HM patient subgroups and their therapeutics are not well known. Additionally, given the high mortality and limited therapeutic options associated with disseminated CA from IPA, it is imperative to have a human-relevant model to advance the understanding of disease pathogenesis for the development of diagnostic and therapeutic tools. Current models for studying CA are limited in their relevance as they do not recapitulate the immune states or natural routes of infection in this disease. Thus, while these existing models have provided a platform for investigating isolated cerebral infection or disseminated infection in an immunocompetent host, they are limited in their applications to human health. Further limiting progress in the prevention and treatment of disseminated CA has been the absence of knowledge regarding the inflammatory and immune responses within the brain during disease. To address these problems, I aimed to i) systematically review the literature to define risk factors specific to disseminated CA in the greatest at-risk population, ii) develop a novel murine model of disseminated CA informed by the results and conclusions generated by the systematic review, and iii) define the inflammatory and immune milieu in the brain resultant from disseminated CA. Completion of these aims has provided invaluable information to move the field closer to reducing the incidence and severity of this highly lethal disease.

CHAPTER 2

A SYSTEMATIC REVIEW TO ASSESS THE RELATIONSHIP BETWEEN DISSEMINATED CEREBRAL ASPERGILLOSIS, LEUKEMIAS AND LYMPHOMAS, AND THEIR RESPECTIVE THERAPEUTICS.

2.1 Introduction

Aspergillus spp. are ubiquitous, opportunistic fungal pathogens that, when inhaled, are readily eliminated from the lung of immunocompetent individuals but can lead to the highly lethal infection IPA in immunocompromised individuals. Patients undergoing immunosuppressive therapies for HMs, stem cell and solid-organ transplants, and exposed to immunomodulating drugs including corticosteroids, are at the greatest risk of developing IPA [22, 59, 136, 137]. *A. fumigatus* is the species most frequently attributed to IPA; however additional species are occasionally identified as the cause of IPA, including *A. niger*, *A. flavus*, and azole-resistant *A. terreus* [138-140]. Dissemination of these fungi most frequently occurs via the hematogenous spread of the fungus from the lungs to subsequent organs [54, 141, 142]. The CNS is often reported as the most frequent site of *Aspergillus* dissemination from the lung resulting in CA; this is particularly true in the immunocompromised population's [2, 140, 142]. In addition to being amongst the most common organs of dissemination, *Aspergillus* infection in the CNS is also regarded as one of the most lethal [48, 49, 143].

IPA is diagnosed in more than 300,000 immunocompromised patients annually and is associated with a 30-80% mortality rate [22, 24, 144]. On average, 20-50% of IPA infections result in disseminated disease, with 10-20% reported to result in CA [145, 146].

However, this is likely a conservative estimate as the population of CA is greatly under-reported, owing partially to the fact that CA is notably difficult to diagnose with some cases not being diagnosed until autopsy [147-150]. Further, as the number of immunosuppressed patients continues to increase, the CA population is likely larger than reported [1, 151, 152]. Disseminated CA is associated with a particularly poor prognosis, resulting in death in up to 70-100% of patients [151-153]. The difficult diagnosis of CA additionally contributes to the high mortality as the symptoms, including fever, headache, mental alteration, or lethargy, etc., are non-specific [57, 138]. The difficulty of diagnosis is also due, in part, to the methods which are often invasive and have variable sensitivity and specificity [154]. Latency to diagnose combined with poor therapeutic tools often result in a fatal infection. Within the immunocompromised population, patients with hematologic malignancies (HMs) (i.e., cancers that affect the blood, bone marrow, and lymph nodes) are considered to be one of the most prevalent populations to be diagnosed with disseminated CA [52, 59]. HM patient subgroups include various leukemias (acute lymphocytic (ALL), chronic lymphocytic (CLL), acute myeloid (AML), chronic myeloid (CML)), myeloma, and lymphoma (Hodgkin's and non-Hodgkin's (NHL)). Additionally, the therapeutics and treatments associated with HMs, such as chemotherapy and stem cell transplants (SCT), leave the patients in a highly immunocompromised state, elevating the risk for opportunistic infections. Given the high proportion of patients reported to have disseminated CA also having HMs, it is essential to identify the most at-risk HM patient subgroups and characteristics for CA so prophylactic measures and therapeutic considerations can be taken.

Up-to-date reports of disseminated CA specifically related to HMs are relatively limited. The risk factors of disseminated CA related to HM patient subgroups and their therapeutics, including cytotoxic drugs, steroids, SCTs, and targeted agents, are also not well documented. This systematic review serves, in part, to clarify the evidence base

available around the relationship between HM patients undergoing therapy related to HMs and CA. Additionally, this review aims to identify any relationships between HM patient subgroups and the prevalence of CA, thus, potentially identifying patient subgroups with increased risk. Further, this review aims to identify the post-infection characteristics of CA patients. Lastly, this review addresses any relationships between various patient characteristics, disseminated CA, and mortality. We systematically reviewed the literature using the Preferred Reporting Items for Systematic Reviews and Meta-Analyses (PRISMA) guidelines to address these objectives. A systematic review was performed on the selected study population comparing patients receiving chemotherapy, SCT, corticosteroids, and/or targeted therapies before diagnosis with IPA with disseminated CA. Post-infection characteristics were also compared, including anti-fungal treatment, surgical intervention, *Aspergillus* spp., and mortality. Studies included in this review were published on or before May 18th, 2021, and were accessed through four online databases.

2.2 Methods

The systematic review was conducted according to PRISMA guidelines. The study protocol for this systematic review was registered with the PROSPERO database (<https://www.crd.york.ac.uk/PROSPERO/>), with the registration number CRD42021288469 [155].

Search strategy and study selections

Data sources used for this systematic review were PubMed/Medline, Embase, Cumulative Index to Nursing and Allied Health Literature (CINAHL) Plus, Web of Science, and GreyLit. All databases were searched from inception to May 18, 2021, and all relevant peer-reviewed studies published were included for systematic review. No limits were placed for language, publication type, etc., in the initial search. The literature search strategy combined all synonyms for the disease “cerebral aspergillosis” combined with “disseminated,” combined with all synonyms for diseases resulting from “hematologic malignancies,” and all synonyms describing “chemotherapy” and related “immunosuppression.” Table A1 contains all MeSH terms and keywords that comprise the search strategies used for each database.

All articles retrieved through database searching were imported into Covidence systematic review software (Veritas Health Innovation, Melbourne, Australia), where duplicate records were automatically removed. In Covidence, studies were screened first by title and abstract review and second by full-text review by two independent reviewers (BNS and MAB) in duplicate. Following the first and second reviews, those studies kept and rejected were compared between reviewers, and any discrepancies were resolved by consensus.

Eligibility criteria

Research articles that met the following defined inclusion criteria were selected for systematic review. Eligible studies needed to include patients with leukemia or lymphoma (any age/gender), diagnosed IPA + CA (proven, any *Aspergillus* spp.) with the primary infection being in the lung and without any concurrent infections by other yeasts, viruses, and/or bacteria, etc., and the outcome of fungal infection. Studies additionally needed to include one or all of the following regarding whether or not patient(s) included in the study were receiving chemotherapy, SCT, and/or another therapeutic for HM. Studies without patients with CA were excluded, and patients without CA in studies included were excluded from the analysis. Study design: any full-text peer-reviewed reports available in English containing original clinical data were considered; this primarily included case reports and series. Further, preprint articles and articles with no full text available were not included. The primary outcomes of interest were mortality and prevalence of CA within HM patient subgroups. Comparison or control groups were not applicable.

Data abstraction

Data were abstracted independently and in duplicate by two reviewers using standardized data extraction criteria for case reports and studies. The Covidence systematic review software was utilized for data abstraction for case reports. For case series, Google Sheets was used. For case series in which cohort data was additionally available, individual patient data were preferentially used as they provided more-detailed information about underlying HMs, treatment, and outcomes. Two independent investigators (BNS, MAB) abstracted the following data, when available, from eligible articles: general study information (including title, authors, PMID, country study was conducted in, year of infection diagnosis, and year of publication), study characteristics (case study versus series), participant characteristics (including age, gender, type of

leukemia or lymphoma, neutropenic status, absolute neutrophil count (ANC) or white blood cell count (WBC), and additional sites of dissemination if any), information about the interventions (including chemotherapy regimen, SCT, any non-cytotoxic therapeutics pre- or post-IPA, prophylactic anti-fungal regimens, therapeutic interventions for aspergillosis, and surgical interventions), type of *Aspergillus*, and outcome measures (survival). Abstracted data were compared between the two reviewers, and any discrepancies were resolved by consensus. Upon resolving discrepancies, data were synthesized into a single form that was maintained on Google Sheets.

Assessment of study quality

The included publications were assessed for risk of bias for selection, ascertainment, causality, and reporting based on the modified Pearson Case Report Quality scale proposed by Murad and colleagues [156]. For each bias domain, levels of bias were rated as high, low, or unclear, based upon the response of no, yes, or unclear, respectively, to the prompting questions. The overall risk of bias of a study was deemed low if the study had a low risk of bias for all domains. The overall risk of bias was considered unclear if a study had an unclear risk of bias for at least one domain. Lastly, the overall risk of bias was deemed high if a study had a high risk of bias for at least one domain. All responses were recorded through Covidence systematic review software (Table A2). The consensus of quality was reached by two independent researchers (BNS, MAB) for each study.

Data synthesis and analysis

A narrative summary approach was used to detail the key study characteristics and systematic review findings. As each study represented an individual patient or patients, the data was synthesized and described in this way. The data were pooled to

determine the prevalence of underlying HM patient subgroups, treatments, outcome, and other pertinent variables in the patient population. In some analyses, studies were excluded if relevant data were not available. For this reason, the number of patients varies in each analysis. Further, due to heterogeneity in study design, statistical analysis of the data collected from the 47 studies was not undertaken.

2.3 Results

Search results

The PRISMA flow diagram [157] detailing the search results is shown in Figure 2.1. A search of PubMed, Embase, CINAHL, Web of Science, and GreyLit was conducted and yielded 761 records. After removing 165 duplicates by Covidence, 596 records were screened for title and abstract. This initial screening resulted in 191 records being sought for retrieval, 180 reports were assessed for eligibility, and 11 were unable to be retrieved. A total of 133 records were deemed ineligible and were excluded. Studies were excluded for the following reasons: the primary infection was not in the lung, there was no infection in the brain, the manuscript was not available in English, the patients did not have an HM prior to infection, or the HM patient subgroup was not specified/proven, the infection was not *Aspergillus* or was not proven to be, patients had a co-current infection with another yeast, bacteria, virus, etc., the study was a duplicate that Covidence did not remove in the initial screening, the article was a review, and/or the study was the wrong design where no relevant data could be extracted. Many studies met multiple criteria for exclusion but were only tagged with one exclusion criterion. The remaining 47 case reports, case series, and observational studies, all of which contained one or more patients with IPA + CA, underwent data extraction and were included in the final systematic review. Seventy-six HM patients with CA disseminated from IPA were included from the 47 studies, summarized in Table 2.1.

Quality appraisal

Each study's quality was assessed and detailed in Table A2. The overall outcome of quality appraisal is synthesized in Figure A1. For evaluating the selection bias of patients included, it was assessed if the patient(s) included in the case report or series represented the whole experience of the investigator. Overall, there was a relatively low

risk of selection bias, with 97.87% of studies being deemed as having a low risk of bias and 2.13% with an unclear risk of bias. There was a low risk of ascertainment bias for evaluating the exposure and outcome of each study, with 100% of studies for both criteria being considered as having a low risk of ascertainment bias. Each study was evaluated to determine if other alternative causes that may explain the observation were ruled out when assessing causality bias. 55.32% of studies had a low risk of causality bias, 31.91% had an unclear risk of bias, and 12.77% had a high risk of causality bias. Causality bias was further ascertained by evaluating the follow-up time to determine the outcome, and 97.87% of studies were found to have a relatively low risk of causality bias, and 2.13% with an unclear risk of bias. Overall, the causality bias was moderate, with 76.60% of studies having low risk of causality bias, 17.02% with unclear risk of bias, and 6.38% of studies with a high risk of causality bias. Finally, the risk of reporting bias was determined by evaluating whether the case(s) were described with enough detail for researchers and/or practitioners to replicate to make inferences related to their practice. Here 63.83% of studies were found to have low risk of reporting bias, 27.66% have unclear risk of bias, and 8.51% have a high risk of bias. Essentially, most case reports and studies had a low risk of bias, with 65.96% with low risk, 31.91% with an unclear risk of bias, and 2.13% having a high risk of bias.

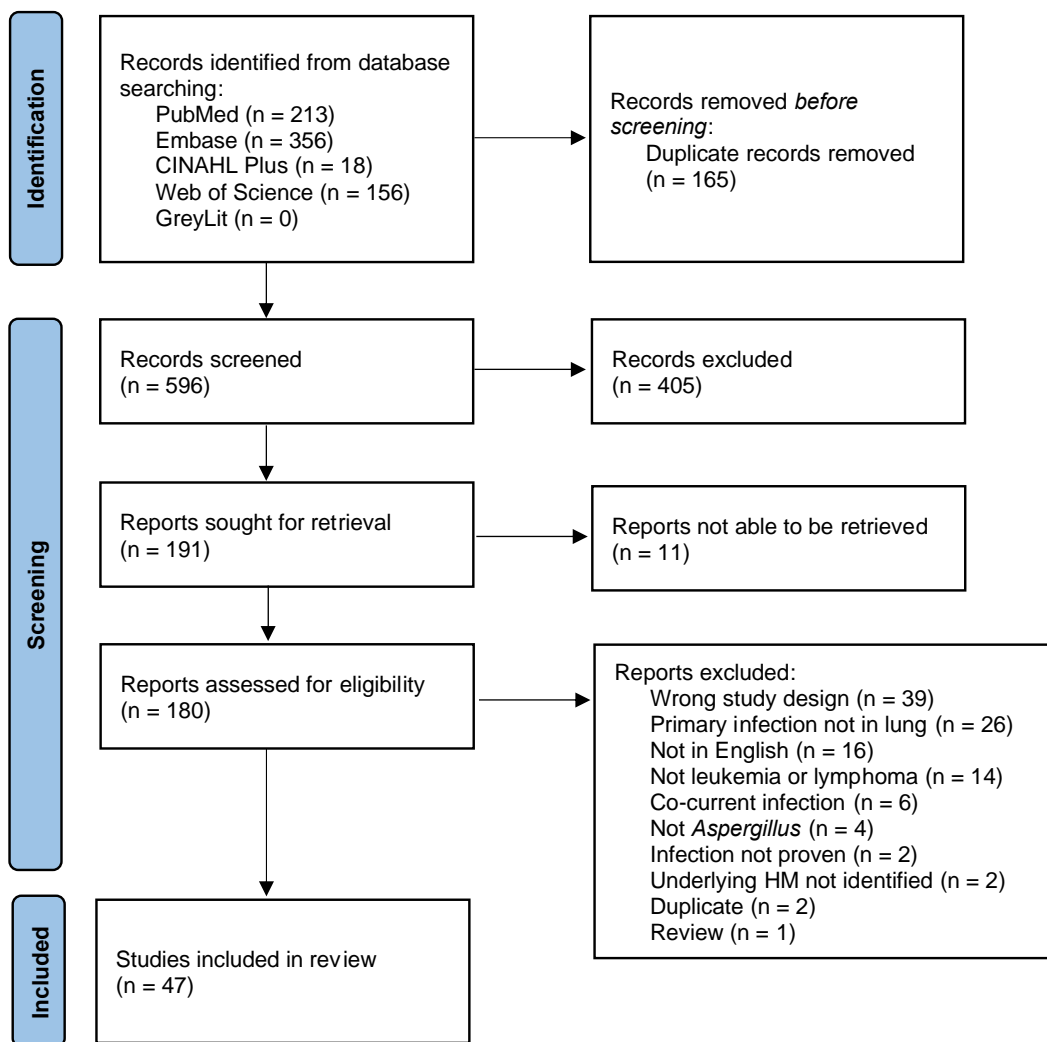


Figure 2.1. PRISMA flow chart

Table 2.1. Characteristics of included studies.

Ref.	Country of diagnosis	Year of diagnosis	Patient #	Gender	Age (years)	HM	<i>Aspergillus</i> species	Outcome
[158]	France	2017	1	M	75	CLL	<i>A. fumigatus</i>	Survived
			2	M	65	CLL	<i>A. fumigatus</i>	Survived
[159]	Germany	1992	3	M	17	ALL	<i>Aspergillus</i> spp.	Survived
			4	M	16	ALL	<i>A. fumigatus</i>	Died
			5	M	58	AML	<i>Aspergillus</i> spp.	Died
[160]	Spain	2011-2017	6	M	52	AML	<i>Aspergillus</i> spp.	Died
			7	M	56	MM	<i>Aspergillus</i> spp.	Died
			8	F	12	ALL	<i>A. fumigatus</i> , <i>A. flavus</i>	Survived
[161]	Germany	2002	9	F	63	AML	<i>A. fumigatus</i>	Died
		2003	10	F	4	ALL	<i>A. fumigatus</i>	Survived
[162]	USA	1985-1990	11	NA	NA	NHL	<i>A. flavus</i>	Died
			12	NA	NA	NHL	<i>A. flavus</i>	Died
			13	NA	NA	NHL	<i>A. flavus</i>	Died
[163]	USA	1985-1994	14	F	36	NHL	<i>A. flavus</i>	Died
			15	M	38	NHL	<i>A. flavus</i>	Died
			16	M	16	ALL	<i>A. fumigatus</i>	Died
[164]	USA	1997-1999	17	M	16	ALL	<i>Aspergillus</i> spp.	Died
			18	M	6	AML	<i>Aspergillus</i> spp.	Survived
[165]	Japan	1995	19	F	71	AML	<i>Aspergillus</i> spp.	Died
		1978-1995	20	F	71	AML	<i>Aspergillus</i> spp.	Died
			21	F	57	ALL	<i>Aspergillus</i> spp.	Died
[166]	Germany	1988	22	M	49	ALL	<i>Aspergillus</i> spp.	Survived
		1989	23	F	23	AML	<i>Aspergillus</i> spp.	Died
[167]	USA	2014-2016	24	M	65	NHL	<i>A. fumigatus</i>	Died
			25	F	87	NHL	<i>A. fumigatus</i>	Died
			26	M	49	NHL	<i>A. fumigatus</i>	Survived
[168]	USA	2001	27	F	6	AML	<i>Aspergillus</i> spp.	Survived
			28	M	6	AML	<i>Aspergillus</i> spp.	Survived
[169]	Italy	2015	29	F	65	AML	<i>Aspergillus</i> spp.	Died
			30	F	60	AML	<i>Aspergillus</i> spp.	Survived

[170]	Unknown	2014-2017	31	M	67	CLL	<i>Aspergillus</i> spp.	Died
			32	M	71	CLL	<i>Aspergillus</i> spp.	Died
[171]	Netherlands	2019	33	F	18	ALL	<i>A. fumigatus</i>	Survived
			34	F	15	ALL	<i>A. fumigatus</i>	Survived
[172]	USA	1982-1990	35	F	22	AML	<i>A. flavus</i>	Died
			36	F	31	ALL	<i>Aspergillus</i> spp.	Died
			37	F	57	AML	<i>Aspergillus</i> spp.	Died
			38	F	32	ALL	<i>Aspergillus</i> spp.	Died
			39	F	20	AML	<i>A. flavus</i>	Died
			40	F	21	ALL	<i>Aspergillus</i> spp.	Died
[173]	Netherlands	2007-2009	41	F	13	NHL	<i>A. fumigatus</i>	Died
		2007-2010	42	M	60	AML	<i>A. fumigatus</i>	Survived
[52]	USA	1956-1985	43	M	60	AML	<i>Aspergillus</i> spp.	Survived
			44	F	62	AML	<i>Aspergillus</i> spp.	Survived
			45	M	59	NHL	<i>Aspergillus</i> spp.	Died
			46	M	14	ALL	<i>Aspergillus</i> spp.	Died
[174]	USA	1995-2002	47	NA	10	AML	<i>A. flavus</i>	Died
[175]	Taiwan	1987-2005	48	M	11	AML	<i>Aspergillus</i> spp.	Survived
[176]	Netherlands	2007	49	F	16	ALL	<i>A. fumigatus</i>	Survived
[177]	United Kingdom	2006	50	M	34	AML	<i>A. fumigatus</i>	Survived
[178]	USA	1991	51	F	6	ALL	<i>A. fumigatus</i>	Survived
[179]	USA	1981	52	M	23	AML	<i>A. terreus</i>	Died
[180]	France	1994-1995	53	M	61	AML	<i>A. fumigatus</i>	Died
[181]	Israel	2018	54	M	37	NHL	<i>A. fumigatus</i>	Died
[182]	Spain	1997	55	M	43	ALL	<i>Aspergillus</i> spp.	Died
[183]	Japan	2017	56	M	15	AML	<i>Aspergillus</i> spp.	Died
[184]	India	2011	57	M	14	ALL	<i>Aspergillus</i> spp.	Died
[185]	Thailand	1991-2000	58	F	36	ALL	<i>A. fumigatus</i>	Died
[186]	China	2012	59	M	53	AML	<i>Aspergillus</i> spp.	Survived
[187]	USA	Before 1987	60	F	32	AML	<i>Aspergillus</i> spp.	Survived
[188]	Japan	1995	61	M	41	AML	<i>A. flavus</i>	Died
[189]	Italy	2000	62	F	53	CLL	<i>A. flavus</i>	Survived
[190]	Germany	1996	63	F	62	AML	<i>Aspergillus</i> spp.	Survived
[191]	Germany	2003	64	F	9	AML	<i>A. fumigatus</i>	Survived
[192]	Korea	2011	65	F	31	AML	<i>Aspergillus</i> spp.	Survived

[193]	Germany	1980	66	M	12	ALL	<i>A. fumigatus</i>	Survived
[194]	France	1999	67	F	30	CML	<i>A. fumigatus</i>	Died
[195]	USA	2009	68	M	17	ALL	<i>Aspergillus</i> spp.	Survived
[196]	USA	2015	69	M	76	CLL	<i>A. fumigatus</i>	Survived
[197]	USA	2017	70	M	62	CLL	<i>A. fumigatus</i>	Survived
[198]	Italy	2017	71	F	3	ALL	<i>Aspergillus</i> spp.	Survived
[199]	France	2002	72	M	57	AML	<i>Aspergillus</i> spp.	Survived
[200]	Australia	2018	73	M	66	CLL	<i>A. felis</i>	Survived
[201]	Greece	2004	74	M	2	ALL	<i>A. fumigatus</i>	Survived
[154]	Iran	2018	75	M	1.5	ALL	<i>A. fumigatus, A. niger</i>	Died
[202]	Italy	2015	76	F	0.5	ALL	<i>Aspergillus</i> spp.	Survived

Abbreviations: Ref. = reference; M = Male; F = Female; NA = Data not available; AML = Acute myeloid leukemia; ALL = Acute lymphocytic leukemia; CML = Chronic myeloid leukemia; CLL = Chronic lymphocytic leukemia; NHL = non-Hodgkin's lymphoma; MM = Multiple myeloma; A. = *Aspergillus*; spp. = *Aspergillus* species

Demographic characteristics

The demographic characteristics of all patients included are detailed in Table 2.2. Reported gender amongst all patients is approximately half male-identifying (54.17%, n = 39) and half female-identifying (45.83%, n = 33), the gender of 4 patients was not reported. The age (n = 73) of patients ranged from 0.5 to 87 years (mean = 32.5; SD = 21.9). The number children (< 18 years), young adults (18-49 years), and older adults (\geq 50 years) was relatively similar between all groups.

Table 2.2. Demographic characteristics of all included studies.

Age of all patients ($N^a = 73$) (Mean \pm SD (Years))	32.5 \pm 21.9
	% (n^b)
< 18 years	34.25% (25)
\geq 18, < 50 years	27.40% (20)
\geq 50 years	38.36% (28)
Identify as male ($N = 72$)	54.17% (39)

^aN = total number of patients with available data for characteristic. ^bn = number of patients with defined characteristic within group. % = # with defined characteristic/# with available data for characteristic. Abbreviations: SD = standard deviation

Underlying disease

The details regarding HM patient subgroup reported amongst all patients are included in Table 2.3. AML was the most frequently reported HM patient subgroup followed closely by ALL. Reported less frequently amongst the population included herein were NHL and CLL. For CML and myeloma, only one patient was reported for each HM amongst the patient population. No cases of disseminated CA included were reported in patients with Hodgkin's lymphoma.

Table 2.3. Patient characteristics.

	%(n ^a)
Underlying HM patient subgroup (N^b = 76)	
AML	39.47% (30)
ALL	32.89% (25)
CML	1.32% (1)
CLL	10.53% (8)
NHL	14.47% (11)
MM	1.32% (1)
Neutropenic (N = 51)	78.43% (40)
Immunosuppressive therapies	
Chemotherapy (N = 67)	88.06% (59)
Phase (N = 23)	
Induction	73.91% (17)
Consolidation	26.09% (6)
Type + regimen (N = 27)	
Mono therapy	18.52% (5)
Multi therapy	81.48% (22)
Regimen includes Cytarabine	66.66% (18)
Regimen includes Daunorubicin	40.74% (11)
Regimen includes Vincristine	33.33% (9)
SCT (N = 58)	
Allogenic	78.57% (11)
Autologous	21.43% (3)
Corticosteroids (N = 54)	
Type (N = 21)	
Prednisone	61.90% (13)
Dexamethasone	38.10% (8)
Prophylactic anti-fungal	
Yes (N = 48)	47.91% (23)
Type + Regimen (N = 13)	
AmB ^c	61.54% (8)
Fluconazole	23.08% (3)
Itraconazole	7.69% (1)
AmB + fluconazole	7.69% (1)

^an = number of patients with defined characteristic within group. ^bN = total number of patients with available data for characteristic. ^c1 patient received broad-spectrum anti-microbials in addition to AmB. % = # with defined characteristic/# with available data for characteristic. Abbreviations: HM = Hematologic malignancy AML = Acute myeloid leukemia; ALL = Acute lymphocytic leukemia; CML = Chronic myeloid leukemia; CLL = Chronic lymphocytic leukemia; NHL = Non-Hodgkin lymphoma; MM = Multiple myeloma; SCT = Stem cell transplant; AmB = amphotericin B

Prevalence of known risk factors for IPA in the IPA + CA population

Prior to onset of infection, neutropenia, a common risk factor for, was identified in 40 out of the 51 patients where data was available regarding WBC or ANC levels (Table 2.3). Herein, neutropenia was defined as an ANC or WBC \leq 1500 cells/ μ l. Individual patient data regarding WBC or ANC is detailed in table A3. All patients that were considered as neutropenic, except for one, were also receiving chemotherapy related to their underlying HM. Within HM patient subgroups, at least 75% of patients within each group were identified as being neutropenic, apart from CLL in which only 50% of patients with data available were neutropenic.

Chemotherapy was given to 88.06% (n = 59) of patients prior to infection (Table 2.3). In patients with data available regarding the chemotherapy regimen (n = 27), the most prevalent chemotherapy given was cytarabine (n = 18). Cytarabine was most frequently given in combination with one or more other chemotherapies (88.89%), such as daunorubicin/doxorubicin (n = 7), etoposide (n = 5), vincristine (n = 4), methotrexate (n = 4), fludarabine (n = 4), and idarubicin (n = 4). Most patients receiving chemotherapy had at least two or three (n = 7) chemotherapeutic agents in their therapeutic regimen. In patients in which the stage of chemotherapy was reported, 73.91% (n = 17) were in the induction phase, with the remaining 26.09% (n = 6) in the consolidation phase. In most HM patient subgroups, at least 75% of patients within each were receiving chemotherapy, except for CLL patients, in which only 37.5% (n = 3) of patients received chemotherapy at the time of infection (Table 2.4).

Several targeted, non-chemotherapeutic, anti-cancer therapies were reported. Most notable is ibrutinib (n = 11), which was included in the therapeutic regimen for 87.50% of CLL (n = 7) and 36.36% of NHL (n = 4) patients and was frequently given with rituximab (n = 6), and/or corticosteroids (n = 8). In patients who received ibrutinib, 45.45% (n = 5) were not on chemotherapy, and only 18.18% (n = 2) of patients on ibrutinib were

Table 2.4. Risk factors for disease per HM patient subgroup.

HM	Chemotherapy (<i>N</i> ^a = 59)	Corticosteroids (<i>N</i> = 33) % (n^b)	SCT (<i>N</i> = 21)	Anti-fungal prophylaxis (<i>N</i> = 23)
AML (<i>N</i> = 30)	73.33% (22)	30% (10)	30% (10)	23.33% (7)
ALL (<i>N</i> = 25)	88% (22)	48% (12)	12% (3)	28% (7)
CML (<i>N</i> = 1)	100% (1)	100% (1)	100% (1)	-
CLL (<i>N</i> = 8)	37.5% (3)	50% (4)	-	33.33% (2)
NHL (<i>N</i> = 11)	90.91% (10)	45.45% (5)	54.55% (6)	54.55% (6)
MM (<i>N</i> = 1)	100% (1)	100% (1)	100% (1)	100% (1)

^a*N* = total number of patients with characteristic. ^b*n* = number of patients with characteristic within group. % = # with defined risk factor/# with HM. Abbreviations: HM = Hematologic malignancy AML = Acute myeloid leukemia; ALL = Acute lymphocytic leukemia; CML = Chronic myeloid leukemia; CLL = Chronic lymphocytic leukemia; NHL = Non-Hodgkin lymphoma; MM = Multiple myeloma; SCT = Stem cell transplant

on prophylactic antifungal. Overall, 45.45% (n = 5) succumbed to infection, and 88.89% of patients *Aspergillus spp.* identified were found to have *A. fumigatus*.

Less frequently reported were other targeted therapies such as venetoclax (n = 1), immunotherapies such as obinutuzumab (n = 2), immunoglobulin (n = 4), interleukin-2 (IL-2) (n = 2), alemtuzumab (n = 1), anti-CD52 (n = 1), and biologics such as granulocyte-colony stimulating factor (G-CSF) (n = 2) and L-asparaginase (n = 7).

Prior to infection, SCTs were done in 36.21% (n = 21) of the population. In the cases in which the type of SCT was identified (n = 14), the majority were allogenic (78.57%, n = 11) as compared to autologous (21.43%, n = 3) (Table 2.3). In groups with more than one patient, NHL patients had the highest prevalence of SCT prior to infection (54.55%, n = 6), and ALL patients had the least (12%, n = 3) (Table 2.4).

At the time of infection, 61.11% (n = 33) of patients were taking corticosteroids (Table 2.3). In the patient population in which the type of steroid prescribed was identified (n = 21), the most prevalent corticosteroid taken was prednisone (61.90%; n = 13), followed by dexamethasone (38.10%; n = 8). In most HM patient subgroups, approximately half of the patients were receiving corticosteroids prior to infection, apart from AML patients, of which 30% were being given corticosteroids at the time of infection (Table 2.4).

To determine if there was a combinatorial effect of risk factors relative to the incidence of cerebral dissemination, the presence and/or absence of multiple variables was evaluated (Table 2.5). Corticosteroids and chemotherapy together were the most prevalent combination of risk factors, with approximately half of patients with reported data receiving both prior to infection. Less prevalent was SCT combined with chemotherapy or corticosteroids prior to infection as only about one-quarter of patients were reported to have received those therapies prior to infection.

Table 2.5. Multiple risk factors for dissemination.

	% (n^a)
Chemotherapy, SCT	N^b = 49
yes, yes	28.57% (14)
yes, no	57.14% (28)
no, yes	2.04% (1)
no, no	12.24% (6)
Corticosteroid, SCT	N = 39
yes, yes	23.08% (9)
yes, no	30.77% (12)
no, yes	5.13% (2)
no, no	41.03% (16)
Chemotherapy, Corticosteroid	N = 52
yes, yes	53.85% (28)
yes, no	30.77% (16)
no, yes	7.69% (4)
no, no	7.69% (4)

^aN = total number of patients with characteristic. ^bn = number of patients with defined characteristics within group. % = # with defined characteristic/# total number of patients with characteristic. Abbreviations: SCT = stem cell transplant.

Prophylactic anti-fungal treatment

Data was available regarding the prescription of anti-fungal prophylaxis for 48 patients, of which 47.91% (n = 23) were taking anti-fungal drugs at the time of fungal infection (Table 2.3). Details for the type and regimen of anti-fungal were available for 13 patients. Amphotericin B (AmB) was the most prevalent anti-fungal drug used, with it being prescribed for 69.23% (n = 9) of patients before fungal infection. The second most prevalent was fluconazole, accounting for about 30.77% (n = 4) of patients given prophylactic anti-fungal drugs. Itraconazole was given to one patient (7.69%). All anti-fungal prophylactics were primarily given singularly, with only one patient receiving AmB + fluconazole in combination [190].

Further, the prevalence of anti-fungal prophylaxis in patients receiving immunosuppressive therapies before fungal infection was evaluated (Table 2.6). Approximately 45% of patients undergoing chemotherapy received anti-fungal prophylaxis. In patients who were given corticosteroids or who received SCT prior to infection, about one-quarter of those patients also received anti-fungal drugs preceding the invasive fungal infection (IFI).

The prevalence of anti-fungal prophylaxis in most HM sub-populations ranged from approximately 25-35%, except for NHL patients, in which more than 50% were receiving anti-fungal prophylaxis at the time of infection (Table 2.4).

Table 2.6. Traditional risk factors with or without antifungal prophylaxis.

	% (n^a)
chemotherapy, anti-fungal prophylaxis	N^b = 46
yes, yes	45.65% (21)
yes, no	39.13% (18)
no, yes	2.17% (1)
no, no	13.04% (6)
corticosteroid, anti-fungal prophylaxis	N = 39
yes, yes	25.64% (10)
yes, no	28.21% (11)
no, yes	15.38% (6)
no, no	30.77% (12)
SCT, anti-fungal prophylaxis	N = 44
yes, yes	27.27% (12)
yes, no	9.09% (4)
no, yes	22.73% (10)
no, no	40.91% (18)

^aN = total number of patients with characteristic. ^bn = number of patients with defined characteristics within the group. % = # with defined characteristic/# total number of patients with characteristic.

Abbreviations: SCT = stem cell transplant.

Treatment

Following the diagnosis of proven infection, 91.30% (n = 66) of patients were given antifungal therapy (Table 2.7). In cases where the specific anti-fungal(s) used were detailed (n = 61), the top anti-fungal therapy given, either alone or in combination with additional therapeutics, was AmB, with 80.33% (n = 49) of patients receiving it as part of their regimen. Liposomal AmB (L-AmB) was given to 19.67% (n = 12) patients. 22.95% (n = 14) of patients were given AmB singularly. When given in combination with additional anti-fungals, AmB was most frequently given with voriconazole alone (16.39%, n = 10) or in combination with other antifungals (18.03%, n = 11). AmB was given with fluconazole in 14.75% (n = 9) or with itraconazole in 8.19% (n = 5) of patients. The second most reported anti-fungal therapy prescribed to patients was voriconazole, accounting for 49.18% (n = 30) of patients, most often included as a part of a therapeutic regimen. Voriconazole was often given with caspofungin with (8.19%, n = 5) or without AmB (4.92%, n = 3). Posaconazole was included in the treatment regimen of several patients (6.56%, n=4), and was given along with voriconazole for all patients, with AmB for 3/4 , and caspofungin for 2/4. Other anti-fungal drugs, including echinocandin (n = 2), isavuconazole (n = 2), micafungin (n = 2), natamycin (n = 1), and fluconazole (n = 1), were occasionally included in patients therapeutic regimens, albeit less frequently than others mentioned above.

Of the 58 patients with data regarding surgical interventions following diagnosis, 44.83% (n = 26) of patients underwent surgical intervention for the IFI (Table 2.7).

Species

Among the 39 patients in which *Aspergillus* isolates were identified to the species level, the most frequent species identified was *A. fumigatus* (64.10%, n = 25), followed by *A. flavus* (25.64%, n = 10). Single cases of *A. terreus*, *A. felis*, *A. niger* were identified amongst the patient population included (Table 2.8). Two patients were found to have two species of *Aspergillus* identified. The first patient was a 12-year-old with ALL who had a co-infection by *A. fumigatus* and *A. flavus*, they survived the infection [161]. The second patient was an 18-month-old with ALL who had co-infection by *A. fumigatus* and *A. niger*, the patient did not survive [154].

Table 2.7. Antifungal therapy.

	% (n^a)
Antifungal therapy (N^b = 69)	91.30% (63)
Type of therapy (N = 61)	
Mono therapy	31.15% (19)
Multiple therapy	68.84% (42)
Regimen (N = 61)	
Included AmB	80.33% (49)
DAmB	75.51% (37)
L-AmB	24.49% (12)
Included Voriconazole	50.82% (31)
Included Caspofungin	18.03% (11)
Included Itraconazole	16.39% (10)
Included Flucytosine	13.11% (8)
Included Posaconazole	6.55% (4)
Voriconazole + AmB^c	24.59% (15)
Voriconazole + Caspofungin^c	4.92% (3)
Voriconazole + AmB + Caspofungin^c	9.84% (6)
Other	11.48% (7)
Type not disclosed	7.35% (5)
Surgery (N = 58)	65.38% (38)

^an = number of patients with defined characteristics within the group. ^bN = total number of patients with available data for characteristic. ^cPatients may have received an additional regimen to the combination. % = # with defined characteristic/# with available data for characteristic. Abbreviations: AmB = Amphotericin B; DAmB = Deoxycholate Amphotericin B; L-AmB = Liposomal Amphotericin B.

Mortality

Overall, ~54% (n = 41) of patients included succumbed to CA (Table 2.9). Evaluation of the overall mortality in each HM patient subgroup demonstrated patients with acute lymphomas (AML, ALL) succumbed to infection at a rate of 50% (n = 15) and 48% (n = 12), respectively. The mortality rate was much higher in the NHL population with 90.91% (n = 10) of patients with NHL succumbing to the IFI.

Examining mortality according to pre-infection risk factors showed patients exposed to chemotherapy or corticosteroids before infection to have a mortality rate of 59.32% (n = 35) and 60.61% (n = 20), respectively. In patients that did not receive corticosteroids before infection, the mortality rate was lower, with 33.33% (n = 7) of patients succumbing to infection. In patients that underwent SCT before IFI 76.19% (n = 16) died due to the infection (Table 2.9).

For patients that received anti-fungal therapy, 51.52% (n = 34) succumbed to infection, while 100% (n = 3) of patients that did not receive anti-fungal treatment died due to infection (Table 2.9).

Patients that underwent surgical intervention had a mortality rate of 34.62% (n = 9) associated with the infection. Conversely, patients who did not undergo surgical intervention had higher mortality rates with 62.50% (n = 20) of patients succumbing to infection. When the surgical intervention was combined with anti-fungal therapy, the mortality rate was 36% (n = 9) (Table 2.9).

The *Aspergillus* spp. associated with the highest mortality rate was *A. flavus*, with 90.00% (n = 9) of patients infected by that species succumbing to infection (Table 2.8). The most-reported species identified in patients, *A. fumigatus*, was associated with a 47.62% (n = 10) mortality rate.

Table 2.8. *Aspergillus* species* identity and related mortality.

	Patients (N^a = 39)	Survived	Died
		% (n^b)	
<i>Aspergillus fumigatus</i>	64.10% (25)	60.00% (15)	40.00% (10)
<i>A. fumigatus</i> + <i>A. flavus</i>^c	2.56% (1)	100% (1)	
<i>A. fumigatus</i> + <i>A. niger</i>^d	2.56% (1)		100% (1)
<i>Aspergillus flavus</i>	25.64% (10)	10.00% (1)	90.00% (9)
<i>Aspergillus terreus</i>	2.56% (1)		100% (1)
<i>Aspergillus felis</i>	2.56% (1)	100% (1)	

^aN = total number of patients with available data for characteristic. ^bn = number of patients with defined characteristic within group. ^c1 patient positive for *Aspergillus fumigatus* and *flavus*. ^d1 patient positive for *Aspergillus fumigatus* and *niger*. % = # with defined characteristic/# total number of patients with characteristic. *n = 37 species not identified. Abbreviations: A. = *Aspergillus*.

Table 2.9. Potential factors associated with mortality.

	% Mortality (n^a)
Overall mortality	53.95% (41)
Age	
< 18 years (N^b = 25)	36.00% (9)
≥ 18, < 50 years (N = 20)	70.00% (14)
≥ 50 years (N = 39)	53.57% (15)
Mortality rate according to HM	
AML (N = 30)	50.00% (15)
ALL (N = 25)	48.00% (12)
CML (N = 1)	100.00% (1)
CLL (N = 8)	25.00% (2)
NHL (N = 11)	90.91% (10)
MM (N = 1)	100.00% (1)
Mortality rate according to chemotherapy at time of IPA diagnosis	
Chemotherapy (N = 59)	59.32% (35)
No (N = 8)	25.00% (2)
Mortality rate according to SCT prior to IPA diagnosis	
SCT (N = 21)	76.19% (16)
No (N = 37)	35.14% (13)
Mortality rate according to corticosteroids at time of IPA diagnosis	
Steroids (N = 33)	60.61% (20)
No (N = 21)	33.33% (7)
Mortality rate according to prophylactic anti-fungal	
Anti-fungal prophylaxis (N = 23)	73.91% (17)
No (N = 25)	28.00% (7)
Mortality rate according to therapeutic anti-fungal	
Anti-fungal therapy (N = 66)	51.52% (34)
No (N = 3)	100.00% (3)
Mortality rate according to surgical intervention post-diagnosis	
Surgical intervention (N = 26)	34.62% (9)
No (N = 32)	62.50% (20)
Mortality rate according to therapeutic anti-fungal & surgical intervention	
Surgical intervention, anti-fungal therapy (N = 25)	36.00% (9)
No Surgical intervention, anti-fungal therapy (N = 26)	61.54% (16)

^an = number of patients died within characteristic group. ^bN = total number of patients with characteristic. % = # died within characteristic group / # total number of patients with characteristic. Abbreviations: HM = hematologic malignancy AML = acute myeloid leukemia; ALL = acute lymphocytic leukemia; CML = chronic myeloid leukemia; CLL = chronic lymphocytic leukemia; NHL = non-Hodgkin's lymphoma; MM = multiple myeloma; SCT = stem cell transplant.

2.4 Discussion

To our knowledge, this is the first comprehensive systematic review of the literature focusing on disseminated CA following IPA in patients with HMs. In this study we examined the characteristics of a large number of disseminated CA cases following IPA in HM patients published as single case reports, case series, or as a part of larger observational studies. All cases included had a proven *Aspergillus* spp. infection. The mortality rate due to CA was 53.95% overall for patients included in this systematic review.

Like studies focusing on IPA in patients with HMs, we found the predominant HM patient subgroup diagnosed with disseminated CA to be AML, closely followed by ALL [67, 80, 203, 204]. Interestingly, estimates of the global incidence and prevalence of HMs have demonstrated the top reported HM patient subgroups to be NHL and CLL; however, in studies of IPA, and disclosed within this systematic review, have demonstrated those to be of mid-level prevalence. Conversely, the most prevalent HM patient subgroups for IPA and disseminated CA, AML and ALL, are globally regarded as mid-to low-level prevalence [205, 206]. This suggests that the high prevalence of AML and ALL patients diagnosed with IPA or IPA coupled with disseminated CA is potentially due, at least in part, to the anti-cancer therapeutic regimen(s) given to those patients. In fact, several reports have linked the prevalence of IFIs and the chemotherapeutic regimens used in the acute leukemia populations [207, 208]. Indeed, the top two cytotoxic drugs reported in the cases included in this systematic review were cytarabine and daunorubicin, longstanding chemotherapeutics for acute leukemia. However, in our systematic review of the literature, we did not find anti-fungal prophylaxis to be more prevalent in the acute leukemia population compared to other HM patient subgroups; rather, it was less than other populations, like those with NHL (Table 2.4). Altogether, more aggressive monitoring prevention, and implementation of anti-fungal drugs into the therapeutic regimen of HM

patients, particularly those with acute leukemias, is likely required for the prevention and/or reduction of the highly fatal CA.

Immunosuppression related to the treatment of HMs has long been considered a primary risk factor for IPA. Historically, immunosuppression in patients with HMs has been related to (i) prolonged neutropenia, primarily resulting from the use of chemotherapeutic agents, (ii) immunosuppressive drugs for the prevention and/or treatment of graft versus host disease (GvHD) following allogeneic hematopoietic-SCT and (iii) corticosteroids prescribed for a range of indications during cancer care, including the reduction of chemotherapy side-effects, anticancer effects, and as a non-specific immunosuppressant following SCT. On average, 50-90% of IPA patients with underlying HMs received chemotherapy before infection [80, 209]. Likewise, 88.06% and 78.43% of IPA patients with disseminated CA patients included in this systematic review of the literature received chemotherapeutic agents and were neutropenic, respectively, prior to infection. SCT is conducted in about 20-35% of HM patients with IPA, with allogeneic being more prevalent than autologous [80, 146, 203]. In the population of HM patients with disseminated CA following IPA, similar results were found, with about 36% of patients receiving SCT prior to infection, most of whom received allogeneic SCTs. In studies of IPA, approximately 25-45% of patients with underlying HMs were reported to be receiving corticosteroids at the time of infection [146, 203]. Interestingly, greater than 60% of the CA patients included herein were prescribed corticosteroids at the time of infection. The elevated prevalence of corticosteroids in HM patients with CA disseminated from IPA compared to HM patients with IPA alone points to a potential factor that increased the susceptibility of developing disseminated CA. Although, it is difficult to draw definitive conclusions related to specific treatments and their impact on developing CA as there is no way to account for all potential variables. The data presented here indicate that HM patients with corticosteroids included

in their anti-cancer therapy should be closely monitored and receive prophylactic anti-fungal drugs to prevent the development of this severe disease.

Recently, targeted anti-cancer therapies have become more frequently attributed to increased risk of IFIs, including IPA [210]. One of the most prominent targeted therapies is ibrutinib, a bruton tyrosine kinase (BTK) inhibitor, primarily prescribed to CLL and NHL patients. Ibrutinib is used as a single-agent therapy or as a part of combination therapy with other anti-cancer drugs such as rituximab, an anti-CD20 monoclonal antibody. Although CLL and NHL have not historically been considered as high-risk for developing IPA, the addition of ibrutinib and/or rituximab has been associated with increased prevalence of IPA in these patients [211]. Herein we report that 85.70% of CLL and 36.36% of NHL patients were given ibrutinib, frequently given in combination with rituximab and/or corticosteroids. Most patients receiving ibrutinib at the time of infection had received chemotherapy prior to initiating ibrutinib [158, 167, 170, 181, 196, 200]. Only two patients were treatment naïve prior to ibrutinib therapy, and one patient began ibrutinib co-currently with chemotherapy [158, 167, 197]. Recently, there have been several reports of CA in patients receiving Ibrutinib [212-217]. While the number of reports at this time is relatively small, it bears noting as historically, the number of CLL patients diagnosed with CA has been relatively low in comparison to patients with other HMs. Thus, this indicates the importance of investigating the incidence of CA in patients receiving Ibrutinib therapy to potentially identify an at-risk population.

Other targeted therapies, immunotherapies, and biologics given to HM patients prior to fungal infection, such as L-asparaginase, immunoglobulins, and venetoclax, among others, were administered to only a few patients, which does not permit us to make any inferences regarding their influence for the susceptibility for disseminated CA in this population. However, given the mechanisms of action of some of these drugs and previously published reports, it is reasonable that they could have impacted the immune

status of patients [210, 218, 219]. More reports on non-chemotherapeutic drugs given to HM patients are required to draw any substantial conclusions.

Anti-fungal prophylaxis has become a common addition to the treatment regimen of HM patients, with and without SCTs [220-222]. The addition of anti-fungal prophylaxis is thought to contribute to the overall reduction of IPA cases amongst immunocompromised individuals [220, 221]. Further, anti-fungal prophylaxis in HM patients is a positive predictor of survival in breakthrough cases of IPA [220, 223]. The number of HM patients prescribed antifungal drugs prophylactically typically ranges from ~15-45% [224, 225]. It should be noted, however, that the prevalence of antifungal prophylaxis in HM patients is on the rise with the development of new antifungal drugs and repeated demonstration of the efficacy of using these drugs prophylactically [95, 209, 226]. Here, we report that 47.91% of HM patients had breakthrough IPA with disseminated CA. Although, data for this was only retrievable from two-thirds of the studies, which is likely attributable to the age of some studies and the lack of antifungal prophylaxis.

Posaconazole is a prophylactic antifungal that has been consistently found to be the most effective at preventing IPA, with as little as 1% of neutropenic patients on prophylactic posaconazole with breakthrough IPA [209, 220]. No patients included in this systematic review received Posaconazole prophylactically. Instead, the majority of patients received AmB, followed by fluconazole (Table 2.3), both of which have been found to be less efficacious in preventing IPA, notably fluconazole [209]. However, it is unknown whether the infection was due to wrong anti-fungal drug choice, insufficient drug levels in the CNS or host, or fungus-specific issues and thus warrants further investigation.

Historically, AmB has been considered as the standard of care for patients with IPA. However, one study compared voriconazole with AmB as primary treatment for IPA infections and overall exhibited improved survival and response rates [227]. Improved response with voriconazole was further demonstrated through higher successful

outcomes in HM patients, patients with extrapulmonary involvement, and others suggesting voriconazole to be superior to AmB at ameliorating *Aspergillus* driven infections. Further still, treatment with voriconazole resulted in significantly fewer adverse events. Another study examining the inclusion or exclusion of voriconazole in the treatment of IPA in HM patients found the overall mortality of those receiving voriconazole to be 5%, significantly lower than the 49% mortality rate associated without voriconazole [223]. By and large, in the population of disseminated CA disclosed herein, AmB was the number one therapeutic prescribed, whether singularly or in combination. The second most prescribed in the patients included within this systematic review was Voriconazole, which was often given in combination with AmB and/or other anti-fungal drugs such as caspofungin and posaconazole. Generally, the inclusion of voriconazole reduced the overall mortality of disseminated CA. The inclusion of voriconazole with or without AmB was associated with ~30% mortality, while AmB in the absence of voriconazole was associated with ~75% mortality. While it is difficult to draw conclusions due to the inability to exclude confounding factors, the reduction of mortality associated with voriconazole suggests its therapeutic potential for CA and warrants further investigation.

In agreement with previously published cases of IPA in HM patients, *A. fumigatus* was the most common isolate identified in this systematic review [203, 204, 228, 229]. Here, *A. flavus* was the second most common isolate identified in HM patients with IPA disseminated to CA. However, the trends observed in reports of HM patients with IPA are inconsistent, with some reporting *A. flavus* or *A. terreus* as the second most common isolate identified in HM patients with IPA [146, 203, 223, 228]. In the cases included in this systematic review, only one report of infection by *A. terreus* was identified. Of note, while the population of *A. flavus* was less than half of the *A. fumigatus* population, infection by *A. flavus* was associated with a 90% mortality, approximately double that of *A. fumigatus* (Table 2.9).

2.5 Limitations

One of the primary limitations of the study was missing data. While most single case series provided adequate detail about patient history, treatment regimens, and outcome, this was not always the case for the case series and observational studies. Additionally, while many studies detailed whether, for example, chemotherapy and corticosteroids were included in patient treatment regimens, details on the type, dosing, and duration were often excluded. More to this point, disclosure of ANC levels was frequently neglected, despite neutropenia being a well-established risk factor for infection that as is often resultant from chemotherapy. Further, several studies included were published over a decade ago, and thus missing data could not be retrieved. A limitation of the wide range of dates in which the studies were conducted is that therapeutic standards have changed vastly with advancements in modern medicine, thus often making it difficult to make direct or meaningful comparisons. An additional limitation pertaining to the range of dates of the studies included is that the tools and criteria for diagnosing proven *Aspergillus* infection have changed throughout time, thus we had to rely on standards appropriate for the time of diagnosis and best judgment to determine whether a case met our stringent criteria for inclusion. In doing so, it is possible that articles were excluded or included when others would not have made that judgment, thus introducing potential bias.

Further, during the screening process, many studies with CA patients had to be excluded because they did not provide adequate information about patients included with CA. Rather, the characteristics provided were for all patients, and thus no population data specific to CA could be retrieved from those articles. For this reason, single case reports, case series, and observational studies in which individual data could be retrieved were preferentially used. Ultimately, the lack of patient data at that level severely limited the number and types of articles that could be included, and thus it is possible some important information was excluded. Further, as we were unable to retrieve CA cohort data from

larger studies investigating aspergillosis, a meta-analysis was not able to be conducted. Due to this, we were unable to potentially identify distinguishing factors amongst patient cohorts with disseminated CA that may have provided critical information to better identify high-risk populations. Therefore, for improved analysis of this population and potential identification of critical risk factors, more articles are required that distinguish and detail cohort characteristics for those with disseminated CA in the invasive aspergillosis population.

2.6 Conclusions

Disseminated cerebral aspergillosis poses a significant risk to the immunocompromised population as it is associated with a high mortality rate. Historically one of the most at-risk populations for IPA has been those with HMs, which is often attributed to the neutropenia associated with chemotherapy. With the brain being amongst the top sites of dissemination and the subsequent disease being associated with a high mortality rate, delineating the HM populations and characteristics associated with CA posed a critical need. Despite the limitations, this systematic review provides a comprehensive evidence base and analysis of a large population of HM patients with IPA with disseminated CA. Overall, the outcome of this systematic review highlights the need for more stringent incorporation of anti-fungal drugs in high-risk HM patient subgroups such as those with acute leukemias receiving chemotherapy and/or corticosteroids to reduce the incidence and mortality of this highly deadly disease.

CHAPTER 3

DEVELOPMENT OF A PRECLINICAL MOUSE MODEL OF DISSEMINATED CEREBRAL ASPERGILLOSIS IN AN IMMUNOSUPPRESSED HOST

3.1 Introduction

Invasive aspergillosis is a leading cause of death in immunocompromised patients that has become more common as the number of patients exposed to immunosuppressive agents increases. During IPA, a disease most attributed to *A. fumigatus*, which is readily eliminated from the lung in immunocompetent patients through phagocytotic clearance. However, this is not the case for immunocompromised individuals. At-risk populations include patients exposed to immunosuppressive therapies associated with HMs, stem cell and solid-organ transplants, and chronic pulmonary diseases. Prolonged neutropenia, graft-versus-host disease, high-dose corticosteroid treatment, and other immunosuppressive regimens are considered top risk factors. During IPA, unchecked fungal growth results in tissue damage and potential dissemination to other organs. Disseminated disease occurs in approximately 20-50% of the IPA population and most frequently occurs via hematogenous spread from the lungs to subsequent organs [54, 145, 146]. The brain is often reported as the most frequent site of *Aspergillus* dissemination, with CA occurring in up to 40% of some immunocompromised populations [1, 48-51, 145, 146]. Disseminated CA is also considered the most fatal form of aspergillosis, with mortality rates approaching 90% in certain populations [2, 52, 53]. Symptoms of CA, often wide-ranging and often non-specific, include antibacterial resistant fever, headache, altered mental status, nausea and vomiting, and seizures [1, 52, 54-56].

There are many clinical presentations of CA, including meningitis, encephalitis, mycotic aneurysms, granuloma, cerebral blood vessel invasion, or hemorrhage. The most frequent clinical manifestation of CA is single or multiple brain abscesses [48, 52, 54-59]. Mortality resultant from CA is often rapid, occurring in as few as 5 days post-infection. Hemorrhagic and/or ischemic events resulting from CA are amongst the top causes of death in this disease [48, 59]. While the continued development and implementation of anti-fungal drugs have greatly improved the outcome of IPA patients, for the treatment of CA, very few available therapeutics are effective in the CNS. Thus, there is a clear need for a platform in which to better evaluate treatment strategies to improve patient outcomes in the growing invasive aspergillosis population. Further, unlike IPA, there are no *in vivo* models available that effectively mimic human disease, with primary pulmonary infection and dissemination through the blood resulting in CA. Current models depend on a singular, direct inoculation into either the brain or the blood, neither of which are physiological routes of infection [60, 62]. As such, the potential for significant improvements in the understanding and development of therapeutics and diagnostic tools has been limited. Further improvements in disease outcomes depend on gaining deeper insight into and translating advances to promote anti-*Aspergillus* immunity.

To this end, we detail the development of a novel preclinical murine model of CA. As corticosteroids are a significant risk factor that are used for most at-risk populations, we have implemented immunosuppression through high-dose corticosteroids to model this disease. Mice were infected via a “two-hit” inoculation regimen via the lung to establish primary experimental IPA and the blood to promote secondary disseminated disease. To study disease progression, CA infection was intended to be universally and reproducibly lethal within several days. At disease termination, fungal burden was quantified in the lung and brain. Altogether, corticosteroid-induced immunosuppression in the two-hit

disseminated CA model disclosed herein resulted in reproducible fungal infection within the brain with pathology that mimics human disease.

3.2 Methods

Animals

Male and female, age-matched C57BL/6 mice, 6–10 weeks of age, were obtained from The Jackson Laboratory (Bangor, ME). All animals were housed in a specific pathogen-free, Association for Assessment and Accreditation of Laboratory Animal Care–certified facility and handled according to Public Health Service Office of Laboratory Animal Welfare policies after review by the Tulane Institutional Animal Care and Use Committee (IACUC). All animal research was conducted under approved Tulane IACUC Protocol #1589. Mice were sacrificed following anesthesia with ketamine/xylazine (100/10 mg kg⁻¹ intraperitoneally (IP); MWI Veterinary Supply, Boise, ID). No animals were excluded from the analyses unless the animal died prematurely. ‘*n*’ reported in the manuscript represents the number of animals in each group that were euthanized as scheduled at the end of the study unless otherwise stated.

Preparation of *A. fumigatus*

A. fumigatus isolate 13073 (American Type Culture Collection, Manassas, VA) was maintained on potato dextrose agar for 5–7 d at 37°C. Conidia were harvested by washing the culture flask with 50 ml of sterile PBS (Thermo Fisher Scientific, Waltham, MA) supplemented with 0.1% Tween-20 (Bio-Rad, Hercules, CA). The conidia were then passed through a sterile 40-mm nylon membrane to remove hyphal fragments and conidial clusters and enumerated on a hemacytometer.

Immunosuppression

For the corticosteroid-induced immunosuppression model, mice were given Kenalog-40™ or sterile PBS as an immunocompetent control [230, 231]. Briefly, subcutaneous (SC) injections at 40 mg/kg Kenalog-40™ (triamcinolone acetonide; Bristol-

Myer Squibb, Princeton, NJ) of body weight in sterile PBS for a final volume of 100ul 24h before fungal inoculation [232]. Immunocompetent mice were injected SC with 100ul of sterile PBS 24h before fungal inoculation.

Infection

For pulmonary infection, mice were lightly anesthetized with isoflurane, and administered 2×10^6 , 7×10^6 , or 1×10^7 *A. fumigatus* conidia suspended in sterile PBS in a volume of 30 ul intranasally (IN) 1-day post immunosuppression, as previously described [233]. Briefly, mice are held in a horizontal, supine, position, and a pipette is used to deliver the 30 ml inoculum dropwise to the nares, where normal breathing results in fluid aspiration into the lungs. For hematologic infection, mice were administered 100 ul 1×10^5 or 7×10^6 of resting or pre-swollen for 5h at 37°C *A. fumigatus* conidia given IV through the lateral tail vein [234]. “Two-hit” model mice received IV inoculation 2-days following Kenalog-40 immunosuppression (1-day post IN inoculation with 30ul *A. fumigatus* or PBS control), whereas IV only were inoculated on DPI 0. IN-only control mice in the “two-hit” model were administered 100ul of sterile PBS incubated at 37°C IV 1-day post IN inoculation.

Monitoring disease severity

Mice were weighed daily, and total weight loss was calculated at study completion. Following infection, mice were scored daily beginning 1-day post IN inoculation for morbidity and mortality up to ten days, using a modified scoring system as previously described [235]. Morbidity was scored from 0 to 5 as follows: 0) healthy, 1) minimal disease (e.g. ruffled fur), 2) moderate disease (e.g. ungroomed, hunched), 3) severe disease (e.g. severely hunched, altered gait, low motility, head-tilt), 4) moribund (e.g.

spinning in cage or when suspended by tail, unable to move freely around cage, >25% weight loss) and 5) deceased. Mice that received a score of 4 were sacrificed.

Survival studies

Cages were inspected daily. All animals were observed for symptom severity, weight loss, and morbidity for 10 days after initial IN infection. Morbidity was recorded for mice that reached a clinical score of 4 or 5. Mice that survived to day 10 were euthanized.

Lung and brain fungal burden assessment

For lung fungal burden analysis, the left lungs were collected at 96h postexposure and homogenized in 1ml of PBS. Total RNA was extracted per manufacturer instructions from 0.1ml of unclarified lung homogenate using the MasterPure Yeast RNA Purification Kit (Lucigen Corporation, Middletown, WI), which includes a DNase treatment step to eliminate genomic DNA as previously reported because DNA is not predictive of organism viability in this assay [236].

For brain fungal burden analysis, the right hemisphere was collected at 96h postexposure and homogenized in 0.6ml of PBS. Total RNA was extracted in the same manner as the lung from 0.3ml of unclarified brain homogenate using the MasterPure Yeast RNA Purification Kit, with the exception of extraction reagent and proteinase K volumes, which were doubled, and the incubation at 70°C, which was increased from 10 to 15 minutes.

Lung and brain *A. fumigatus* burden was analyzed with reverse transcription quantitative PCR (RT-qPCR) measurement of the *A. fumigatus* 18S rRNA (Integrated DNA Technologies; Forward: 5'-GGC CCT TAA ATA GCC CGG T-3'; Reverse: 5'-TGA GCC GAT AGT CCC CCT AA-3'; Probe: 5'-/56-FAM/AGC CAG CGG CCC GCA AAT G/3BHQ_1/-3') and quantified using a standard curve of *A. fumigatus* 18S rRNA

synthesized by GenScript via *in vitro* transcription. The final RNA sequence of the 18s fragment (562nt) is as follows:

TCGCAAGGCTGAAACTTAAAGAAATTGACGGAAGGGCACCACAAGGCGTGGAGCC
 TGCGGCTTAATTTGACTCAACACGGGGAAACTCACCAGGTCCAGACAAAATAAGGA
 TTGACAGATTGAGAGCTCTTTCTTGATCTTTTGGATGGTGGTGCATGGCCGTTCTTA
 GTTGGTGGAGTGATTTGTCTGCTTAATTGCGATAACGAACGAGACCTCGGCCCTTA
 AATAGCCCGGTCCGCATTTGCGGGCCGCTGGCTTCTTAGGGGGACTATCGGCTCA
 AGCCGATGGAAGTGCGCGGCAATAACAGGTCTGTGATGCCCTTAGATGTTCTGGG
 CCGCACGCGCGCTACACTGACAGGGCCAGCGAGTACATCACCTTGGCCGAGAGGT
 CTGGGTAATCTTGTTAAACCCTGTCGTGCTGGGGATAGAGCATTGCAATTATTGCTC
 TTCAACGAGGAATGCCTAGTAGGCACGAGTCATCAGCTCGTGCCGATTACGTCCCT
 GCCCTTTGTACACACCGCCCGTCGCTACTACCGATTGAATGGCTCGGTGAGGCCTT
 CGGA.

The RT-qPCR reaction was performed with the CFX96 Real-Time System C1000 Touch thermal cycler (Bio-Rad).

Histology

The left hemisphere of the brain was collected and fixed in 10% neutral buffered formalin. The fixed brains were paraffin-embedded and then processed and stained with Hematoxylin & Eosin (H&E) or Grocott's methenamine silver (GMS) by GNO Histology Consultants (New Orleans, LA). Imaging was performed using a Swift Optical Instruments M10T-P Trinocular LED Microscope equipped with a Motic Moticam 5 + 5-megapixel digital camera.

Statistics

Data were analyzed using GraphPad Prism, version 9.0, statistical software (GraphPad Software, San Diego, CA). Comparisons between groups for normally distributed data were made with the Student's t-test or two-way analysis of variance (ANOVA). Significance was accepted at a p value < 0.05 .

3.3 Results

Induction of IPA in immunosuppressed mice dose not result in cerebral dissemination.

In the clinical population of CA, the disease occurs most commonly as a secondary infection, disseminated from the primary pulmonary infection IPA. Further, this disease most frequently occurs in the severely immunosuppressed population, with corticosteroids being one of the most prevalent immunosuppressive agents amongst these patients. Therefore, we hypothesized that through corticosteroid-induced immunosuppression and primary pulmonary infection, we could achieve successful CA. To test this, we infected mice that had been immunosuppressed with corticosteroids and infected IN with two different conidial doses (Figure 3.1a). Mice were inoculated IN with either 7×10^6 or 1×10^7 to (i) determine if CA would occur subsequent to IPA and (ii) if dissemination was dose-dependent. Mice were evaluated daily for weight loss and monitored for signs of severe infection, including labored breathing, latency to move around the cage or inability to walk. Overall, we observed that the mice challenged with a higher conidial dose (1×10^7) were observed to have significantly greater weight loss and a higher, albeit insignificant, percentage of mice displayed signs of severe disease, 42% vs 29%, by study completion (Figure 3.1b, c). Mice were sacrificed at 3-days post-infection as signs of severe disease were observed at that point, and RT-qPCR was performed on RNA isolated from the lungs and brain to quantify fungal burden. Both inoculum concentrations resulted in fungal infection within the lung. However, the increased inoculum concentration did not result in significantly greater infection (Figure 3.1d). Further, no fungal organism was detected within the brain at either inoculum concentration, despite considerable pulmonary infection (Figure 3.1d). As such, we concluded that induction of IPA through high doses of *A. fumigatus* in corticosteroid immunosuppressed mice does not result in the dissemination of *Aspergillus* into the brain following IPA.

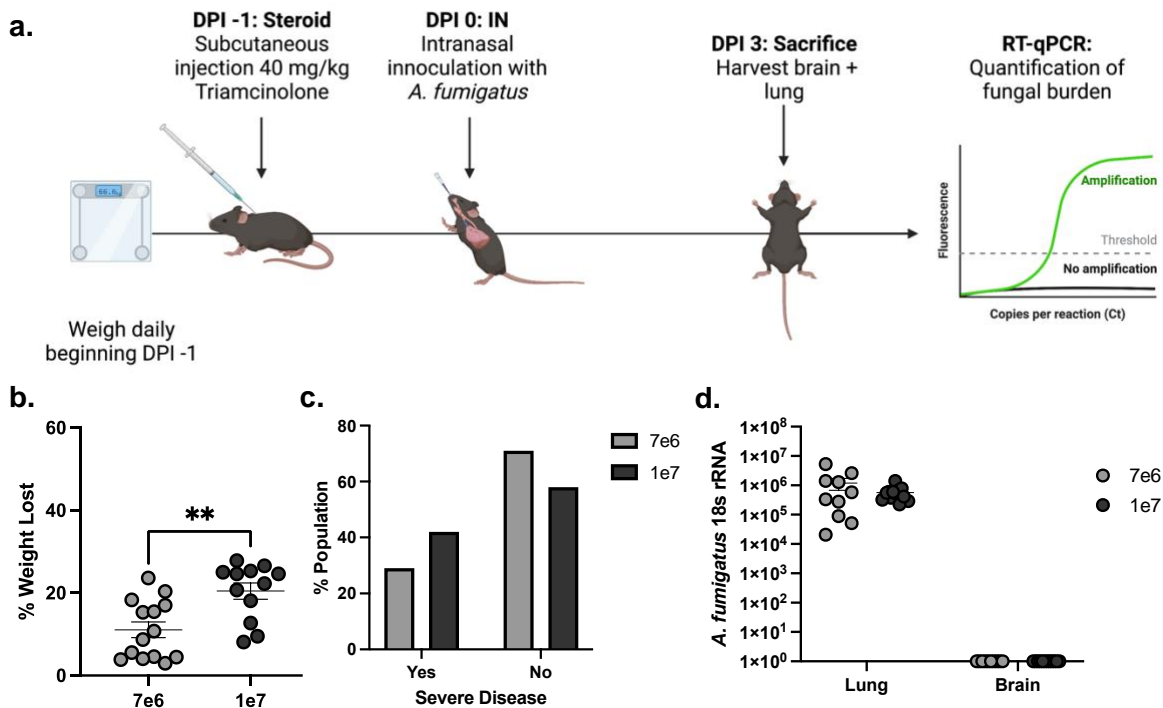


Figure 3.1. Induction of IPA does not result in cerebral dissemination, regardless of the conidial dose.

a. WT C57Bl/6 male and female mice were subjected to experimental IPA with mice immunosuppressed at DPI -1 with triamcinolone acetate SC and IN inoculated with either 7e6 or 1e7 resting *A. fumigatus* conidia. Mice were weighed daily beginning from the study initiation (DPI -1) through study completion. Mice were monitored daily for signs of severe disease. Mice were sacrificed, and tissue was harvested for RT-qPCR at DPI 3. Image created with BioRender.com **b.** Mice were weighed daily, and total weight loss was determined by comparing initial weight to weight at study completion. **c.** Mice were assessed daily for signs of severe disease; data represents the presence (yes) or absence (no) signs of severe disease at the time of sacrifice. **d.** Lung and brain fungal burden were assessed by RT-qPCR analysis of *A. fumigatus* 18S rRNA levels. The Figures illustrate cumulative data from three independent studies (n = 4-5 mice per group, per study). Each data point/dot represents a single mouse, and the lines in each group correspond to the mean + SEM. **b, d.** ** indicates p = 0.0023, unpaired two-tailed Student's t-test. **c.** Fisher's exact test.

Successful induction of disseminated CA via IV inoculation

Next, as infection through IN administration did not lead to disseminated CA, we sought to determine whether successful infection in the brain could be achieved through IV inoculation. For this, we evaluated weight loss, signs of severe disease via a clinical scoring system, and fungal burden in immunocompetent mice inoculated IV with 7×10^6 *A. fumigatus* or PBS (control). For clinical scoring, beginning DPI 1, mice were monitored for clinical signs using a 0-5 scoring system, with 0 being no symptoms and 5 being death. In comparison to sham control mice, mice that received *A. fumigatus* IV lost a significant percentage of body weight by study completion, as well as exhibited signs of increasing disease severity, with all mice reaching severe disease by DPI 3. At that point, they were sacrificed (Figure 3.2b-c). Following sacrifice, the brains and lungs were harvested and evaluated for fungal burden by RT-qPCR. Mice that received *A. fumigatus* IV had fungal burden in both brain and lung (Figure 3.2d), while sham control mice were absent of fungal burden in both tissues (data not shown). The mice that received *A. fumigatus* had significantly greater fungal burden within the brain in comparison to the lung (Figure 3.3d). To better visualize this and evaluate the pathology in the brain, histology staining on the brain tissue with GMS stain, which stains for fungi within the tissue, as well as with H&E, was done (Figure 3.2e-h). In the sham control mice, no fungi were found, and morphologically the tissue appeared healthy. In the IV *A. fumigatus* mice, hyphal bodies and robust inflammatory cell infiltration were observed within the tissue. Overall, we were able to successfully induce a cerebral infection with *A. fumigatus* in immunocompetent mice through IV infection with a high conidial dose. Through this, severe disease was achieved as demonstrated via weight loss and clinical scoring. Further, significant infection within the brain was observed, with some fungal infiltration into the lung as well. While this does not effectively recapitulate the human disease, we were able to demonstrate that successful cerebral infection could be achieved via IV inoculation.

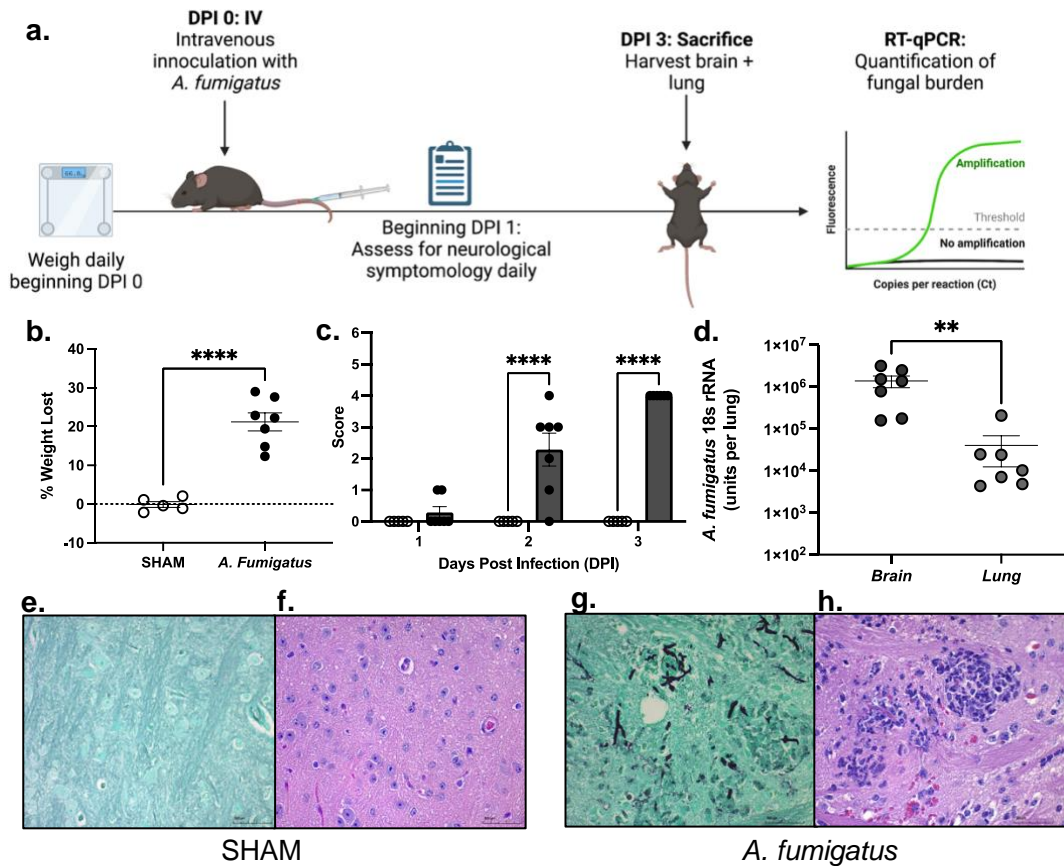


Figure 3.2. Successful induction of disseminated CA via IV inoculation.

a. WT C57Bl/6 male and female mice were IV inoculated with 7×10^6 resting *A. fumigatus* conidia. Mice were weighed daily beginning from the study initiation (DPI 0) through study completion. Following initial infection on DPI 0, mice were assessed daily for clinical signs of disease and assigned a score ranging from 0-5. Mice were sacrificed, and tissue was harvested for RT-qPCR at DPI 3. Image created with BioRender.com. **b.** Percent total weight loss was determined by comparing weight at the study start to that at study completion. **c.** Daily clinical scores for DPI 1-3. **d.** Fungal burden was assessed in RNA isolated from brains and lungs by RT-qPCR analysis of *A. fumigatus* 18s rRNA levels. **e, g.** Representative GMS-stained brain sections from **(e)** sham and **(g)** *A. fumigatus*-infected mice. **f, h.** Representative H&E-stained brain sections from **(f)** sham and **(h)** *A. fumigatus*-infected mice. **e-h.** original magnification $\times 40$. Scale bar, $100 \mu\text{m}$. The figure illustrates data from two independent studies ($n = 2-4/\text{group}$) each data point represents a single mouse, and the line in each group corresponds to the mean + SEM. For all graphs, ** and **** represent P values of 0.0089 and < 0.0001 , respectively. **b, d.** unpaired two-tailed Student's t -test, **c.** Two-Way ANOVA (mixed effects) with post-hoc Tukey's multiple comparisons test.

Development of an immunosuppression-based “two-hit” disseminated cerebral aspergillosis model.

CA was achieved in immunocompetent mice through IV infection with a high conidial dose, whereas IN inoculation resulted in IPA without any detectable cerebral involvement. Thus, we hypothesized that, in immunosuppressed mice, IN inoculation chased one day later with IV inoculation could result in pulmonary and cerebral infections. Although inoculation through both the lung and blood is artificial, our hypothesis was that this method would accurately model the disease pathophysiology commonly observed in humans with disseminated CA. For this, male and female WT mice were immunosuppressed with a high dose of corticosteroids one day before infection. Weight was recorded daily beginning one day before infection. Infection for the disseminated CA model was established through a ‘two-hit’ method, where IN inoculation on DPI 0 with resting *A. fumigatus* conidia was done to establish IPA, and IV inoculation on DPI 1 with pre-swollen *A. fumigatus* conidia to establish disseminated infection (IN+IV+steroids). Control groups included an immunosuppressed control, where mice were subjected to immunosuppression with corticosteroids and IN inoculation without IV inoculation (IN+steroids). Additionally, an immunocompetent control was included, where mice were not given corticosteroids but received inoculation IN and IV (IN+IV) (Figure 3.3a). To assess the morbidity associated with the disseminated CA model, mice were monitored daily from all three groups through DPI 10. Death was recorded for mice who succumbed to the disease (a score of 5) or for mice who met the criteria that necessitated humane sacrifice (a score of 4). The disseminated CA group resulted in rapid mortality, with 50% of mice succumbing to disease by DPI 4 and 100% by DPI 5 (Figure 3.3b). In the immunocompetent control group, approximately one-third of mice succumbed by DPI 4; approximately 40% succumbed by DPI 10, and 60% survived through DPI 10. In the immunosuppressed control, about 20% of mice succumbed by DPI 7, 30% by DPI 9, and

about 70% survived through DPI 10. Disseminated CA had a significantly reduced overall survival rate in comparison to both control groups (Figure 3.3b). Thus DPI 4 was chosen as the study endpoint, and all subsequent assays were conducted on tissue collected from mice sacrificed at DPI 4.

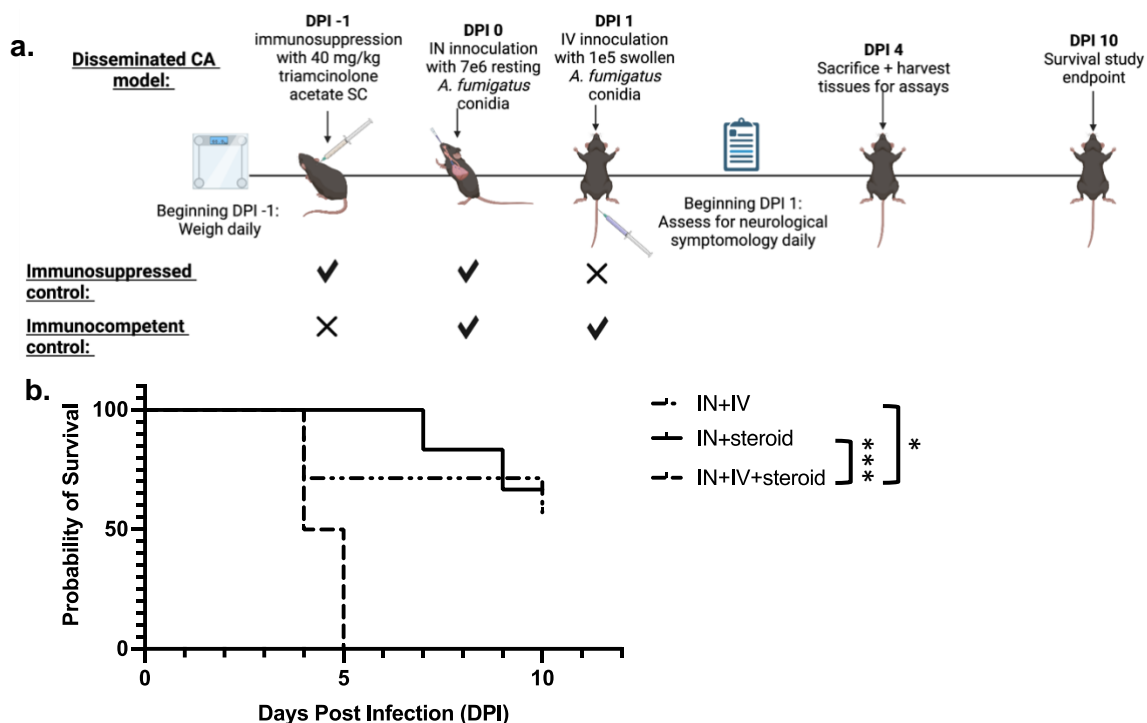


Figure 3.3. The experimental disseminated CA model results in profound mortality.

a. WT C57Bl/6 male and female mice were subjected to experimental disseminated CA with mice being immunosuppressed at DPI -1 with triamcinolone acetate SC, IN inoculated with 7×10^6 resting *A. fumigatus* conidia on DPI 0, and IV inoculated with 1×10^5 swollen *A. fumigatus* conidia via the lateral tail vein on DPI 1. Mice were weighed daily beginning from the study initiation (DPI -1) through study completion. Beginning DPI 1, mice were assessed for disease symptomology daily and assigned a score ranging from 0-5. For survival assessment, mice were monitored through DPI 10; for all assays, mice were sacrificed at DPI 4, at which point tissue was harvested. Image created with BioRender.com. **b.** Mice were infected as in **(a)** and monitored twice daily for survival through 10 DPI. The figure illustrates cumulative data from two independent studies ($n = 3-4$ mice per group per study). * $p = 0.026$ and *** $p = 0.0009$ (graph created by Kaplan–Meier estimator and the groups analyzed by the Mantel–Cox log-rank test).

Disease severity in an immunosuppression-based “two-hit” disseminated cerebral aspergillosis model

As the IN+IV+steroid group had a significantly reduced overall survival rate early and overall, compared to both control groups, day 4 post-infection was chosen for additional analyses. At the study initiation (DPI -1), weight was recorded daily. Beginning one day after IN challenge, mice were assessed through a clinical scoring system through day 4. Death was recorded for mice who succumbed to the disease (a score of 5) or for mice who met the criteria that necessitated humane sacrifice (a score of 4). Overall, mice subjected to immunosuppression (IN+IV+steroid and IN+steroid) had significantly more weight loss than immunocompetent mice (IN+IV) (Figure 3.4a). In line with mortality, mice in the IN+IV+steroid group lost a significantly greater percentage of total body weight than the other groups (Figure 3.4a). Both groups immunosuppressed with corticosteroids lost a significant amount of weight by study completion in comparison to the immunocompetent control. However, IN+IV+steroid lost a significantly greater portion of weight than IN+steroid. Likewise, disease severity was also significantly worse in the IN+IV+steroid compared to the other groups by study completion (Figure 3.4b). Further, in comparison to IN+IV mice, IN+IV+steroid mice had significantly higher clinical scores throughout the study, beginning one day following IV infection (DPI 2). Thus, the “two-hit” disseminated CA model results in substantial weight loss and severe clinical signs in comparison to mice with IPA alone (IN+steroid) and immunocompetent mice (IN+IV). Altogether, this suggests that the “two-hit” IN+IV+steroid model results in severe disease.

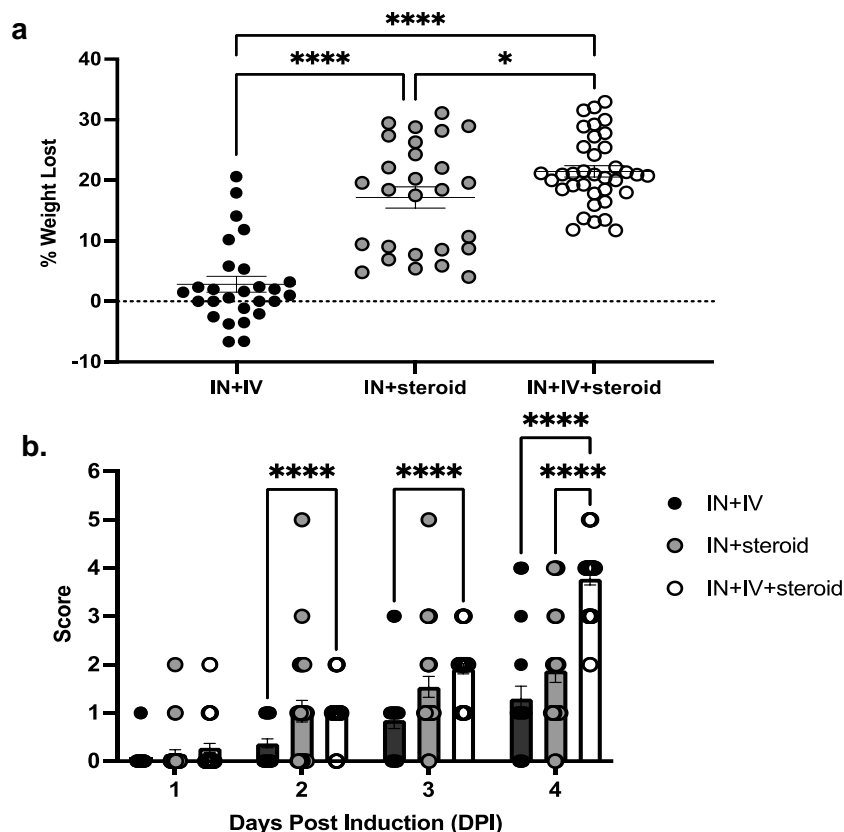


Figure 3.4. Disease severity in an immunosuppression-based “two-hit” disseminated cerebral aspergillosis model.

a, b. C57Bl/6 mice were randomly assigned to the experimental disseminated CA, immunocompetent control, or immunosuppressed control group and subjected to immunosuppression and inoculation with *A. fumigatus* as in Figure 3.3a. Mice were monitored for weight and symptomology daily. **a.** Total percent weight loss was calculated by comparing the mouse weight at the study endpoint (DPI 4) with the weight at the study initiation (DPI -1). **b.** Beginning DPI 1, mice were assessed for disease severity and assigned a score between 0-5 correlating to the symptomology. The Figures illustrate cumulative data from eight independent studies. For all graphs, * and **** represent *P* values of <0.05 and <0.0001, respectively; *n* = 3-4 mice/group for each study; each data point/dot represents a single mouse and the line in each group corresponds to the mean + SEM. **a.** unpaired two-tailed Student’s *t*-test, **b.** Two-Way ANOVA (mixed effects) with post-hoc Tukey’s multiple comparisons test.

The fungal burden is greater in the lungs and brain of disseminated CA model mice

Human IPA and subsequent disseminated CA are associated with fungal infiltration and germination at the sites of infection. To quantify the fungal burden in the lung and brain associated with our novel model of disseminated CA, RT-qPCR was employed. The disseminated CA model mice had significantly higher fungal burden in both the lung and the brain than immunocompetent control mice (Figure 3.5a, b). Compared to immunosuppressed control mice singularly infected by IN, disseminated CA model mice had more significant fungal burden in the brain but not the lung (Figure 3.5a, b). In the brain, 100% of disseminated CA model mice had fungal burden, while one-third of immunocompetent control mice and zero immunosuppressed control mice had fungal burden. Taken together, this data suggests that not only does corticosteroid-induced immunosuppression contribute significantly to the severity of the pulmonary infection but also to the severity of CA. Further, this data demonstrates the need for immunosuppression and introduction of *A. fumigatus* into the blood to achieve a pre-clinical model with consistent disseminated cerebral infection in combination with pulmonary infection as is seen in the human population.

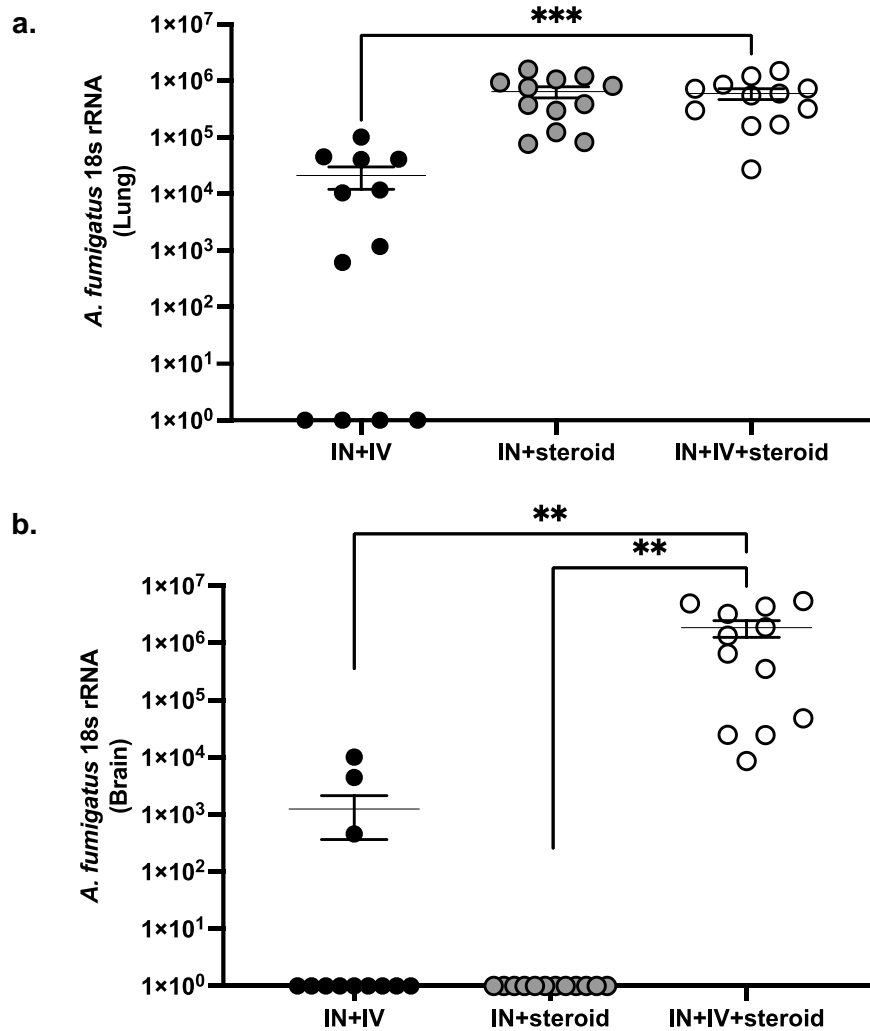


Figure 3.5 The disseminated CA model results in significant fungal infection in the lung and brain.

a, b. C57Bl/6 mice were randomly assigned to the experimental disseminated CA, immunocompetent control, or immunosuppressed control group and subjected to immunosuppression and inoculation with *A. fumigatus* as in Figure 3.3a. At DPI 4, half of the brain was collected and subsequently homogenized, from which RNA was isolated. **a.** Lung and **b.** brain fungal burden at DPI 4 was assessed by RT-qPCR analysis of *A. fumigatus* 18S rRNA levels. The Figures illustrate cumulative data from two independent studies. For all graphs, ** represents a P value of <0.01; n = 3-4 mice/group for each study; each data point represents a single mouse, and the line in each group corresponds to the mean + SEM. Unpaired two-tailed Student's t-test.

Severe pathology in the brain of disseminated CA model mice

In the brains of CA patients, common features observed during histological analysis include necrosis, hemorrhage, inflammation, cellular infiltrates, and fungal organisms [237, 238]. To assess if our model of disseminated CA resulted in similar pathological features, we employed staining of brain tissue by GMS and H&E (Figure 3.6). Demonstrated are representative images. However, from the sagittal sections of the brain stained and analyzed by microscopy, we saw no remarkable features in any of the immunocompetent and immunosuppressed controls (Figure 3.6a, b). Whereas fungal organisms and pathological features were observed in the brains of disseminated CA model mice (Figure 3.6c). Specifically, fungal hyphae, necrosis, cellular infiltrates, and hemorrhage were observed (Figure 3.6d). The presence of these pathological features further suggests that the disseminated CA model successfully recapitulates key aspects of the human disease.

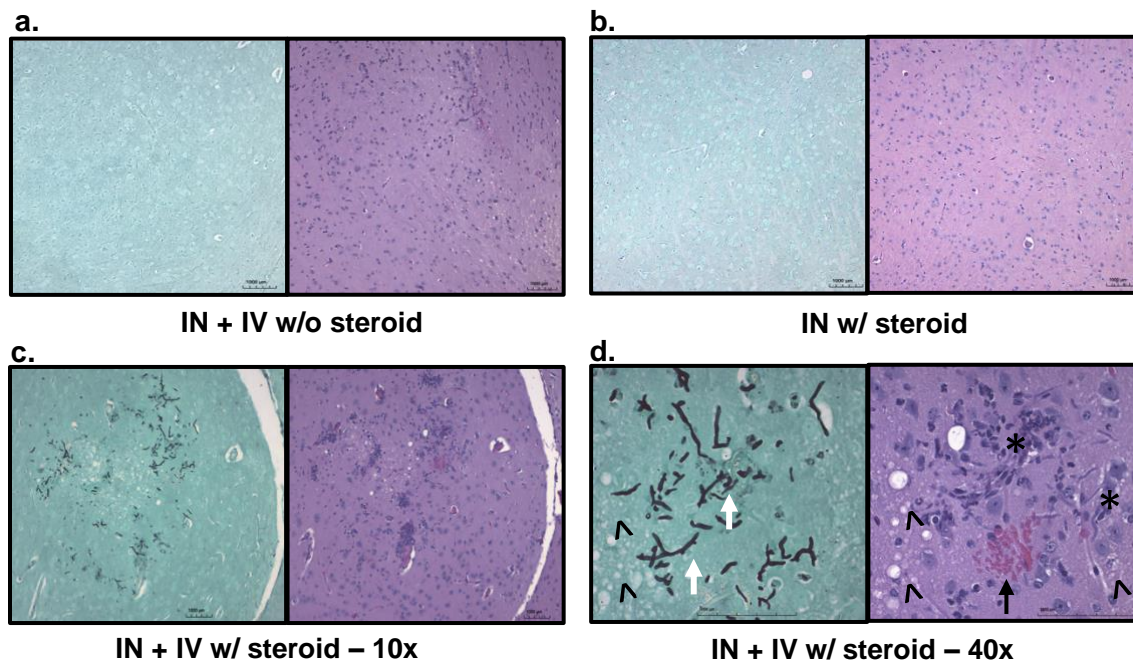


Figure 3.6. The disseminated CA model results in distinct pathological in the brain.

a – d. C57Bl/6 mice were randomly assigned to the experimental disseminated CA, immunocompetent control, or immunosuppressed control group and subjected to immunosuppression and inoculation with *A. fumigatus* as in Figure 3.3a. At DPI 4, one hemisphere was collected, fixed with 10% neutral buffered formalin, following which the tissue was paraffin-embedded and sectioned along the sagittal plane, and stained for histological analysis. **a – c (left).** Representative GMS-stained brain sections from: **a.** immunocompetent control, **b.** immunosuppressed control, and **c.** experimental CA mice. Original magnification x10. Scale bar, 1000 μ m. **a – c (right).** Representative H&E-stained brain sections from: **a.** immunocompetent control, **b.** immunosuppressed control, and **c.** experimental CA mice. Original magnification x10. Scale bar, 1000 μ m. **d.** Representative GMS (**left**) and H&E (**right**) images from the same slide represented in **c.** Original magnification x40. Scale bar, 1000 μ m. White arrows indicate representative fungal hyphae, ^ represents areas of necrosis, * indicates cellular infiltrated, and black arrows represent hemorrhage.

The primary pulmonary infection decreases dissemination and prevents rapid mortality in CA model mice

Lastly, in developing the disseminated CA model, we sought to define the role of the primary pulmonary infection in this model. For this, corticosteroid-induced immunosuppressed mice were either infected IN+IV as described above or infected IV only (Figure 3.7a). At the study initiation, weight was recorded daily. Beginning one day after IN challenge, i.e. on the day of the IV challenge, disease severity was assessed daily through clinical scoring. Death was recorded for mice who succumbed to the disease (a score of 5), or for mice who met the criteria that necessitated humane sacrifice (a score of 4). Overall, mice subjected to IN and IV challenge (IN+IV+steroid) lost significantly more weight than mice challenged IV only (IV+steroid) (Figure 3.7b). However, disease severity was significantly greater in the IV+steroid in comparison to the IN+IV+steroid group by study completion (Figure 3.7c). In fact, despite the shorter overall exposure to *A. fumigatus*, 80% of IV+steroid mice succumbed to infection by study completion. In contrast, no IN+IV+steroid mice died, although most mice exhibited signs of severe disease (i.e., a score of 4). Further, while tissue could only be collected from 20% of IV+steroid mice due to rapid mortality, compared to IN+IV+steroid mice, IV+steroid mice had significantly higher fungal burden in the brain (Figure 3.7e). Whereas IN+IV+steroid mice had elevated, though not significant, fungal burden in the lung compared to IV+steroid mice (Figure 3.7d). Limitations of this study include the rapid mortality of IV+steroid mice and the inability to harvest tissue. However, taken together, this data suggests that not only does the IN+IV+steroid disseminated CA model successfully recapitulate the pathophysiology observed in the human disease, but the initial pulmonary infection likely elicits an immune response that mitigates the cerebral infection. Thus, the “two-hit” IN+IV+steroid model results in severe disease but not rapid mortality, providing an opportunity to manipulate the model and further investigate this disease.

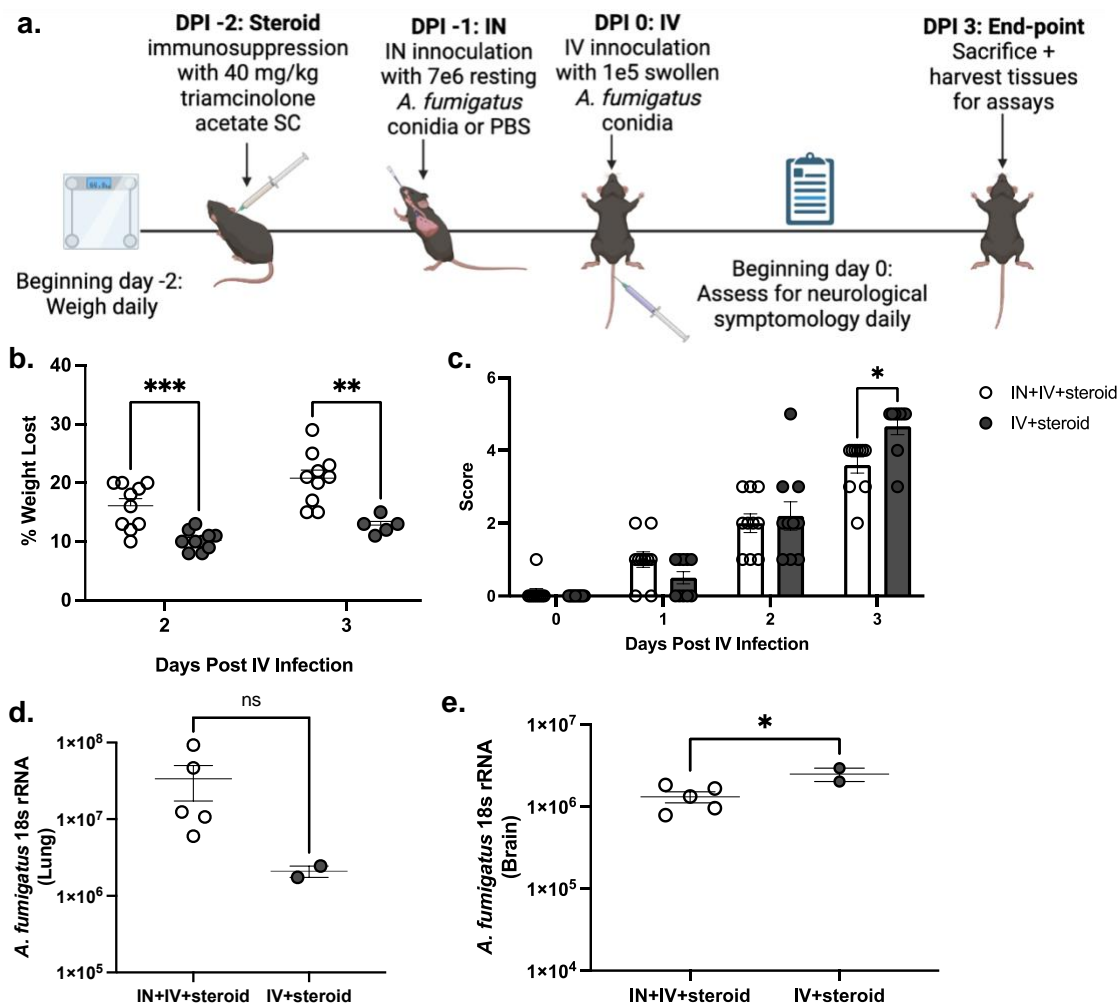


Figure 3.7. The primary pulmonary infection decreases dissemination and prevents rapid mortality in CA model mice.

a. WT C57Bl/6 male and female mice were immunosuppressed with triamcinolone acetate SC, one day after immunosuppression IN inoculated with 7e6 resting *A. fumigatus* conidia or sham inoculated with PBS IN, and IV inoculated with 1e5 swollen *A. fumigatus* conidia via the lateral tail vein. Mice were weighed daily beginning from the study initiation through study completion. Mice were additionally assessed for disease severity through daily clinical scoring (scores ranging from 0-5). Image created with BioRender.com. **b.** Total percent weight loss was calculated by comparing the mouse weight at the study endpoint (DPI 3) with the weight at the study initiation (DPI -2). **c.** Beginning DPI 0, mice were assessed for disease severity and assigned a score between 0-5 correlating to the symptomology. (Figure description continued on next page.)

Figure 3.7. The primary pulmonary infection decreases dissemination and prevents rapid mortality in CA model mice (continued).

d, e. At DPI 3, the left lung and half of the brain were collected and subsequently homogenized, from which RNA was isolated. **d.** lung and **e.** brain fungal burden at DPI 3 was assessed by RT-qPCR analysis of *A. fumigatus* 18S rRNA levels. The Figures illustrate cumulative data from two independent studies. For all graphs, *, **, and *** represent a P value of <0.05, 0.0018, and 0.0003, respectively; n = 5 mice/group for each study; each data point represents a single mouse, and the line in each group corresponds to the mean + SEM. **b, d, e.** unpaired two-tailed Student's t-test, **c.** Two-Way ANOVA (mixed effects) with post-hoc Tukey's multiple comparisons test.

3.4 Discussion

To our knowledge, this is the first pre-clinical model of disseminated CA that utilizes both the pulmonary and hematogenous components of this disease to more accurately mimic the pathogenesis observed in humans. In this study, we examined the progress and outcome of disease following multiple inoculum doses and routes of administration in corticosteroid-immunosuppressed mice. Altogether we have developed a "two-hit" model of disseminated CA that results in predictable and robust fungal infection in the brain. This model can be used in further studies for defining host response during infection, studying the effects of immunomodulation, and evaluating therapeutic strategies during cerebral infection.

IPA is a disease characterized by uncontrolled growth of the opportunistic mold *A. fumigatus* resulting in lung tissue damage and potential dissemination to other organs. On average, 20-50% of IPA infections result in disseminated disease, with ~20% reported to result in CA [145, 146]. However, this is likely a conservative estimate as the population of CA is greatly under-reported, owing partially to the fact that CA is notably difficult to diagnose, with some cases not being diagnosed until autopsy [44, 145]. Further, as the number of immunosuppressed patients continues to increase, the CA population is likely larger than reported [44, 71].

Recently, the use of corticosteroids, alone and in conjunction with therapeutics resulting in neutropenia, has been regarded as one of the most notable risk factors of IPA, given their frequent use in transplant recipients and patients with various HMs [59, 167, 239]. For example, in a post-transplant epidemiological study, corticosteroid use was a significant risk factor for IPA as 87.5% of bone marrow transplant recipients diagnosed with IPA had been treated with corticosteroids [99]. Similarly, a 20-year retrospective study of CA in patients with various underlying conditions found corticosteroids to be amongst

the top risk factors, with more than 50% of patients with CA having undergone steroid treatment prior to infection [59].

During IPA, upon reaching the alveoli, inhaled resting *A. fumigatus* conidia swell and germinate, producing hyphae, all forms of which enter the pulmonary parenchyma [42, 43]. *A. fumigatus* swollen conidia and hyphae invade the blood vessels through the endothelial cell lining by passing from the abluminal to the luminal surface, whereby swollen conidia and hyphal fragments can break off and disseminate through the bloodstream [42, 43]. In the profoundly immunosuppressed host, invasion of the pulmonary vasculature can result in widespread hematogenous dissemination to organs such as the brain, kidneys, heart, spleen, and liver [44]. Thus, for our model, we elected to employ resting conidia for the initial pulmonary infection, and pre-swollen conidia for the hematogenic infection. Further, during IPA and disseminated infection, the number of conidia and hyphae that enter the blood during dissemination is likely significantly reduced in comparison to the amount that was initially inhaled due to the relatively complicated route of dissemination. Thus, in our model, the hematogenous infection was conducted with a greatly reduced conidial dose compared to the pulmonary infection.

Previous models of CA are relatively limited in their reproduction of disease pathogenesis as seen in humans. Particularly, current models do not accurately mimic the route of infection, immune status, and/or state of conidia during the fungal challenge. One of the most frequently used models of CA, developed twenty years ago, infects mice by injecting a high dose of resting conidia directly into the brain of outbred neutropenic mice [60]. While this model has been previously used to assess the therapeutic efficacy of anti-fungal drugs *in vivo*, this method of infection is highly improbable in human patients. It thus lacks physiological relevance [240-242]. This inoculation method has also been conducted in immunocompetent subjects [243]. Though this model provides a space to understand the disease mechanism without any predisposing factors, the data garnered has little

relevance to human disease. The other frequently utilized route of inoculation is IV. While this route results in rapid fungal dissemination throughout the bloodstream, it is most frequently done in immunocompetent mice with high doses of resting conidia [61]. Thus, IV alone does not accurately recapitulate disseminated infections that are most typically preceded by a primary pulmonary infection. For this reason, in an effort to make a model as physiologically accurate as possible, we developed the “two-hit” method of infection in corticosteroid immunosuppressed mice to have both the primary pulmonary infection and secondary hematologic infection with resting and swollen conidia, respectively, as occurs in humans.

Another limitation within the field has been the method by which fungal load is measured in tissue following *in vivo* studies. Several methods that are regularly utilized for evaluating the fungal burden within a tissue of interest include qPCR on total isolated DNA, quantification of colony forming units (CFU) and/or histology, and galactomannan detection [244, 245]. However, these methods of quantifying fungal burden are highly variable, lack sensitivity, and are often not reflective of the level of live fungal bodies within the tissue. Particularly, quantification from CFU and histology are highly susceptible to subjectivity as (i) *A. fumigatus* has been demonstrated to colonize readily thus, the enumeration of individual spores is near impossible, and (ii) histology is representative of one small section of the tissue of interest, and thus quantification cannot be accurately applied to the tissue as a whole [246, 247]. Detection of galactomannan, secreted by *A. fumigatus* and frequently used as a diagnostic marker in the clinical setting, through enzyme-linked immunoassay is considered a strong tool for detecting *A. fumigatus* infection; however, given that galactomannan is secreted the application of this method is significantly limited [248, 249]. Whereas for DNA, which can be extracted from organisms no longer alive, the use of DNA for qPCR results in the quantification of total *A. fumigatus*, even though it is entirely possible that a considerable fraction is no longer viable and thus

no longer pathogenic [236]. Here, we report quantifying fungal burden within brain (and lung) tissue from purified RNA. We are, to our knowledge, the first to describe utilizing RT-qPCR to quantify *A. fumigatus* RNA from brain tissue. By utilizing this method, we were able to quantify the level of live *A. fumigatus* in the brain with great specificity and sensitivity.

Acknowledging the predisposing quality of corticosteroids for IPA and CA, the limitations of current animal models, and the fact that entry of *A. fumigatus* resting conidia into the bloodstream is highly improbable, we developed a “two-hit” model of infection incorporating (i) a relevant immunosuppression strategy known to be associated with CA development in humans (corticosteroid therapy) (ii) a lung component (intranasal inoculation of *A. fumigatus* resting conidia) and (iii) a dissemination component (intravenous inoculation of *A. fumigatus* swollen conidia into the bloodstream). Although we recognize that employing intravenous inoculation is suboptimal, we felt that combining the above strategy had the best chance to mimic the pathogenesis of human disease and produce a predictable infection within the brain more effectively. Through this immunosuppression-based “two-hit” disseminated CA model (IN+IV+steroid), successful primary IPA and secondary disseminated CA was achieved, allowing for the characterization of pathogenicity and the neuroimmune response. In addition to severe weight loss and neurologic symptomology, we observed fungal burden in the brain of 100% of the mice and pathology consistent with that observed in the brain of humans with CA [237, 238]. Moreover, mortality in the immunosuppression-based “two-hit” disseminated CA model was high, mimicking that observed in humans with CA [2, 49, 160].

3.5 Limitations

One of the most notable limitations associated with these studies is the artificial introduction of *A. fumigatus* into the bloodstream. Natural introduction of fungus into the blood most often occurs following pulmonary infection. Direct intravenous introduction from an IV or catheter, for example, is exceedingly rare. Thus, by the nature of the “two-hit” model, directly introducing a low-dose of pre-swollen *A. fumigatus* conidia through IV inoculation limits the physiological relevance, despite the fungus consistently and effectively entering the brain. Another limitation is the ability of the fungus to enter the brain in absence of the primary pulmonary infection. While, based on our findings, we consider the primary pulmonary infection to play a seemingly protective role, the exact impact of the pulmonary infection is currently unknown. However, this presents a promising avenue for discovering host defense mechanisms that occur despite severe immunosuppression with corticosteroids that may be able to be leveraged as therapeutic targets or biomarkers for early intervention.

3.6 Conclusions

We have developed a human-relevant, novel model of disseminated CA by utilizing corticosteroid-induced immunosuppression and a “two-hit” inoculation method with *A. fumigatus*. With this model, we achieved severe neurological symptomology, 100% mortality, and significant fungal burden in both the lung and the brain in 100% of the mice. Further, we found corticosteroid-induced immunosuppression significantly blunted infiltration of specific immune cells as well as inflammatory cytokine and chemokine responses in the brain during CA. Finally, we demonstrate that corticosteroid-induced immunosuppression is superior at inducing disseminated CA to chemotherapy-induced immunosuppressed and neutropenia-induced immunosuppression. In conclusion, this model of disseminated CA following IPA in an immunosuppressed host provides a novel platform for studying the efficacy of antifungal drugs and immunotherapies for improving disease outcomes.

CHAPTER 4

NEUROIMMUNE RESPONSE IS SIGNIFICANTLY IMPACTED BY CORTICOSTEROID IMMUNOSUPPRESSION IN AN EXPERIMENTAL MODEL OF CEREBRAL ASPERGILLOSIS

4.1 Introduction

In the lung, following the inhalation of *A. fumigatus* spores (conidia), the early immune response is mediated by immune effector cells such as neutrophils, circulating macrophages, and DCs, amongst others. These professional phagocytotic cells are primarily recruited to the lung via inflammatory cytokines and chemokines expressed by alveolar macrophages, the prototypic first line of immune defense in the lung, following the recognition of *A. fumigatus* [15, 31]. As the infection progresses, *A. fumigatus* interacts with the innate immune system through pattern recognition receptors (PRRs), such as dectin-1, which recognize pathogen-associated molecular patterns (PAMPs), such as β -1,3-glucan, expressed on the surface of germinating conidia [250, 251]. Different cells of the innate immune system uniquely express and interact with PRRs and PAMPs, respectively, eliciting important responses for the initiation of anti-*A. fumigatus* host defense [234, 252].

Cytokines and chemokines expressed by the various cells of the innate immune response against *A. fumigatus* coordinate to induce adaptive immune cells such as T-cells and B-cells. Successful clearance of *A. fumigatus* from the lung relies on a balance between adaptive immune cells to produce cytokines and chemokines to enhance phagocytotic activity and provide protective immunity. Important are CD4⁺ T-cells, including Th1-, Th2-, and Th17-type, whose differential responses are mediated by

cytokines produced by innate immune cells following exposure to *A. fumigatus* conidia or hyphae [36]. Particularly, an imbalance of Th1/Th2 that favors Th2 has been found to contribute to the exacerbation of disease [253-255]. As the host defense against *A. fumigatus*

relies on a concerted coordinated response between immune cells, any alteration to immune cell function is likely to be detrimental.

While both host and fungal properties influence the virulence of *A. fumigatus*, it is the host immune response that is most implicated in the development of invasive aspergillosis. Indeed, immunosuppression from agents such as chemotherapy and corticosteroids are heavily associated with the development of IPA and subsequent secondary infections, including CA [94, 239]. The immune response involved in the clearance of *A. fumigatus* from tissue in the immunosuppressed host has generally been understudied however, several articles have found immunosuppressive agents to both quantitatively and qualitatively impact the immune response to *A. fumigatus* [108, 110, 112]. The interaction between the inhaled conidia and immune effector cells is critical during IPA. As such, the role of inflammatory and immune responses is imperative for disease resolution. Despite widespread clinical prevalence, the immune and inflammatory response involved in the clearance of *A. fumigatus* from tissue in the immunosuppressed host remains poorly understood, particularly for infection in the brain.

As *A. fumigatus* poses a significant threat to an ever-growing immunocompromised population, many efforts have been made to improve prevention and treatment. However, these efforts have been primarily focused on the development of novel antifungal drugs [256, 257]. While antifungal drugs are extremely beneficial for preventing and treating *A. fumigatus*-related diseases, these (i) have poor penetration into the brain for those with CA, (ii) are not effective in all populations, and (iii) do not improve the host immune defense in immunocompromised patients. To this end, we have

employed the experimental model of disseminated CA to generate an in-depth understanding of the immune and inflammatory responses against *A. fumigatus* lung within the brain in corticosteroid-induced immunocompromised mice. It is hoped that identifying immune and inflammatory responses within the brain will enhance the understanding of protective antifungal responses. Providing information that can be used to develop novel approaches to boost host resistance.

4.2 Methods

Animals

Male and female, age-matched C57BL/6 mice, 6–10 weeks of age, were obtained from The Jackson Laboratory (Bangor, ME). All animals were housed in a specific pathogen-free, Association for Assessment and Accreditation of Laboratory Animal Care–certified facility and handled according to Public Health Service Office of Laboratory Animal Welfare policies after review by the Tulane Institutional Animal Care and Use Committee (IACUC). All animal research was conducted under approved Tulane IACUC Protocol #1589. Mice were sacrificed following anesthesia with ketamine/xylazine (100/10 mg kg⁻¹ IP; MWI Veterinary Supply, Boise, ID). No animals were excluded from the analyses unless the animal died prematurely. ‘*n*’ reported in the manuscript represents the number of animals in each group that were euthanized as scheduled at the end of the study unless otherwise stated.

Preparation of *A. fumigatus*

A. fumigatus isolate 13073 (American Type Culture Collection, Manassas, VA) was maintained on potato dextrose agar for 5–7 d at 37°C. Conidia were harvested by washing the culture flask with 50 ml of sterile PBS (Thermo Fisher Scientific, Waltham, MA) supplemented with 0.1% Tween-20 (Bio-Rad, Hercules, CA). The conidia were then passed through a sterile 40-mm nylon membrane to remove hyphal fragments and conidial clusters and enumerated on a hemacytometer.

Immunosuppression

For the corticosteroid-induced immunosuppression model, mice were given Kenalog-40™ or sterile PBS as immunocompetent control [230, 231]. Briefly, SC injections at 40 mg/kg Kenalog-40™ (triamcinolone acetonide; Bristol-Myer Squibb, Princeton, NJ)

of body weight in sterile PBS for a final volume of 100 μ l 24h before fungal inoculation [232]. Immunocompetent mice were injected SC with 100ul of sterile PBS 24h prior to fungal inoculation.

Infection

For pulmonary infection, mice were lightly anesthetized with isoflurane and administered 7×10^6 *A. fumigatus* conidia in a volume of 30 μ l IN 1-day post immunosuppression as previously described [233]. Briefly, mice are held in a horizontal, supine, position, and a pipette is used to deliver the 30 ml inoculum dropwise to the nares, where normal breathing results in fluid aspiration into the lungs. For disseminated infection, 1-day post IN inoculation, mice were administered 100 μ l 1×10^5 *A. fumigatus* conidia pre-swollen for 5h at 37°C IV [234]. IN only control mice were administered 100ul of sterile PBS incubated at 37°C IV 1-day post IN inoculation.

Flow cytometry

Following euthanasia at DPI 4, whole brains were extracted, mononuclear cells were dissociated from CNS tissue, separated on a density gradient, blocked for nonspecific antibody binding, and stained as previously described, with minor modification [258]. Briefly, brain tissues from individual animals were minced gently in RPMI 1640 medium (Thermo Fisher Scientific) with scissors and incubated with collagenase D (1 mg/ml; Roche) and DNase I (50 μ g/ml; Roche) for 30 min in a shaking incubator at 37°C. Digested tissues were passed through a 100 μ m cell strainer (Corning, Corning, NY) to remove cell debris and obtain single-cell suspensions. Cells were spun down at 256 x g for 5 min at 4°C. The resultant cell pellets from brain tissues were resuspended in ice-cold 90% Percoll PLUS solution (Cytiva, Marlborough, MA) and overlaid with 60% Percoll

PLUS solution followed by 40% Percoll PLUS solution and subsequently 1x HBSS (Thermo Fisher Scientific) gently. All Percoll solutions were diluted in 1x HBSS. Cells were isolated by centrifugation at 514 x g for 20 min at RT with the brake disengaged. The cell fraction (containing mononuclear cells) located between the 60% and 40% interphase was carefully aspirated. Cell suspensions were washed with 1x HBSS and were centrifuged at 348 x g for 10 min at 4°C. Resultant cell pellets were resuspended in 500 µl FACS buffer (PBS + 2% BSA + 1mM EDTA + 0.09% Sodium Azide).

Cells were washed, and Fc receptors were blocked with Mouse TruStain FcX™ (CD16/32; BioLegend, San Diego, CA), following which cells were stained with a single-color LIVE/DEAD Aqua Fixable Dead Cell Stain (Invitrogen), then labeled with specific immune cell surface or intracellular markers. The following staining parameters were employed: Microglia: CD45^{int}CD11b⁺TMEM119⁺, M1 microglia: CD45^{int}CD11b⁺TMEM119⁺CD86⁺CD206⁻, M2 microglia: CD45^{int}CD11b⁺TMEM119⁺CD86⁻CD206⁺, Astrocytes: CD45⁻CD11b⁻ASCA-2⁺A2B5⁺, Reactive astrocytes: CD45⁻CD11b⁻ASCA-2⁺A2B5⁺GFAP⁺, Macrophages: CD45^{hi}CD11b⁺TMEM119⁻, Eosinophils: CD45⁺CD11b⁺SiglecF⁺, Neutrophils: CD45⁺CD11b⁺Ly6G⁺, Monocytes: CD45⁺CD11b⁺CD11c⁻Ly6C⁺, Dendritic cells (DCs): CD45⁺CD11c⁺Ly6C⁺MHCII⁺, CD4⁺T-Cells: CD45⁺CD3⁺CD4⁺, CD8⁺T-Cells CD45⁺CD3⁺CD8⁺, iNKTs: CD45⁺CD3⁺CD1d⁺, γδT-Cells: CD45⁺CD3⁺TCRgd⁺, NKs: CD45⁺CD3⁻NK1.1⁺. Specific antibodies used are detailed in Table B1, and representative gating strategies are included in Figures B1-3. Samples were acquired using a 4-laser, 20-parameter analytic BDLSRFortessa, and data were analyzed using FlowJo software (Tree Star, Inc., Ashland, OR). Unstained brain leukocytes served as a control for background fluorescence and gating. Appropriately stained UltraComp eBeads (Thermo Fisher Scientific) served as single-color controls unless otherwise indicated.

Inflammatory cytokine analysis

Following euthanasia at DPI 4, the right hemisphere of the brain was flash-frozen and stored at -80°C until processing. The flash-frozen brain tissue was homogenized as previously described, with minor modifications [259]. Briefly, brain tissue was homogenized in a buffer containing 20 mmol/L Tris-HCl (pH 7.5; Fisher Scientific, Hampton, NH), 150 mmol/L NaCl (Fisher Scientific), 0.05% Tween-20, and a cocktail of protease inhibitors (Roche, Basel, Switzerland), and freshly added 1 mmol/L PMSF (Roche). The homogenate was sonicated for 30 seconds and clarified by centrifugation (12,000g for 10min at 4°C). Clarified brain homogenate supernatants were analyzed for the protein levels of 32 inflammatory cytokines and chemokines using the Luminex based Milliplex multiplex suspension cytokine array (MilliporeSigma, Burlington, MA), according to the manufacturer's instructions. Specific cytokines and chemokines evaluated are detailed in Table B2. The data were analyzed using Bio-Plex Manager software (Bio-Rad).

VEGF treatment

Mice were treated with either 200 ng recombinant mouse vascular endothelial growth factor 164 (rm-VEGF₁₆₄) or vehicle control (sterile PBS with 0.01% BSA) (R&D Systems, Minneapolis, MN). rm-VEGF₁₆₄ or vehicle were administered SC daily beginning on DPI 0 until study completion. Dosing and route of administration were selected based on prior studies demonstrating safety, efficacy, and clearance rate [260, 261].

Statistics

Data were analyzed using GraphPad Prism, version 9.0, statistical software (GraphPad Software, San Diego, CA). Comparisons between groups for normally distributed data were made with the Student's t-test or two-way analysis of variance (ANOVA). Significance was accepted at a p value < 0.05 .

4.3 Results

Immune cell infiltration into the brain in an immunosuppression-based “two-hit” disseminated cerebral aspergillosis model

Cells of the myeloid and lymphoid lineage are vital for the immune response to *A. fumigatus* in the lung. However, their response within the brain has not been characterized [77, 262]. Immune cell suppression by corticosteroids is well-documented as a contributor to the development of severe disease during IPA [15, 17, 98, 116]. Utilizing the model described previously (Figure 1.1a), mice in the disseminated CA model (IN+IV+steroid), compared to immunocompetent control mice (IN+IV), had significantly lower numbers of inflammatory monocytes (Figure 4.1a), eosinophils (Figure 4.1b), and DCs (Figure 4.1c) in the brain. However, in comparison to immunosuppressed control mice (IN+steroid), the number of monocytes, eosinophils, macrophages (Figure 4.1d), and neutrophils (Figure 4.1e) was significantly elevated in the brain of the disseminated CA model mice, presumably because of the higher fungal burden in these mice. Interestingly, no differences in the number of neutrophils and macrophages in the brain of IN+IV+steroid mice compared to IN+IV mice were observed. Comparatively, most lymphoid lineage cells were affected by corticosteroid immunosuppression. The number of CD4 (Figure 4.1f), CD8 (Figure 4.1g), iNKT (Figure 4.1h), $\gamma\delta$ T cells (Figure 4.1i), and NK cells (Figure 4.1j) were all lower in the brain of the IN+IV+steroid group compared to the IN+IV group. No differences in lymphoid cell number were observed between immunosuppressed groups IN+IV+steroid and IN+steroid (Figures 4.1f-i), further indicating the impact of corticosteroid immunosuppression on lymphoid cell response. The number and activation state of primary resident immune mediators in the brain, microglia, and astrocyte subsets, was unchanged in immunocompetent vs. immunosuppressed control mice (Figure B4a-f). Thus, despite germinating organisms in the brain, immune cell infiltration into the CNS was dramatically impaired due to corticosteroid-induced immunosuppression.

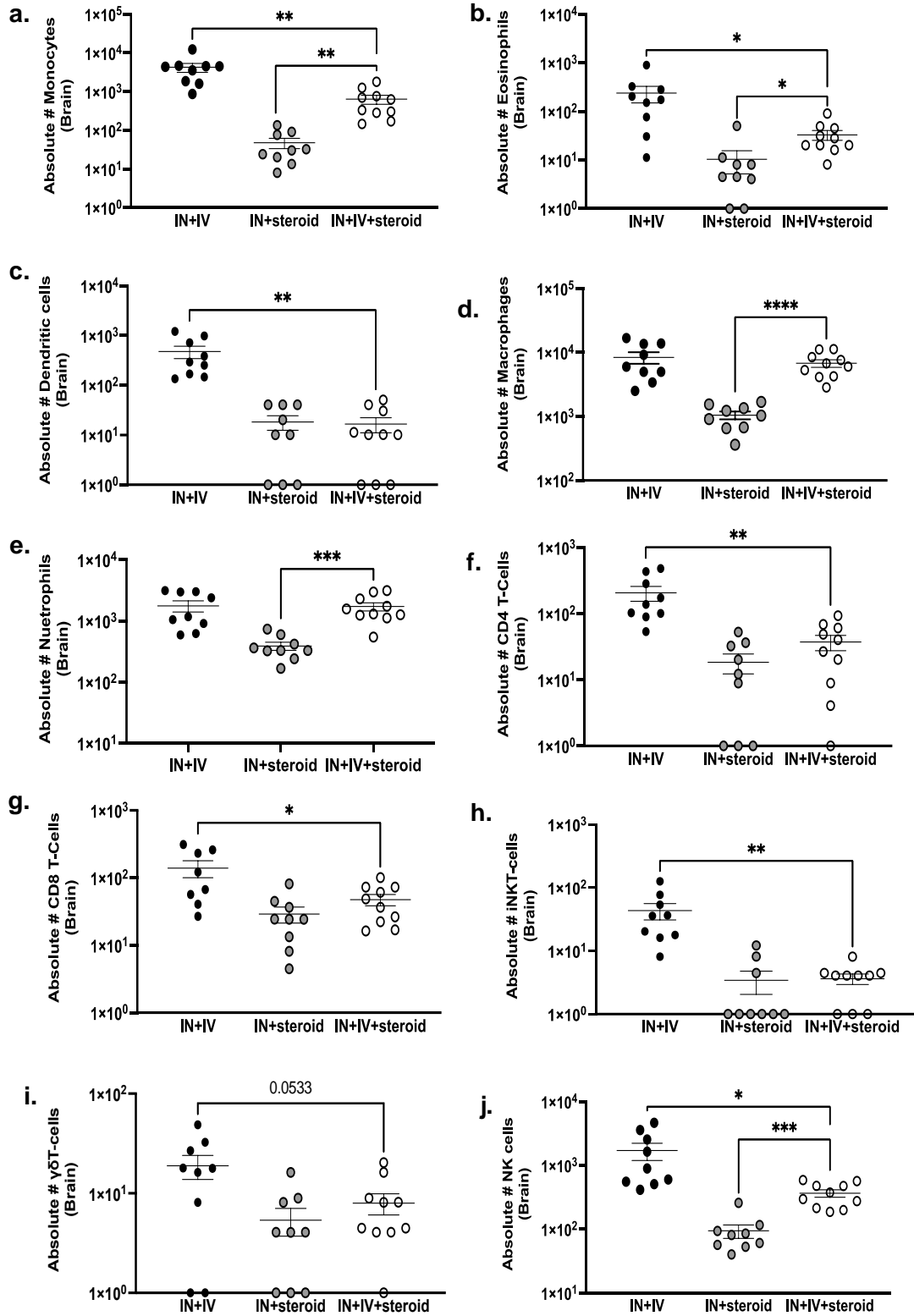


Figure 4.1 The disseminated CA model results in a significant impact to the immune cell infiltration into the brain. (Figure legend on next page.)

Figure 4.1 The disseminated CA model results in a significant impact to the immune cell infiltration into the brain.

a – j. C57Bl/6 mice were randomly assigned to the experimental disseminated CA, immunocompetent control, or immunosuppressed control group and subjected to immunosuppression and inoculation with *A. fumigatus* as in Figure 3.3a. At DPI 4 whole brains were collected, mononuclear cells isolated following enzymatic digestion, and quantified by flow cytometry. **a.** monocytes (CD45+CD11b+CD11c-Ly6C+), **b.** eosinophil (CD45+CD11b+Siglec F+), **c.** dendritic cells (CD45+CD11c+Ly6C+MHC II+), **d.** macrophage (CD45^{hi}CD11b+TMEM119-), **e.** neutrophils (CD45+CD11b+Ly6G+) **f.** CD4 T-cells (CD45+CD3+CD4+), **g.** CD8 T-cells (CD45+CD3+CD8+), **h.** iNKT-cells (CD45+CD3+CD1d+) **i.** $\gamma\delta$ T-cells (CD45+CD3+TCR $\gamma\delta$ +), **j.** NK cells (CD45+CD3-NK1.1+), were quantified by flow cytometry. The figure illustrates cumulative data from three independent studies (n = 3–4 mice per group per study). Each data point represents an individual sample. Line within a given group represents the mean + SEM. For all graphs, *, **, ***, and **** represent P values of <0.05, <0.01, <0.001, and <0.0001 respectively; (unpaired two-tailed Student's t-test).

Inflammatory cytokine and chemokine responses in an immunosuppression-based “two-hit” disseminated cerebral aspergillosis model

Multiple inflammatory mediators, such as interleukin (IL)-1 α , IL-1 β , IL-6, IL-17A, and tumor necrosis factor-alpha (TNF- α), are required for protection against IPA [263]. Moreover, mediators such as granulocyte-macrophage colony-stimulating factor (GM-CSF; Sargramostim/Leukine®) have been approved to shorten the time of immunosuppression and to reduce the incidence of infection associated with chemotherapy and bone marrow transplantation, whereas interferon-gamma (IFN γ ; Actimmune®) has been approved for the treatment of infectious fungal complications associated with chronic granulomatous disease [264-268]. To gain insight into inflammatory mediator pathways that may be critical for defense in the CNS, we focused on the levels of mediators in the brain that significantly differed between the IN+IV+steroid group and the IN+IV group. First, it was interesting to note that despite only 25% of the mice in the IN+IV group having detectable *A. fumigatus* in the brain, 100% of the mice had detectable levels of multiple inflammatory mediators. This analysis revealed that IL-1 β (Figure 4.2a), IL-6 (Figure 4.2b), IL-17A (Figure 4.2c), C-C Motif Chemokine Ligand (CCL) 3 (Figure 4.2d), C-X-C motif chemokine ligand (CXCL) 10 (Figure 4.2e), and vascular endothelial growth factor (VEGF) (Figure 4.2f) were decreased in the IN+IV+steroid group despite the presence of higher fungal burden. In contrast, mediators that were elevated in the IN+IV+steroid group included IL-1 α (Figure 4.2g), CXCL1 (Figure 4.2h), granulocyte-colony-stimulating factor G-CSF (Figure 4.2i), and Eotaxin (Figure 4.2j). Surprisingly, the mediators potentially used for the treatment of IPA, GM-CSF, and IFN- γ , were not different between the groups (Figures 4.2k and 4.2l).

Comparisons of chemokine and cytokine levels in immunosuppressed mice were made between the disseminated CA mice (IN+IV+steroid) and immunosuppressed controls (IN+steroid). This was done to better understand the impact of fungal presence

in the brain on inflammatory mediator levels under corticosteroid immunosuppression. When comparing IN+IV+steroid with IN+steroid IL-6, CXCL10, IL-1 α , CXCL1, G-CSF, and Eotaxin levels were found to be significantly elevated in the IN+IV+steroid group, despite all those mediators being significantly reduced in the same group when compared with immunocompetent IN+IV. This trend was also observed for IL-13 (Table B3). Interestingly, like the results when compared with IN+IV, VEGF was found to be significantly reduced in IN+IV+steroid, when compared to IN+steroid. Inflammatory mediators that are likely important for host-defense in the brain in the corticosteroid immunosuppressed host are MCP-1, MIP-2, LIF, M-CSF, and TNF- α , all of which were significantly elevated in the brain of IN+IV+steroid mice compared to IN+steroid mice, but not different from immunocompetent IN+IV mice (Table B3). Although only a portion of IN+IV mice had detectable *A. fumigatus* in the brain compared to the IN+IV+steroid group, which had 100% detectable *A. fumigatus*, the presence of comparable levels of certain cytokines and chemokines points to the importance of these during infection despite corticosteroid immunosuppression. Thus, mediators suppressed by corticosteroids vs. those enhanced by elevated fungal burden may represent important CNS host defense pathways during CA.

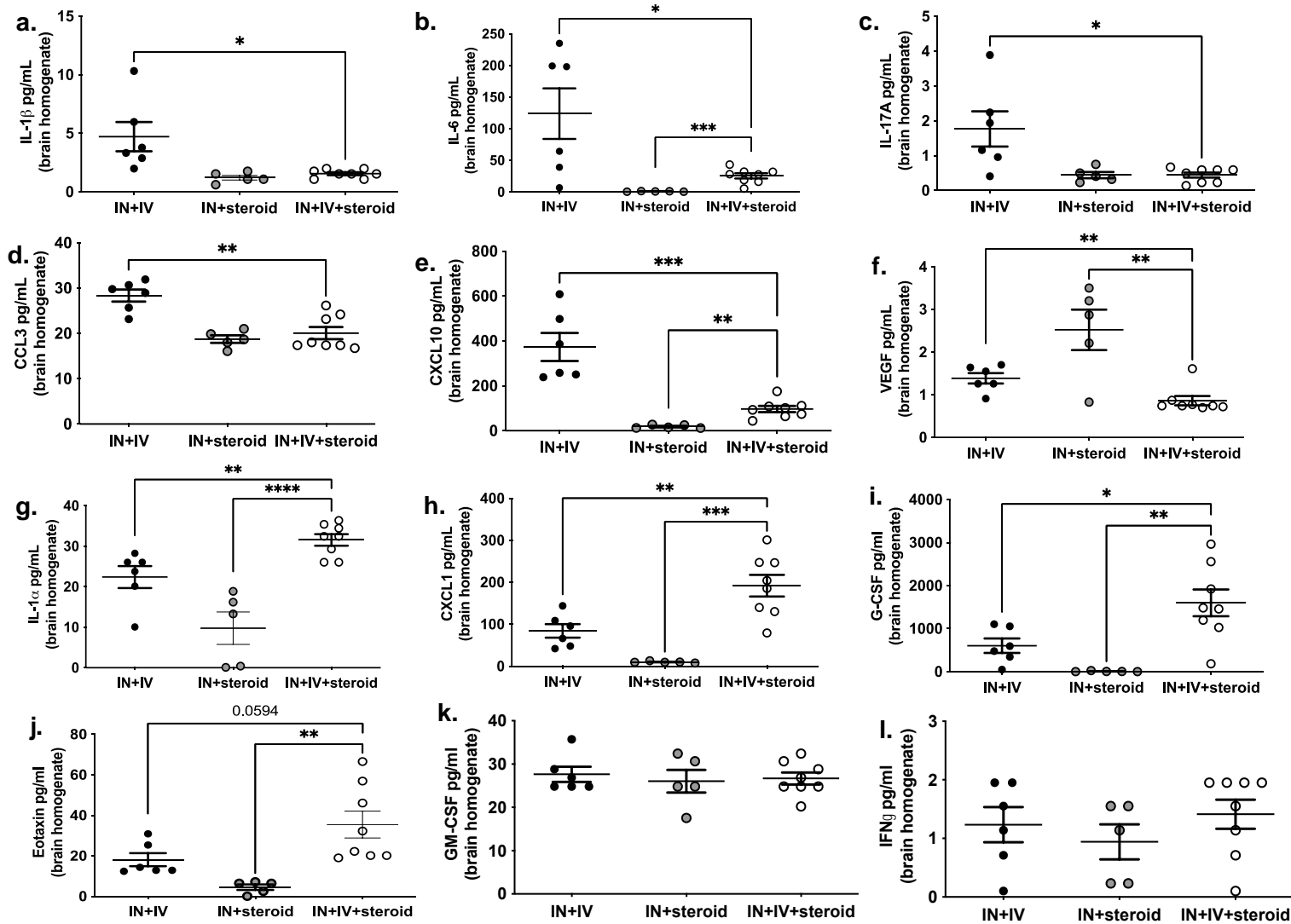


Figure 4.2 The disseminated CA model results in a significant impact to the inflammatory cytokine and chemokine population in the brain. (Figure legend on next page.)

Figure 4.2 The disseminated CA model results in a significant impact to the inflammatory cytokine and chemokine population in the brain.

a – l. C57Bl/6 mice were randomly assigned to the experimental disseminated CA, immunocompetent control, or immunosuppressed control group and subjected to immunosuppression and inoculation with *A. fumigatus* as in Figure 3.3a. At DPI 4, half of the brain was collected for cytokine and chemokine analysis, homogenized, and clarified. **a.** IL-1 β , **b.** IL-6, **c.** IL-17a, **d.** CCL3, **e.** CXCL10, **f.** VEGF, **g.** IL-1 α , **h.** CXCL1, **i.** G-CSF, **j.** Eotaxin, **k.** GM-CSF, and **l.** IFN γ levels were quantified from clarified homogenates by Luminex-based MILLIPLEX assessment. The figure illustrates cumulative data from two independent studies (n = 3–4 mice per group per study). Each data point represents an individual sample. A line within a given group represents the mean + SEM. For all graphs, *, **, and *** represent P values of <0.05, <0.01, and <0.001, respectively; (unpaired two-tailed Student's t-test).

VEGF is not therapeutic in the “two-hit” model of disseminated cerebral aspergillosis

Because VEGF was significantly reduced in IN+IV+steroid in comparison to both IN+steroid and IN+IV controls, we hypothesized that VEGF could be a therapeutic target in the “two-hit” disseminated CA model. In animal studies, VEGF administered SC was found to have the longest clearance rate; thus, we compared treatment with rm-VEGF₁₆₄ delivered via SC daily beginning on the day of IN infection to the vehicle control in the “two-hit” disseminated cerebral aspergillosis model (Figure 4.3a) [260]. Male and female WT mice were immunosuppressed with a 40mg/kg triamcinolone acetate one day before infection. On the day of primary infection, mice were inoculated IN with resting *A. fumigatus* conidia to establish IPA. On DPI 1, mice were inoculated IV with pre-swollen *A. fumigatus* conidia to establish disseminated infection. rm-VEGF₁₆₄ treatment began on DPI 0 following IN infection, and mice were treated daily through DPI 3 for a total of 4 doses. rm-VEGF₁₆₄ treated mice were compared with vehicle control mice in the “two-hit” disseminated CA model.

Weight was recorded daily beginning one-day preceding infection, and mice were monitored for clinical symptomology beginning day 1 after infection. No significant difference in weight loss was observed between VEGF and vehicle control mice (Figure 4.3b). Disease severity was not significantly different between either group, though most mice in both groups exhibited signs of severe disease on DPI 4 (Figure 4.3c). No significant differences in fungal burden in the lung (Figure 4.3d) or brain (Figure 4.3e) were detected. Thus, although a reduction of VEGF was observed in mice with significant and severe disease in the brain, treatment with rm-VEGF₁₆₄ did not reduce the signs of disease or fungal burden. Altogether, VEGF alone is not a promising therapeutic target for disseminated CA.

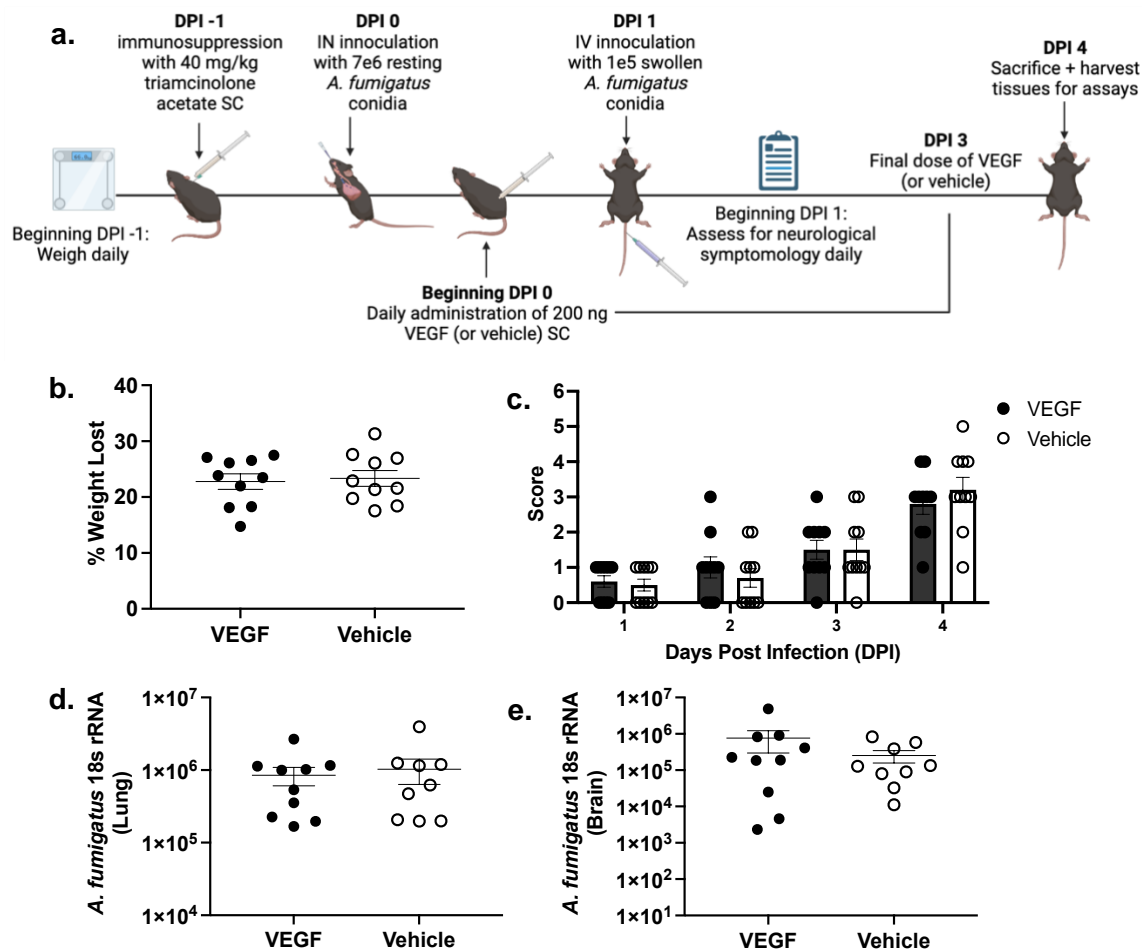


Figure 4.3. VEGF is not therapeutic in the “two-hit” model of disseminated cerebral aspergillosis.

a. WT C57Bl/6 male and female mice were subjected to experimental disseminated CA with mice being immunosuppressed at DPI -1 with triamcinolone acetate SC, IN inoculated with 7e6 resting *A. fumigatus* conidia, IV inoculated with 1e5 swollen *A. fumigatus* conidia via the lateral tail vein on DPI 1. 100ul of 200ng of rm-VEGF₁₆₄ was administered SC daily from DPI 0-3 for a total of 4 doses. rm-VEGF₁₆₄ treated mice were compared to vehicle (PBS+ 0.1% BSA) control mice given 100ul vehicle on the same dosing schedule as rm-VEGF₁₆₄. Mice were weighed daily beginning from the study initiation (DPI -1) through study completion. Beginning DPI 1, mice were assessed for disease symptomology daily and assigned a score ranging from 0-5. Mice were sacrificed at DPI 4, For fungal burden quantification. (*Figure legend continues on next page.*)

Image created with BioRender.com **b – e**. C57Bl/6 mice were randomly assigned to either rm-VEGF₁₆₄ or vehicle control, and all mice were infected on DPI 0 via the experimental disseminated CA method. **b**. Total percent weight loss was calculated by comparing the mouse weight at the study endpoint (DPI 4) with the weight before immunosuppression (DPI -1). **c**. Beginning DPI 1, mice were assessed for disease severity and assigned a score between 0-5 correlating to the symptomology. **d, e**. Lung and brain fungal burden at DPI 4 was assessed by RT-qPCR analysis of *A. fumigatus* 18S rRNA levels. The Figures illustrate cumulative data from two independent studies. n = 5 mice/group for each study; each data point represents a single mouse, and the center line in each group corresponds to the mean + SEM. **b, d, e**. unpaired two-tailed Student's t test, **c**. Two-Way ANOVA (mixed effects) with post-hoc Tukey's multiple comparisons test.

4.4 Discussion

A. fumigatus dissemination and penetration into the brain are dependent on several factors. These include fungal growth, germination, hyphal extravasation, as well as penetration of the BBB. While the inflammatory milieu induced by *A. fumigatus* promotes dissemination and BBB permeability, immunosuppression increases the likelihood [120, 143, 269]. In the corticosteroid-treated host, the widespread suppression of immune response impacts practically every cell implicated in the immune response, including barrier cells, providing an ideal environment for IPA and dissemination to the brain [108, 114, 270, 271]. As such, we previously demonstrated that with corticosteroid-based immunosuppression “two-hit” disseminated CA model (IN+IV+steroid), successful primary IPA and secondary disseminated CA were achieved. This model allowed for the characterization of pathogenicity and the neuroimmune response. For IPA, the immune response and host defense have been extensively characterized. However, until now, the same could not be said for CA.

It is well known that leukocytes such as monocytes, macrophages, neutrophils, DCs, eosinophils, NKs, and various T-cells have significant, independent, and conserved roles in response to and elimination of *A. fumigatus* in the lungs [35, 272-274]. In a murine model of IPA, the number of DCs and monocytes in the lung was significantly blunted in corticosteroid-induced immunosuppressed mice, while there was little difference for neutrophils and macrophages in comparison to immunocompetent mice [112]. Here, in the brain of immunocompetent mice (IN+IV), we observed infiltration of monocytes, eosinophils, DCs, CD4 T-cells, CD8 T-cells, iNKT-cells, $\gamma\delta$ T-cells, and NK cells, all of which were significantly lower in IN+IV+steroid mice, except for the number of $\gamma\delta$ T-cells which approached significance but did not meet our criteria for significance. Intriguingly, no difference in macrophages or neutrophils was observed between immunocompetent and immunosuppressed mice IN+IV infected mice. Given the significantly elevated fungal

burden in the brain of IN+IV+steroid mice, we can speculate that the recruitment of or activation of one or more of the above cell types is negatively affected by corticosteroids. In contrast, IN+IV+steroid mice had significant infiltration of monocytes, eosinophils, macrophages, neutrophils, and NK cells compared to IN+steroid mice without CA, suggesting that the presence of *A. fumigatus* in the brain induces infiltration of certain leukocytes, regardless of immune status, even if it is not sufficient for clearing the fungal infection.

Many cytokines and chemokines are known to play essential roles in anti-fungal immunity during IPA [77, 275, 276]. Our analysis revealed that IL-1 β , IL-6, IL-17A, CCL3, CXCL10, and VEGF were decreased in the IN+IV+steroid group despite the presence of higher fungal burden, in comparison with the immunocompetent control, IN+IV. In contrast, IL-1 α , CXCL1, G-CSF, and Eotaxin were increased in the IN+IV+steroid group. It could be argued that lower mediators in the IN+IV+steroid group are important in CNS antifungal defense. However, the decreased levels of these mediators may be a result of corticosteroid-mediated suppression. Alternatively, it could be argued that higher mediators in the IN+IV+steroid group are important in CNS antifungal defense, as these were resistant to corticosteroid-mediated suppression. However, the increased levels of these mediators may simply reflect the increased fungal burden in these mice. Nevertheless, we have made some compelling findings. Specifically, previous studies in the lung have shown that IL-1 α , which is constitutively expressed, was essential for initiating leukocyte recruitment, while IL-1 β , which is predominantly expressed under inflammatory conditions, was determined to be a critical mediator of antifungal activity against *A. fumigatus* hyphae [277]. Interestingly, in IN+IV+steroid mice, there was an imbalance between IL-1 α and IL-1 β in the brain, with IL-1 α significantly elevated and IL-1 β significantly decreased. As IL-1 β expression has been reported to be significantly impacted by corticosteroids, we can speculate here that corticosteroid

immunosuppression during CA blunts antifungal activity within the brain by inhibiting IL-1 β [278].

The pleiotropic cytokine IL-6, known to have increased cerebral expression in numerous CNS diseases, was significantly elevated in the brain of immunocompetent IN+IV control mice, despite only a fraction of these mice having detectable fungal burden in the brain [279, 280]. Whereas in contrast, IN+IV+steroid mice, with significant fungal burden in the brain, had blunted IL-6 in the brain in comparison to IN+IV mice. Suggesting that, while *A. fumigatus* infection leads to a significant upregulation in IL-6 in the brain, corticosteroids significantly inhibit this response. To further support this notion, IN+steroid mice, despite having significant pulmonary infections, had no detectable IL-6 in the brain, even though, per the response observed from IN+IV mice, cerebral production of IL-6 would be expected, despite the absence of cerebral infection. IL-6 is further thought to be a critical component in directing the transition from innate to acquired immunity [281]. As such, the significant reduction of IL-6 in corticosteroid-treated mice may directly correlate to the significant reduction of lymphoid-derived immune cells in the brain compared to immunocompetent mice.

During IPA, IL-6 is critically involved in the phagocytic activity of lung leukocytes, the absence of which results in increased fungal burden in the lungs and decreased survival [282]. Further, IL-6 is known to be a potent regulator of macrophage and DC differentiation from monocytes [283]. Production of CXCL10 by neutrophils has likewise been identified as a critical mediator of DC recruitment to the lung during IPA [274]. Here, IL-6 and CXCL10 were found to be significantly lower in the brain of IN+IV+steroid mice. As macrophage and DC recruitment into the brain during CA was blunted in IN+IV+steroid mice, this may result from the reduced production of IL-6 and CXCL10, respectively.

Mice deficient in CCL3 are more susceptible to disseminated aspergillosis, whereas neutralization of CCL3 in neutropenic mice results in decreased survival and

increase lung *A. fumigatus* burden [284, 285]. Blockade of the receptor for CXCL1, and CXCR2, results in increased mortality, higher *A. fumigatus* lung burden, and lower neutrophil recruitment to the lung during IPA [286]. Likewise, we have reported that the levels of CCL3 and CXCL1 directly correlate with levels of neutrophils in the lung during IPA [287-289]. Similar to IL-1 α and IL-1 β , there was an imbalance between CCL3 and CXCL1, with CCL3 being decreased in the IN+IV+steroid group and CXCL1 increased when compared to immunocompetent control mice (IN+IV). This may explain why neutrophils were not significantly different in IN+IV+steroid mice compared to IN+IV mice, despite the significant elevation in fungal burden in IN+IV+steroid mice. Indeed, CCL3 release from macrophages has been previously found to be downregulated following exposure to corticosteroids, whereas CXCL1 is seemingly unaffected by corticosteroid exposure [290, 291].

IL-17A is a critical cytokine for mediating both neutrophil-mediated immunity and activating the antimicrobial response of epithelial cells [292-297]. Previously, we reported that IL-17A functions as a critical antifungal cytokine during IPA, with its levels directly correlating with the level of *A. fumigatus* lung burden but not necessarily with the level of neutrophils [35, 287, 288, 298, 299]. Although IL-17A is thought to be immunopathogenic in the brain during such inflammatory diseases as experimental autoimmune encephalomyelitis, its role in CNS infections is not well-described [300]. However, acknowledging the importance of IL-17A in IPA and the observation of lower IL-17A in the brains of IN+IV+steroid mice, we cannot exclude a protective role for IL-17A during CA.

Further, we have previously found CCL3 and IL-17A expression to be Dectin-1 dependent, and impaired production or loss of these mediators significantly impairs *A. fumigatus* clearance from the lung during experimental IPA [287, 301]. Interestingly, corticosteroids have been previously found to inhibit Dectin-1 mediated activation of autophagy and antigen-presenting cells [302, 303]. Dectin-1, the β -glucan receptor, is

critical for innate immunity against *A. fumigatus* [234]. Given the i) reduced expression of the proinflammatory cytokines and chemokines, ii) reduced recruitment of critical immune cells, and iii) increased fungal burden in the presence of corticosteroids, it can be hypothesized that Dectin-1 expression within the brain is blunted by corticosteroids, contributing to a more severe disease state.

Interestingly, the only cytokine that was reduced in IN+IV+steroid mice, compared to both IN+IV and IN+steroid mice, was VEGF. This proangiogenic cytokine is significantly modulated by *A. fumigatus*, where, specifically, gliotoxins along with other secondary metabolites produced by *A. fumigatus* have anti-angiogenic effects [304]. As such, VEGF is likely suppressed in the presence of *A. fumigatus*. Thus, it is probable that the significantly reduced levels of VEGF in the brain of IN+IV+steroid result from the significant levels of fungal burden observed within the brain. Whether VEGF is protective in the brain is currently unknown. However, in a murine model of IPA in immunosuppressed mice, treatment with recombinant VEGF was found to prolong survival, although it did not reduce fungal burden [261]. Further in this model, treatment with recombinant basic fibroblast growth factor (bFGF) was found to prolong survival and reduce fungal burden in the lung. These results suggest that targeting angiogenesis may potentially be protective against the incidence of CA. Additionally, to date, several cases of IA in cancer patients treated with new anti-cancer therapeutics, bevacizumab, a VEGF inhibitor, or pazopanib, a VEGFR inhibitor, have been reported [305-307]. While the data is anecdotal in humans at this point, investigations into VEGF as a potential therapeutic for *A. fumigatus* infections should be considered to clarify its role and potentially reduce the incidence and/or severity of IPA. Thus, reducing incidence of CA.

While VEGF was elevated in the brain of mice without fungal infection, treatment with VEGF did not significantly reduce the incidence or severity of disseminated CA. VEGF, essential for early blood vessel formation and angiogenesis, has been found to

stimulate neurogenesis and act as an autocrine/paracrine neuroprotective factor in multiple models of CNS inflammation and injury *in vivo* [308-310]. VEGF has also, however, been implicated in pathology, as on its own, VEGF induces early angiogenesis but is not capable of producing mature blood vessels, so vascular leakage may occur [311, 312]. Several studies have found the coadministration of another growth factor, such as angiopoietin-1 (Ang-1), broadly involved in later-stage blood vessel formation, to result in the therapeutic vascularization [312, 313]. Thus, even though VEGF is reduced, it is possible that in our model, VEGF alone is not an adequate therapeutic, but the addition of Ang-1, for example, could improve the outcome of “two-hit” disseminated CA.

Most studies investigating host defense mechanisms related to *A. fumigatus*-mediated infections have done so in immunocompetent subjects. While this has provided immense and invaluable evidence for advancing diagnostic and therapeutic targets, the understanding of the impact of immunosuppressors on these has been limited. Further, studies investigating the immune and inflammatory responses to *A. fumigatus* have done so with the exclusion of the brain. It is critical to understand not only the immunological and inflammatory mediators during CA but to additionally understand how corticosteroid immunosuppression impacts these responses as a vast number of patients with CA are on corticosteroid therapy related to their underlying comorbidity. Even though some differences between murine and human responses likely exist, the data included herein have provided insight into the inflammatory and immune responses within the brain during CA. Further, by employing immunocompetent and immunosuppressed controls, we have gleaned an understanding of the difference in the immunological responses between the normal and immunosuppressed hosts. Therefore, identifying and understanding these differences may be key for diagnosing and treating CA based on the immune status of the host.

4.5 Limitations

These studies are limited by multiple factors. To start, we exclusively evaluated the immune and inflammatory response at one singular timepoint. As these responses are well documented to be dynamic and ever changing through disease progression, it is likely there are critical responses that are currently being missed. Additionally, we only examined the responses from homogenates, and as evidenced by the histopathology, we know the inflammatory and immune landscape changes with the presence or absence of *A. Fumigatus* hyphae. Thus, it is entirely possible that important inflammatory and immune dynamics localized to the areas of fungal invasion were missed. This is particularly likely for the microglia and astrocyte response. Further, these studies were solely conducted under a singular immunosuppressive regimen and therefore we cannot compare between corticosteroid and chemotherapy immunosuppressed mice. As both of these are highly implicated in the incidence of disseminated CA it is important to understand how the immunosuppressive regimens impact the inflammatory and immune response so treatment can be more specific and targeted. Lastly, when evaluating the therapeutic potential, only one dose was tested, and we did not measure the levels of VEGF in the brain to determine if treatment resulted in elevated levels. Thus, we are limited in the conclusions we can derive from this data. All limitations considered, however, present promising future directions for advancing our knowledge of disseminated CA and the development of therapeutics.

4.6 Conclusion

Taken together, we have demonstrated a significant disruption in the inflammatory and immune responses in the brain resultant from both *A. fumigatus* and corticosteroids in a model of disseminated CA. We have highlighted important differences in the response to *A. fumigatus*, that are seemingly in direct correlation with the host immune status. For example, the response of many critical myeloid and lymphoid-derived immune cells within the brain was significantly blunted in IN+IV+steroid mice compared to IN+IV mice, demonstrating the impact of corticosteroids on the host defense against *A. fumigatus*. Further still, we found that the secretion of many critical mediators of inflammation was significantly blunted in the presence of corticosteroids. Thus, while it is important to define the inflammatory and immune responses to *A. fumigatus* in the immunocompetent host, it is equally, if not more, important to define these responses in the immunosuppressed host, as that is directly reflective of the human population.

CHAPTER 5

NEUTROPENIA IS LESS EFFECTIVE FOR INDUCING EXPERIMENTAL DISSEMINATED CEREBRAL ASPERGILLOSIS THAN CORTICOSTEROIDS

5.1 Introduction

Neutropenia is one of the most serious and well-known risk factors for invasive aspergillosis. In the neutropenic host, angioinvasion by *A. fumigatus* is well documented, which contributes to the higher frequency of dissemination to other organs such as the skin and brain [23]. Therapeutics associated with HMs and SCTs are frequently attributed to the occurrence of neutropenia. Thus, patients receiving drugs associated with HMs and SCTs are at high risk of developing IPA and increased risk of CA. Indeed, we previously reported chemotherapy and SCT to be common risk factors before the occurrence of disseminated CA following IPA in HM patients [239]. One of the most at-risk populations for IPA are those with AML, 10% of whom are reported to develop IPA [68, 71]. In agreement with this, we found patients with AML to be the most prevalent HM patient subgroup with CA, and further, the chemotherapy agents commonly administered to AML patients to be the most frequently given to patients before CA [239].

Given the high frequency of AML patients diagnosed with IPA and subsequently CA, we sought to develop an experimental disseminated CA model utilizing the chemotherapy regimen given to one of the most at-risk populations. This therapeutic regimen, known as 7+3-induction chemotherapy, consists of the patient receiving cytarabine for 7 days, along with an anthracycline such as daunorubicin on each of the first 3 days. As the diagnosis, treatment, and pathogenesis of IPA are well known to be heavily influenced by the type of immunosuppression, it was important to take this into

consideration for developing an experimental model of disseminated CA. Therefore, to effectively recapitulate the immunosuppressive state of AML patients we utilized a “5+3” regimen, modified for murine suitability, like the 7+3 induction chemotherapy regimen [314]. Thus, here we show the “two-hit” disseminated CA model in a neutropenic host.

5.2 Methods

Mice

Male and female, age-matched C57BL/6 mice, 6–10 weeks of age, were obtained from The Jackson Laboratory (Bangor, ME). All animals were housed in a specific pathogen-free, Association for Assessment and Accreditation of Laboratory Animal Care–certified facility and handled according to Public Health Service Office of Laboratory Animal Welfare policies after review by the Tulane Institutional Animal Care and Use Committee (IACUC). All animal research was conducted under the approved Tulane IACUC Protocol #1589. Mice were sacrificed following anesthesia with ketamine/xylazine (100/10 mg kg⁻¹ IP; MWI Veterinary Supply, Boise, ID). No animals were excluded from the analyses unless the animal died prematurely. ‘*n*’ reported in the manuscript represents the number of animals in each group that were euthanized as scheduled at the end of the study unless otherwise stated.

Preparation of *A. fumigatus*

A. fumigatus isolate 13073 (American Type Culture Collection, Manassas, VA) was maintained on potato dextrose agar for 5–7 days at 37°C. Conidia were harvested by washing the culture flask with 50 ml of sterile PBS (Thermo Fisher Scientific, Waltham, MA) supplemented with 0.1% Tween-20 (Bio-Rad, Hercules, CA). The conidia were then passed through a sterile 40-mm nylon membrane to remove hyphal fragments and conidial clusters and enumerated on a hemacytometer.

Immunosuppression

For the corticosteroid-induced immunosuppression model, mice were given Kenalog-40™ or sterile PBS as an immunocompetent control [230, 231]. Briefly, SC injections at 40 mg/kg Kenalog-40™ (triamcinolone acetonide; Bristol-Myer Squibb,

Princeton, NJ) of body weight in sterile PBS for a final volume of 100 μ l 24 hours before fungal inoculation [232]. Immunocompetent mice were injected SC with 100 μ l of sterile PBS 24h before fungal inoculation. For the 5 + 3 chemotherapy-induced immunosuppression, mice were given a regimen of cytarabine (Hospira, Lake Forest, IL) and daunorubicin HCL (Selleck Chemicals, Houston, TX), as previously described [314, 315]. Briefly, IV injections of 50mg/kg cytarabine and 1.6 mg/kg daunorubicin of body weight in sterile PBS for a final volume of 100 μ l were administered daily for three days beginning five days prior to fungal inoculation. Two days prior to fungal inoculation, mice were weighed and given daily IV injections of 50 mg/kg cytarabine in sterile PBS for a final volume of 100 μ l for two days. For neutrophil-depletion immunosuppression, mice were given anti-mouse Ly6g antibody (clone: 1A8; BioXcel, West Lebanon, NH) to induce neutropenia or isotype IgG2a (clone: 2A3; BioXcel) for the nonneutropenic control as previously described [273, 316]. Briefly, IP injections of 200 μ g 1A8 or IgG2a in sterile PBS for a final volume of 100 μ l were administered one day before IN fungal inoculation and one day following IV fungal inoculation to ensure continuous neutropenia for the duration of the experiment.

Infection

For pulmonary infection, mice were lightly anesthetized with isoflurane and administered 7×10^6 *A. fumigatus* conidia in a volume of 30 μ l IN one-day post immunosuppression as previously described [233]. Briefly, mice are held in a horizontal, supine, position, and a pipette is used to deliver the 30 μ l inoculum dropwise to the nares, where normal breathing results in fluid aspiration into the lungs. For disseminated infection, one-day following IN inoculation, mice were administered 100 μ l 1×10^5 *A. fumigatus* conidia pre-swollen for 5 hours at 37°C IV [234].

Monitoring disease severity

Mice were weighed daily, and the percent total weight loss between study initiation and completion was calculated. Following infection, mice were scored daily beginning one-day post IN inoculation for morbidity and mortality up to ten days, using a modified scoring system as previously described [235]. Morbidity was scored from 0 to 5 as follows: 0) healthy, 1) minimal disease (e.g. ruffled fur), 2) moderate disease (e.g. ungroomed, hunched), 3) severe disease (e.g. severely hunched, altered gait, low motility, head-tilt), 4) moribund (e.g. spinning in cage or when suspended by tail, unable to move freely around cage, >25% weight loss) and 5) deceased. Mice that received a score of 4 were sacrificed.

Lung and brain fungal burden assessment

For lung fungal burden analysis, the left lungs were collected at day post-induction (DPI) 4 and homogenized in 1 ml of PBS. Total RNA was extracted from 0.1 ml of unclarified lung homogenate using the MasterPure Yeast RNA Purification Kit (Lucigen Corporation, Middletown, WI), which includes a DNase treatment step to eliminate genomic DNA as previously reported because DNA is not predictive of organism viability in this assay [236].

For brain fungal burden analysis, the right hemisphere was collected at DPI 4 and homogenized in 0.6 ml of PBS. Total RNA was extracted in the same manner as the lung from 0.3 ml of unclarified brain homogenate using the MasterPure Yeast RNA Purification Kit, except for extraction reagent and proteinase K volumes, which were doubled, and incubation at 70°C, which was increased from 10 to 15 minutes.

Lung and brain *A. fumigatus* burden was analyzed with RT-qPCR measurement of the *A. fumigatus* 18S rRNA (Integrated DNA Technologies; Forward: 5'-GGC CCT TAA

ATA GCC CGG T-3'; Reverse: 5'-TGA GCC GAT AGT CCC CCT AA-3'; Probe: 5'-/56-FAM/AGC CAG CGG CCC GCA AAT G/3BHQ_1/-3') and quantified using a standard curve of *A. fumigatus* 18S rRNA synthesized by GenScript via *in vitro* transcription. The final RNA sequence of the 18s fragment (562nt) is as follows:

TCGCAAGGCTGAAACTTAAAGAAATTGACGGAAGGGCACCACAAGGCGTGGAGCC
 TGCGGCTTAATTTGACTCAACACGGGGAAACTCACCAGGTCCAGACAAAATAAGGA
 TTGACAGATTGAGAGCTCTTTCTTGATCTTTTGGATGGTGGTGCATGGCCGTTCTTA
 GTTGGTGGAGTGATTTGTCTGCTTAATTGCGATAACGAACGAGACCTCGGCCCTTA
 AATAGCCCGGTCCGCATTTGCGGGCCGCTGGCTTCTTAGGGGGACTATCGGCTCA
 AGCCGATGGAAGTGCGCGGCAATAACAGGTCTGTGATGCCCTTAGATGTTCTGGG
 CCGCACGCGCGCTACTGACAGGGCCAGCGAGTACATCACCTTGGCCGAGAGGT
 CTGGGTAATCTTGTTAAACCCTGTCGTGCTGGGGATAGAGCATTGCAATTATTGCTC
 TTCAACGAGGAATGCCTAGTAGGCACGAGTCATCAGCTCGTGCCGATTACGTCCCT
 GCCCTTTGTACACACCGCCCGTCGCTACTACCGATTGAATGGCTCGGTGAGGCCTT
 CGGA.

The RT- qPCR reaction was performed with the CFX96 Real-Time System C1000 Touch thermal cycler (Bio-Rad).

Statistics

Data were analyzed using GraphPad Prism, version 9.0, statistical software (GraphPad Software, San Diego, CA). Comparisons between groups for normally distributed data were made with the Student's t-test or two-way analysis of variance (ANOVA). Significance was accepted at a p-value < 0.05.

5.3 Results

Comparison between corticosteroid-mediated immunosuppression and chemotherapy-mediated immunosuppression in the “two-hit” disseminated cerebral aspergillosis model

Because neutropenia resulting from chemotherapy is a top risk factor for the development of IPA and CA, we sought to develop a disseminated CA model with chemotherapy-induced immunosuppression. We previously identified AML as the primary HM associated with CA, disseminating from IPA (Chapter 2). Induction chemotherapy that is often employed in AML is the “7+3” regimen with the chemotherapeutic drugs cytarabine and daunorubicin (both drugs given for the first three days with cytarabine given an additional four days alone) [317]. In animal studies, a modified “5+3” regimen is often employed [314, 315]. As such, we compared the “5+3” immunosuppressive strategy with the corticosteroid-mediated “two-hit” disseminated cerebral aspergillosis model (Figure 5.1a). For the chemotherapy disseminated CA model, male and female WT mice were immunosuppressed with 50mg/kg cytarabine and 1.6mg/kg daunorubicin IV daily for three days beginning five days before infection, and 50mg/kg cytarabine alone IV daily for the two days immediately before infection. Chemotherapy-induced immunosuppressed disseminated CA mice were infected in the same manner as described above. On the day of primary infection, mice were inoculated IN with resting *A. fumigatus* conidia to establish IPA. On DPI 1, mice were inoculated IV with pre-swollen *A. fumigatus* conidia to establish disseminated infection. Chemotherapy disseminated CA model mice were compared to corticosteroid disseminated CA model mice.

Weight was recorded daily beginning five days before infection to account for weight loss associated with the 5+3 regimen. Mice were monitored for clinical symptomology beginning on day 1 after infection. Mice included in the corticosteroid disseminated CA group (IN+IV+steroid) lost a significantly greater percentage of total body weight compared to the chemotherapy disseminated CA mice (IN+IV+chemo) (Figure

5.1b). Disease severity was also significantly greater in the corticosteroid disseminated CA group (IN+IV+steroid) compared to the chemotherapy disseminated CA group (IN+IV+chemo) (Figure 5.1c). In turn, corticosteroid-treated mice had higher lung and brain fungal burden than chemotherapy-treated mice (Figure 5.1d, e). Thus, despite a known association with both corticosteroids and the 7+3 regimen for CA dissemination from IPA, corticosteroid treatment was superior, with 100% of mice in this group having fungal burden in the brain compared to only 50% of chemotherapy-treated mice.

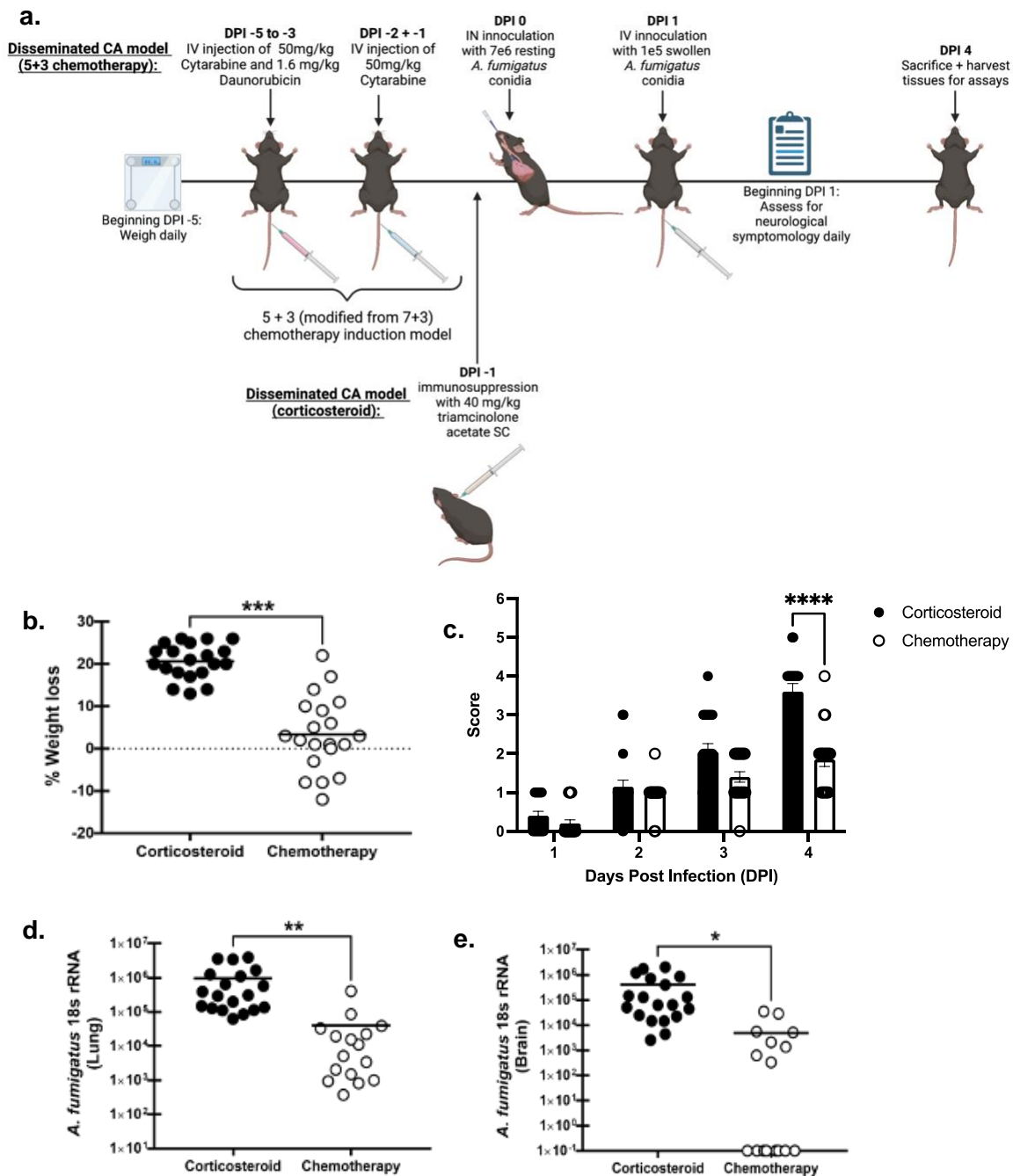


Figure 5.1 Comparison between corticosteroid-mediated immunosuppression and chemotherapy-mediated immunosuppression in the “two-hit” disseminated cerebral aspergillosis model (Figure legend on next page).

Figure 5.1 Comparison between corticosteroid-mediated immunosuppression and chemotherapy-mediated immunosuppression in the “two-hit” disseminated cerebral aspergillosis model.

a. WT C57Bl/6 male and female mice were subjected to experimental disseminated CA with mice being immunosuppressed by chemotherapy beginning DPI -5, IN inoculated with 7e6 resting *A. fumigatus* conidia, and IV inoculated with 1e5 swollen *A. fumigatus* conidia via the lateral tail vein. Chemotherapy disseminated CA mice were compared to corticosteroid immunosuppressed mice given triamcinolone acetate SC at DPI -1. Mice were weighed daily beginning from the study initiation (DPI -1) through study completion. Following initial infection (DPI 1) mice were assessed for disease symptomology daily and assigned a score ranging from 0-5. For fungal burden quantification mice were sacrificed at DPI 4 at which point tissue was harvested. Image created with BioRender.com. **b-e.** C57Bl/6 mice were randomly assigned to either corticosteroid or chemotherapy immunosuppression, all mice were infected on DPI 0 via the experimental disseminated CA method. Mice were monitored for weight and symptomology daily and sacrificed on DPI 4 for fungal burden analysis. **b.** Total percent weight loss was calculated by comparing the mouse weight at the study endpoint (DPI 4) with the weight prior to immunosuppression (DPI -1). **c.** Beginning DPI 1, mice were assessed for disease severity and assigned a score between 0-5 correlating to the symptomology. **d, e.** Lung and brain fungal burden at DPI 4 was assessed by RT-qPCR analysis of *A. fumigatus* 18S rRNA levels. The Figures illustrate cumulative data from four independent studies. For all graphs, *, **, ***, and **** represent P values of <0.05, 0.0059, <0.001, and <0.0001, respectively; n = 4-5 mice/group for each study; each data point represents a single mouse and the line in each group corresponds to the mean + SEM. **b, d, e.** unpaired two-tailed Student's t-test, **c.** Two-Way ANOVA (mixed effects) with post-hoc Tukey's multiple comparisons test.

Evaluation of neutropenia in the “two-hit” disseminated cerebral aspergillosis model

Neutropenia is widely considered as the primary risk factor for the development of IPA [23, 32, 33]. However, we were surprised to observe no differences in brain neutrophil numbers between IN+IV and IN+IV+steroid, despite dramatic differences in fungal burden. To evaluate the impact of neutropenia on the development of disseminated CA, we implemented an anti-mouse Ly6G neutralizing antibody (1A8) to deplete neutrophils effectively. For this, male and female WT mice were neutrophil depleted with 200 ug 1A8 IP one-day prior to infection induction. Mice were induced with the “two-hit” disseminated CA model infection regimen in the same manner described above. As neutrophil depletion is known to be maintained for 3-4 days, on DPI 2, mice were administered a second dose of 200 ug 1A8 IP [316]. Neutropenic mice induced with disseminated CA were compared to IgG2a isotype control mice induced with disseminated CA mice (Fig. 5.2a).

Weight was recorded daily beginning one-day preceding infection and mice were monitored for clinical symptomology beginning day 1 after infection. Results showed that neutropenic mice (IN+IV+neutropenia) lost a significantly greater percentage of total body weight in comparison to the isotype control group (IN+IV+Iso) (Figure 5.2b). Disease severity was not significantly different between either group. However, some IN+IV+1A8 treated mice did display severe symptomology at DPI 4 (Figure 5.2c). Neutropenia did, however, result in a higher fungal burden in the brain (Figure 5.2d), albeit 33% of neutropenic mice did not have detectable *A. fumigatus* (compared to 77% of non-neutropenic mice). Thus, although neutropenia was associated with an increased presence of *A. fumigatus* in the brain, this was less consistent than in corticosteroid-treated mice. Altogether, neutropenia-mediated immunosuppression was insufficient to induce a severe and consistent model of disseminated CA.

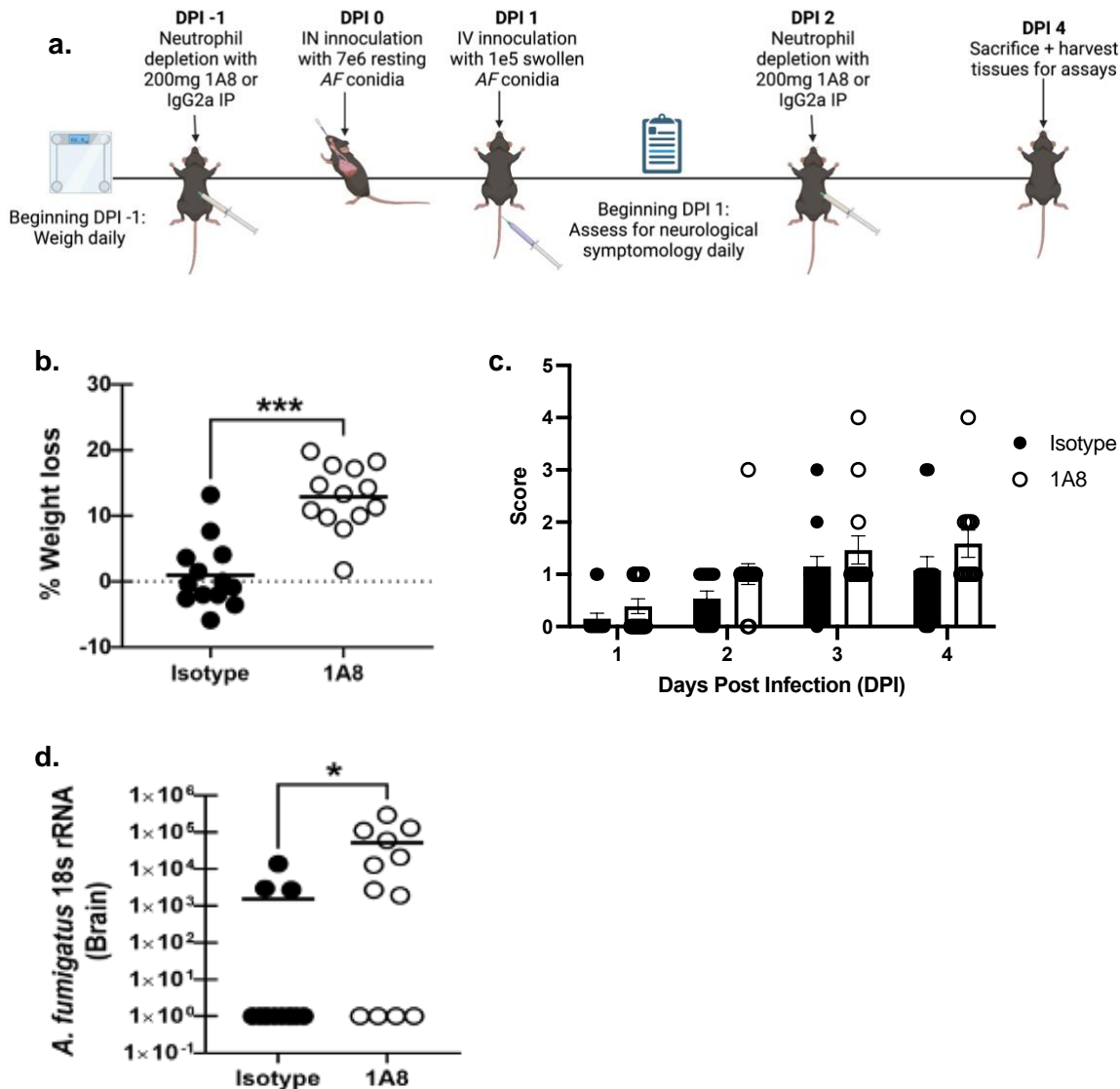


Figure 5.2 Evaluation of neutropenia in the “two-hit” disseminated cerebral aspergillosis model.

a. WT C57Bl/6 male and female mice were subjected to experimental disseminated CA with mice being immunosuppressed by 200ug anti-mouse Ly6g (1A8) given IP 1 day prior to infection, IN inoculated with 7e6 resting *A. fumigatus* conidia, IV inoculated with 1e5 swollen *A. fumigatus* conidia via the lateral tail vein on DPI 1, and 200ug 1A8 given IP on DPI 2. Neutropenic mice were compared to nonneutropenic isotype control mice given 200 ug IgG2a on the same dosing schedule as 1A8. Mice were weighed daily beginning from the study initiation (DPI -1) through study completion. (*Figure legend continues on next page*).

Figure 5.2 Experimental design, Ly6G-antibody induced neutropenia in the “two-hit” disseminated CA model (continued).

Beginning DPI 1, mice were assessed for disease symptomology daily and assigned a score ranging from 0-5. For fungal burden quantification, mice were sacrificed at DPI 4, at which point tissue was harvested. Image created with BioRender.com. **b – d.** C57Bl/6 mice were randomly assigned to either 1A8 or isotype control. All mice were infected on DPI 0 via the experimental “two-hit” disseminated CA method. Mice were monitored for weight and symptomology daily and sacrificed on DPI 4 for fungal burden analysis. **b.** Total percent weight loss was calculated by comparing the mouse weight at the study endpoint (DPI 4) with the weight before immunosuppression (DPI -1). **c.** Beginning DPI 1, mice were assessed for disease severity and assigned a score between 0-5 correlating to the symptomology. **d.** Brain fungal burden at DPI 4 was assessed by RT-qPCR analysis of *A. fumigatus* 18S rRNA levels. The Figures illustrate cumulative data from three independent studies. * and **** represent a P value of <0.05 and <0.0001, respectively; n = 4-6 mice/group for each study; each data point represents a single mouse + SEM. **b, d.** unpaired two-tailed Student’s t-test, **c.** Two-Way ANOVA (mixed effects) with post-hoc Tukey’s multiple comparisons test.

5.4 Discussion

As neutropenia is considered a top risk factor for developing IPA and subsequent CA, we sought to develop a model of disseminated CA utilizing the “two-hit” infection method in chemotherapy-treated and neutropenic mice. While we were able to achieve successful cerebral infection in 50% of mice immunosuppressed via chemotherapy, the number of mice infected, and the level of infection was significantly reduced in comparison to corticosteroid-induced immunosuppressed mice. We further investigated whether direct neutrophil depletion was sufficient for inducing disseminated CA and found that while a greater number of mice had a detectable fungal infection within the brain than chemotherapy-induced immunosuppressed mice, this immunosuppression method was not as robust as corticosteroids. Overall, neutropenia-based immunosuppression was inferior to corticosteroid-induced immunosuppression for inducing cerebral infection with the “two-hit” method of disseminated CA.

A limitation in understanding the development of, pathogenicity, and immune responses during CA is a direct result of a lack of an experimental animal model. A review of the literature examining the development of or models for CA identified a diverse array of models, yet not any that exactly replicate the acquisition of IPA/CA as it relates to HMs. Early models employed cyclophosphamide for immunosuppression, and direct intracranial inoculation of *A. fumigatus*, which clearly resulted in CA, albeit this model does not replicate the natural dissemination of the organism from the respiratory tract to the brain [60, 318]. Other models employed cyclophosphamide for immunosuppression and intravenous inoculation; again, a model that results in *A. fumigatus* in the CNS/brain but again lacks the dissemination from the lung component [319, 320]. Some studies have employed the neutrophil depleting antibody 1A8 with an intravenous challenge, or intravenous challenge without any immunosuppression [321-323]. We found only a single study that employed a relevant cyclophosphamide-cortisone acetate immunosuppression

model and administered *A. fumigatus* intratracheally, which resulted in 100% mortality by day 5 [324]. Although live organism was detected in the lung in 100% of these mice, only 50% of the mice had detectable *A. fumigatus* in the brain [324].

The dominant patient population at risk for developing IPA and subsequent mortality include those with leukemia or lymphoma, especially if these individuals undergo HSCT along with immunosuppression [71, 325]. Of these, IPA and CA are a significant concern in patients with AML [146, 325]. Neutropenia has historically been considered the predominant risk factor for IPA, particularly for HM patients undergoing induction chemotherapy [326]. For patients with AML, a 7+3-induction chemotherapy regimen is often implemented. This involves treatment with two chemotherapy drugs, cytarabine and an anthracycline drug such as daunorubicin, with the resulting neutropenia often associated with the development of infection [80, 327]. Although these chemotherapeutic agents are extensively used in AML, and there are numerous reports of aspergillosis occurring in patients administered these drugs, we did not find any reports that have examined daunorubicin in an aspergillosis animal model, and only a single report of a rabbit model that employed cytarabine + methylprednisolone for immunosuppression [328]. Although we employed a similar 5+3 regimen in mice that uses human equivalent dosing to effectively mimic the immunosuppressive state frequently associated with *A. fumigatus* infection, development of disseminated CA occurred at a lower level in terms of fungal burden in the brain and in fewer mice compared to mice immunosuppressed with corticosteroids (IN+IV+steroid) [68, 314, 315].

One of the most serious and notable side effects of chemotherapy is neutropenia. However, neutrophils are not the sole immune cell impacted by chemotherapy. The murine 5+3 chemotherapy dosing regimen results in rapid weight loss, low white blood cell counts, neutropenia, and reduced red blood cell count. Indicating that this model induces significant changes to the bone marrow cellularity [314]. Specifically, the population of

lineage-negative cells and LSK progenitor cells were both significantly increased in the bone marrow of 5+3 mice, a similar effect as observed in human AML patients during induction therapy [329]. This data suggests that this chemotherapy regimen is cytotoxic to mature blood cells such as T and B lymphocytes, NK cells, granulocytes, and macrophages/monocytes, but not hematopoietic stem cells, generating a relative imbalance between progenitor and mature bone marrow-derived cells. Conversely, the neutrophil-depleting antibody 1A8 is specific for neutrophils. The use of this Ly6G-specific antibody has been shown to result in a nearly complete depletion of neutrophils while monocyte/macrophage, T-cell, DC, and NK cell levels remained unaffected [316, 330].

Depletion of neutrophils with antibodies is artificial in terms of human disease and does not truly represent how neutrophil depletion occurs because of chemotherapy regimens. However, to evaluate neutropenia-based immunosuppression more directly for modeling disseminated CA, we employed the IN+IV model with the neutrophil-depleting antibody 1A8. By implementing the antibody, a more specific investigation into the role of neutrophils during disseminated was conducted, which could not be done through chemotherapy as multiple cell types are impacted by the cytotoxic drugs. The induction of neutropenia was less efficient at developing disseminated CA than in corticosteroid-induced immunosuppressed mice. Although data with 1A8 supports a role for neutrophils in *A. fumigatus* infection, it is unclear if the lack of neutrophils is required to control *A. fumigatus* in the brain vs. the lack of neutrophils resulting in an increased escape of *A. fumigatus* from the lung.

5.5 Limitations

A potential limitation of these studies is the acute neutropenia preceding infection. Namely, prolonged neutropenia has been heavily implicated in the occurrence of IPA and subsequently CA. Approximately 40 years ago, Gerson et al. conducted a small, case-control study of patients with acute leukemia where they found the duration of neutropenia to be correlative to the incidence of IPA [64]. However, in this study, only one-third of patients with prolonged neutropenia ultimately developed IPA. Following this study, prolonged neutropenia has since been considered a top risk factor for IPA and subsequently disseminated CA [32, 331]. Neutropenia is typically defined as <500 absolute neutrophil count (ANC) at the time of infection, and prolonged neutropenia is typically considered as exceeding ten days. By these standards, a large cohort of patients is excluded. More recently, a large retrospective study conducted primarily on patients with HMs or bone marrow transplants with proven or probable IPA found neutropenia of any duration to be a more robust predictor of infection than prolonged neutropenia, specifically [72]. Another recent retrospective study of cerebral fungal infections in HM and SCT patients found neutropenia of any duration to be strongly correlated with the incidence of fungal infection, with about three-quarters of patients being neutropenic at the onset of infection [332]. About half of the patients were found to have severe neutropenia of varying durations. Overall, these recent studies suggest that a state of neutropenia before the infection is of greater priority for inducing IPA and CA than the duration of neutropenia. Although, given that neutropenia was less effective in the “two-hit” disseminated CA model, prolonged severe neutropenia is worth investigating in this model.

5.6 Conclusion

Here, we investigated the occurrence of disseminated CA via the “two-hit” model, in mice immunosuppressed via 5+3-induction chemotherapy, the most common chemotherapy employed for the highest risk underlying disease, AML. We further evaluated the effect of neutropenia in our “two-hit” model with neutrophil-depleted mice, as neutropenia has historically been considered a top risk factor for IPA and subsequent CA. Altogether, successful cerebral infection was achieved in a percentage of chemotherapy-induced neutropenic and neutrophil-specific depleted mice. However, these neutrophil-targeted immunosuppression methods were inferior at inducing disseminated CA in comparison to corticosteroids. Although these models may not be ideal for modeling disseminated CA, they are promising tools for investigating host defense during disease in a neutropenic state. Particularly the chemotherapy-induced immunosuppression “two-hit” disseminated CA model, which can be leveraged to gain insight into mechanisms precluding disseminated disease in a human-relevant immunosuppression model, given that only a portion becomes cerebrally infected.

CHAPTER 6

CONCLUSIONS AND FUTURE WORKS

6.1 Conclusions

Here, we identified the patient characteristics related to HM patient subgroups and their therapeutics associated with increased risk for the development of disseminated CA following IPA. Incidence of IPA is frequently attributed to those with HMs and is often linked to severe and prolonged neutropenia associated with chemotherapy. As the brain is often reported as a top site of dissemination and the subsequent disease poses a serious threat to life, delineating the HM populations and characteristics associated with CA posed a critical need. Thus, a systematic review of the literature was conducted to identify those most at risk for disseminated CA within the HM population and define their characteristics. From this, patients with acute leukemias receiving chemotherapy and/or corticosteroids were identified as the largest population(s) at risk for developing disseminated CA.

Informed by the results and conclusions generated from our systematic literature review, we developed a human-relevant model of disseminated CA pathogenesis. We demonstrated a novel, pre-clinical model of disseminated CA developed using corticosteroid-induced immunosuppression and a “two-hit” inoculation method with *A. fumigatus*. This model achieved severe clinical disease, mortality, and significant fungal burden in both the lung and the brain in 100% of the mice. Overall, we established a novel model that i) utilized an immunosuppressive regimen relevant to the most at-risk human populations, ii) reflected the natural route by which disseminated CA is acquired, and iii) resulted in consistent, reproducible, and severe disease.

Additionally, corticosteroid-induced immunosuppression significantly blunted the infiltration of specific immune cells and inflammatory cytokine and chemokine responses in the brain during CA. Finally, corticosteroid-induced immunosuppression was superior for inducing disseminated CA to chemotherapy-induced immunosuppression and neutropenia-induced immunosuppression.

Altogether, the outcome of this work highlights the need for more rigorous incorporation of anti-fungal drugs in high-risk HM patient subgroups such as those with acute leukemias receiving chemotherapy and/or corticosteroids to reduce the incidence and mortality of this highly deadly disease. Furthermore, developing this model of disseminated CA following IPA in an immunosuppressed host provides a novel platform and improved human-relevant model with a wide range of potential applications. For example, this model can be leveraged to study the efficacy of anti-fungal drugs and immunotherapies, enhance understanding of disease pathogenesis, identify novel diagnostic and therapeutic targets, and identify early biomarkers to improve detection. Because of the “two-hit” inoculation method we developed for this model, with a delay between the primary pulmonary and secondary disseminated infection, in the future, this model could be used to investigate prophylactic strategies to prevent the progression from IPA to CA or to define therapeutic windows once the disease is already established for the prevention of disseminated disease. All of these can be used to reduce disease incidence and severity and reduce mortality associated with this devastating disease.

6.2 Future direction 1: Define the systemic and local immune and inflammatory responses in the brain of chemotherapy-induced immunosuppressed mice with and without fungal burden.

In mice immunosuppressed via 5+3-induction chemotherapy, only 50% of mice were found to have detectable fungal burden within the brain, while 100% were demonstrated to have fungal infection in the lung. One consideration is that it is possible that our method of detecting the presence of *A. fumigatus* within the brain is not sensitive enough to detect low levels of the fungus. Thus, it could be that infection did occur in the 50% of mice without detectable fungal burden within the brain; however, it was simply missed. To our knowledge, the method of detecting and quantifying the fungal burden we have employed is the most sensitive in the field to date. As such, despite mice being exposed to one of the top identified risk factors for disseminated CA, 50% of mice were seemingly protected against the dissemination of *A. fumigatus* to the brain. Due to this, we will next investigate the host-defense response within the blood and brain of chemotherapy-immunosuppressed mice infected via the “two-hit” disseminated CA model and compare those with detectable fungal burden in the brain to those without. Because it is unclear what is protecting mice without cerebral infection from this disease, we will use several measures to delineate the inflammatory and immune response to identify any differences between infected and uninfected mice that could contribute to susceptibility to infection. One limitation is that which mice will have disseminated CA versus those that will cannot be predicted at this time. To overcome this and identify underlying factors contributing to the incidence of cerebral infection, serum will be sampled at multiple time points through the course of immunosuppression and infection. For serum collected throughout the study, we will perform RNAseq and a multiplex assay for common inflammatory cytokines and chemokines. These results can potentially identify critical biomarkers that may be used to further inform populations with increased susceptibility

and vulnerability. This analysis will additionally provide information for the dynamics of the immune response throughout the course of infection, as it is highly likely that early immune responses will inform just as much, if not more, regarding those that are infected versus those that are not at study completion. Altogether the results of this study are expected to identify other biomarkers and critical components of host defense that be targeted, potentially through the development of novel therapeutics, to reduce the incidence of disseminated CA.

6.3 Future direction 2: Investigating the relationship between primary pulmonary infection and secondary hematogenic infection

Early on, we demonstrated that the primary pulmonary infection, while not necessary for the induction of cerebral infection in this model, has a seemingly protective role against severe and rapid dissemination of *A. fumigatus* to the brain. As such, our next goal is to improve the understanding of the contribution of primary pulmonary infection to disseminated CA. To achieve this, we will evaluate the fungal migration patterns and the dynamics of the host defense over the course of infection. To assess the migration patterns of *A. fumigatus* during both steps of the “two-hit” infection, we will be employing a fluorescently tagged *A. fumigatus* strain. Specifically, mice will be infected IN with the fluorescently labeled *A. fumigatus* strain and infected IV with unlabeled *A. fumigatus*, and vice versa. Our early studies show that *A. fumigatus* cannot be detected by current standards within the brain in corticosteroid immunosuppressed mice infected IN only. However, using fluorescence imaging, we would be able to understand better if and where *A. fumigatus* traffics outside of the lung and the brain, in this model. Further, it is currently unknown if the hematologic infection increases the likelihood of dissemination from the lung. Thus, these studies will provide information to improve our understanding of each administration route's contribution to dissemination. Second, to identify the primary

pulmonary infection's role in host defense during secondary hematologic disorder, we will investigate circulating immune cells, cytokines, and chemokines following the pulmonary disease, immediately before IV inoculation, and at intervals following blood infection. Altogether, these future studies will help identify the primary infection's dynamic role in disseminated CA. This information can be used to identify biomarkers and potential therapeutic targets for preventing and treating disseminated infections.

6.4 Future direction 3: Susceptibility for disseminated CA in mice exposed to standard targeted therapies in AML patients.

The scope of this current thesis centered on the development of a model of disseminated CA that was relevant to and reflective of the largest at-risk patient groups. However, other underlying factors and treatments are associated with an increased risk for infection by *A. fumigatus*. More recently, in oncology, targeted therapies have become more prevalent. As targeted therapies are a newer addition to the patient treatment regimens, the potential risk these therapies pose for susceptibility to IFI is not fully understood. Within a sub-population of AML patients, targeted inhibitors against tyrosine Fms-like tyrosine kinase 3 (FLT3) and B-cell lymphoma-2 (BCL-2) protein have become more common. More than 30% of newly diagnosed AML patients have been found to have activating mutations in the *FLT3* gene, whereas *BCL2* gene overexpression has been detected in up to 60% of the AML population, both of which have been implicated in a high probability of relapse, chemotherapeutic resistance, and poor prognosis [333, 334]. Small-molecule inhibitors of activated FLT3 specifically inhibit the proliferation of leukemia cells and have been shown to have good efficacy in the clinical setting as stand-alone therapies and in conjunction with chemotherapy [335]. BCL-2 small-molecule inhibitors specifically inhibit the BCL-2 anti-apoptotic pathway, ultimately promoting leukemic cell death [336]. BCL-2 inhibitors are often used alongside chemotherapies to target chemo-

resistant leukemic cells [336]. Recently, several studies have been published correlating FLT3 or BCL-2 inhibitors with the occurrence of IPA and subsequent disseminated CA [337, 338]. To better understand the relationship between these therapies and disseminated CA incidence, we will employ our two-hit model in mice exposed to FLT3 or BCL-2 inhibitors. We will be testing these inhibitors on their own and in conjunction with frequently associated chemotherapies to further understand i) the specific impact of these on the immune system that would contribute to increased vulnerability for fungal infection and ii) to determine if these therapies have a synergistic effect with chemotherapy for suppressing the immune response and increasing vulnerability for infection.

6.5 Applications

The “two-hit” model of disseminated CA described herein can be used for many applications. One of the leading and potentially most impactful applications is the discovery, development, and optimization of new therapeutics that could target the brain specifically to reduce the severity of CA. Currently, there are no available therapeutics with cerebral specificity, and those that are used for CA are limited in their ability to cross the BBB. This model, recapitulating the natural dissemination route, will be invaluable for investigating drugs for patients with disseminated CA following IPA. This model, because there is a delay between the pulmonary infection and hematogenic dissemination, can also be implemented for investigating prophylactic strategies, drug regimens, and identifying optimal therapeutic windows to reduce the incidence of dissemination. These factors additionally make it optimally suited for investigating novel prophylactic therapeutics. This model can also be easily manipulated with different immunosuppressors, states of immunity (i.e., genetic manipulation), and disease states to identify those that may increase the incidence and severity of disseminated CA to better

identify vulnerable populations. All of these applications can and will reduce the overall incidence and mortality associated with this disease.

6.6 Final thoughts

Overall, the development of this model provides an invaluable tool that can be used for investigating host dynamics, drug targets, and therapeutic testing. This model can be readily manipulated to investigate various states of immunity, using different immune suppressors, genetically modified mice, or specific immune cell depletion, for example. Given the prior absence of animal models that reconstitute the natural route of infection of the CNS, it has been difficult to fully understand the progression of and identify therapeutic targets for the disease. The human-relevant model of disseminated CA disclosed and described can and will be used to generate discoveries that will, with all luck, reduce the overall incidence and mortality associated with this devastating disease.

Developing a model with seemingly endless applications and modifications has been exciting. There are so many questions surrounding IPA and disseminated CA that could be potentially answered through the use and adaptation of this model. My greatest hope for this project is that those who come after me, who use this model for their research and discoveries, will help move the needle forward on improving overall human health.

APPENDIX A

SUPPORTING INFORMATION FOR CHAPTER 2

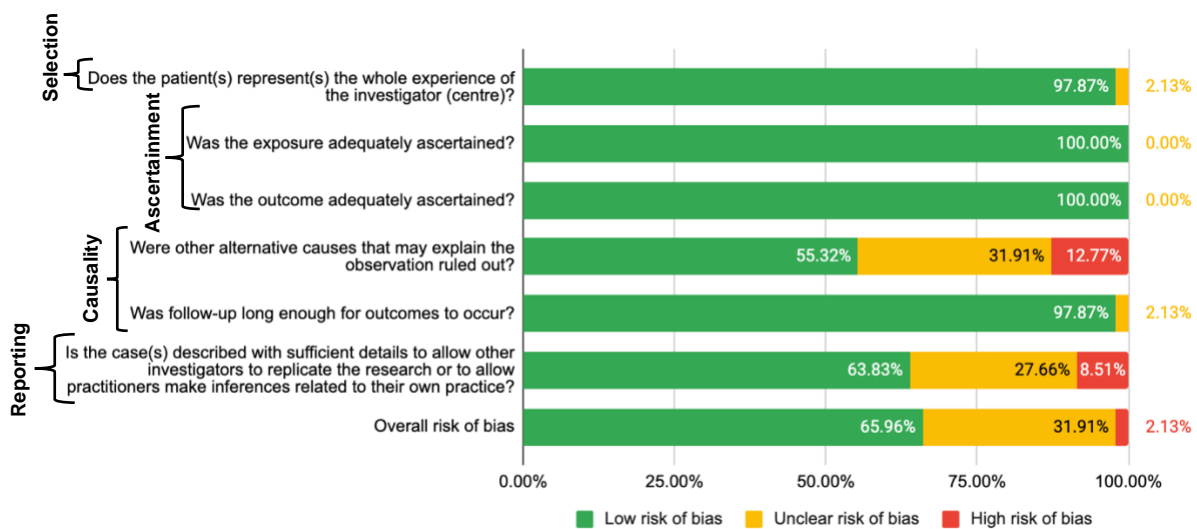


Figure A1. Overall synthesis of quality assessment and risk of bias.

Table A1. Literature search results

Date of Search	Database	Search String	Total results retrieved	Search Details
18-May-21	PubMed	(("Aspergillosis"[Mesh] AND disseminat*[tw]) OR (disseminat*[tw] AND aspergillosis[tw]) OR "Neuroaspergillosis"[Mesh] OR "neuroaspergillosis"[tw] OR "nervous system invasive aspergillosis"[tw] OR "cerebral aspergillosis"[tw] OR "central nervous system aspergillosis"[tw] OR "CNS aspergillosis"[tw] OR "brain aspergillosis"[tw] OR "intracranial aspergillosis"[tw] OR "cranial aspergillosis"[tw]) AND ("Antineoplastic Agents"[Mesh] OR "Antineoplastic"[tw] OR "Antineoplastic Agent"[tw] OR "Antineoplastic Agents"[tw] OR "Antineoplastic Drug"[tw] OR "Antineoplastic Drugs"[tw] OR Antineoplastic[tw] OR "Antitumor Drug"[tw] OR "Antitumor Drugs "[tw] OR "Antitumor Agent"[tw] OR "Antitumor Agents"[tw] OR "Cancer Chemotherapy Drug"[tw] OR "Cancer Chemotherapy Drugs"[tw] OR "Cancer Chemotherapy Agent"[tw] OR "Cancer Chemotherapy Agents"[tw] OR "Chemotherapy, Cancer, Regional Perfusion"[Mesh] OR "Neoplasms/drug therapy"[Mesh] OR "Neoplasms/administration and dosage"[Mesh] OR ((cancer*[tw] OR neoplasm*[tw] OR "hematologic malignancy"[tw] OR "hematologic malignancies"[tw] OR leukemia[tw] OR lymphoma[tw]) AND (chemotherapy[tw] OR antineoplastic[tw] OR antitumor[tw] OR antitumour[tw] OR anti-angiogenic[tw] OR immunomodulatory[tw] OR cytotoxic[tw] OR chemotherapeutic*[tw] OR immunomodulator*[tw] OR immunosuppressant*[tw] OR immunocompromis*[tw])))	213	
18-May-21	Embase	((disseminated NEAR/5 aspergillosis) OR (dissemination NEAR/5 aspergillosis) OR 'central nervous system aspergillosis'/exp OR 'central nervous system aspergillosis' OR 'neuroaspergillosis' OR 'nervous system invasive aspergillosis' OR 'cerebral aspergillosis' OR 'CNS aspergillosis' OR 'brain aspergillosis' OR 'intracranial aspergillosis' OR 'cranial aspergillosis') AND ('cancer chemotherapy'/exp OR (cancer NEAR/5 chemotherapy) OR 'antineoplastic agent'/exp OR 'antineoplastic agent' OR (('neoplasm' OR 'hematologic malignancy' OR 'leukemia' OR 'lymphoma') AND ('chemotherapy' OR 'antineoplastic' OR 'antitumor' OR 'antitumour' OR 'anti-angiogenic' OR 'immunomodulatory' OR 'cytotoxic' OR 'chemotherapeutic' OR 'immunomodulator' OR 'immunosuppressant' OR	356	All fields

		'immunocompromised')) AND 'article'/it AND 'human'/de		
18-May-21	CINAHL Plus with Full Text	((disseminated N5 aspergillosis) OR (dissemination N5 aspergillosis) OR central nervous system aspergillosis OR central nervous system aspergillosis OR neuroaspergillosis OR nervous system invasive aspergillosis OR cerebral aspergillosis OR CNS aspergillosis OR brain aspergillosis OR intracranial aspergillosis OR cranial aspergillosis) AND (cancer chemotherapy OR (cancer N5 chemotherapy) OR antineoplastic agent OR ((neoplasm OR hematologic malignancy OR leukemia OR lymphoma) AND (chemotherapy OR antineoplastic OR antitumor OR antitumour OR anti-angiogenic OR immunomodulatory OR cytotoxic OR chemotherapeutic OR immunomodulator OR immunosuppressant OR immunocompromised)))	18	All fields
18-May-21	Web of Science - Science Index Expanded	((disseminated NEAR aspergillosis) OR (dissemination NEAR aspergillosis) OR central nervous system aspergillosis OR central nervous system aspergillosis OR neuroaspergillosis OR nervous system invasive aspergillosis OR cerebral aspergillosis OR CNS aspergillosis OR brain aspergillosis OR intracranial aspergillosis OR cranial aspergillosis) AND (cancer chemotherapy OR (cancer NEAR chemotherapy) OR antineoplastic agent OR ((neoplasm OR hematologic malignancy OR leukemia OR lymphoma) AND (chemotherapy OR antineoplastic OR antitumor OR antitumour OR anti-angiogenic OR immunomodulatory OR cytotoxic OR chemotherapeutic OR immunomodulator OR immunosuppressant OR immunocompromised)))	156	Topic
18-May-21	www.greylit.org	((disseminated aspergillosis) OR (dissemination aspergillosis) OR central nervous system aspergillosis OR central nervous system aspergillosis OR neuroaspergillosis OR nervous system invasive aspergillosis OR cerebral aspergillosis OR CNS aspergillosis OR brain aspergillosis OR intracranial aspergillosis OR cranial aspergillosis) AND (cancer chemotherapy OR (cancer chemotherapy) OR antineoplastic agent OR ((neoplasm OR hematologic malignancy OR leukemia OR lymphoma) AND (chemotherapy OR antineoplastic OR antitumor OR antitumour OR anti-angiogenic OR immunomodulatory OR cytotoxic OR chemotherapeutic OR immunomodulator OR immunosuppressant OR immunocompromised)))	0	

Table A2. Quality assessment for each article used in the systematic review and overall level of bias.

Study ID	Does the patient(s) represent(s) the whole experience of the investigator (centre)?	Was the exposure adequately ascertained?	Was the outcome adequately ascertained?	Were other alternative causes that may explain the observation ruled out?	Was follow-up long enough for outcomes to occur?	Is the case(s) described with sufficient details to allow other investigators to replicate the research?	Overall level of Bias
Zwitserloot 2008	Yes	Yes	Yes	Yes	Yes	Yes	Low
Yeh 2007	Yes	Yes	Yes	Yes	Yes	Unclear	Low
Wright 2003	Yes	Yes	Yes	Yes	Yes	Unclear	Low
Wandroo 2006	Yes	Yes	Yes	Yes	Yes	Yes	Low
Walsh 1985	Yes	Yes	Yes	Yes	Yes	Unclear	Low
Van der Linden 2011	Yes	Yes	Yes	Yes	Yes	Unclear	Low
Trigg 1993	Yes	Yes	Yes	Yes	Yes	Yes	Low
Tracy 1983	Yes	Yes	Yes	Yes	Yes	Yes	Low
Tattevin 2004	Yes	Yes	Yes	Unclear	Yes	Unclear	Unclear
Sparano 1992	Yes	Yes	Yes	Yes	Yes	Unclear	Low
Schauwvlieghe 2020	Yes	Yes	Yes	Yes	Unclear	Yes	Low
Schamroth Pravda 2019	Yes	Yes	Yes	Yes	Yes	Unclear	Low
Sancho 1997	Yes	Yes	Yes	Yes	Yes	Yes	Low
Sakata 2021	Yes	Yes	Yes	Unclear	Yes	Yes	Low
Ruchlemer 2019	Yes	Yes	Yes	Unclear	Yes	Unclear	Unclear
Prakash 2012	Yes	Yes	Yes	Yes	Yes	Yes	Low
Pongbhaesaj 2004	Yes	Yes	Yes	Unclear	Yes	Unclear	Unclear
Peng 2015	Yes	Yes	Yes	Unclear	Yes	Yes	Low
Pascale 2015	Yes	Yes	Yes	Unclear	Yes	Yes	Low
Palmisani 2017	Yes	Yes	Yes	No	Yes	Yes	Unclear
Nov 1984	Yes	Yes	Yes	Yes	Yes	Yes	Low

Mori 1998	Yes	Yes	Yes	Yes	Yes	Yes	Low
Middelhof 2005	Yes	Yes	Yes	Yes	Yes	Yes	Low
Marbello 2003	Yes	Yes	Yes	Yes	Yes	Yes	Low
Mahlknecht 1997	Yes	Yes	Yes	Unclear	Yes	Yes	Low
Lionakis 2017	Yes	Yes	Yes	Unclear	Yes	Yes	Low
Kurdow 2005	Yes	Yes	Yes	Yes	Yes	Yes	Low
Kreisel 1991	Yes	Yes	Yes	Yes	Yes	No	Unclear
Kawanami 2002	Yes	Yes	Yes	Yes	Yes	Unclear	Low
Kaste 2000	Yes	Yes	Yes	Unclear	Yes	Unclear	Unclear
Iwen 1997	Yes	Yes	Yes	Unclear	Yes	Unclear	Unclear
Iwen 1993	Yes	Yes	Yes	Unclear	Yes	Unclear	Unclear
Im 2012	Yes	Yes	Yes	No	Yes	Yes	Unclear
Hummel 2006	Unclear	Yes	Yes	Unclear	Yes	No	High
Henze 1982	Yes	Yes	Yes	No	Yes	Yes	Unclear
Guermazi 2002	Yes	Yes	Yes	No	Yes	Yes	Unclear
Groll 1999	Yes	Yes	Yes	Unclear	Yes	Yes	Low
Gaye 2018	Yes	Yes	Yes	Yes	Yes	Yes	Low
Flatt 2012	Yes	Yes	Yes	No	Yes	Yes	Unclear
Faisal 2019	Yes	Yes	Yes	Yes	Yes	No	Unclear
Eichenberger 2020	Yes	Yes	Yes	Yes	Yes	No	Unclear
DeLeonardis 2020	Yes	Yes	Yes	No	Yes	Yes	Unclear
Damaj 2004	Yes	Yes	Yes	Yes	Yes	Yes	Low
Beresford 2019	Yes	Yes	Yes	Yes	Yes	Yes	Low
Athanassiadou 2005	Yes	Yes	Yes	Unclear	Yes	Yes	Low
Anciones 2018	Yes	Yes	Yes	Unclear	Yes	Yes	Low
Amanati 2020	Yes	Yes	Yes	Yes	Yes	Yes	Low

Low bias = 1 or fewer questions with the answer of “unclear,” Unclear bias = 2 questions with the answer of “unclear” or 1 with the answer of “no,” high risk of bias = 3 or more questions with the answer of “unclear” or 2 questions with the answer of “unclear” and 1 with the answer of “no” or 2 questions with the answer of “no”

Table A3. Data for HM, neutropenia status, inclusion of chemotherapy, and outcome of individual patients from included studies.

Patient #	Underlying Disease	Reported ANC or WBC Status (cells/ul)	Chemotherapy	Outcome
1	CLL	<100	yes	Survived
2	CLL	7100	no	Survived
3	ALL	≤500	yes	Survived
4	ALL	≤500	yes	Died
5	AML	NA	NA	Died
6	AML	NA	yes	Died
7	MM	Neutropenic	yes	Died
8	ALL	NA	NA	Survived
9	AML	NA	NA	Died
10	ALL	NA	NA	Survived
11	NHL	>550	yes	Died
12	NHL	≤500	yes	Died
13	NHL	≤500	yes	Died
14	NHL	<500	yes	Died
15	NHL	<500	yes	Died
16	ALL	<500	yes	Died
17	ALL	NA	NA	Died
18	AML	NA	NA	Survived
19	AML	<100	yes	Died
20	AML	<100	yes	Died
21	ALL	<100	yes	Died
22	ALL	Granulocytopenia	yes	Survived
23	AML	Granulocytopenia	yes	Died
24	NHL	NA	yes	Died
25	NHL	Not neutropenic	yes	Died
26	NHL	<500	yes	Survived
27	AML	NA	yes	Survived
28	AML	NA	yes	Survived
29	AML	NA	yes	Died
30	AML	NA	yes	Survived
31	CLL	NA	yes	Died
32	CLL	Not neutropenic	no	Died
33	ALL	NA	yes	Survived
34	ALL	NA	yes	Survived
35	AML	<100	yes	Died
36	ALL	<100	yes	Died
37	AML	<100	yes	Died
38	ALL	<100	yes	Died
39	AML	<100	yes	Died
40	ALL	<100	yes	Died
41	NHL	NA	NA	Died

42	AML	NA	NA	Survived
43	AML	1,200^	yes	Survived
44	AML	10,200^	no	Survived
45	NHL	650^	yes	Died
46	ALL	220^	yes	Died
47	AML	<500	yes	Died
48	AML	NA	yes	Survived
49	ALL	480	yes	Survived
50	AML	100	yes	Survived
51	ALL	NA	yes	Survived
52	AML	1100^	yes	Died
53	AML	NA	yes	Died
54	NHL	1500	yes	Died
55	ALL	4500^ (38% neutrophils)	yes	Died
56	AML	3393	no	Died
57	ALL	3900^	yes	Died
58	ALL	NA	yes	Died
59	AML	NA	no	Survived
60	AML	NA	yes	Survived
61	AML	Neutropenic	yes	Died
62	CLL	<100	yes	Survived
63	AML	<500	yes	Survived
64	AML	Neutropenic	yes	Survived
65	AML	2,420^	NA	Survived
66	ALL	NA	yes	Survived
67	CML	Neutropenic	yes	Died
68	ALL	<500	yes	Survived
69	CLL	1000	no	Survived
70	CLL	3200^	no	Survived
71	ALL	Neutropenic	yes	Survived
72	AML	Neutropenic	yes	Survived
73	CLL	2600	no	Survived
74	ALL	Neutropenic	yes	Survived
75	ALL	Neutropenic	yes	Died
76	ALL	NA	yes	Survived

^ = White blood cell count. Abbreviations: ANC = Absolute neutrophil count; WBC = White blood cell; NA = Data not available; AML = Acute myeloid leukemia; ALL = Acute lymphocytic leukemia; CML = Chronic myeloid leukemia; CLL = Chronic lymphocytic leukemia; NHL = non-Hodgkin's lymphoma; MM = Multiple myeloma.

APPENDIX B

SUPPORTING INFORMATION FOR CHAPTER 4

Table B1: Antibodies for flow cytometry

ANTIBODY	FLUOROCHROME	DILUTION (1:___)	CAT#	VENDOR
LIVE/DEAD	Aqua	-	L34957	Invitrogen
CD45	APC/Cy7	200	103116	BioLegend
CD11B	BV605	200	101257	BioLegend
CD11C	PE	100	117308	BioLegend
LY6C[^]	PerCP/Cy5.5	100	128012	BioLegend
MHC II	PE/Cy7	200	107630	BioLegend
LY6G	AF700	50	127622	BioLegend
SIGLEC F	APC	200	130-102-241	Miltenyi Biotec
CD3	AF700	100	100216	BioLegend
CD4	PE/Cy7	200	100422	BioLegend
CD25	PE	200	101903	BioLegend
CD1D[^]	APC	100	55059	Tetramer Core NIH
TCRGD	PerCP/Cy5.5	100	118117	BioLegend
CD8	PE/Dazzle	125	100762	BioLegend
NK1.1	FITC	100	11-5941-82	eBioscience
CD19	BV605	200	115540	BioLegend
CD206	PE/Dazzle	50	141731	BioLegend
CD86	AF700	100	105024	BioLegend
ASCA-2	PE	50	130-123-284	Miltenyi Biotec
A2B5	FITC	100	FAB1416G	R&D
GFAP[*]	eFluor660	100	50-9892-82	eBioscience
TMEM119[*]	PE/Cy7	100	ab209064	Abcam

[^]Compensation stained on live cells

^{*}Intracellular

Table B2: Bioplex Mouse Cytokine/Chemokine Magnetic Bead Panel - Premixed 32 Plex - Immunology Multiplex Assay

Analytes			
Eotaxin/CCL11	G-CSF	GM-CSF	IFN- γ
IL-1 α	IL-1 β	IL-2	IL-3
IL-4	IL-5	IL-6	IL-7
IL-9	IL-10	IL-12 (p40)	IL-12 (p70)
IL-13	IL-15	IL-17	IP-10/CXCL10
KC/CXCL1	LIF/CXCL9	LIX/CXCL5	MCP-1/CCL2
M-CSF	MIG/CXCL9	MIP-1 α	MIP-1 β
MIP-2	RANTES	TNF- α	VEGF

Table B3: Additional bioplex data

Chemokines and cytokines	IN+IV		IN+Steroid		IN+IV+Steroid		<i>P</i>	<i>P</i>
	Mean (pg/ml)	SEM	Mean (pg/ml)	SEM	Mean (pg/ml)	SEM	IN+IV : IN+IV+Steroid	IN+Steroid : IN+IV+Steroid
<i>IL-2</i>	9.6	1.7	8.5	1.5	9.9	1.3	0.6493	0.4964
<i>IL-7</i>	1.2	0.39	1	0.49	1.2	0.35	0.963	0.8402
<i>IL-10</i>	11.7	2.9	7.5	1.5	11.5	1.9	0.9674	0.1752
<i>IL-12 (p40)</i>	1.5	0.69	0.49	0.39	2.5	0.79	0.3771	0.0915
<i>IL-12 (p70)</i>	5.9	0.5	5.9	0.45	7.1	0.72	0.2207	0.2362
<i>IL-13</i>	126.4	3.8	101.7	0.97	11.8	2.9	0.0098 (**)	0.0245 (*)
<i>IL-15</i>	50.5	2.3	54.9	5.3	49.5	1.4	0.6789	0.2495
<i>MCP-1</i>	65.29	11.6	14.9	4	69.3	6.5	0.7554	<0.0001 (****)
<i>MIP-1β</i>	15.3	1.7	10.8	0.99	12.8	1.2	0.24	0.2782
<i>MIP-2</i>	86.8	14.5	35.5	3.3	78.6	12.8	0.6821	0.0254 (*)
<i>TNF-α</i>	1.9	0.22	0.2	0.1	2.2	0.43	0.5147	0.0036 (**)
<i>LIF</i>	6.8	2.8	0.44	0.15	2.6	0.37	0.1003	0.0011 (**)
<i>M-CSF</i>	21.7	1.1	14	0.55	20.5	1.1	0.4629	0.0010 (***)

Info for Table C3. The disseminated CA model results in a significant impact to the inflammatory cytokine and chemokine population in the brain. C57Bl/6 mice were randomly assigned to the experimental disseminated CA, immunocompetent control, or immunosuppressed control group and subjected to immunosuppression and inoculation with *A. fumigatus* as in Figure __. At DPI 4 half of the brain was collected for cytokine and chemokine analysis, homogenized, and clarified. The levels were quantified by Luminex-based MILLIPLEX assessment. The table illustrates cumulative data from two independent studies (n = 3–4 mice per group per study). Unpaired two-tailed Student's t-test.

Note: IL-3, IL-4, IL-5, IL-9, LIX, MIG, RANTES were measured but expression was either absent amongst the groups, or the concentration was too low to detect within the sample.

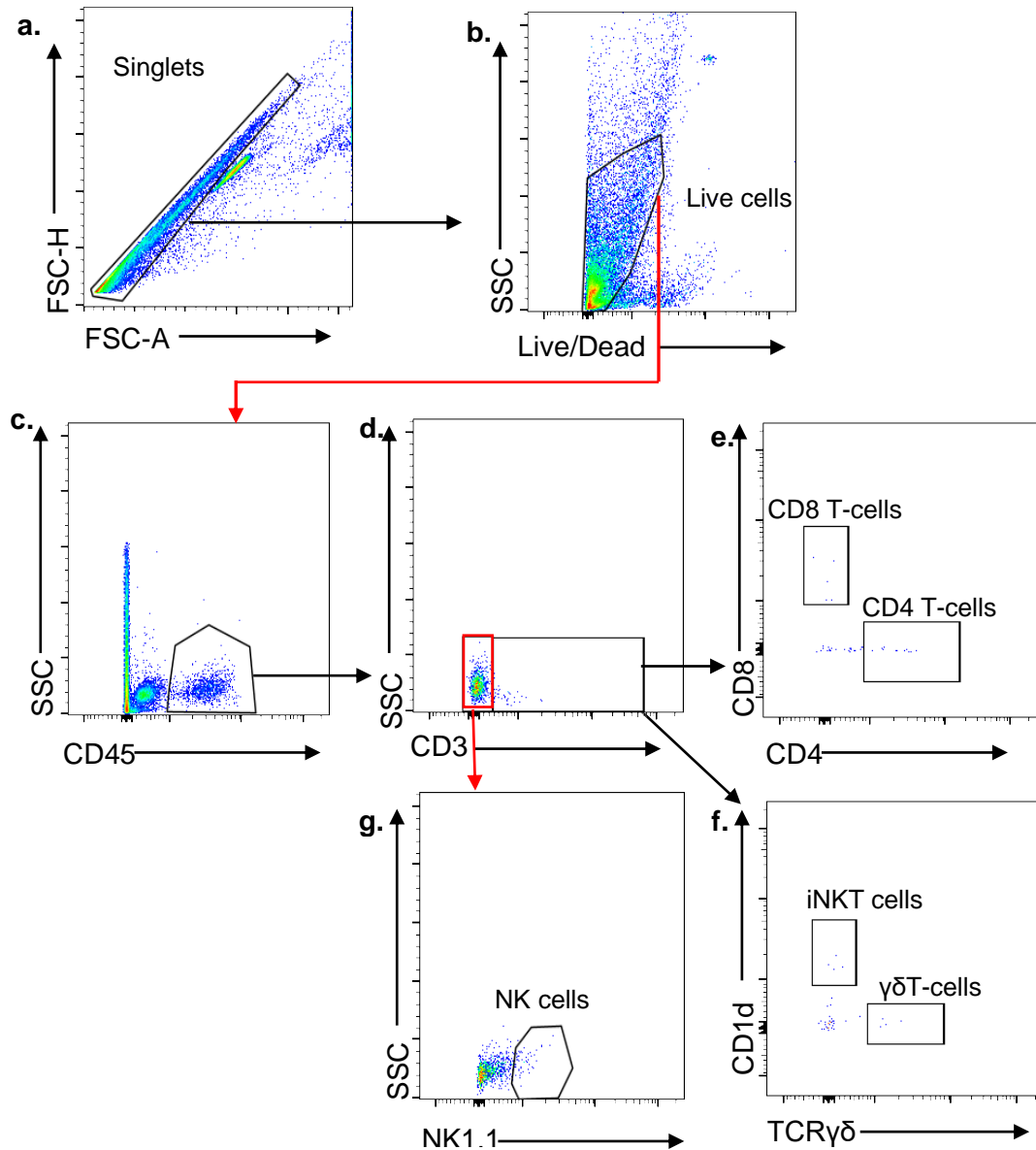


Figure B1. Gating strategy for flow cytometry for lymphoid-lineage cells in the brain.

Representative flow cytometry profiles from individual central nervous system suspensions, showing gating strategy used for flow cytometry for lymphoid-lineage cells. **a.** First doublets were excluded based on FSC-H, FSC-A, **b.** from which a live gate was established, **c.** then a CD45 gated was established, **d.** followed by a CD3 gate. **e.** CD45^{hi}CD3⁺ T-cell populations were discriminated based on CD8 (CD8 T-cells) and CD4 (CD4 T-cells) expression, **f.** or CD1d (iNKT cells) and $\gamma\delta$ TCR ($\gamma\delta$ T-cells) expression. **g.** CD45⁺CD3⁻ population was further gated on NK1.1 (NK cells) expression.

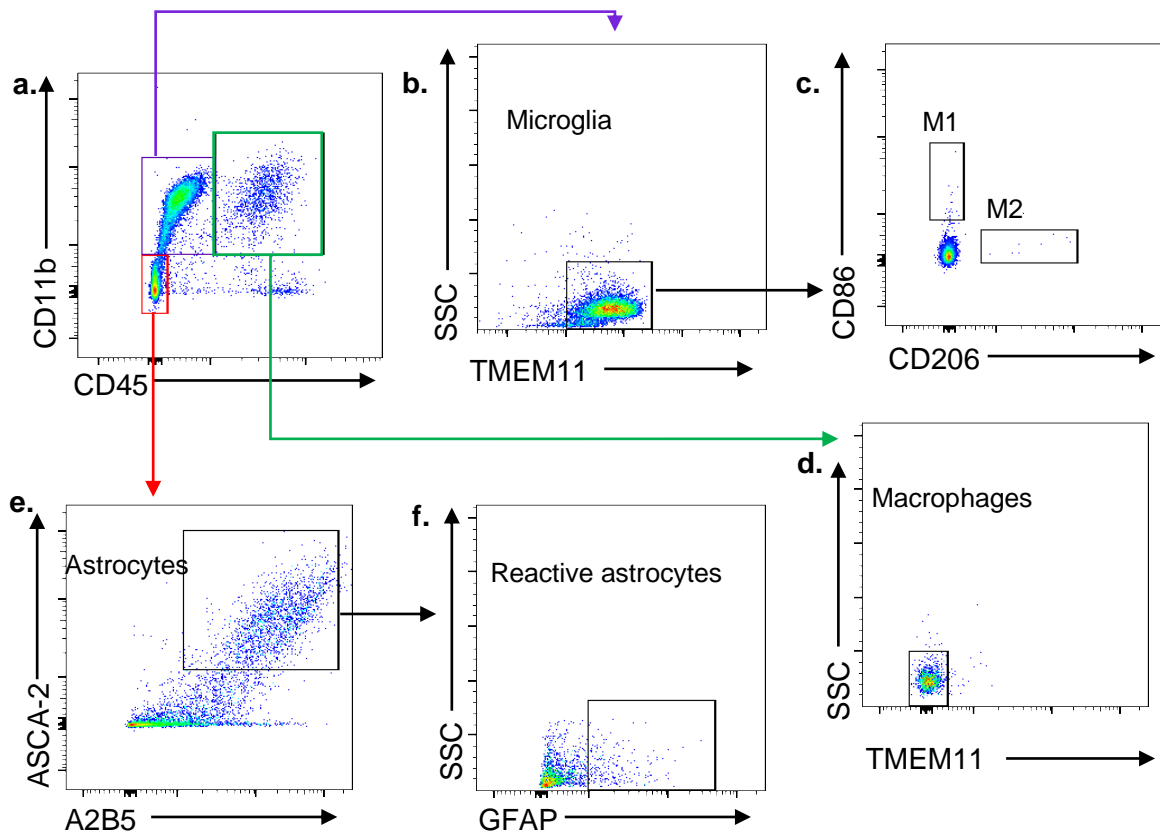


Figure B2. Gating strategy for flow cytometry for resident immune cells in the brain and infiltrating macrophages.

Representative flow cytometry profiles from individual central nervous system suspensions, showing gating strategy used for flow cytometry for resident immune cells in the brain and infiltrating macrophages. **a-f.** First doublets were excluded based on FSC-H, FSC-A from which a live gate was established as per Figure C1. **a.** A CD45 CD11b gate was established from the live cell singlet gates. **b.** Microglia were gated on CD11b+ CD45^{lo} expression (purple, **a.**), then further discriminated by TM119+ expression. **c.** From this, the microglia subsets were established based on CD86 (M1) and CD206 (M2) expression. **d.** Macrophages were discerned from the CD11b+ CD45^{hi} (green, **a.**) expression and further established by exclusion of TMEM119 expression. **e.** Astrocytes discrimination was initiated by absence of CD45 and CD11b (red, **a.**) expression followed by gating for ASCA-2+ and A2B5+ expression. **f.** Reactive astrocytes were discriminated from ASCA-2+ and A2B5+ gated cells and discriminated by GFAP expression.

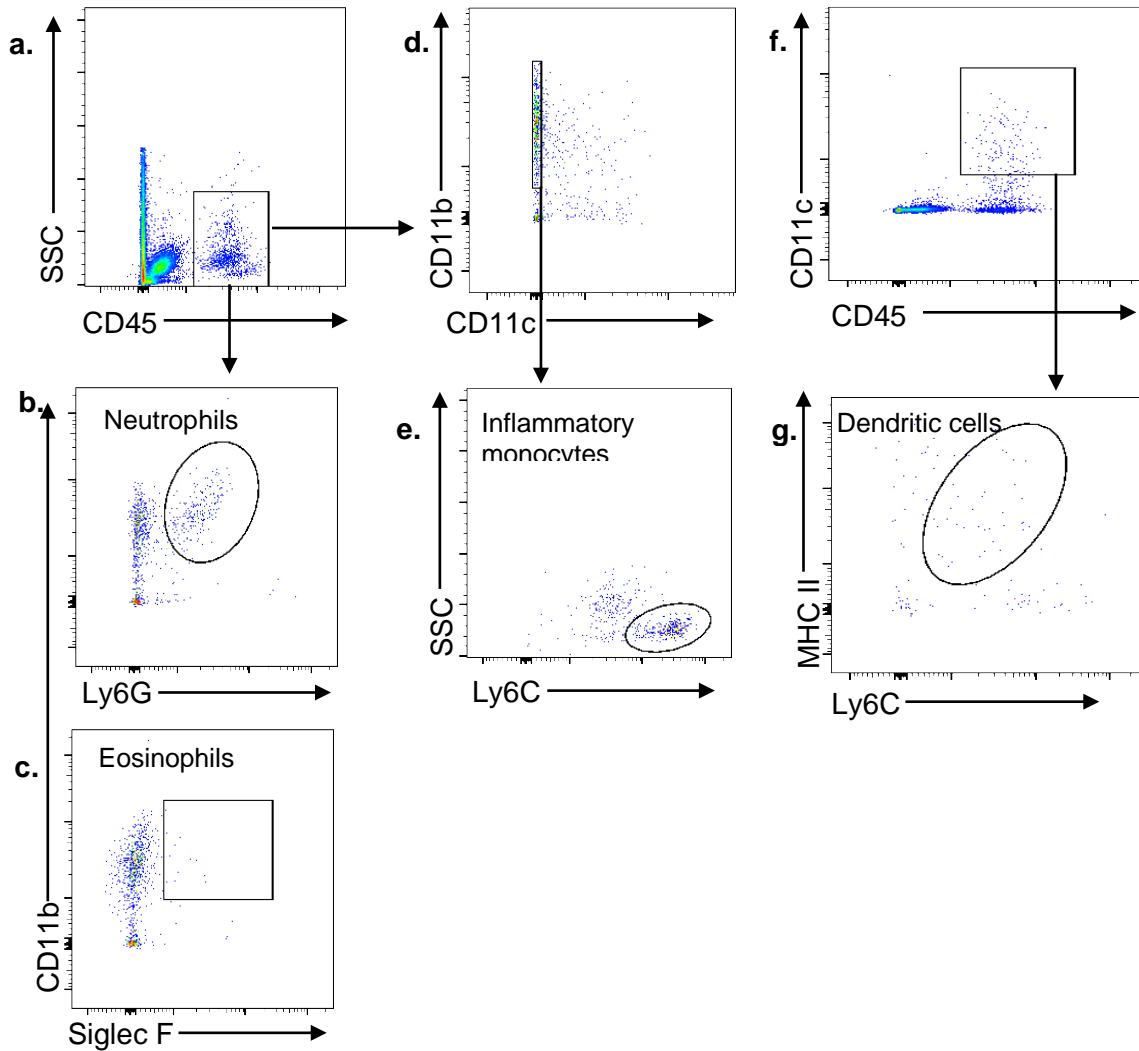


Figure B3. Gating strategy for flow cytometry for infiltrating myeloid-derived cells in the brain.

Representative flow cytometry profiles from individual central nervous system suspensions, showing gating strategy used for flow cytometry for infiltrating myeloid-derived cells. **a-e.** First doublets were excluded based on FSC-H, FSC-A from which a live gate was established as per Figure C1. **a.** A CD45 gate was established from the live cell singlet gates. **b.** Neutrophils were discriminated from CD45^{hi} cells by CD11b⁺ and Ly6G⁺ expression. **c.** Eosinophils were discriminated from CD45^{hi} cells by CD11b⁺ and Siglec F⁺ expression. **d.** Inflammatory monocytes were discriminated from CD45^{hi} cells first establishing a CD11b⁺ and CD11c⁻ gate, **e.** followed by gating for Ly6C^{hi} expression. **f.** A CD45⁺ CD11c⁺ gate was established from the live cell singlet gates. **g.** Dendritic cells were discriminated by MHC II⁺ and Ly6C⁺ expression.

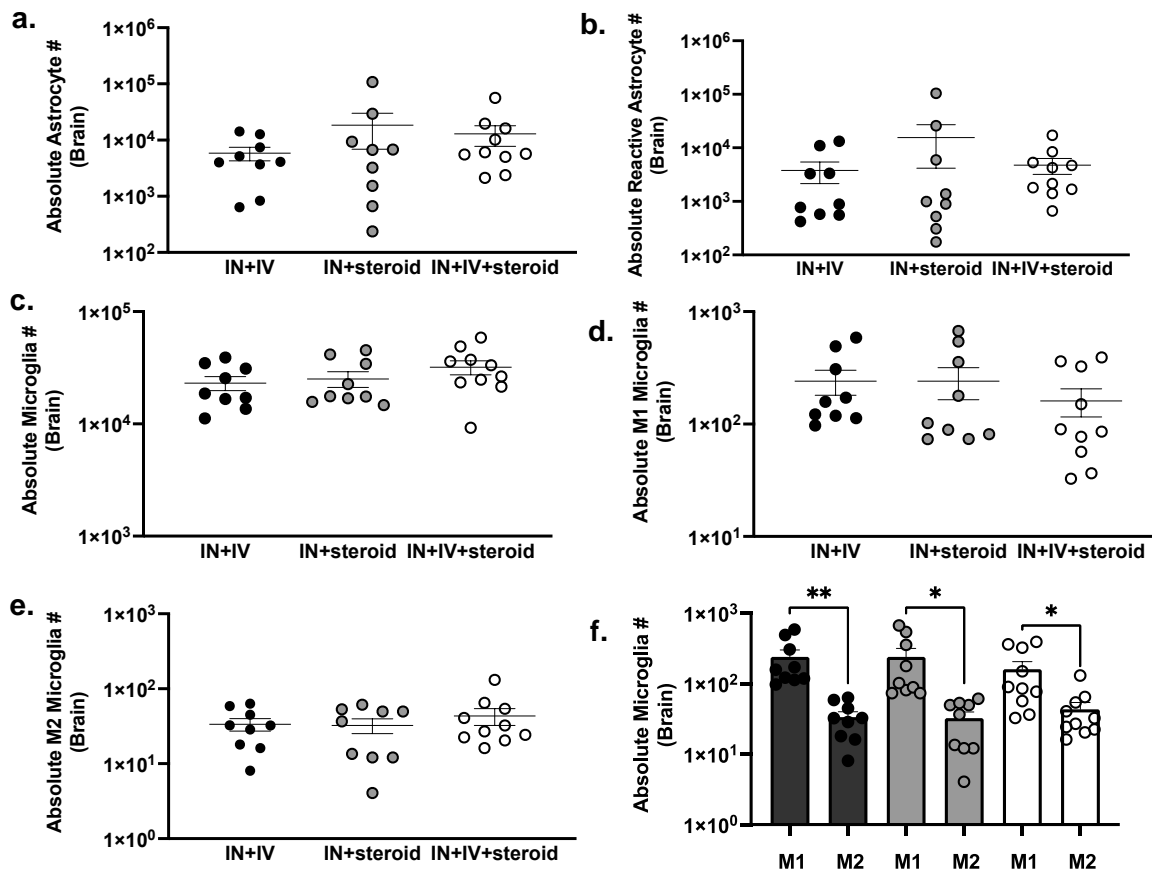


Figure B4. Certain cell populations were unaffected in the brain of disseminated CA model mice compared to control mice.

a – f. C57Bl/6 mice were randomly assigned to the experimental disseminated CA model, IN+IV control, or IN+steroid control group and subjected to immunosuppression and infection with *A. fumigatus* as in Figure 3.3. At DPI 4, whole brains were collected, mononuclear cells isolated following enzymatic digestion, and quantified by flow cytometry. **a.** Astrocytes (CD45-CD11b-ASCA-2+A2B5+), **b.** reactive astrocytes (CD45-CD11b-ASCA-2+A2B5+GFAP+) **c.** Microglia (CD45intCD11b+TMEM119+), **d.** M1 microglia (CD45intCD11b+TMEM119+CD86+CD206-), **e.** M2 microglia (CD45intCD11b+TMEM119+CD86-CD206+), were quantified by flow cytometry. **f.** M1:M2 ratios were compared between each group. The figure illustrates cumulative data from three independent studies ($n = 3-4$ mice per group per study). Each data point represents an individual sample. The line within a given group represents the mean + SEM. For all graphs, * and ** represent P values of <0.05 and <0.01 , respectively; (unpaired two-tailed Student's t-test.)

APPENDIX C

AGE-ASSOCIATED NEUROLOGICAL COMPLICATIONS OF COVID-19: A SYSTEMATIC REVIEW AND META-ANALYSIS

C.1 Introduction

Infectious disease, ranging in severity from symptoms of a mild cold to severe acute respiratory distress are attributed to coronaviruses (CoV)s. The majority of this large family of viruses are transmitted among non-human species, however, occasional zoonosis has resulted in seven known CoV strains that infect and cause disease in humans. Of these, three human CoVs (huCoVs) strains have emerged over the past two decades that can promote severe disease and even death. Severe acute respiratory coronavirus (SARS-CoV) and Middle East respiratory syndrome (MERS)-CoV, emerged in 2003 and 2012, respectively, causing significant global illness and mortality [339, 340]. In December 2019, a novel CoV strain, now designated SARS-CoV-2, was first reported to infected humans and cause severe disease, termed CoV disease-19 (COVID-19). While most individuals with COVID-19 experience mild to moderate symptoms, others develop more severe disease, leading to death in a subset of these patients. Rapid transmission of the virus has resulted in a global pandemic resulting in hundreds of millions of infections and millions of deaths, worldwide, that remains on-going at the time of this review [341, 342].

Although primarily considered a virus impacting the respiratory system, an increasing number of case studies have highlighted substantial neurological consequences of SARS-CoV-2 infection. Indeed, the Centers for Disease Control (CDC) lists new confusion or

the inability to arouse as indicators of severe COVID-19 presentation, necessitating emergency medical attention [343]. Early reports from Wuhan, China alerted the neuroinvasive potential of SARS-CoV-2, as multiple patients developed headache and dizziness, anosmia, and/or ageusia, which were often reported as initial symptoms of infection and disease [341, 344-346]. In addition, acute onset of more serious neurological symptoms, including altered mental status (encephalopathy), meningoencephalitis, demyelinating diseases, and stroke are increasingly reported in SARS-CoV-2 infected patients [347-352]. Many reports that reveal the age of the subjects studied suggest that patients older than 50 years are more likely to experience severe neurological complications, however, varying new onset neurological manifestations have also been reported among younger individuals and appear to be a common complication of COVID-19. As such, there is a critical need for investigating the impact of COVID-19 on the central nervous system (CNS). Here, we present evidence for a direct or indirect role of SARS-CoV-2 in promoting neurological disease in individuals across the lifespan via a systematic review of the literature and meta-analyses. We also discuss potential pathophysiology of SARS-CoV-2-associated CNS injury and the potential for long-term neurological complications of infection in recovered patients, including the potential impact of disease on pathological brain aging.

C.2 Methods

Search strategy and study selections

A systematic review was conducted for the purposes of identifying the population of COVID-19 patients diagnosed with new onset neurological condition(s) during the disease course. This review was designed and organized in accordance with the Preferred Reporting Items for Systematic Reviews (PRISMA) guidelines [353]. The database PubMed-NCBI was systematically searched for peer-reviewed literature presenting original clinical data of COVID-19 patients diagnosed with a neurological condition. The search of PubMed-NCBI alone is considered comprehensive and reliable, as over 90% of MEDLINE is covered by this database, thus the search of additional databases was deemed unnecessary [354]. Manuscripts published from 2019 – April 4, 2021 were interrogated using the following search terms: (“COVID-19” OR “SARS-CoV-2”) AND (“Brain” OR “Neuro” OR “Stroke” OR “Seizure” OR “Anosmia” OR “Ageusia” OR “Guillain-Barré” OR “Headache” OR “Dizziness” OR “Confusion” OR “Impaired Consciousness” OR “Seizure” OR “Encephalopathy” OR “Meningitis”) NOT “review”. The search was restricted to full text peer-reviewed reports available in English containing original clinical data. Preprint articles were not included. The purpose of this systematic review and meta-analysis was to assess the type and incidence of neurological complications of COVID-19 in relation to age. As such, only published articles with original clinical data containing the following criteria were included: (1) age of patient(s) featured in the study, (2) a diagnosis of new onset neurological manifestations, and (3) laboratory-confirmed SARS-CoV-2 infection. Exclusion criteria included: (1) any known pre-existing neurological conditions, (2) known co-current viral or parasitic infection, and/or (3) opinions, viewpoints, personal anecdotes, and reviews. Seizure was reported in a SARS-CoV-2 positive 6-week-old male [355], however, this case was excluded from analysis because a history of seizure could not be ruled out, due to the young age. An 80-year-old woman with Alzheimer’s dementia,

who developed stroke [356] and a 52-year-old HIV-infected woman with posterior reversible encephalitic syndrome (PRES) [357] were also excluded from analyses, as these comorbidities could not be ruled-out as significant confounders to the development of neurological disease in the context of COVID-19.

Data extraction and synthesis

Articles vetted for inclusion were independently reviewed by BNS and TF, and the following information was extracted for analysis: age, gender, neurological manifestation, COVID-19 symptom severity, comorbidities, and presence of virus in CSF or autopsied brain. All data were captured and maintained in a Microsoft Excel workbook. Any disagreement regarding inclusion was resolved by discussion.

To reduce the effects of heterogeneity among the case reports, neurological diagnoses/symptoms were evaluated and categorized as cerebrovascular disease (CVD), peripheral neuropathy, encephalopathy, demyelinating disease, smell and/or taste disorder, and CNS inflammatory disease. The category “other” was included to capture patients who exhibited neurological symptoms, but the underlying cause was not determined or identified. This is expanded in Supplementary Table C1. Dichotomous outcomes were created for each category of CNS disease for statistical tests. Reported comorbidities were also reduced to dummy variables for assessing potential relationships with hypertension (HTN), diabetes mellitus (DM), lipid disorder, obesity, none, and other. This is expanded in Supplementary Table C2. For analyses, comorbidities were scaled based on their overall relationship with CVD, which had the strongest association with age and COVID-19 severity. Scores were designed as follows: None = 0, other = 1, obesity = 2, lipid disorder = 3, DM = 4, HTN = 5. This allowed for the inclusion of multiple reported comorbidities by synthesizing a “comorbidity score” for each patient equal to the sum of the individual scores. For example, a patient with HTN and DM would have a comorbidity

score = 9. “None” includes only reports that specifically stated no comorbidities. Reports that did not include comorbidities were excluded from analyses that required these data. COVID-19 severity was converted to ordinal variables as follows: asymptomatic = 0, mild = 1, moderate = 2, severe = 3, critical = 4.

Statistical analyses

Statistical tests were performed using Prism 9 for MacOS (v9.1.1) and the on-line statistics software, Intellectus Statistics (2021; <https://analyze.intellectusstatistics.com>). Graphs were constructed with Prism and Microsoft Excel. Summary statistics for individual patient data were calculated for each variable. A general assessment of the relationship between age and each neurological disease category was conducted through simple linear regression using dummy coding (dichotomous outcomes) for the neurological disease category. Pearson correlation matrices were constructed to assess pair-wise relationships between variables. Cohen's standard was used to evaluate the strength of the relationships, where coefficients between ± 0.10 and ± 0.29 represent a small effect size, coefficients between ± 0.30 and ± 0.49 represent a moderate effect size, and coefficients of ± 0.50 and above indicate a large effect size [358]. The result of the correlations was examined using Holm corrections to adjust for multiple comparisons based on $\alpha = 0.05$. Analysis of variance (ANOVA) was conducted to assess if there were significant differences in COVID-19 severity or comorbidities score between the levels of neurological disease category. Tukey pairwise comparisons were conducted for all significant effects based on $\alpha = 0.05$. For each statistical test, only data from patients with all variables investigated were included. Cases with missing data were excluded from analysis. As such, the n for each test or summary is reported.

Table C1. Total number (n=584) and percent of each neurological condition reported in patients diagnosed with COVID-19 per decade of age.

Age range	≤ 9	10-19	20-29	30-39	40-49	50-59	60-69	70-79	≥ 80
# Cases reported	7	22	19	60	72	100	154	121	29
Neurological Diagnosis	N (%) [reference]								
Cerebrovascular Diseases	2 (28.6) [356, 359]	3 (13.6) [360-362]	3 (15.8) [361, 363, 364]	19 (31.7) [363, 365-379]	31 (43.1) [363, 366, 368, 375, 377, 378, 380-394]	46 (46.0) [356, 368, 370, 371, 374, 375, 377, 378, 382, 384, 387-391, 393, 395-410]	70 (45.5) [356, 357, 360, 368, 370, 371, 375-379, 382, 386, 387, 390, 393, 397, 400, 401, 403, 406, 410-429]	69 (57.0) [356, 368, 371, 374, 375, 378, 382, 386, 391-393, 397-401, 403, 405, 406, 421, 430-438]	21 (72.4) [356, 368, 375, 379, 400, 403, 406, 415, 430, 431, 433, 439]
Peripheral Neuropathies		2 (9.1) [440, 441]	2 (10.5) [442, 443]	6 (10.0) [444-449]	8 (11.1) [450-457]	15 (15.0) [443, 447, 451, 454, 458-469]	12 (7.8) [443, 466, 470-479]	16 (13.2) [443, 448, 451, 452, 457, 478, 480-484]	2 (6.9) [452, 454]
Encephalopathies	2 (28.6) [485, 486]		2 (10.5) [392, 487]	7 (11.7) [379, 488-493]	9 (12.5) [489, 494-501]	11 (10.0) [357, 383, 405, 499, 502-508]	25 (16.2) [379, 417, 419, 424-426, 489-492, 494, 499, 500, 505, 506, 509-512]	14 (11.6) [391, 401, 405, 498, 500, 505, 506, 510, 513-518]	2 (6.9) [379, 500]
Demyelinating Diseases		1 (4.5) [519]		2 (3.3) [392, 520]	2 (2.8) [521, 522]	7 (7.0) [520, 522-527]	4 (2.6) [410, 427, 470, 509]	3 (2.5) [520, 528, 529]	

Smell and/or Taste Disorder	8 (36.4) [530-533]	5 (26.3) [487, 534-537]	9 (15.0) [449, 538-540]	8 (11.1) [452, 457, 501, 538, 539, 541, 542]	4 (4.0) [402, 538, 543]	10 (6.5) [477, 500, 538, 544-547]	4 (3.3) [452, 457]	2 (6.9) [538, 546]	
CNS Inflammatory Diseases	3 (42.9) [548-550]	4 (4.5) [551-553]	3 (15.8) [536, 554, 555]	7 (11.7) [490, 556-560]	5 (6.9) [392, 393, 561-563]	13 (13.0) [393, 400, 564-567]	18 (11.7) [393, 400, 512, 547, 568-571]	6 (5.0) [393, 400]	1 (3.4) [400]
Other	4 (18.2) [531, 572]	4 (21.1) [573-575]	10 (16.7) [379, 448, 491, 573, 576, 577]	9 (12.5) [393, 542, 573, 574]	4 (4.0) [393, 578, 579]	15 (9.7) [379, 393, 491, 544, 545, 573, 574, 580, 581]	9 (7.4) [393, 448, 574, 582-584]	1 (3.4) [379]	

C.3 Results

Search results and population characteristics

Of an initial 4,611 records retrieved, 4,372 were excluded as per our exclusion criteria (Figure C1). A total of 239 articles were included in an overall assessment for the prevalence of neurological conditions reported in all patients with confirmed COVID-19 ($n = 2,307$) (Figure C2). The prevalence of COVID-19 patients with neurological conditions were assessed by age (years) from a total of 230 articles ($n = 584$) in which individual ages could be extracted (Table C1). Patient diagnoses were categorized under the following general neurological conditions: cerebrovascular disease (CVD), peripheral neuropathies, encephalopathies, demyelinating diseases, smell and/or taste disorders, and CNS inflammatory diseases. An additional category of 'other' was ascribed to patients who exhibited neurological symptoms, but the underlying cause was not determined or identified (Figure C2). Smell and/or taste disorders were the most prevalent neurological manifestation with 1,303 cases identified, or 56.5% of the total. CVD, including stroke and microhemorrhages, was seen less frequently, but impacted approximately one quarter of the total ($n = 584$). Each of the remaining neurological conditions comprised less than ten percent of the total reported with encephalopathy and 'other' accounting for 5.3% ($n = 122$) and 6.8% ($n = 156$), respectively. Less prevalent, but nonetheless significant neurological conditions also reported include peripheral neuropathy [e.g., Guillain-Barré Syndrome (GBS) and critical illness neuromyopathy (CIM)], CNS inflammatory disease (e.g., encephalitis and myelitis), and demyelinating disease [e.g., multifocal demyelinating lesions and acute disseminated encephalomyelitis (ADEM)], constituting a respective 3.3% ($n = 75$), 2.1% ($n = 49$), and 0.8% ($n = 18$) of the total subjects.

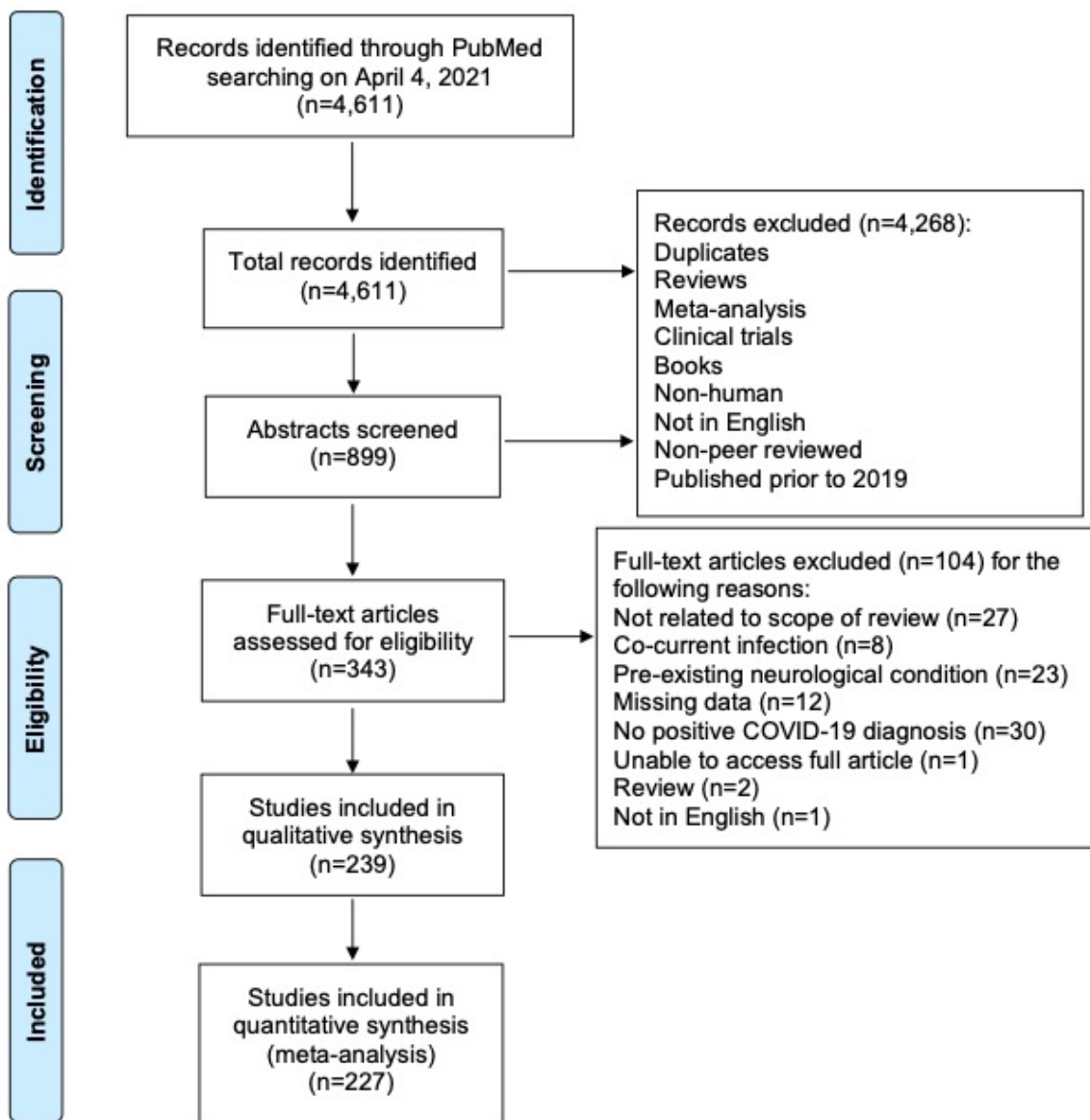


Figure C1. Flow chart of systematic literature search and screening for studies of COVID-19 patients with neurological conditions

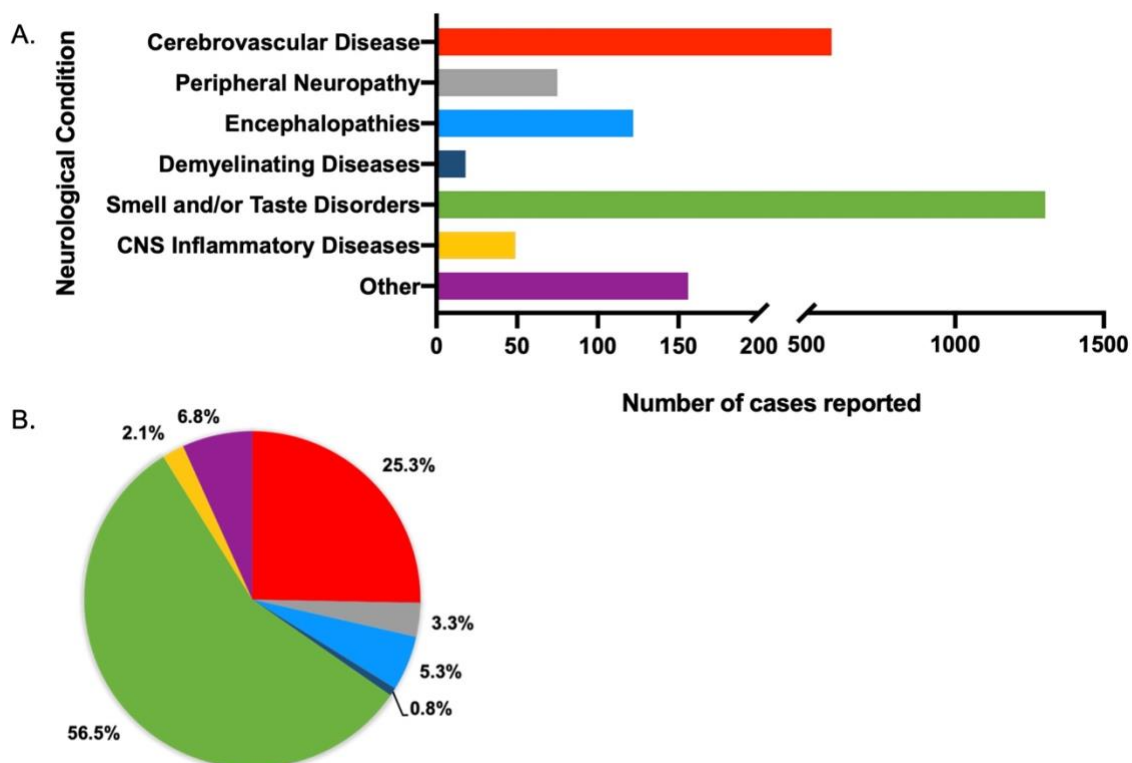


Figure C2. Total number (A) and percent of (B) reported neurological conditions occurring in patients, regardless of demographics (total $n = 2,390$). Individual diagnoses have been categorized as cerebrovascular diseases ($n = 592$), peripheral neuropathies ($n = 75$), encephalopathies ($n = 175$), demyelinating diseases ($n = 23$), smell and/or taste disorders ($n = 1,303$), CNS inflammatory diseases ($n = 45$), and other (neurological symptoms that cannot be attributed to a specific neurological condition, such as headache, seizure, ataxia, aphasia) ($n = 177$).

Summary of individual patient data for meta-analyses

Data of 510 patients were extracted from 227 published reports, from which age and neurological complication could be matched. When possible, sex, COVID-19 severity, comorbidities, and the presence of detectable virus in cerebrospinal fluid (CSF) were also captured. As described above, neurological diagnoses were broadly categorized under CVD, CNS inflammatory disease, demyelinating disease, encephalopathy, peripheral neuropathy, taste/smell disorders, and other. Frequencies and percentages of individual diagnoses included under these categories are listed in Supplementary Table C1. The most frequently reported CVD was stroke of various types ($n = 230$, 89%). Among CNS inflammatory diseases, meningoencephalitis was most frequently observed ($n = 22$, 47%). Acute disseminated encephalomyelitis (ADEM) was the most frequently reported demyelinating disease ($n = 9$, 60%). Within the category of encephalopathy, a diagnosis of various types of encephalopathy were reported with the highest frequency ($n = 47$, 83%), while different manifestations of GBS were the most frequently observed peripheral neuropathy ($n = 54$, 84%). Loss of smell (anosmia) was the most frequent complication of taste/smell disorders ($n = 11$, 31%) and various manifestations of headache ($n = 18$, 49%) were the most frequently reported neurological manifestation categorized as “other”, which includes neurological manifestations for which the underlying cause was not identified.

Comorbidities were reported for 363 of the 510 patients for which individual patient data could be extracted. Risk factors for cardiovascular disease, including hypertension (HTN), diabetes mellitus (DM), obesity, and hyperlipidemia, were the most frequent comorbidities among COVID-19 patients with neurological manifestations (Supplementary Table C2). To assess the association of the stated comorbidities with neurological manifestations, comorbidities were limited to HTN, DM, obesity, and lipid disorders, which includes hyperlipidemia, dyslipidemia, and hypercholesterolemia. All other reported comorbidities were included as “other”.

Although the number of males outnumbered females, the mean age did not differ significantly between the two sexes, or from the mean age of a cohort of individuals for which sex was not specified (Table C2). Summary statistics for individual patient data were calculated for each variable, and frequencies and percentages were split by sex and reported in Table C3. Frequencies and percentages were only calculated on available data (*n/a* = not available excluded). This is reflected in the *n* reported for each variable. The most frequently observed neurological disease category for all patients regardless of sex, specified or not, was cerebrovascular disease (*n* = 257, 50% of total). Moderate COVID-19 severity was most often reported for all male and female subjects, however, patients for which sex was not specified (*n* = 57), severe COVID-19 was most frequently reported. Although no comorbidities (none) appear to be most frequently reported among all subjects (*n* = 131, 36%), when taken together, HTN, with and without additional comorbidities, is most frequently reported *in toto* (*n* = 165, 45%), as well as separately among males (*n* = 96, 46%) and persons for which sex was not specified (*n* = 27, 57%). No comorbidities (none) and HTN, with and without additional comorbidities, were equally reported among females (*n* = 42, 39%). CSF was assessed for detectable virus in 122 of the total 510 patients but only identified in four cases (Table C3), including a 31-year-old male and a 74-year-old female with altered mental status, a 24-year-old male with meningoencephalitis, and a 68-year-old male who developed stroke [411, 515, 554, 585].

Finally, frequencies and percentages were calculated for neurological disease category split by COVID-19 severity (*n* = 495; Table C4). Regardless of disease severity, CVD was the most frequently observed category of neurological disease, which may reflect a more serious injury, such as stroke, being more likely to prompt a case report. It is important to note, however, that CVD may be seen in the context of SARS-COV-2 infection among individuals with few or no other symptoms typically associated with COVID-19.

Table C2. Summary statistics for age of patients in toto and by sex.

Sex	Mean age (years)	<i>SD</i>	<i>n</i>	<i>SE_M</i>	Min (years)	Max (years)
all subjects	55.37	18.16	510	0.80	2	94
male	55.55	17.75	278	1.06	2	94
female	54.33	19.99	175	1.51	3	92
not specified	57.67	13.74	57	1.82	31	93

Table C3. Frequencies and percentages of neurological disease, COVID-19 severity, comorbidities, and detectable virus in CSF by sex.

Variable	<i>n</i>	female	male	not specified
Neurological disease category	510			
Cerebrovascular disease		68 (39%)	133 (48%)	56 (98%)
CNS inflammatory disease		20 (11%)	26 (9%)	0 (0%)
Demyelinating disease		6 (3%)	8 (3%)	1 (2%)
Encephalopathy		25 (14%)	32 (12%)	0 (0%)
Taste/smell disorders		21 (12%)	15 (5%)	0 (0%)
Peripheral neuropathy		19 (11%)	44 (16%)	0 (0%)
Other		16 (9%)	20 (7%)	0 (0%)
COVID-19 severity	495			
asymptomatic		20 (12%)	16 (6%)	3 (5%)
mild		21 (12%)	44 (16%)	2 (4%)
moderate		61 (36%)	73 (27%)	10 (18%)
severe		31 (18%)	67 (25%)	35 (61%)
critical		37 (22%)	68 (25%)	7 (12%)
Comorbidities (reclassified)	363			
none		42 (39%)	78 (37%)	11 (23%)
DM		2 (2%)	17 (8%)	2 (4%)
DM, lipid disorder		1 (1%)	1 (0%)	2 (4%)
DM, obesity		1 (1%)	0 (0%)	0 (0%)
DM, other		1 (1%)	1 (0%)	1 (2%)
HTN		20 (19%)	27 (13%)	8 (17%)
HTN, DM		5 (5%)	24 (11%)	0 (0%)
HTN, DM, lipid disorder		1 (1%)	3 (1%)	5 (11%)
HTN, DM, lipid disorder, other		0 (0%)	1 (0%)	3 (6%)
HTN, DM, obesity		1 (1%)	4 (2%)	0 (0%)
HTN, DM, obesity, lipid disorder,		1 (1%)	0 (0%)	0 (0%)
other				
HTN, DM, obesity, other		1 (1%)	2 (1%)	0 (0%)
HTN, DM, other		2 (2%)	6 (3%)	0 (0%)
HTN, lipid disorder		1 (1%)	10 (5%)	5 (11%)
HTN, lipid disorder, other		3 (3%)	0 (0%)	2 (4%)
HTN, obesity		1 (1%)	4 (2%)	0 (0%)
HTN, obesity, lipid disorder		0 (0%)	1 (0%)	0 (0%)
HTN, obesity, lipid disorder,		1 (1%)	0 (0%)	0 (0%)
other				
HTN, obesity, other		0 (0%)	1 (0%)	0 (0%)
HTN, other		5 (5%)	13 (6%)	4 (9%)
lipid disorder		1 (1%)	1 (0%)	3 (6%)
lipid disorder, other		0 (0%)	1 (0%)	0 (0%)
obesity		4 (4%)	5 (2%)	1 (2%)
obesity, other		5 (5%)	0 (0%)	0 (0%)
other		8 (7%)	9 (4%)	0 (0%)
Virus in CSF	122			
no		50 (98%)	67 (96%)	1 (100%)
yes		1 (2%)	3 (4%)	0 (0%)

Note. Due to rounding errors, column wise percentages may not equal 100%. **Abbreviations:** Central nervous system (CNS); Diabetes mellitus (DM); Hypertension (HTN); Cerebral spinal fluid (CSF)

Table C4. Frequencies and percentages of observed neurological disease split by COVID-19 severity

(N = 495) Neurological disease category	n (%)				
	asymptomatic	mild	moderate	severe	critical
Cerebrovascular disease	18 (46)	25 (37)	55 (38)	88 (66)	58 (52)
CNS inflammatory disease	2 (5)	4 (6)	15 (10)	6 (5)	17 (15)
Demyelinating disease	1 (3)	1 (1)	1 (1)	2 (2)	10 (9)
Encephalopathy	4 (10)	7 (10)	10 (7)	24 (18)	12 (11)
Loss of taste/smell	7 (18)	10 (15)	16 (11)	0 (0)	3 (3)
Peripheral neuropathy	5 (13)	15 (22)	19 (13)	12 (9)	12 (11)
Other	2 (5)	5 (7)	28 (19)	1 (1)	0 (0)

Note. Due to rounding errors, column wise percentages may not equal 100%.

Age-associated neurological complications of COVID-19

Neurological conditions were evaluated by age, where the individual age or cohort age range was able to be determined and stratified to assess the overall frequency of specific types of neurological complications affecting children (< 19 years), young adults (19-50 years), and older adults (> 50) infected with SARS-CoV-2 (Figure C3). More specific details relating the number and percent of COVID-19 patients diagnosed with neurological conditions are stratified by decade of age and included in Table C1. Overall, patients 60-69 years showed the greatest population with neurological conditions ($n = 154$) and those less than or equal to 9 years of age had the least ($n = 7$) (Table C1, Figure C4). Age and other available population characteristics of multicenter, retrospective, and observational studies with large cohorts reporting neurological conditions from which individual matched patient data could not be discerned is detailed in Supplementary Table 3. Instances where data were able to be extracted from these reports is detailed.

Linear regression analyses were conducted to assess whether age significantly predicted any category of neurological complications of SARS-CoV-2 infection (Figure C5). The results of the linear regression model were significant for CVD, $F(1,508) = 30.08$, $p < 0.001$, $r^2 = 0.06$, indicating that approximately 6% of the variance in CVD is explainable by increased age (Figure C5a). In contrast, taste/smell disorder was associated with decreased age, $F(1,508) = 28.73$, $p < .001$, $r^2 = 0.05$, indicating that approximately 5% of the variance in this category is explainable by age (Figure C5f). A mild, but nonetheless statistically significant inverse relationship between age and CNS inflammatory disease or other was also observed. Approximately 1% of the variance in observation of COVID-19 patients with CNS inflammatory disease [$F(1,508) = 7.19$, $p = 0.008$, $r^2 = 0.01$] or other [$F(1,508) = 6.70$, $p = 0.01$, $r^2 = 0.01$] is also explainable by decreased age (Figure C5d, g). Age did not explain a significant proportion of variation in the observed frequencies of encephalopathy, peripheral neuropathy, or demyelinating disease (Figure C5b, c, e).

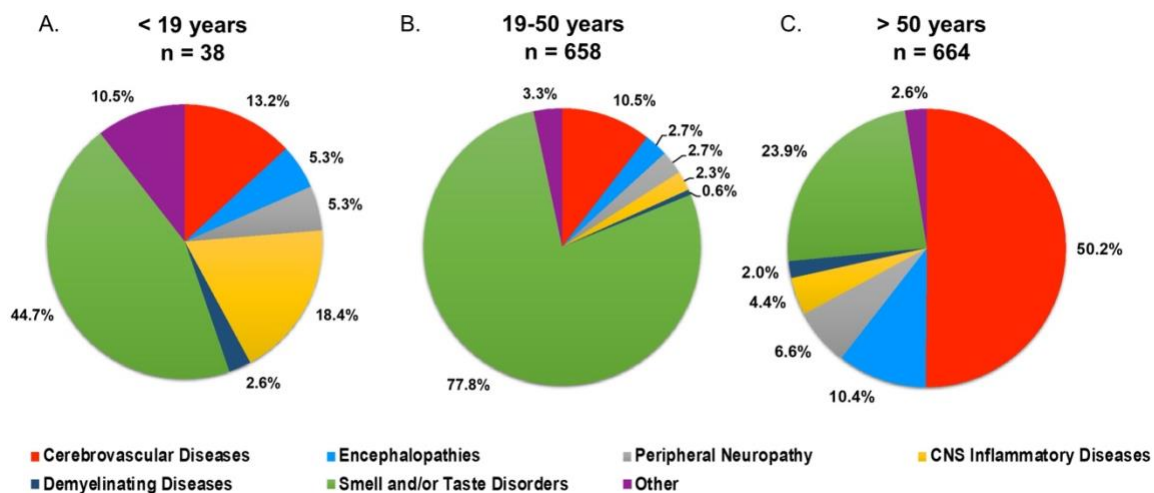


Figure C3. Percent of total neurological conditions ($n = 1,360$) occurring in (A) children (<19 years), (B) young adults (19-50 years), and (C) older adults (>50 years) diagnosed with COVID-19.

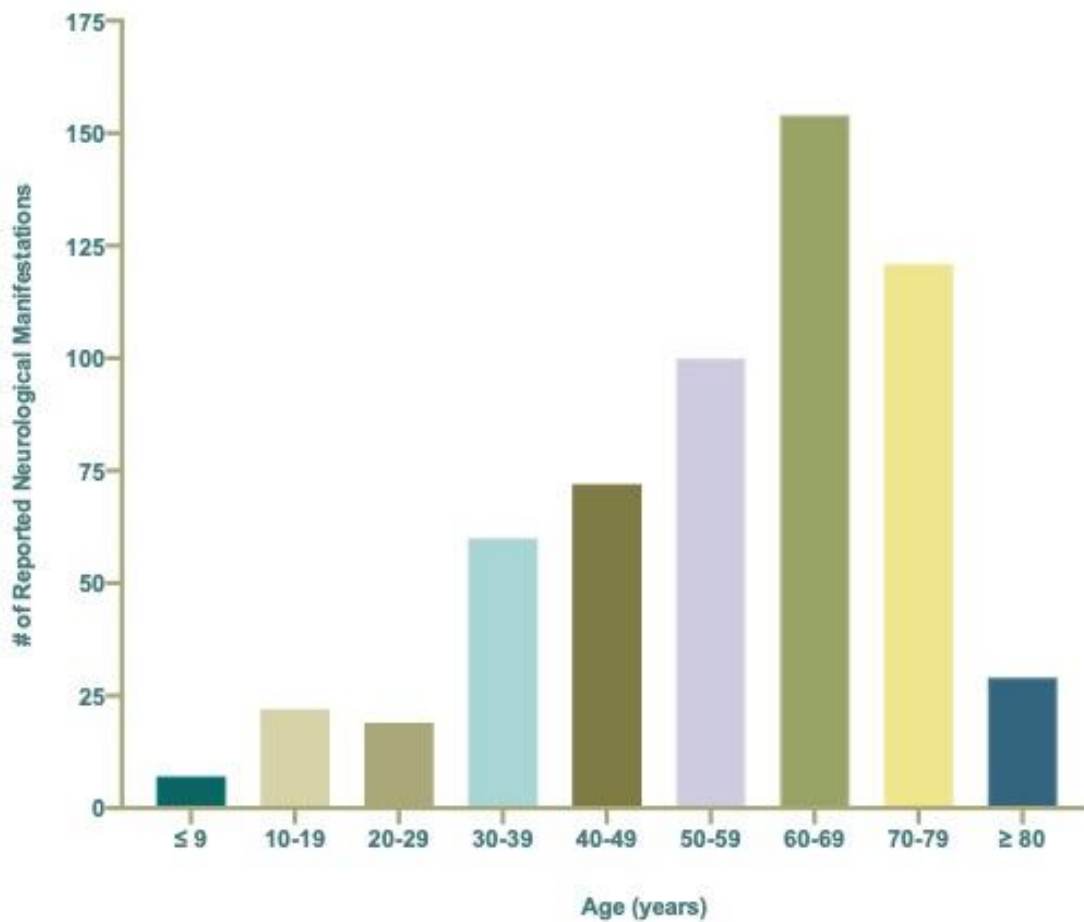


Figure C4. Total number ($n = 584$) of reported neurological manifestations occurring in patients with COVID-19 per decade ranging from ≤ 9 to ≥ 80 years of age.

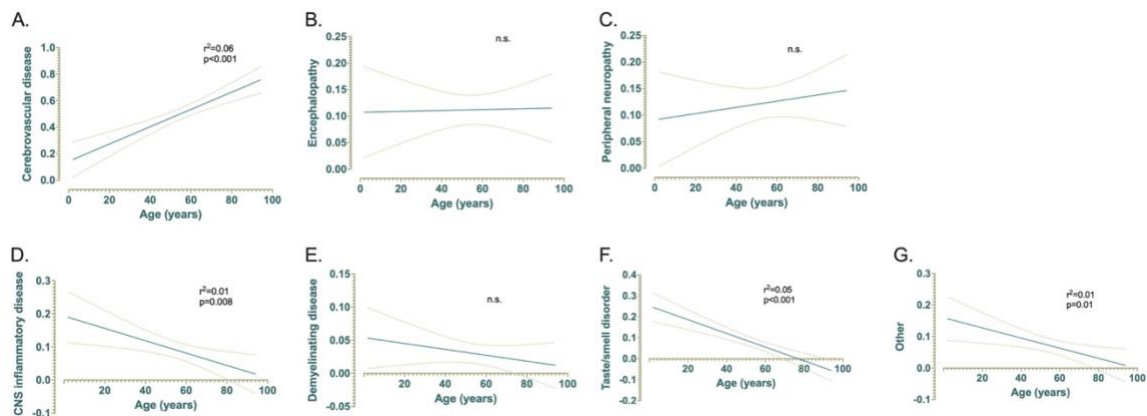


Figure C5. Simple linear regressions. Demonstrating the effect of age on (A) cerebrovascular disease, (B) encephalopathy, (C) peripheral neuropathy, (D) CNS inflammatory disease, (E) demyelinating disease, (F) taste and/or smell disorders, and (G) other non-specific neurological symptoms and their relationships with age (years) for patients with COVID-19 ($n = 510$).

Relationship of age, COVID-19 severity, and comorbidities on neurological manifestations of COVID-19

A Pearson correlation analysis was conducted among age, sex, each category of neurological disease, COVID-19 severity, and individual comorbid factors to assess the relationship among these variables and displayed as heat maps based on the coefficient between variables (Figure C6). Cases with incomplete data for the variables being assessed were excluded from analysis, resulting in a different n for each analysis.

In agreement with the linear regression analyses, a significant positive correlation between age and CVD was seen ($p < 0.001$) with a coefficient (r_p) of 0.24, indicating a small effect size (Figure C6A). Small effect size was also observed with age and CNS inflammatory disease ($r_p = -0.12$, $p = 0.008$), smell and/or taste disorder ($r_p = -0.23$, $p < 0.001$), and other ($r_p = -0.11$, $p = 0.01$), all of which show a negative correlation with age (Figure C6a). The relationship between age and COVID-19 severity was statistically significant for all disease severities (Figure C6b). A negative relationship was observed between age and asymptomatic ($r_p = -0.13$, $p = 0.005$), mild ($r_p = -0.15$, $p < 0.01$), or moderate ($r_p = -0.09$, $p = 0.046$) COVID-19 severity, while a positive correlation was seen between age and severe ($r_p = 0.18$, $p < 0.001$) or critical ($r_p = 0.11$, $p = 0.013$) disease (Figure C6b).

Apart from obesity, the relationship between age and comorbidities was statistically significant for all types examined (Figure C6c). A moderate effect size ($r_p = -0.40$, $p < 0.001$) between age and stated no comorbidities (none) was observed, indicating that as age increases, the category of “none” tends to decrease. In contrast, significant positive relationship between age and HTN ($r_p = 0.37$, $p < 0.001$), DM ($r_p = 0.16$, $p = 0.002$), or lipid disorders ($r_p = 0.11$, $p = .042$), suggesting that increased incidence of comorbid cardiovascular risk factors may contribute to the increased risk for CVD and/or severe-critical COVID-19 observed. Although age and “other” was found to be statistically

significant with a small effect size ($r_p = 0.12$, $p = 0.023$), the wide variety of conditions included in this category do not point to any one condition as being significant.

Relationships among all variables was also assessed and displayed in Figure 7. This revealed additional associations with neurological disease among patients for which all variables were available ($n = 350$). Age retained the strongest relationship with CVD, however, a significant positive correlation with HTN ($r_p = 0.14$, $p = 0.013$), DM ($r_p = 0.14$, $p = .017$), and critical COVID-19 ($r_p = 0.13$, $p = 0.027$) were also seen. Encephalopathy correlated positively with severe COVID-19 ($r_p = 0.26$, $p < 0.001$) and was seen most frequently among individuals with comorbid conditions categorized as “other” ($r_p = 0.13$, $p = 0.025$). CNS inflammatory disease showed a positive correlation with moderate COVID-19 severity ($r_p = 0.16$, $p = 0.005$), as well as patients without comorbid disease ($r_p = 0.17$, $p = 0.003$). No significant relationship between comorbidities and demyelinating disease was observed, however it did correlate with critical COVID-19 ($r_p = 0.20$, $p < 0.001$). These results, however, may be less reliable due to a low number of patients in this neurological disease category ($n = 12$). There appears to be a small positive relationship between demyelinating disease and obesity, however, this did not reach statistical significance. Like demyelinating disease, obesity had a positive association with critical COVID-19 ($r_p = 0.30$, $p < 0.001$). Peripheral neuropathy correlated with mild COVID-19 ($r_p = 0.18$, $p = 0.001$) but not with any comorbid condition. Interestingly, impaired taste/smell only reached significant positive associations with asymptomatic COVID-19 ($r_p = 0.19$, $p < 0.001$) and no comorbidities ($r_p = 0.24$, $p < 0.001$). Although the reason for this is unclear, in the absence of more critical symptoms, impairments in taste and/or smell may be more discernable by patients.

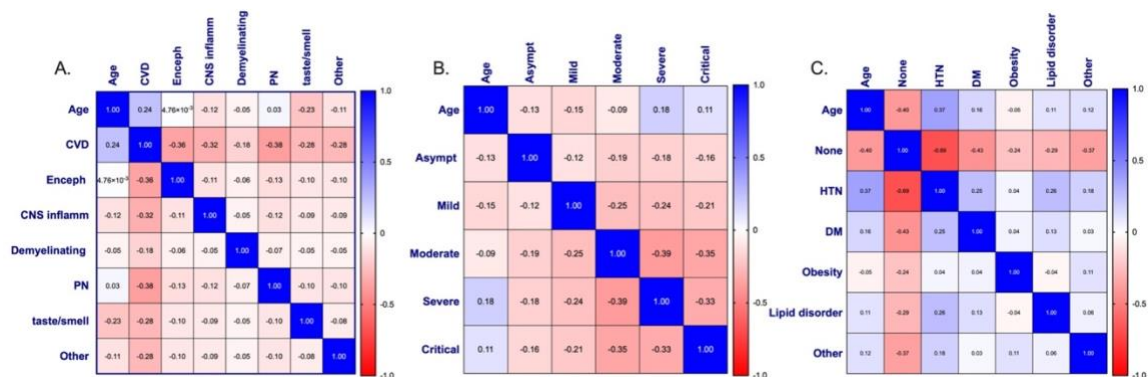


Figure C6. Pearson's correlation matrices and heatmaps. (A) age and neurological disease ($n = 510$), (B) age and COVID-19 symptom severity ($n = 495$), and (C) age and comorbidities ($n = 363$) of patients with COVID-19 and diagnosed with a neurological condition(s). Pearson's correlation coefficients are displayed and assigned color based on the distance from zero, with blue representing positive and red representing negative correlations.

Abbreviations: Cerebrovascular disease (CVD); Encephalopathy (Enceph); Central nervous system inflammatory disease (CNS inflamm); Peripheral neuropathy (PN); Asymptomatic (Asympt); Hypertension (HTN); Diabetes mellitus (DM)

Effect of COVID-19 severity and comorbidities on neurological disease outcome

In addition to age, COVID-19 severity and comorbidities appeared to associate with the observance of specific neurological disease (Figure C7). Multivariate analysis of covariance (MANCOVA) to assess if there were significant differences in the linear combination of COVID-19 severity and comorbidities score between the levels of neurological disease category after controlling for age were attempted, however, these tests failed assumptions of homogeneity of covariance and covariate-independent variable independence. As such, ANOVAs were performed separately to assess whether there were significant differences in COVID-19 severity or comorbidities score by neurological disease category. This demonstrated significant differences in the mean COVID-19 severity and comorbidities score among the different neurological disease categories (Figure C8). Demyelinating disease, CVD, and encephalopathy had the highest mean COVID-19 severity and comorbidities score, while loss of taste/smell had the lowest for both, demonstrating a relationship between disease severity and comorbid conditions. To aid viewing, neuronal disease categories were reordered by increasing mean of the two variables (Figure C8).

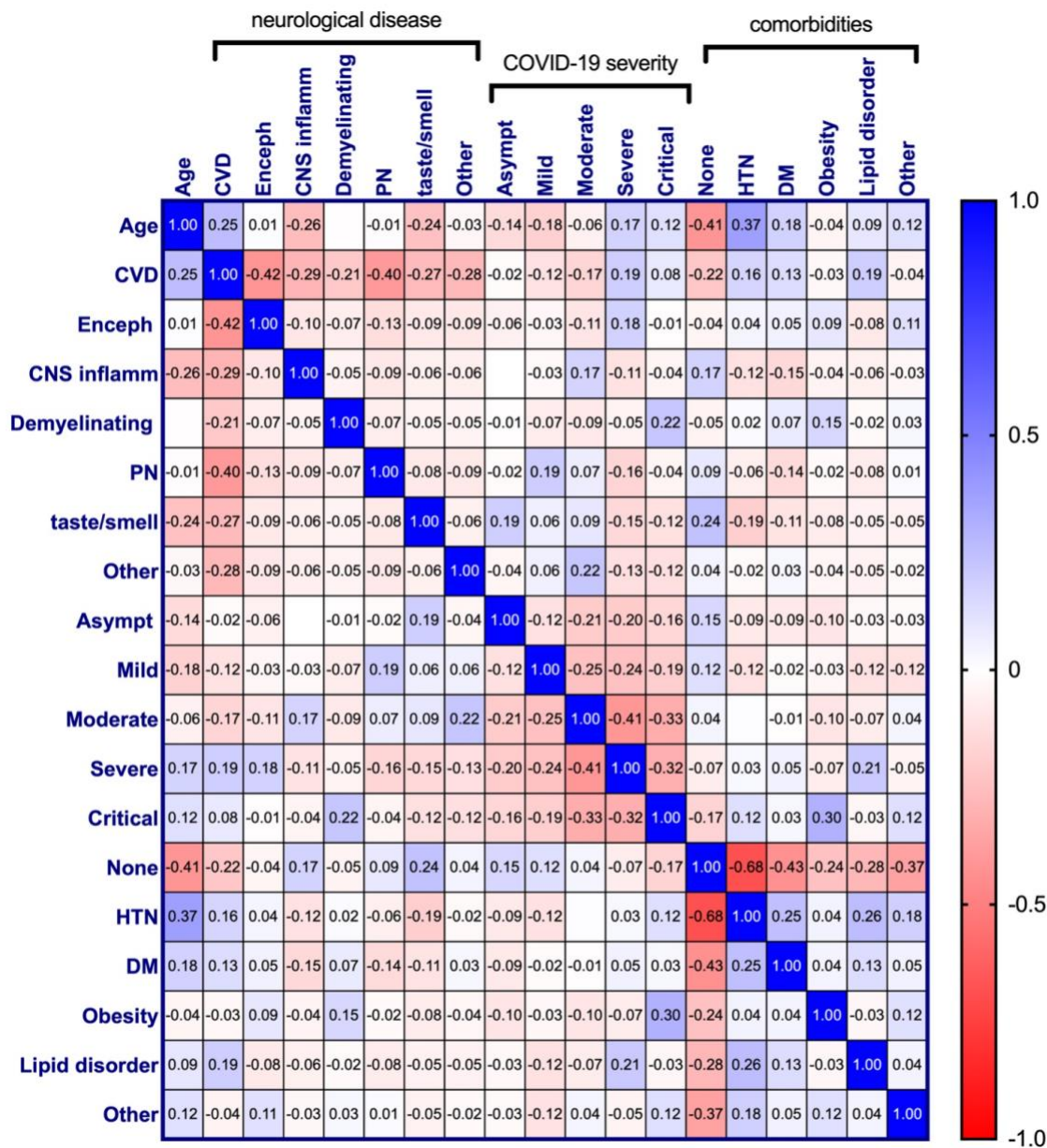


Figure C7. Pearson correlation matrix for age, neurological disease, COVID-19 symptom severity, and comorbidities of COVID-19 patients diagnosed with a neurological condition(s) (n=303). Pearson's correlation coefficients are displayed and assigned color based on the distance from zero, with blue representing positive and red representing negative correlations.

Abbreviations: Cerebrovascular disease (CVD); Encephalopathy (Enceph); Central nervous system inflammatory disease (CNS inflamm); Peripheral neuropathy (PN); Asymptomatic (Asympt); Hypertension (HTN); Diabetes mellitus (DM).

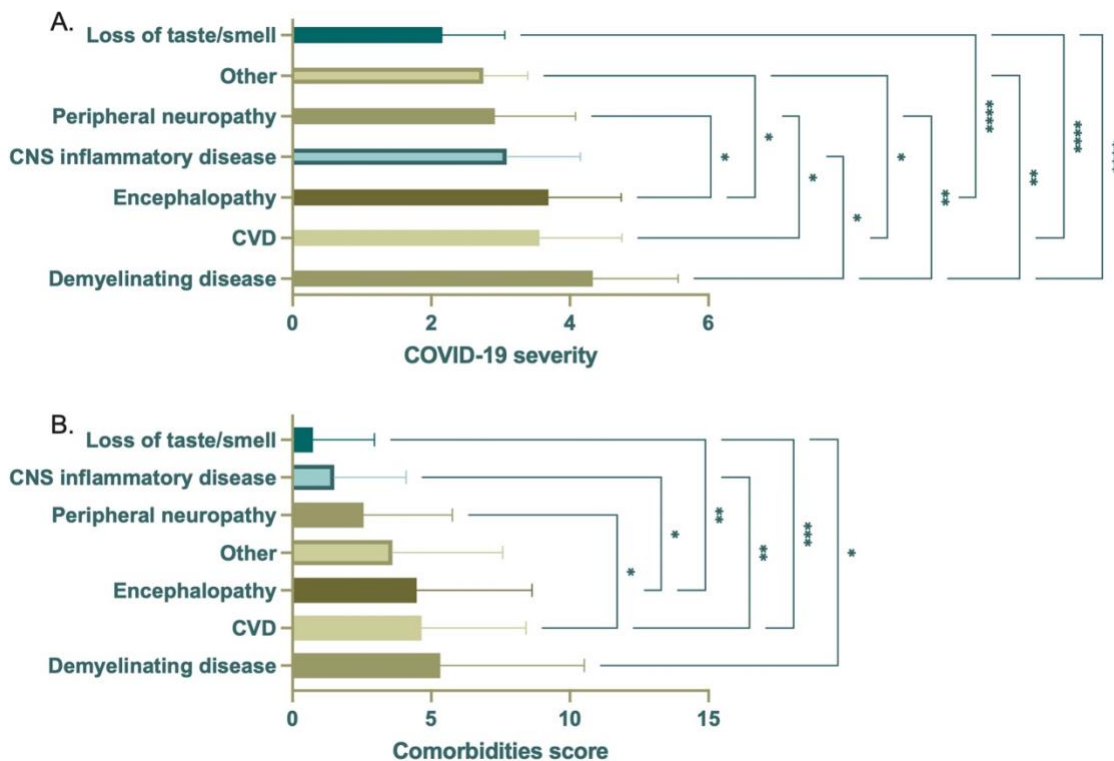


Figure C8. ANOVA of COVID-19 severity or comorbidities score by neurological disease category ($n = 350$). Significant differences in mean COVID-19 severity (A) were seen among all neurological disease categories. Demyelinating disease had the highest mean, with CVD and encephalopathy second and third. Similarly, demyelinating disease had the highest mean comorbidities score, with CVD and encephalopathy second and third (B). Loss of taste/smell had the lowest mean COVID-19 severity and comorbidities score. Data were derived from the same subjects. * $p < 0.05$; ** $p < 0.01$; *** $p < 0.001$; **** $p < 0.0001$.

C.4 Discussion

Neurological manifestations are a significant complication of SARS-CoV-2 infection and COVID-19. Although many anecdotal and case study reports have suggested relationships between neurological complications of disease with age, disease severity, and comorbid conditions, significant associations among these variables remain unclear. Through a systematic review of peer-reviewed, published patient reports spanning the entirety of 2020 through April 4, 2021, and meta-analyses, we report that while smell and/or taste disorders are the most common neurological manifestation of SARS-CoV-2 infection, CVD, manifesting almost entirely as stroke, is a major neurological complication of infection, affecting just over a quarter of individuals in this study. Other clinically significant CNS complications, broadly categorized as encephalopathy, CNS inflammatory disease, demyelinating disease, and peripheral neuropathy have been reported less frequently. Other symptoms, including headache, seizure, aphasia, and ataxia have also been reported in connection with infection without identification of the underlying cause and are categorized as “other” in this report.

When investigating a potential relationship between the type of neurological disorder and age, smell and/or taste disorders remained the most common neurological complication affecting infected individuals 50 years of age and younger. For infected individuals over 50, however, CVD became the most common neurological injury, where it was observed in over half of individuals in this age group. Linear regression analysis, however, suggests only 6% of the variance in CVD is explainable by age. Known risk factors for vascular disease, HTN and DM, as well as critical COVID-19, showed a positive correlation with CVD but with a small effect size. Additionally, stroke affected individuals across the lifespan, including individuals with reported no comorbidities and/or asymptomatic disease. Together, this suggests other factors, which may include virus and/or the host’s response to infection, contribute to the development of CVD.

Although a higher incidence of CVD is seen among infected persons over 50, there is currently no clear indicator as to which patients will suffer stroke, several risk factors for stroke in aged individuals have been reported in COVID-19 patients, such as coagulopathy, elevated D-dimer levels, and vascular endothelial dysfunction. A large retrospective study evaluating risk factors for mortality of COVID-19 patients found coagulopathy to be a significant indicator, affecting ~50% of non-survivors [586]. Additionally, marked elevation ($<0.5\mu\text{g/L}$) of D-dimer, a by-product of blood clotting that is often elevated in response to acute vascular disease, has been reported in COVID-19 patients and found to be predictive of severe disease and mortality [341, 344, 586-588].

Endothelial cell infection and/or injury may also contribute to increased risk for CVD with COVID-19. ACE2, the principal receptor used for viral entry, is reportedly expressed by endothelial cells throughout the body, including brain [589, 590], indicating the potential for viral infection in the endothelium in the CNS. In support of this notion, a post-mortem investigation reported the presence of endothelial cell infection and endotheliitis across the vascular beds of several organs [591]. Although the brain was not evaluated in this study, the presence of endothelial infection of multiple organs reveals the potential for widespread disruption of vascular homeostasis, increasing the susceptibility of infected patients to CVD. Interestingly, endotheliopathy without evidence of infection has been reported in a cohort of COVID-19 patients (mean age = 62 years), which was associated with severe disease [592]. This suggests that the host response to infection may sufficiently promote endothelial cell inflammation and injury, without direct involvement of the virus.

In agreement with endotheliopathy in the CNS, several autopsy and neuroimaging reports demonstrate the presence of brain microvascular lesions and microhemorrhages in COVID-19 patients [553, 593-598]. Autopsy findings reveal intact endothelium, suggesting that microbleeds may form due to inflammation of endothelial cells that allows

for extravasation of red blood cells into the brain parenchyma [592, 599]. Cerebral microhemorrhages are associated with age and systemic disease, increasing the risk for microhemorrhage development in older patients with COVID-19. Moreover, the integrity of the blood-brain barrier (BBB) decreases with age and is posited to precede and contribute to the development of CVD [600]. The mechanisms of BBB dysfunction in aging are not completely clear; however, small atheromatous plaques, HTN, and endothelial cell inflammation are believed to play a prominent role and may help explain why individuals with underlying comorbidities, including DM and HTN, appear to be at greater risk for developing more severe COVID-19. Additionally, chronic, subclinical inflammation is a common feature of aging that increases the susceptibility of individuals to age-related disease [601]. Chronic inflammation can induce cellular stress and injury that weakens tissues and reduces the ability of cells to counter additional insults. It is reasonable, therefore, that aging-associated inflammation promotes endotheliitis and endotheliopathy, leading to increased “leakiness” of the vasculature that is made more severe with COVID-19.

In addition to CVD, more frequent observations of clinically significant encephalopathy and peripheral neuropathy are also seen in patients over 50 years. Patients with encephalopathy, which is broadly characterized as disease or damage to the brain that affects brain function, present with altered mental status ranging from mild confusion to more severe dementia or coma. Several case reports detail infected patients presenting with acute encephalopathic episodes, irrespective of COVID-19 severity, including acute necrotizing encephalopathy and posterior reversible encephalopathy syndrome (PRES). Encephalopathy accounted for only 5.3% of the total population of COVID-19 patients with neurological manifestations and 10.4% of those over 50 years of age. It is highly probable, however, that due to the strong inflammatory response to infection in the periphery, which

can negatively impact the CNS, encephalopathy among infected individuals occurs more frequently but not widely reported in case studies.

Peripheral neuropathy, including Guillain-Barré syndrome (GBS) and critical illness neuromyopathy, have emerged as one of the more serious neurological complications of COVID-19 infection. GBS is a neuromuscular disorder defined as an acute paralytic neuropathy, often preceded by an infection, and clinically characterized by symmetric weakness of the limbs [602]. This disease is considered, primarily, to be an affliction of the peripheral nerves that has a 5% fatality rate and results in the severe disability of up to 20% of GBS patients [602, 603]. Critical illness neuromyopathy is characterized by muscle wasting and paralysis and often culminates into a severely disabling weakness of the muscles and/or paralysis [604, 605]. In this review, we found that peripheral neuropathy was most frequent among older adults (6.6%, $n = 44$), with zero cases of critical illness neuromyopathy reported in patients younger than 60 years of age.

Less frequent observations of CNS inflammatory disease, demyelinating disease, and smell and/or taste disorders was seen among older adults, as compared to younger adults and patients under 19 years of age (children). CNS inflammatory disorders, which includes encephalitis, myelitis, and meningitis, was most frequently reported among patients under 19 years, while demyelinating disease was similar in frequency among the three age categories. Interestingly, the demyelinating disease, acute disseminated encephalomyelitis (ADEM), which is a rare but serious complication of viral infection most commonly affecting by young children, was seen more frequently in older adults (72.8%, $n = 8$), as compared to younger adults (18.1%, $n = 2$) and children (9.1%, $n = 1$), in this review. Impaired smell and/or taste was seen at a high frequency in all age groupings but was the principal manifestation affecting children and young adults and the second most common complication among individuals over 50 years.

Pathophysiology of neurological involvement

How SARS-CoV-2 infection promotes the development of neurological complications is unclear and may involve several factors (Figure C9). Brain autopsy and CSF analyses seldom report detectable virus in the CNS compartment, however, the neuroinvasive character of other huCoVs suggest SARS-CoV-2 may also infect the CNS [606] and has been demonstrated in a limited number of infected individuals [554, 564, 607, 608]. While the presence of virus in the CNS compartment and mechanism of entry is not fully elucidated, it is highly likely that SARS-Cov-2 is able to gain access to the brain through nasal epithelial cell. ACE2 is highly expressed in nasal epithelial cells, pointing to the olfactory bulb as a probably point of entry [609]. Infected olfactory epithelial cells may then transfer virus to closely situated olfactory neurons, allowing for retrograde axonal transport into the CNS compartment. In support of this, unilateral ablation of the olfactory bulb prior to intranasal inoculation of a neurotropic coronavirus prevented CNS entry and viral spread in mouse brain [610].

Hematological entry of virus into the CNS also cannot be ruled. SARS-CoV-2 has been detected in endothelial cells throughout the body of infected subjects and, given the prevalence of endothelial ACE2 expression, SARS-CoV-2 may be found in brain endothelium [589, 591]. Post-mortem analyses of human and non-human primate brain revealed hCoV-299E in brain endothelial cells [611]. Viral infection of the endothelial cells by coronavirus has been found to cause inflammation of the endothelial cells which disrupts vascular homeostasis and coagulation, suggesting an increased risk for CVD, as a result [591, 611].

Even in the absence of direct neuronal or neural cell infection, hypoxia/hypoxemia, coagulopathy, and uncontrolled inflammation or 'cytokine storm' can also negatively impact the CNS and cognition (Figure C9). Indeed, most clinical evidence suggests neurological complications of COVID-19 are due to secondary effects of infection,

including reduced O₂ and hyperimmune responses, often referred to as “cytokine storm”. Serum levels of pro-inflammatory cytokines [e.g., interleukin (IL)-6, IL-8, tumor necrosis factor- α (TNF- α)] in COVID-19 patients are significantly predictive and/or correlative to the severity of infection and mortality [341, 586, 587, 612]. Previously, SARS-CoV patients with severe disease were found to have elevated levels of pro-inflammatory cytokines and chemokines, and reduced levels of anti-inflammatory cytokines (IL-10), in comparison to patients with mild disease [613]. Indeed, virus-associated diseases of the nervous system, such as acute necrotizing encephalopathy, are associated with high levels of pro-inflammatory cytokines in serum and CSF. As such, elevated pro-inflammatory cytokines in serum of severe COVID-19 patients may promote inflammation in brain and contribute to the neurological manifestations of disease [614, 615].

Long-term impact of COVID-19 on the nervous system

The long-term consequences of COVID-19-associated nervous system injury and/or dysfunction is currently unknown, however, reports continue to emerge describing persistent symptoms of disease months after resolution of infection, including impaired smell and/or taste, chronic fatigue, and impaired cognition. Long-term complications of infection are referred to as post-acute sequelae of COVID-19 (PASC) or Long COVID and evidence for this complication is seen with other viruses that induce neurological disease, including human immunodeficiency virus (HIV), West Nile virus, and multiple herpes- and picornaviruses. It is not entirely clear if SARS-CoV-2 directly infects neurons and/or non-neuronal cells of the CNS and, if so, whether virus is eradicated from these sites with recovery of COVID-19. The significance of this important consideration is seen in a single case report of a 78-year-old woman who recovered from COVID-19 but succumbed to a sudden cardiac arrest prior to hospital discharge [616]. Although this individual had three consecutive SARS-CoV-2 PCR negative nasopharyngeal swabs, postmortem

investigation of multiple tissues, excluding brain, revealed residual virus in lung [616]. These findings suggest that the virus may not be completely cleared in some patients that appear to have recovered and raises the possibility that SARS-CoV-2 may evade immune surveillance, at least to some degree. It is important to note that replication-competency of virus found in lung of this patient was not determined and remains an important scientific and clinical question. This would have major implications for the brain if replication-competent virus persists in the CNS compartment after recovery. Even an abortive infection, if present, could negatively impact cell function and impair brain homeostasis. Alternatively, or in addition to direct viral involvement, chronic neuroinflammation can contribute to impaired brain homeostasis through production of soluble factors that directly and/or indirectly impair neuronal function. Clinical follow-up and prospective observational studies are critical for assessing long-term neurological outcomes of patients recovered from COVID-19. While this is a likely standard for follow-up of individuals who were diagnosed with serious neurological manifestations, functional and cognitive decline may continue after recovery among COVID-19 patients for whom neurological disease was not identified. There is significant evidence that supports the notion that these individuals, particularly those recovered from severe COVID-19, may have difficulty performing critical functions long after recovery, including reduced job performance and/or ability to attend to activities of daily living, that may worsen over time.

Limited studies are available that investigate the long-term neurological consequences of COVID-19 and do not include neurological assessments but have relied on neuropsychological testing and self-reports. A large cross-sectional study involving cognitive assessments of subjects who had recovered from COVID-19 demonstrated impairment in a variety of cognitive domains and a lower global cognitive performance score, with worsening performance associated with the severity of respiratory disease [617]. This may suggest irreversible injury to the brain due to reduced oxygen and/or

chronic subclinical unresolved neuroinflammation, two factors that play a major role in pathologic brain aging. Importantly, minor deficits were even seen among individuals who had experienced only mild respiratory symptoms. Additional follow-up of these individuals is needed to assess the course of symptoms with increased recovery time. It is important to note that testing was performed on-line, rather than by a board-certified neuropsychologist. In a separate assessment of self-reports from subjects at 6-months post-infection, sleep difficulties, anxiety, and depression were most common reported complaints, in addition to fatigue and muscle weakness [618].

Evidence of injury at the level of the CNS is very limited at this time, however, a functional imaging study of patients with persistent anosmia following recovery of SARS-CoV-2 infection displayed reduced metabolism in bilateral limbic cortices and the insular cortex of the left hemisphere, as compared to controls [619]. This suggests brain involvement in SARS-CoV-2-associated anosmia that may also impact cognitive function, as these brain regions are involved in multiple cognitive processes, including learning and memory, word, face, and body recognition, and consciousness. The insular cortices are also involved in taste, which is often impaired in SARS-CoV-2 infection, alone or concurrent with impaired smell, which may implicate injury within in this region among individuals suffering loss of taste and/or smell. With the potential for controlling the SARS-CoV-2 pandemic with the world-wide introduction of multiple vaccines, more comprehensive follow-up of recovered patients is likely to become an urgent public health concern, including neurological work-up and neuropsychological and/or psychiatric assessments.

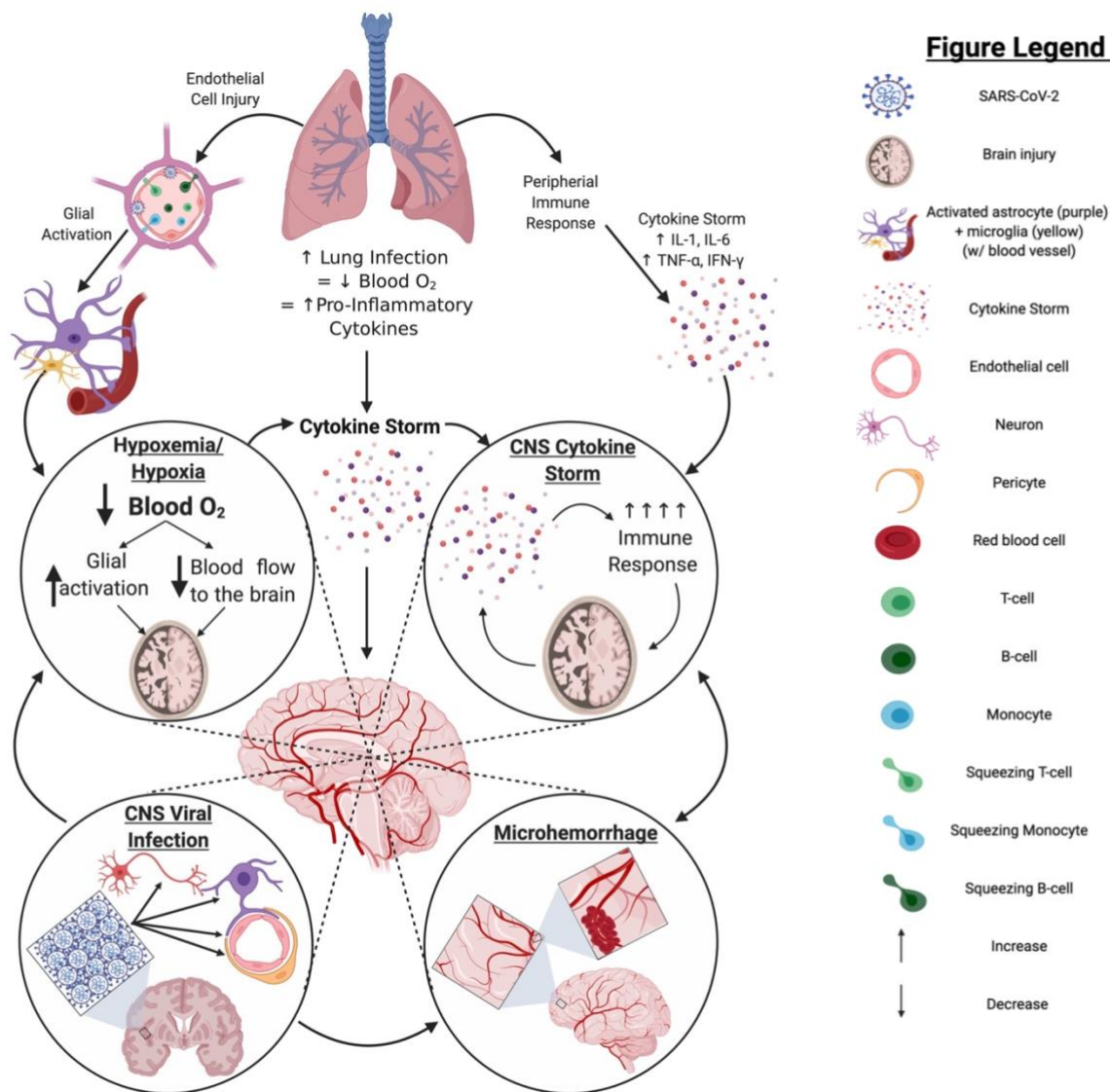


Figure C9. COVID-19 pathology in the CNS: primary impacts and potential mechanisms. Infection by SARS-CoV-2 primarily impacts the lungs, often leading to a hypoxic state and resulting in a robust increase in proinflammatory cytokine production. This may ultimately cause a "cytokine storm" and/or activate glia in the brain. Should such events occur, there is potential for hypoxemia or hypoxia, exacerbated "cytokine storm," and/or infiltration of peripheral immune cells through endothelial cell infection to occur within the brain; any of which can result in significant brain injury to the infected patient. Although currently unclear, if SARS-CoV-2 can establish a productive or even non-productive infection within the CNS compartment, persistent inflammation and/or impaired cell function may result, increasing the potential for serious injury of the brain and/or pathological brain aging. Image created with BioRender.com

C.5 Conclusions

This systematic review of the literature and meta-analysis has demonstrated that neurological manifestations are a common complication of SARS-CoV-2 infection and COVID-19 that affects individuals across the lifespan, with all severities of COVID-19, and with or without comorbidities. Consistently emerging case reports and retrospective studies detailing the neurological impact that COVID-19 point to the necessity to investigate the impact of hyperimmune responses and/or reduced oxygen more thoroughly on neuronal injury. In addition, the neuroinvasive potential of the virus should not be ruled out, as neurological conditions may be seen as a presenting symptom of infection and arise in the absence of respiratory disease. Further, as SARS-CoV-2 infection can lead to devastating neurological diseases irrespective of age, sex, or comorbidities, targeted studies of the COVID-19 population are imperative to better the understanding and elucidate the true impact of COVID-19 on the CNS. Additionally, patients need to be followed for potential long-term neurological sequelae, including pathologic brain aging, that likely plays a key role in post-acute sequelae of COVID-19 (PASC), or “Long COVID”. With multiple vaccines now available, we may continue to see a reduction in new cases and/or disease severity, however, the potential for CNS complications remains a major clinical and public health concern.

Supplementary Table C1. Frequencies and percentages of specific diagnoses included under each category of neurological complications.

Category		<i>n</i>	%
Diagnosis			
Cerebrovascular disease		259	
acute ischemic stroke		1	0.39
acute peripheral artery occlusion and ischemic stroke		1	0.39
bilateral occipital stroke w/loss of vision		1	0.39
CVST, thrombotic stroke		3	1.17
CVT		2	0.78
diffuse microvascular occlusion		4	1.56
embolic stroke		5	1.95
hemorrhage		12	4.67
hemorrhages, encephalopathy		2	0.78
hemorrhages, microhemorrhages		1	0.39
hemorrhagic PRES		2	0.78
hemorrhagic stroke		3	1.17
intraparenchymal hemorrhage		2	0.78
ischemic stroke		16	6.23
ischemic stroke with embolic infarcts		1	0.39
ischemic stroke with large vessel occlusion		1	0.39
large hemorrhage CVT, status epilepticus, encephalopathy		1	0.39
large vessel stroke		6	2.33
microhemorrhage		3	1.17
microhemorrhage, hypoxic injury, edema		10	3.89
microhemorrhage, lesion		1	0.39
microhemorrhages, encephalopathy		1	0.39
microhemorrhages, hypoxic injury, delirium		2	0.78
microhemorrhages, hypoxic injury, delirium, aguesia		1	0.39
microhemorrhages, lesions		1	0.39
multiple embolic strokes, encephalopathy		1	0.39
reversible cerebral vasoconstriction syndrome		1	0.39
SAH		4	1.56
SAH, encephalopathy		2	0.78
stroke		154	60.31
stroke, Balint-Holmes' syndrome, anosmia, ageusia		1	0.39
stroke, microhemorrhage, encephalopathy		1	0.39
stroke, microhemorrhages		1	0.39
stroke, seizures, encephalopathy		1	0.39
thrombotic stroke		6	2.33
vasculitis-related stroke		1	0.39

CNS inflammatory disease	48	
acute hemorrhagic leukoencephalomyelitis	1	2.13
acute hemorrhagic necrotizing encephalitis	2	4.26
acute transverse myelitis, anosmia, dysgeusia	1	2.13
anti-NMDAR encephalitis	2	4.26
CLOCCs	3	6.38
encephalitis	2	4.26
encephalitis and myelitis	1	2.13
encephalitis with seizure	2	4.26
encephalitis with seizure, aphasia	1	2.13
encephalitis, vasculitis	1	2.13
endotheliitis	1	2.13
meningoencephalitis	22	46.81
myelitis	5	10.64
reversible lesion of the corpus callosum	2	4.26
viral cerebellitis	1	2.13
Demyelinating disease	15	
acute demyelination	1	6.67
acute multifocal demyelinating lesions	1	6.67
acute tumefactive demyelination	1	6.67
ADEM	9	60.00
ADEM w/pseudoleukodystrophy	1	6.67
ADEM, GBS	1	6.67
demyelinating polyradiculoneuritis with GBS	1	6.67
Encephalopathy	58	
acute necrotizing encephalopathy	2	3.45
altered mental status	1	1.72
aphasia, behavioural agitation	1	1.72
delirium	3	5.17
disorientation, extreme fatigue, disgeusia	1	1.72
encephalopathy	31	53.45
encephalopathy with aphasia	1	1.72
encephalopathy with reversible splenium lesion	1	1.72
encephalopathy, aguesia	1	1.72
encephalopathy, hyposmia	1	1.72
hyponatremic encephalopathy	1	1.72
hypoxic-ischemic encephalopathy	3	5.17
impaired consciousness, ataxia	1	1.72
impaired consciousness, headache	1	1.72
impaired consciousness, wm lesions	1	1.72
ophthalmoparesis, encephalopathy	1	1.72
ophthalmoparesis, encephalopathy, right hemicranial headache	1	1.72

periventricular and deep wm injury	1	1.72
PRES	4	8.62
Peripheral neuropathy	64	
acute motor axonal neuropathy	1	1.59
AMSAN GBS	5	7.94
anosmia, ageusia, GBS	2	3.17
critical illness neuromyopathy	5	7.94
dysgeusia, GBS	1	1.59
facial nerve palsy, anosmia	1	1.59
GBS	33	52.38
GBS and Bell's Palsy	1	1.59
GBS with dysautonomia	1	1.59
Miller Fisher GBS	3	4.76
Miller Fisher GBS, ataxia	1	1.59
Miller Fisher GBS, ataxia, polyneuritis cranialis	2	3.17
ophthalmoparesis, facial palsy	2	3.17
polyneuritis cranialis GBS	1	1.59
polyneuritis cranialis GBS, hyposmia, ageusia	4	6.35
Smell and/or taste disorders	37	
ageusia	5	13.89
anosmia	11	30.56
anosmia, ageusia	10	27.78
anosmia, ageusia, headache	3	8.33
anosmia, ageusia, hearing impairment, lethargy, headache	1	2.78
anosmia, dysgeusia, olfactory bulb edema	1	2.78
anosmia, headache	2	5.56
anosmia, hypogeusia, akinetic-rigid parkinsonism	1	2.78
anosmia, olfactory bulb atrophy	1	2.78
hypoguesia	1	2.78
Other	37	
cerebral edema	1	2.78
chorioretinopathy, Adie syndrome, headache	1	2.78
headache	2	5.56
headache with photophobia	1	2.78
intracranial hypertension (headache)	13	36.11
moderate neck stiffness, photophobia, somnolence	1	2.78
myclonus	8	22.22
non-remitting headache	1	2.78
seizure	7	19.44
severe brain edema w/seizure	1	2.78

Note. Due to rounding errors, percentages may not equal 100%.

Abbreviations: Cerebral venous sinus thrombosis (CVST); Cerebral venous thrombosis (CVT); Posterior reversible encephalopathy syndrome (PRES); Subarachnoid hemorrhage (SAH); Central nervous system (CNS); N-Methyl-D-aspartate receptor (NMDAR); Cytotoxic lesions of corpus callosum (CLOCC); Acute disseminated encephalomyelitis (ADEM); Guillain-Barré syndrome (GBS); Acute motor-sensory axonal neuropathy (AMSAN)

Supplementary Table C2. Frequencies and percentages of all reported comorbidities

	<i>n</i>	%
Comorbidities		
AKI, obesity	1	0.28
aplastic anemia	1	0.28
asthma	1	0.28
breast cancer	2	0.55
Crohn's disease, obesity	1	0.28
DM	21	5.79
DM, asthma	1	0.28
DM, hyperlipidemia	4	1.10
DM, hyperthyroidism	1	0.28
DM, obesity	1	0.28
DM, CAD	1	0.28
dyslipidemia	2	0.55
dyslipidemia, atrial fibrillation	1	0.28
HTN	55	15.15
HTN, asthma	3	0.83
HTN, atrial fibrillation, smoker	1	0.28
HTN, CKD, smoker	1	0.28
HTN, dyslipidemia	4	1.10
HTN, dyslipidemia, CKD	1	0.28
HTN, dyslipidemia, atrial fibrillation	1	0.28
HTN, heart failure	1	0.28
HTN, hypercholesterolemia	4	1.10
HTN, hyperlipidemia	8	2.20
HTN, hyperlipidemia, asthma	1	0.28
HTN, hyperlipidemia, CAD	1	0.28
HTN, hyperlipidemia, CHF	1	0.28
HTN, kidney failure	1	0.28
HTN, KTR, past smoker	1	0.28
HTN, migraine	2	0.55
HTN, obesity	5	1.38
HTN, obesity, CKD	1	0.28
HTN, obesity, dyslipidemia, sleep apnea, ESRD	1	0.28
HTN, obesity, hyperlipidemia	1	0.28
HTN, smoking	5	1.38
HTN, CAD	3	0.83
HTN, CKD	4	1.10
HTN, DM	29	7.99
HTN, DM, CAD	1	0.28
HTN, DM, cholithiasis	1	0.28

HTN, DM, CKD	4	1.10
HTN, DM, dyslipidemia	3	0.83
HTN, DM, dyslipidemia, ESRD, smoker, sleep apnea	1	0.28
HTN, DM, ESRD	1	0.28
HTN, DM, hyperlipidemia	6	1.65
HTN, DM, hyperlipidemia, CAD	2	0.55
HTN, DM, hyperlipidemia, CAD, CHF	1	0.28
HTN, DM, ischemic heart disease	1	0.28
HTN, DM, obesity	5	1.38
HTN, DM, obesity, AKI	1	0.28
HTN, DM, obesity, CHD	1	0.28
HTN, DM, obesity, hyperlipidemia, CKD	1	0.28
HTN, DM, obesity, smoker	1	0.28
hyperlipidemia	3	0.83
hyperthyroidism	1	0.28
ischemic heart disease	1	0.28
left eye strabismus	1	0.28
migraine	2	0.55
none	131	36.09
obesity	10	2.75
obesity, asthma	3	0.83
obesity, smoking	1	0.28
psoriatic arthritis	1	0.28
RA, allergic alveolitis, monoclonal IgG kappa gammopathy	1	0.28
sickle cell disease	1	0.28
sinusitis	1	0.28
sleep apnea	1	0.28
smoking	1	0.28
ulcer	1	0.28

Note. Due to rounding errors, percentages may not equal 100%.

Abbreviations: Acute kidney injury (AKI); Diabetes mellitus (DM); Coronary artery disease (CAD); Chronic kidney disease (CKD); Coronary heart failure (CHF); Kidney transplant recipient (KTR); End-stage renal disease (ESRD); Rheumatoid arthritis (RA)

LIST OF REFERENCES

1. Jantunen, E., et al., *Central nervous system aspergillosis in allogeneic stem cell transplant recipients*. Bone Marrow Transplantation, 2003. **31**(3): p. 191-196.
2. Lin, S.-J., J. Schranz, and S.M. Teutsch, *Aspergillosis Case-Fatality Rate: Systematic Review of the Literature*. Clinical Infectious Diseases, 2001. **32**(3): p. 358.
3. Bodey, G., et al., *Fungal infections in cancer patients: An international autopsy survey*. European Journal of Clinical Microbiology and Infectious Diseases, 1992. **11**(2): p. 99-109.
4. Archer, D.B. and P.S. Dyer, *From genomics to post-genomics in Aspergillus*. Current opinion in microbiology, 2004. **7**(5): p. 499-504.
5. Wang, K., D.W. Ussery, and S. Brunak, *Analysis and prediction of gene splice sites in four Aspergillus genomes*. Fungal genetics and biology, 2009. **46**(1): p. S14-S18.
6. Chang, Y.C., et al., *THTA, a thermotolerance gene of Aspergillus fumigatus*. Fungal genetics and biology, 2004. **41**(9): p. 888-896.
7. Alonso, V., et al., *Modelling the effect of pH and water activity in the growth of Aspergillus fumigatus isolated from corn silage*. Journal of Applied Microbiology, 2017. **122**(4): p. 1048-1056.
8. Chazalet, V., et al., *Molecular Typing of Environmental and Patient Isolates of Aspergillus fumigatus from Various Hospital Settings*. Journal of Clinical Microbiology, 1998. **36**(6): p. 1494.
9. Latgé, J.-P. and G. Chamilos, *Aspergillus fumigatus and Aspergillosis in 2019*. Clinical microbiology reviews, 2019. **33**(1).
10. Jahn, B., et al., *Isolation and characterization of a pigmentless-conidium mutant of Aspergillus fumigatus with altered conidial surface and reduced virulence*. Infection and Immunity, 1997. **65**(12): p. 5110.
11. Jahn, B., et al., *PKSP-dependent reduction of phagolysosome fusion and intracellular kill of Aspergillus fumigatus conidia by human monocyte-derived macrophages*. Cellular Microbiology, 2002. **4**(12): p. 793-803.
12. Wasylnka, J., M. Simmer, and M.M. Moore, *Differences in sialic acid density in pathogenic and non-pathogenic Aspergillus species*. Microbiology-(UK), 2001. **147**: p. 869-877.
13. Garth, J.M. and C. Steele, *Innate Lung Defense during Invasive Aspergillosis: New Mechanisms*. Journal of innate immunity, 2017. **9**(3): p. 271-280.
14. De Repentigny, L., et al., *Acquired immunity in experimental murine aspergillosis is mediated by macrophages*. Infection and Immunity, 1993. **61**(9): p. 3791-3802.
15. Schaffner, A., H. Douglas, and A. Braude, *Selective protection against conidia by mononuclear and against mycelia by polymorphonuclear phagocytes in resistance to Aspergillus. Observations on these two lines of defense in vivo and in vitro with human and mouse phagocytes*. The Journal of clinical investigation, 1982. **69**(3): p. 617-631.

16. Bozza, S., et al., *Immune Sensing of Aspergillus fumigatus Proteins, Glycolipids, and Polysaccharides and the Impact on Th Immunity and Vaccination*. The Journal of immunology (1950), 2009. **183**(4): p. 2407-2414.
17. Lewis, R.E. and D.P. Kontoyiannis, *Invasive aspergillosis in glucocorticoid-treated patients*. Med Mycol, 2009. **47 Suppl 1**: p. S271-81.
18. Chamilos, G., et al., *Invasive fungal infections in patients with hematologic malignancies in a tertiary care cancer center: an autopsy study over a 15-year period (1989-2003)*. Haematologica, 2006. **91**(7): p. 986.
19. Glass, H.C., et al., *MRI findings in an immunocompromised boy with CNS fungal infection*. Can J Neurol Sci, 2007. **34**(1): p. 88-91.
20. Kontoyiannis, D.P., et al., *Progressive disseminated aspergillosis in a bone marrow transplant recipient: response with a high-dose lipid formulation of amphotericin B*. Clinical infectious diseases : an official publication of the Infectious Diseases Society of America, 2001. **32**(5): p. E94-96.
21. Herbrecht, R., et al., *Risk stratification for invasive aspergillosis in immunocompromised patients*. Annals of the New York Academy of Sciences, 2012. **1272**(1): p. 23-30.
22. A Vazquez, J., et al., *The Changing Epidemiology of Invasive Aspergillosis in the Non-Traditional Host: Risk Factors and Outcomes*. Pulmonary and Critical Care Medicine, 2016. **1**(3).
23. Kosmidis, C. and D.W. Denning, *The clinical spectrum of pulmonary aspergillosis*. Thorax, 2015. **70**(3): p. 270.
24. Bongomin, F., et al., *Global and Multi-National Prevalence of Fungal Diseases-Estimate Precision*. J. Fungi, 2017. **3**(4).
25. Lortholary, O., et al., *Epidemiological trends in invasive aspergillosis in France: the SAIF network (2005–2007)*. Clinical Microbiology and Infection, 2011. **17**(12): p. 1882-1889.
26. Brown, G., et al., *Hidden Killers: Human Fungal Infections*. Sci. Transl. Med., 2012. **4**(165).
27. Benedict, K., et al., *Estimation of Direct Healthcare Costs of Fungal Diseases in the United States*. Clinical Infectious Diseases, 2019. **68**(11): p. 1791-1797.
28. Kim, A., D.P. Nicolau, and J.L. Kuti, *Hospital costs and outcomes among intravenous antifungal therapies for patients with invasive aspergillosis in the United States*. Mycoses, 2011. **54**(5): p. e301-e312.
29. Robin, C., et al., *Mainly Post-Transplant Factors Are Associated with Invasive Aspergillosis after Allogeneic Stem Cell Transplantation: A Study from the Surveillance des Aspergilloses Invasives en France and Société Francophone de Greffe de Moelle et de Thérapie Cellulaire*. Biology of blood and marrow transplantation, 2019. **25**(2): p. 354-361.
30. Cadena, J., r.G.R. Thompson, and T.F. Patterson, *Aspergillosis: Epidemiology, Diagnosis, and Treatment*. Infectious disease clinics of North America, 2021. **35**(2): p. 415-434.
31. Philippe, B., et al., *Killing of Aspergillus fumigatus by Alveolar Macrophages Is Mediated by Reactive Oxidant Intermediates*. Infection and Immunity, 2003. **71**(6): p. 3034-3042.
32. Reichenberger, F., et al., *Diagnosis and treatment of invasive pulmonary aspergillosis in neutropenic patients*. The European respiratory journal, 2001. **19**(4): p. 743-755.
33. Kontoyiannis, D.P., et al., *Impact of unresolved neutropenia in patients with neutropenia and invasive aspergillosis: a post hoc analysis of the SECURE trial*. Journal of antimicrobial chemotherapy, 2018. **73**(3): p. 757-763.

34. Morrison, B.E., *Chemokine-mediated recruitment of NK cells is a critical host defense mechanism in invasive aspergillosis*. The Journal of clinical investigation, 2003. **112**(12): p. 1862-1870.
35. Lilly, L.M., et al., *Eosinophil Deficiency Compromises Lung Defense against Aspergillus fumigatus*. Infection and Immunity, 2014. **82**(3): p. 1315-1325.
36. Bozza, S., et al., *Dendritic Cells Transport Conidia and Hyphae of Aspergillus fumigatus from the Airways to the Draining Lymph Nodes and Initiate Disparate Th Responses to the Fungus*. The Journal of immunology (1950), 2002. **168**(3): p. 1362-1371.
37. Shankar, J., et al., *RNA-Seq Profile Reveals Th-1 and Th-17-Type of Immune Responses in Mice Infected Systemically with Aspergillus fumigatus*. Mycopathologia (1975), 2018. **183**(4): p. 645-658.
38. Cenci, E., et al., *Th1 and Th2 cytokines in mice with invasive aspergillosis*. Infection and Immunity, 1997. **65**(2): p. 564-570.
39. Raijmakers, R.P.H., et al., *Toll-like receptor 2 induced cytotoxic T-lymphocyte-associated protein 4 regulates Aspergillus-induced regulatory T-cells with pro-inflammatory characteristics*. Scientific reports, 2017. **7**(1): p. 11500-9.
40. Olnes, M.J., et al., *Effects of Systemically Administered Hydrocortisone on the Human Immunome*. Scientific reports, 2016. **6**(1): p. 23002-23002.
41. Fauci, A.S., et al., *Mechanisms of corticosteroid action on lymphocyte subpopulations. VI. Lack of correlation between glucocorticosteroid receptors and the differential effects of glucocorticosteroids on T-cell subpopulations*. Cell Immunol, 1980. **49**(1): p. 43-50.
42. Kamai, Y., et al., *Interactions of Aspergillus fumigatus with vascular endothelial cells*. Med Mycol, 2006. **44 Suppl 1**: p. S115-7.
43. Lopes Bezerra, L.M. and S.G. Filler, *Interactions of Aspergillus fumigatus with endothelial cells: internalization, injury, and stimulation of tissue factor activity*. Blood, 2004. **103**(6): p. 2143.
44. Lehrnbecher, T., et al., *Trends in the postmortem epidemiology of invasive fungal infections at a university hospital*. The Journal of infection, 2010. **61**(3): p. 259-265.
45. Groll, A.H., et al., *Trends in the postmortem epidemiology of invasive fungal infections at a University Hospital*. The Journal of infection, 1996. **33**(1): p. 23-32.
46. Jensen, J., et al., *CD4 T cell activation and disease activity at onset of multiple sclerosis*. Journal of Neuroimmunology, 2004. **149**(1-2): p. 202-209.
47. Bokhari, R., et al., *Isolated Cerebral Aspergillosis in Immunocompetent Patients*. World neurosurgery, 2014. **82**(1): p. e325-e333.
48. Pagano, L., et al., *Localization of aspergillosis to the central nervous system among patients with acute leukemia: report of 14 cases. Gruppo Italiano Malattie Ematologiche dell'Adulto Infection Program*. Clinical infectious diseases : an official publication of the Infectious Diseases Society of America, 1996. **23**(3): p. 628.
49. Kourkoumpetis, T.K., et al., *Central nervous system aspergillosis: a series of 14 cases from a general hospital and review of 123 cases from the literature*. Medicine (Baltimore), 2012. **91**(6): p. 328-336.
50. Mattiuzzi, G. and F.J. Giles, *Management of intracranial fungal infections in patients with haematological malignancies*. British journal of haematology, 2005. **131**(3): p. 287-300.
51. Ruhnke, M., et al., *CNS aspergillosis: recognition, diagnosis and management*. CNS Drugs, 2007. **21**(8): p. 659-76.

52. Walsh, T.J., D.B. Hier, and L.R. Caplan, *Aspergillosis of the central nervous system: clinicopathological analysis of 17 patients*. *Ann Neurol*, 1985. **18**(5): p. 574-82.
53. Denning, D.W., *Therapeutic outcome in invasive aspergillosis*. *Clin Infect Dis*, 1996. **23**(3): p. 608-15.
54. Boes, B., et al., *Central Nervous System Aspergillosis: Analysis of 26 Patients*. *Journal of Neuroimaging*, 1994. **4**(3): p. 123-129.
55. Baddley, J.W., D. Salzman, and P.G. Pappas, *Fungal brain abscess in transplant recipients: epidemiologic, microbiologic, and clinical features**. *Clinical Transplantation*, 2002. **16**(6): p. 419-424.
56. Hagensee, M.E., *Brain Abscess following Marrow Transplantation: Experience at the Fred Hutchinson Cancer Research Center, 1984-1992*. *Clinical Infectious Diseases*, 1994. **19**(3): p. 402-408.
57. Torre-Cisneros, J., et al., *CNS aspergillosis in organ transplantation: a clinicopathological study*. *Journal of Neurology, Neurosurgery & Psychiatry*, 1993. **56**(2): p. 188.
58. Ho, C.L. and M.J. Deruytter, *CNS aspergillosis with mycotic aneurysm, cerebral granuloma and infarction*. *The European Journal of Neurosurgery*, 2004. **146**(8): p. 851-856.
59. Kleinschmidt-DeMasters, B.K., *Central nervous system aspergillosis: a 20-year retrospective series*. *Hum Pathol*, 2002. **33**(1): p. 116-24.
60. Chiller, T.M., et al., *Development of a murine model of cerebral aspergillosis*. *J. Infect. Dis.*, 2002. **186**(4): p. 574-577.
61. High, K.P. and R.G. Washburn, *Invasive Aspergillosis in Mice Immunosuppressed with Cyclosporin A, Tacrolimus (FK506), or Sirolimus (Rapamycin)*. *The Journal of infectious diseases*, 1997. **175**(1): p. 222-225.
62. Desoubeaux, G. and C. Cray, *Rodent Models of Invasive Aspergillosis due to Aspergillus fumigatus : Still a Long Path toward Standardization*. *Frontiers in microbiology*, 2017. **8**: p. 841-841.
63. Kontoyiannis, D.P., et al., *Prospective Surveillance for Invasive Fungal Infections in Hematopoietic Stem Cell Transplant Recipients, 2001–2006: Overview of the Transplant-Associated Infection Surveillance Network (TRANSNET) Database*. *Clinical infectious diseases*, 2010. **50**(8): p. 1091-1100.
64. Gerson, S.L., et al., *Prolonged granulocytopenia: the major risk factor for invasive pulmonary aspergillosis in patients with acute leukemia*. *Annals of internal medicine*, 1984. **100**(3): p. 345-351.
65. Weinberger, M., et al., *PATTERNS OF INFECTION IN PATIENTS WITH APLASTIC-ANEMIA AND THE EMERGENCE OF ASPERGILLUS AS A MAJOR CAUSE OF DEATH*. *Medicine (Baltimore)*, 1992. **71**(1): p. 24-43.
66. Patterson, T.F., et al., *Invasive aspergillosis. Disease spectrum, treatment practices, and outcomes. I3 Aspergillus Study Group*. *Medicine (Baltimore)*, 2000. **79**(4): p. 250-60.
67. Pagano, L., et al., *The epidemiology of fungal infections in patients with hematologic malignancies: the SEIFEM-2004 study*. *Haematologica (Roma)*, 2006. **91**(8): p. 1068-1075.
68. Pagano, L., et al., *Invasive aspergillosis in patients with acute myeloid leukemia: a SEIFEM-2008 registry study*. *Haematologica (Roma)*, 2010. **95**(4): p. 644-650.
69. Pagano, L., et al., *Mucormycosis in patients with haematological malignancies: a retrospective clinical study of 37 cases*. *British Journal of Haematology*, 1997. **99**(2): p. 331-336.

70. Miyakoshi, S., et al., *Invasive Fungal Infection Following Reduced-Intensity Cord Blood Transplantation for Adult Patients with Hematologic Diseases*. *Biology of blood and marrow transplantation*, 2007. **13**(7): p. 771-777.
71. van de Peppel, R.J., et al., *The burden of Invasive Aspergillosis in patients with haematological malignancy: A meta-analysis and systematic review*. *The Journal of infection*, 2018. **76**(6): p. 550-562.
72. Abers, M.S., et al., *A Critical Reappraisal of Prolonged Neutropenia as a Risk Factor for Invasive Pulmonary Aspergillosis*. *Open forum infectious diseases*, 2016. **3**(1): p. ofw036-ofw036.
73. Gazendam, R.P., et al., *Human Neutrophils Use Different Mechanisms To Kill Aspergillus fumigatus Conidia and Hyphae: Evidence from Phagocyte Defects*. *The Journal of immunology (1950)*, 2016. **196**(3): p. 1272-1283.
74. Branzk, N., et al., *Neutrophils sense microbe size and selectively release neutrophil extracellular traps in response to large pathogens*. *Nature immunology*, 2014. **15**(11): p. 1017-1025.
75. Mircescu, M.M., et al., *Essential Role for Neutrophils but not Alveolar Macrophages at Early Time Points following Aspergillus fumigatus Infection*. *The Journal of infectious diseases*, 2009. **200**(4): p. 647-656.
76. Shevchenko, M.A., et al., *Aspergillus fumigatus Infection-Induced Neutrophil Recruitment and Location in the Conducting Airway of Immunocompetent, Neutropenic, and Immunosuppressed Mice*. *Journal of immunology research*, 2018. **2018**: p. 5379085-12.
77. Hohl, T.M., *Immune responses to invasive aspergillosis: new understanding and therapeutic opportunities*. *Current opinion in infectious diseases*, 2017. **30**(4): p. 364-371.
78. Lionakis, M.S. and S.M. Levitz, *Host Control of Fungal Infections: Lessons from Basic Studies and Human Cohorts*. *Annual review of immunology*, 2018. **36**(1): p. 157-191.
79. Nosari, A., et al., *Invasive aspergillosis in haematological malignancies: clinical findings and management for intensive chemotherapy completion*. *Am J Hematol*, 2001. **68**(4): p. 231-6.
80. Nicolle, M.-C., et al., *Invasive aspergillosis in patients with hematologic malignancies: incidence and description of 127 cases enrolled in a single institution prospective survey from 2004 to 2009*. *Haematologica*, 2011. **96**(11): p. 1685.
81. Upton, A., et al., *Invasive Aspergillosis following Hematopoietic Cell Transplantation: Outcomes and Prognostic Factors Associated with Mortality*. *Clinical infectious diseases*, 2007. **44**(4): p. 531-540.
82. Drummond, R.A., et al., *CARD9-Dependent Neutrophil Recruitment Protects against Fungal Invasion of the Central Nervous System*. *PLoS pathogens*, 2015. **11**(12): p. e1005293.
83. Kaufman, D.W., et al., *Relative incidence of agranulocytosis and aplastic anemia*. *American journal of hematology*, 2006. **81**(1): p. 65-67.
84. Woods, D. and J.J. Turchi, *Chemotherapy induced DNA damage response: Convergence of drugs and pathways*. *Cancer biology & therapy*, 2013. **14**(5): p. 379-389.
85. Cheung-Ong, K., G. Giaever, and C. Nislow, *DNA-Damaging Agents in Cancer Chemotherapy: Serendipity and Chemical Biology*. *Chemistry & biology*, 2013. **20**(5): p. 648-659.
86. Pillay, J., et al., *In vivo labeling with 2H2O reveals a human neutrophil lifespan of 5.4 days*. *Blood*, 2010. **116**(4): p. 625-627.

87. Craig, M., A.R. Humphries, and M.C. Mackey, *An upper bound for the half-removal time of neutrophils from circulation*. Blood, 2016. **128**(15): p. 1989-1991.
88. Saraf, S. and H. Ozer, *Practice Guidelines for the Use of rHuG-CSF in an Oncology Setting*. 2011, Springer Basel: Basel. p. 109-149.
89. Hamdan, D., et al., *Re-exploring immune-related side effects of docetaxel in an observational study: Blood hypereosinophilia*. Cancer medicine (Malden, MA), 2019. **8**(5): p. 2005-2012.
90. Valdés-Ferrada, J., et al., *Peripheral Blood Classical Monocytes and Plasma Interleukin 10 Are Associated to Neoadjuvant Chemotherapy Response in Breast Cancer Patients*. Frontiers in immunology, 2020. **11**: p. 1413.
91. Liu, P., et al., *Administration of cyclophosphamide changes the immune profile of tumor-bearing mice*. J Immunother, 2010. **33**(1): p. 53-9.
92. Abdel-Razeq, H. and H. Hashem, *Recent update in the pathogenesis and treatment of chemotherapy and cancer induced anemia*. Critical reviews in oncology/hematology, 2020. **145**: p. 102837-102837.
93. Verma, R., et al., *Lymphocyte depletion and repopulation after chemotherapy for primary breast cancer*. Breast cancer research : BCR, 2016. **18**(1): p. 10-10.
94. Baddley, J.W., *Clinical risk factors for invasive aspergillosis*. Med Mycol, 2011. **49 Suppl 1**: p. S7-S12.
95. Robenshtok, E., et al., *Antifungal Prophylaxis in Cancer Patients After Chemotherapy or Hematopoietic Stem-Cell Transplantation: Systematic Review and Meta-Analysis*. Journal of clinical oncology, 2007. **25**(34): p. 5471-5489.
96. Neofytos, D., et al., *Invasive aspergillosis in solid organ transplant patients: diagnosis, prophylaxis, treatment, and assessment of response*. BMC infectious diseases, 2021. **21**(1): p. 296-11.
97. Nivoix, Y., et al., *Factors associated with overall and attributable mortality in invasive aspergillosis.(Clinical report)*. Clinical Infectious Diseases, 2008. **47**(9): p. 1176.
98. Palmer, L.B., H.E. Greenberg, and M.J. Schiff, *Corticosteroid treatment as a risk factor for invasive aspergillosis in patients with lung disease*. Thorax, 1991. **46**(1): p. 15-20.
99. Wald, A., et al., *Epidemiology of Aspergillus Infections in a Large Cohort of Patients Undergoing Bone Marrow Transplantation*. The Journal of Infectious Diseases, 1997. **175**(6): p. 1459-1466.
100. Choi, Y.R., et al., *Invasive aspergillosis involving the lungs and brain after short period of steroid injection: a case report*. Tuberculosis and respiratory diseases, 2012. **72**(5): p. 448.
101. Lake, K.B., et al., *Fatal disseminated aspergillosis in an asthmatic patient treated with corticosteroids*. Chest, 1983. **83**(1): p. 138-139.
102. Guirao-Arrabal, E., et al., *Disseminated aspergillosis in an immunocompetent patient treated with corticosteroids: value of PCR for diagnosis*. Revista espanola de quimioterapia : publicacion oficial de la Sociedad Espanola de Quimioterapia, 2019. **32**(3): p. 273.
103. Marr, K.A., et al., *Invasive aspergillosis in allogeneic stem cell transplant recipients: changes in epidemiology and risk factors*. Blood, 2002. **100**(13): p. 4358.
104. Carter, M., et al., *Disseminated Aspergillosis: An Unfortunate Complication Of Systemic Steroid Use In The Treatment Of Ards*. Am. J. Respir. Crit. Care Med., 2015. **191**.

105. Escribano, P., et al., *Genotyping of Aspergillus fumigatus Reveals Compartmentalization of Genotypes in Disseminated Disease after Invasive Pulmonary Aspergillosis*. Journal of clinical microbiology, 2017. **55**(1): p. 331.
106. Reddy, H., S. Saraf, and M. Singh, *Invasive aspergillosis in a HIV patient on prolonged steroid therapy*. Annals of Tropical Medicine and Public Health, 2013. **6**(2): p. 245-247.
107. Langhoff, E., K. Olgaard, and J. Ladefoged, *The immunosuppressive potency in vitro of physiological and synthetic steroids on lymphocyte cultures*. Int J Immunopharmacol, 1987. **9**(4): p. 469-73.
108. Boss, B., et al., *Influence of corticosteroids on neutrophils, lymphocytes, their subsets, and T-cell activity markers in patients with active rheumatoid arthritis, compared to healthy controls*. Ann N Y Acad Sci, 1999. **876**: p. 198-200.
109. Balow, J.E., D.L. Hurley, and A.S. Fauci, *Immunosuppressive effects of glucocorticosteroids: differential effects of acute vs chronic administration on cell-mediated immunity*. J Immunol, 1975. **114**(3): p. 1072-6.
110. Moser, M., et al., *Glucocorticoids down-regulate dendritic cell function in vitro and in vivo*. Eur J Immunol, 1995. **25**(10): p. 2818-24.
111. Ganter, S., et al., *Growth control of cultured microglia*. J Neurosci Res, 1992. **33**(2): p. 218-30.
112. Kalleda, N., et al., *Dynamic Immune Cell Recruitment After Murine Pulmonary Aspergillus fumigatus Infection under Different Immunosuppressive Regimens*. Frontiers in microbiology, 2016. **7**: p. 1107-1107.
113. Chang, J.Y. and L.-Z. Liu, *Inhibition of Microglial Nitric Oxide Production by Hydrocortisone and Glucocorticoid Precursors*. Neurochemical research, 2000. **25**(7): p. 903-908.
114. Gudewicz, P.W., *The effects of cortisone therapy on lung macrophage host defense function and glucose metabolism*. Circ Shock, 1981. **8**(1): p. 95-103.
115. Kleinert, H., et al., *Glucocorticoids inhibit the induction of nitric oxide synthase II by down-regulating cytokine-induced activity of transcription factor nuclear factor-kappa B*. Mol Pharmacol, 1996. **49**(1): p. 15-21.
116. Ng, T.T.C., G.D. Robson, and D.W. Denning, *Hydrocortisone-enhanced growth of Aspergillus spp.: implications for pathogenesis*. Microbiology (Society for General Microbiology), 1994. **140**(9): p. 2475-2479.
117. Müller, M.B., et al., *Neither major depression nor glucocorticoid treatment affects the cellular integrity of the human hippocampus*. The European journal of neuroscience, 2001. **14**(10): p. 1603-1612.
118. Melo-Filho, A.A., et al., *Corticosteroids Reduce Glial Fibrillary Acidic Protein Expression in Response to Spinal Cord Injury in a Fetal Rat Model of Dysraphism*. Pediatric neurosurgery, 2009. **45**(3): p. 198-204.
119. Tsuneishi, S., et al., *Effects of dexamethasone on the expression of myelin basic protein, proteolipid protein, and glial fibrillary acidic protein genes in developing rat brain*. Brain research. Developmental brain research, 1991. **61**(1): p. 117-123.
120. Patel, R., et al., *Glutotoxin penetrates and impairs the integrity of the human blood-brain barrier in vitro*. Mycotoxin Research, 2018. **34**(4): p. 257-268.
121. Park, S., et al., *Neurotoxic effects of aflatoxin B1 on human astrocytes in vitro and on glial cell development in zebrafish in vivo*. Journal of hazardous materials, 2020. **386**: p. 121639.
122. Behrens, M., et al., *Efflux at the Blood-Brain Barrier Reduces the Cerebral Exposure to Ochratoxin A, Ochratoxin α , Citrinin and Dihydrocitrinone*. Toxins, 2021. **13**(5).

123. Górska, K., J. Blaszkowska, and M. Dzikowiec, *Neuroinfections caused by fungi*. Infection, 2018. **46**(4): p. 443-459.
124. Speth, C., et al., *Gliotoxin as putative virulence factor and immunotherapeutic target in a cell culture model of cerebral aspergillosis*. Molecular immunology, 2011. **48**(15-16): p. 2122-2129.
125. Speth, C., et al., *Culture supernatants of patient-derived Aspergillus isolates have toxic and lytic activity towards neurons and glial cells*. FEMS immunology and medical microbiology, 2000. **29**(4): p. 303-313.
126. Rivera, A., et al., *Dectin-1 diversifies Aspergillus fumigatus-specific T cell responses by inhibiting T helper type 1 CD4 T cell differentiation*. The Journal of experimental medicine, 2011. **208**(2): p. 369-381.
127. Heldt, S., et al., *Levels of interleukin (IL)-6 and IL-8 are elevated in serum and bronchoalveolar lavage fluid of haematological patients with invasive pulmonary aspergillosis*. Mycoses, 2017. **60**(12): p. 818-825.
128. Dagenais, T.R.T. and N.P. Keller, *Pathogenesis of Aspergillus fumigatus in Invasive Aspergillosis*. Clinical Microbiology Reviews, 2009. **22**(3): p. 447-465.
129. Lionakis, M.S., et al., *Organ-Specific Innate Immune Responses in a Mouse Model of Invasive Candidiasis*. Journal of innate immunity, 2011. **3**(2): p. 180-199.
130. Flores-Maldonado, O.E., et al., *Distinct innate immune responses between sublethal and lethal models of disseminated candidiasis in newborn BALB/c mice*. Microbial pathogenesis, 2021. **158**: p. 105061-105061.
131. Kaufman-Francis, K., et al., *The Early Innate Immune Response to, and Phagocyte-Dependent Entry of, Cryptococcus neoformans Map to the Perivascular Space of Cortical Post-Capillary Venules in Neurocryptococcosis*. The American journal of pathology, 2018. **188**(7): p. 1653-1665.
132. Uicker, W.C., J.P. McCracken, and K.L. Buchanan, *Role of CD4+ T cells in a protective immune response against Cryptococcus neoformans in the central nervous system*. Med Mycol, 2006. **44**(1): p. 1-11.
133. Dufaud, C., et al., *Naïve B cells reduce fungal dissemination in Cryptococcus neoformans infected Rag1-/- mice*. Virulence, 2018. **9**(1): p. 173-184.
134. Pathakumari, B., G. Liang, and W. Liu, *Immune defence to invasive fungal infections: A comprehensive review*. Biomedicine & pharmacotherapy, 2020. **130**: p. 110550.
135. Mueller-Loebnitz, C., et al., *Immunological Aspects of Candida and Aspergillus Systemic Fungal Infections*. Interdisciplinary perspectives on infectious diseases, 2013. **2013**: p. 102934-7.
136. Hessel Carvalho-Dias, V.M., et al., *Invasive Aspergillosis in Hematopoietic Stem Cell Transplant Recipients: A Retrospective Analysis*. The Brazilian journal of infectious diseases, 2008. **12**(5): p. 385-389.
137. Segal, B.H., *Aspergillosis*. The New England journal of medicine, 2009. **360**(18): p. 1870-1884.
138. Deigendesch, N., J. Costa Nunez, and W. Stenzel, *Parasitic and fungal infections*. Handbook of Clinical Neurology, 2018. **145**: p. 245-262.
139. Henao-Martínez, A.F. and D. Vela-Duarte, *Chapter 13 - Cryptococcal Meningitis and Other Opportunistic Fungal Infections of the Central Nervous System: Epidemiology, Pathogenesis, Diagnosis, and Treatment*. 2018, Elsevier Inc. p. 261-278.
140. Patterson, T.F., et al., *Invasive Aspergillosis Disease Spectrum, Treatment Practices, and Outcomes*. Medicine (Baltimore), 2000. **79**(4): p. 250-260.

141. Economides, M.P., et al., *Invasive mold infections of the central nervous system in patients with hematologic cancer or stem cell transplantation (2000-2016): Uncommon, with improved survival but still deadly often*. Journal of Infection, 2017. **75**(6): p. 572-580.
142. Cadena, J., r.G.R. Thompson, and T.F. Patterson, *Invasive Aspergillosis: Current Strategies for Diagnosis and Management*. Infectious disease clinics of North America, 2016. **30**(1): p. 125-142.
143. Baddley, J.W., et al., *Factors Associated with Mortality in Transplant Patients with Invasive Aspergillosis*. Clinical infectious diseases, 2010. **50**(12): p. 1559-1567.
144. Chan, J.F.-W., et al., *A 10-year study reveals clinical and laboratory evidence for the 'semi-invasive' properties of chronic pulmonary aspergillosis*. Emerging microbes & infections, 2016. **5**(1): p. e37-7.
145. Hori, A., et al., *Clinical significance of extra-pulmonary involvement of invasive aspergillosis: a retrospective autopsy-based study of 107 patients*. J Hosp Infect, 2002. **50**(3): p. 175-82.
146. Subira, M., et al., *Invasive pulmonary aspergillosis in patients with hematologic malignancies: survival and prognostic factors*. Haematologica (Roma), 2002. **87**(5): p. 528-534.
147. Ramos Fernández, V., et al., *Angio-invasive disseminated aspergillosis: autopsy diagnosis in leukemic patients*. Anales de medicina interna (Madrid, Spain : 1984), 1993. **10**(7): p. 337-340.
148. Chierichini, A., et al., *Autopsy Analysis On Epidemiology and Site of Involvement Of Invasive Fungal Infections (IFI) In Hematological Malignancies : A Retrospective Study at Hematologic Tertiary Care Department*. Blood, 2013. **122**(21): p. 5589-5589.
149. Ueno, M., et al., *An autopsy case with cerebral hemorrhaging due to disseminated aspergillosis during glucocorticoid therapy for overlap syndrome of systemic lupus erythematosus and systemic sclerosis*. Internal Medicine, 2019. **58**(7): p. 1023-1027.
150. Mylonakis, E., et al., *Central nervous system aspergillosis in patients with human immunodeficiency virus infection: Report of 6 cases and review*. Medicine, 2000. **79**(4): p. 269-280.
151. Dotis, J., E. Iosifidis, and E. Roilides, *Central nervous system aspergillosis in children: a systematic review of reported cases*. International journal of infectious diseases, 2007. **11**(5): p. 381-393.
152. Schwartz, S. and E. Thiel, *Cerebral aspergillosis: Tissue penetration is the key*. Medical Mycology, 2009. **47**(SUPPL. 1): p. S387-S393.
153. Wang, R.X., et al., *Cerebral aspergillosis: a retrospective analysis of eight cases*. International Journal of Neuroscience, 2017. **127**(4): p. 339-343.
154. Amanati, A., et al., *Cerebral and pulmonary aspergillosis, treatment and diagnostic challenges of mixed breakthrough invasive fungal infections: case report study*. BMC Infect Dis, 2020. **20**(1): p. 535.
155. Sullivan BN, B.M., O'Connell SS, Pickett KM, Steele C, *A systematic review and meta-analysis to assess the relationship between disseminated cerebral aspergillosis and therapeutics used in leukemias and lymphomas*. 2021: PROSPERO.
156. Murad, M.H., et al., *Methodological quality and synthesis of case series and case reports*. BMJ Evid Based Med, 2018. **23**(2): p. 60-63.
157. Page, M.J., et al., *The PRISMA 2020 statement: an updated guideline for reporting systematic reviews*. BMJ (Online), 2021. **372**: p. n71-n71.

158. Gaye, E., et al., *Cerebral aspergillosis: An emerging opportunistic infection in patients receiving ibrutinib for chronic lymphocytic leukemia?* Med Mal Infect, 2018. **48**(4): p. 294-297.
159. Groll, A.H., et al., *Five-year-survey of invasive aspergillosis in a paediatric cancer centre. Epidemiology, management and long-term survival.* Mycoses, 1999. **42**(7-8): p. 431-42.
160. Anciones, C., et al., *Acute Stroke as First Manifestation of Cerebral Aspergillosis.* Journal of Stroke and Cerebrovascular Diseases, 2018. **27**(11): p. 3289-3293.
161. Hummel, M., et al., *Detection of Aspergillus DNA in cerebrospinal fluid from patients with cerebral aspergillosis by a nested PCR assay.* Journal of Clinical Microbiology, 2006. **44**(11): p. 3989-3993.
162. Iwen, P.C., et al., *Nosocomial invasive aspergillosis in lymphoma patients treated with bone marrow or peripheral stem cell transplants.* Infect Control Hosp Epidemiol, 1993. **14**(3): p. 131-9.
163. Iwen, P.C., M.E. Rupp, and S.H. Hinrichs, *Invasive mold sinusitis: 17 cases in immunocompromised patients and review of the literature.* Clinical Infectious Diseases, 1997. **24**(6): p. 1178-1184.
164. Kaste, S.C., et al., *Imaging aspects of neurologic emergencies in children treated for non-CNS malignancies.* Pediatric Radiology, 2000. **30**(8): p. 558-565.
165. Kawanami, T., et al., *Cerebrovascular disease in acute leukemia: a clinicopathological study of 14 patients.* Intern Med, 2002. **41**(12): p. 1130-4.
166. Kreisel, W., et al., *Therapy of invasive aspergillosis with itraconazole: Improvement of therapeutic efficacy by early diagnosis.* Mycoses, 1991. **34**(9-10): p. 385-394.
167. Lionakis, M.S., et al., *Inhibition of B Cell Receptor Signaling by Ibrutinib in Primary CNS Lymphoma.* Cancer Cell, 2017. **31**(6): p. 833-843.e5.
168. Middelhof, C.A., et al., *Improved survival in central nervous system aspergillosis: a series of immunocompromised children with leukemia undergoing stereotactic resection of aspergillomas - Report of four cases.* Journal of Neurosurgery, 2005. **103**(4): p. 374-378.
169. Pascale, S., et al., *Invasive aspergillosis during consolidation chemotherapy for acute myeloid leukemia: report of two simultaneous cases involving central nervous system.* Haematologica, 2015. **100**: p. 140-140.
170. Ruchlemer, R., et al., *Ibrutinib-associated invasive fungal diseases in patients with chronic lymphocytic leukaemia and non-Hodgkin lymphoma: An observational study.* Mycoses, 2019. **62**(12): p. 1140-1147.
171. Schauwvlieghe, A.F.A.D., et al., *Management of cerebral azole-resistant Aspergillus fumigatus infection: A role for intraventricular liposomal-amphotericin B.* Journal of Global Antimicrobial Resistance, 2020. **22**: p. 354-357.
172. Sparano, J.A., et al., *Cerebral infection complicating systemic aspergillosis in acute-leukemia - clinical and radiographic presentation.* Journal of Neuro-Oncology, 1992. **13**(1): p. 91-100.
173. van der Linden, J.W.M., et al., *Clinical implications of azole resistance in Aspergillus fumigatus, The Netherlands, 2007-2009.* Emerging Infectious Diseases, 2011. **17**(10): p. 1846-1854.
174. Wright, J.A., et al., *Prolonged survival after invasive aspergillosis: a single-institution review of 11 cases.* J Pediatr Hematol Oncol, 2003. **25**(4): p. 286-91.
175. Yeh, T.C., et al., *Invasive fungal infection in children undergoing chemotherapy for cancer.* Ann Trop Paediatr, 2007. **27**(2): p. 141-7.
176. Zwitserloot, A.M., et al., *Disseminated aspergillosis in an adolescent with acute lymphoblastic leukemia.* Pediatr Blood Cancer, 2008. **51**(3): p. 423-6.

177. Wandroo, F., P. Stableforth, and Y. Hasan, *Aspergillus brain abscess in a patient with acute myeloid leukaemia successfully treated with voriconazole*. Clin Lab Haematol, 2006. **28**(2): p. 130-3.
178. Trigg, M.E., et al., *Combined anti-fungal therapy and surgical resection as treatment of disseminated aspergillosis of the lung and brain following BMT*. Bone Marrow Transplantation, 1993. **11**(6): p. 493-496.
179. Tracy, S.L., et al., *Disseminated infection by Aspergillus terreus*. Am J Clin Pathol, 1983. **80**(5): p. 728-33.
180. Tattevin, P., et al., *Successful treatment of brain aspergillosis with voriconazole*. Clinical Microbiology and Infection, 2004. **10**(10): p. 928-931.
181. Schamroth Pravda, M., N. Schamroth Pravda, and M. Lishner, *The Muddied Waters of Ibrutinib Therapy*. Acta Haematol, 2019. **141**(4): p. 209-213.
182. Sancho, J.M., et al., *Unusual invasive bronchial aspergillosis in a patient with acute lymphoblastic leukemia*. Haematologica, 1997. **82**(6): p. 701-702.
183. Sakata, N., et al., *Donor-derived myelodysplastic syndrome after allogeneic stem cell transplantation in a family with germline GATA2 mutation*. International Journal of Hematology, 2021. **113**(2): p. 290-296.
184. Prakash, G., et al., *Cerebral aspergillus infection in pediatric acute lymphoblastic leukemia induction therapy*. Indian J Med Paediatr Oncol, 2012. **33**(4): p. 236-8.
185. Pongbhaesaj, P., et al., *Aspergillosis of the central nervous system: A catastrophic opportunistic infection*. Southeast Asian Journal of Tropical Medicine and Public Health, 2004. **35**(1): p. 119-125.
186. Peng, H.L., et al., *Dramatic response to itraconazole in central nervous system aspergillosis complicating acute promyelocytic leukemia*. Infectious Diseases, 2015. **47**(2): p. 104-106.
187. Nov, A.A. and L.D. Cromwell, *Computed tomography of neuraxis aspergillosis*. Journal of Computer Assisted Tomography, 1984. **8**(3): p. 413-415.
188. Mori, T., et al., *Systemic aspergillosis caused by an aflatoxin-producing strain of Aspergillus flavus*. Medical Mycology, 1998. **36**(2): p. 107-112.
189. Marbello, L., et al., *Successful treatment with voriconazole of cerebral aspergillosis in an hematologic patient*. Haematologica, 2003. **88**(3): p. Ecr05.
190. Mahlknecht, U., et al., *Successful treatment of disseminated central nervous aspergillosis in a patient with acute myeloblastic leukemia*. Leuk Lymphoma, 1997. **27**(1-2): p. 191-4.
191. Kurdow, R., et al., *Case report: successful interdisciplinary treatment of cerebrally disseminated invasive pulmonary aspergillosis in a child with acute myeloid leukemia*. J Pediatr Surg, 2005. **40**(7): p. 1191-4.
192. Im, J.H., et al., *Disseminated invasive aspergillosis with multiple brain abscess after allogeneic hematopoietic stem cell transplantation treated successfully with voriconazole and neurosurgical intervention*. Infection and Chemotherapy, 2012. **44**(5): p. 395-398.
193. Henze, G., et al., *Successful treatment of pulmonary and cerebral aspergillosis in an immunosuppressed child*. Eur J Pediatr, 1982. **138**(3): p. 263-5.
194. Guermazi, A., et al., *Cerebral and spinal cord involvement resulting from invasive aspergillosis*. Eur Radiol, 2002. **12**(1): p. 147-50.
195. Flatt, T., et al., *Successful treatment of fanconi anemia and T-cell acute lymphoblastic leukemia*. Case Rep Hematol, 2012. **2012**: p. 396395.
196. Faisal, M.S., et al., *Cerebral aspergillosis in a patient on ibrutinib therapy—A predisposition not to overlook*. Journal of Oncology Pharmacy Practice, 2019. **25**(6): p. 1486-1490.

197. Eichenberger, E.M., et al., *A case of CNS aspergillosis in a patient with chronic lymphocytic leukemia on first-line ibrutinib therapy*. Medical Mycology Case Reports, 2020. **27**: p. 17-21.
198. De Leonardis, F., et al., *Isavuconazole Treatment of Cerebral and Pulmonary Aspergillosis in a Pediatric Patient With Acute Lymphoblastic Leukemia: Case Report and Review of Literature*. Journal of Pediatric Hematology Oncology, 2020. **42**(6): p. E469-E471.
199. Damaj, G., et al., *Rapid improvement of disseminated aspergillosis with caspofungin/voriconazole combination in an adult leukemic patient*. Annals of Hematology, 2004. **83**(6): p. 390-393.
200. Beresford, R., V. Dolot, and H. Foo, *Cranial aspergillosis in a patient receiving ibrutinib for chronic lymphocytic leukemia*. Medical Mycology Case Reports, 2019. **24**: p. 27-29.
201. Athanassiadou, F., et al., *Treatment of disseminated aspergillosis with voriconazole/liposomal amphotericin B in a child with leukemia*. Pediatric Blood & Cancer, 2005. **45**(7): p. 1003-1004.
202. Palmisani, E., et al., *Need of voriconazole high dosages, with documented cerebrospinal fluid penetration, for treatment of cerebral aspergillosis in a 6-month-old leukaemic girl*. J Chemother, 2017. **29**(1): p. 42-44.
203. Pardo, E., et al., *Invasive pulmonary aspergillosis in critically ill patients with hematological malignancies*. Intensive care medicine, 2019. **45**(12): p. 1732-1741.
204. Heo, S.T., et al., *Changes in In Vitro Susceptibility Patterns of Aspergillus to Triazoles and Correlation With Aspergillosis Outcome in a Tertiary Care Cancer Center, 1999-2015*. Clinical infectious diseases, 2017. **65**(2): p. 216-225.
205. Li, J., et al., *Estimating the prevalence of hematological malignancies and precursor conditions using data from Haematological Malignancy Research Network (HMRN)*. Cancer causes & control, 2016. **27**(8): p. 1019-1026.
206. Smith, A., et al., *Incidence of haematological malignancy by sub-type: a report from the Haematological Malignancy Research Network*. British journal of cancer, 2011. **105**(11): p. 1684-1692.
207. Bow, E.J., et al., *Invasive Fungal Disease in Adults Undergoing Remission-Induction Therapy for Acute Myeloid Leukemia: The Pathogenetic Role of the Antileukemic Regimen*. Clinical infectious diseases, 1995. **21**(2): p. 361-369.
208. Barkati, S.M.D., et al., *Incidence of invasive aspergillosis following remission-induction chemotherapy for acute leukemia: a retrospective cohort study in a single Canadian tertiary care centre*. CMAJ open, 2014. **2**(2): p. E86-E93.
209. Lee, C.-H., et al., *Primary Fungal Prophylaxis in Hematological Malignancy: a Network Meta-Analysis of Randomized Controlled Trials*. Antimicrobial agents and chemotherapy, 2018. **62**(8): p. e00355-18.
210. Facchinelli, D., et al., *Invasive Fungal Infections in Patients with Chronic Lymphoproliferative Disorders in the Era of Target Drugs*. Mediterranean journal of hematology and infectious diseases, 2018. **10**(1): p. e2018063-e2018063.
211. Teh, B.W., et al., *High rates of proven invasive fungal disease with the use of ibrutinib monotherapy for relapsed or refractory chronic lymphocytic leukemia*. Leukemia & lymphoma, 2019. **60**(6): p. 1572-1575.
212. Sharman, J.P., A.R. Mato, and M.J. Keating, *Ibrutinib for Chronic Lymphocytic Leukemia*. The New England journal of medicine, 2016. **374**(16): p. 1592.
213. Zhang, H., et al., *Invasive sphenoid sinus aspergillosis mimicking sellar tumor: a report of 4 cases and systematic literature review*. Chin Neurosurg J, 2020. **6**: p. 10.

214. Creuzet, E., et al., *Cerebral aspergillosis in a patient on ibrutinib therapy*. British journal of haematology, 2021. **193**(6): p. 1025-1025.
215. Cummins, K.C., et al., *Isavuconazole for the treatment of invasive fungal disease in patients receiving ibrutinib*. Leukemia & lymphoma, 2019. **60**(2): p. 527-530.
216. Grommes, C., et al., *Single-Agent Ibrutinib in Recurrent/Refractory Central Nervous System Lymphoma*. Blood, 2016. **128**(22): p. 783-783.
217. Ghez, D., et al., *Early-onset invasive aspergillosis and other fungal infections in patients treated with ibrutinib*. Blood, 2018. **131**(17): p. 1955-1959.
218. Aldoss, I., et al., *Invasive fungal infections in acute myeloid leukemia treated with venetoclax and hypomethylating agents*. Blood advances, 2019. **3**(23): p. 4043-4049.
219. Tse, E., R.Y.Y. Leung, and Y.-L. Kwong, *Invasive fungal infections after obinutuzumab monotherapy for refractory chronic lymphocytic leukemia*. Annals of hematology, 2014. **94**(1): p. 165-167.
220. Cornely, O.A., et al., *Posaconazole vs. Fluconazole or Itraconazole Prophylaxis in Patients with Neutropenia*. The New England journal of medicine, 2007. **356**(4): p. 348-359.
221. Ullmann, A.J., et al., *Posaconazole or Fluconazole for Prophylaxis in Severe Graft-versus-Host Disease*. The New England journal of medicine, 2007. **356**(4): p. 335-347.
222. Halpern, A.B., et al., *Primary antifungal prophylaxis during curative-intent therapy for acute myeloid leukemia*. Blood, 2015. **126**(26): p. 2790-2797.
223. Dib, R.W., et al., *Treating invasive aspergillosis in patients with hematologic malignancy: diagnostic-driven approach versus empiric therapies*. BMC Infect Dis, 2018. **18**(1): p. 656.
224. Hoenigl, M., et al., *Epidemiology of invasive fungal infections and rationale for antifungal therapy in patients with haematological malignancies*. Mycoses, 2011. **54**(5): p. 454-459.
225. Fracchiolla, N.S., et al., *Epidemiology and treatment approaches in management of invasive fungal infections in hematological malignancies: Results from a single-centre study*. PloS one, 2019. **14**(5): p. e0216715-e0216715.
226. Ethier, M.C., et al., *Mould-active compared with fluconazole prophylaxis to prevent invasive fungal diseases in cancer patients receiving chemotherapy or haematopoietic stem-cell transplantation: a systematic review and meta-analysis of randomised controlled trials*. British journal of cancer, 2012. **106**(10): p. 1626-1637.
227. Herbrecht, R., et al., *Voriconazole versus Amphotericin B for Primary Therapy of Invasive Aspergillosis*. The New England journal of medicine, 2002. **347**(6): p. 408-415.
228. Taccone, F.S., et al., *Epidemiology of invasive aspergillosis in critically ill patients: clinical presentation, underlying conditions, and outcomes*. Critical care (London, England), 2015. **19**(1): p. 7-7.
229. Denning, D.W., et al., *An EORTC multicentre prospective survey of invasive aspergillosis in haematological patients: Diagnosis and therapeutic outcome*. Journal of Infection, 1998. **37**(2): p. 173-180.
230. Kale, S.D., et al., *Modulation of Immune Signaling and Metabolism Highlights Host and Fungal Transcriptional Responses in Mouse Models of Invasive Pulmonary Aspergillosis*. Scientific reports, 2017. **7**(1): p. 17096-25.
231. Grahl, N., et al., *In vivo hypoxia and a fungal alcohol dehydrogenase influence the pathogenesis of invasive pulmonary aspergillosis*. PLoS pathogens, 2011. **7**(7): p. e1002145-e1002145.

232. Kowalski, C.H., et al., *Heterogeneity among Isolates Reveals that Fitness in Low Oxygen Correlates with Aspergillus fumigatus Virulence*. mBio, 2016. **7**(5): p. e01515-16.
233. Southam, D.S., et al., *Distribution of intranasal instillations in mice: effects of volume, time, body position, and anesthesia*. American journal of physiology. Lung cellular and molecular physiology, 2002. **282**(4): p. 833-L839.
234. Steele, C., et al., *The beta-glucan receptor dectin-1 recognizes specific morphologies of Aspergillus fumigatus*. PLoS pathogens, 2005. **1**(4): p. e42-e42.
235. Amarsaikhan, N., et al., *Isolate-dependent growth, virulence, and cell wall composition in the human pathogen Aspergillus fumigatus*. PLoS One, 2014. **9**(6): p. e100430.
236. Mattila, P.E., et al., *Dectin-1 Fc targeting of aspergillus fumigatus beta-glucans augments innate defense against invasive pulmonary aspergillosis*. Antimicrobial agents and chemotherapy, 2008. **52**(3): p. 1171.
237. Almutairi, B.M., et al., *Invasive aspergillosis of the brain: radiologic-pathologic correlation*. Radiographics, 2009. **29**(2): p. 375-379.
238. Tempkin, A.D., et al., *Cerebral aspergillosis: radiologic and pathologic findings*. Radiographics, 2006. **26**(4): p. 1239-1242.
239. Sullivan, B.N., et al., *A Systematic Review to Assess the Relationship between Disseminated Cerebral Aspergillosis, Leukemias and Lymphomas, and Their Respective Therapeutics*. 2022, *Journal of Fungi* p. 722.
240. Singh, G., et al., *Efficacy of Caspofungin against Central Nervous System Aspergillus fumigatus Infection in Mice Determined by TaqMan PCR and CFU Methods*. Antimicrobial Agents and Chemotherapy, 2005. **49**(4): p. 1369-1376.
241. Imai, J.K., et al., *Efficacy of posaconazole in a murine model of central nervous system aspergillosis*. Antimicrobial Agents and Chemotherapy, 2004. **48**(10): p. 4063-4066.
242. Clemons, K.V., et al., *Comparative Efficacies of Conventional Amphotericin B, Liposomal Amphotericin B (AmBisome), Caspofungin, Micafungin, and Voriconazole Alone and in Combination against Experimental Murine Central Nervous System Aspergillosis*. Antimicrobial Agents and Chemotherapy, 2005. **49**(12): p. 4867.
243. Zimmerli, S., U. Knecht, and S.L. Leib, *A model of cerebral aspergillosis in non-immunosuppressed nursing rats*. Acta neuropathologica, 2007. **114**(4): p. 411-418.
244. Clemons, K.V. and D.A. Stevens, *Conventional or molecular measurement of Aspergillus load*. Med Mycol, 2009. **47** Suppl 1: p. S132-7.
245. Mercier, T., et al., *Galactomannan, a surrogate marker for outcome in invasive aspergillosis: Finally coming of age*. Frontiers in microbiology, 2018. **9**: p. 661-661.
246. Shopova, I., et al., *Extrinsic extracellular DNA leads to biofilm formation and colocalizes with matrix polysaccharides in the human pathogenic fungus Aspergillus fumigatus*. Frontiers in microbiology, 2013. **4**: p. 141-141.
247. Stolz, D.J., et al., *Histological Quantification to Determine Lung Fungal Burden in Experimental Aspergillosis*. Journal of Visualized Experiments, 2018(133).
248. Klont, R.R., M.A.S.H. Mennink-Kersten, and P.E. Verweij, *Utility of Aspergillus Antigen Detection in Specimens Other than Serum Specimens*. Clinical infectious diseases, 2004. **39**(10): p. 1467-1474.
249. D'Haese, J., et al., *Detection of Galactomannan in Bronchoalveolar Lavage Fluid Samples of Patients at Risk for Invasive Pulmonary Aspergillosis: Analytical and Clinical Validity*. Journal of Clinical Microbiology, 2012. **50**(4): p. 1258-1263.

250. Dubey, L.K., et al., *Induction of innate immunity by Aspergillus fumigatus cell wall polysaccharides is enhanced by the composite presentation of chitin and beta-glucan*. Immunobiology (1979), 2013. **219**(3): p. 179-188.
251. Aimanianda, V., et al., *Surface hydrophobin prevents immune recognition of airborne fungal spores*. Nature, 2009. **460**(7259): p. 1117-1121.
252. Patin, E.C., A. Thompson, and S.J. Orr, *Pattern recognition receptors in fungal immunity*. Seminars in cell & developmental biology, 2019. **89**: p. 24-33.
253. Singh, N., *Novel immune regulatory pathways and their role in immune reconstitution syndrome in organ transplant recipients with invasive mycoses*. European journal of clinical microbiology & infectious diseases, 2008. **27**(6): p. 403-408.
254. Roilides, E., et al., *Elevated Serum Concentrations of Interleukin-10 in Nonneutropenic Patients with Invasive Aspergillosis*. The Journal of infectious diseases, 2001. **183**(3): p. 518-520.
255. Allard, J.B., et al., *Th2 allergic immune response to inhaled fungal antigens is modulated by TLR-4-independent bacterial products*. European journal of immunology, 2009. **39**(3): p. 776-788.
256. Roemer, T. and D.J. Krysan, *Antifungal drug development: challenges, unmet clinical needs, and new approaches*. Cold Spring Harbor perspectives in medicine, 2014. **4**(5): p. a019703-a019703.
257. Scorzoni, L., et al., *Antifungal Therapy: New Advances in the Understanding and Treatment of Mycosis*. Frontiers in microbiology, 2017. **8**: p. 36-36.
258. Manglani, M., S. Gossa, and D.B. McGavern, *Leukocyte Isolation from Brain, Spinal Cord, and Meninges for Flow Cytometric Analysis*. Current Protocols in Immunology, 2018. **121**(1): p. e44-n/a.
259. Fox, C., et al., *Minocycline confers early but transient protection in the immature brain following focal cerebral ischemia-reperfusion*. Journal of cerebral blood flow and metabolism, 2005. **25**(9): p. 1138-1149.
260. Rennet, E.S., et al., *Recombinant human VEGF165b protein is an effective anti-cancer agent in mice*. European journal of cancer (1990), 2008. **44**(13): p. 1883-1894.
261. Ben-Ami, R., et al., *Proangiogenic Growth Factors Potentiate In Situ Angiogenesis and Enhance Antifungal Drug Activity in Murine Invasive Aspergillosis*. The Journal of infectious diseases, 2013. **207**(7): p. 1066-1074.
262. Cramer, R.A., A. Rivera, and T.M. Hohl, *Immune responses against Aspergillus fumigatus: what have we learned?* Current opinion in infectious diseases, 2011. **24**(4): p. 315-322.
263. Tischler, B.Y. and T.M. Hohl, *Menacing Mold: Recent Advances in Aspergillus Pathogenesis and Host Defense*. Journal of molecular biology, 2019. **431**(21): p. 4229-4246.
264. Richard, S. and M.W. Schuster, *Stem cell transplantation and hematopoietic growth factors*. Curr Hematol Rep, 2002. **1**(2): p. 103-9.
265. Marciano, B.E., et al., *Long-Term Interferon- γ Therapy for Patients with Chronic Granulomatous Disease*. Clinical infectious diseases, 2004. **39**(5): p. 692-699.
266. Gale, R.P. and A. Vorobiov, *First use of myeloid colony-stimulating factors in humans*. Bone marrow transplantation (Basingstoke), 2013. **48**(10): p. 1358-1358.
267. Rowe, J.M., et al., *A randomized placebo-controlled phase III study of granulocyte-macrophage colony-stimulating factor in adult patients (> 55 to 70 years of age) with acute myelogenous leukemia: a study of the Eastern Cooperative Oncology Group (E1490)*. Blood, 1995. **86**(2): p. 457-62.

268. Safdar, A., et al., *The safety of interferon- γ -1b therapy for invasive fungal infections after hematopoietic stem cell transplantation*. *Cancer*, 2005. **103**(4): p. 731-739.
269. Sheppard, D.C. and S.G. Filler, *Host cell invasion by medically important fungi*. Cold Spring Harbor perspectives in medicine, 2014. **5**(1): p. a019687-a019687.
270. Giles, A.J., et al., *Dexamethasone-induced immunosuppression: mechanisms and implications for immunotherapy*. *Journal for immunotherapy of cancer*, 2018. **6**(1): p. 51-51.
271. Danielson, M., et al., *Effects of methylprednisolone on blood-brain barrier and cerebral inflammation in cardiac surgery-a randomized trial*. *Journal of neuroinflammation*, 2018. **15**(1): p. 283-283.
272. Hohl, T.M., et al., *Inflammatory monocytes facilitate adaptive CD4 T cell responses during respiratory fungal infection*. *Cell host & microbe*, 2009. **6**(5): p. 470-481.
273. Park, S.J., et al., *Neutropenia enhances lung dendritic cell recruitment in response to Aspergillus via a cytokine-to-chemokine amplification loop*. *The Journal of immunology (1950)*, 2010. **185**(10): p. 6190-6197.
274. Guo, Y., et al., *During Aspergillus Infection, Monocyte-Derived DCs, Neutrophils, and Plasmacytoid DCs Enhance Innate Immune Defense through CXCR3-Dependent Crosstalk*. *Cell host & microbe*, 2020. **28**(1): p. 104-116.e4.
275. Thammasit, P., et al., *Cytokine and Chemokine Responses in Invasive Aspergillosis Following Hematopoietic Stem Cell Transplantation: Past Evidence for Future Therapy of Aspergillosis*. *Journal of fungi (Basel)*, 2021. **7**(9): p. 753.
276. Thakur, R., et al., *Cytokines induce effector T-helper cells during invasive aspergillosis; what we have learned about T-helper cells?* *Frontiers in microbiology*, 2015. **6**: p. 429-429.
277. Caffrey, A.K., et al., *IL-1 α signaling is critical for leukocyte recruitment after pulmonary Aspergillus fumigatus challenge*. *PLoS pathogens*, 2015. **11**(1): p. e1004625-e1004625.
278. Langereis, J.D., et al., *Steroids induce a disequilibrium of secreted interleukin-1 receptor antagonist and interleukin-1 β synthesis by human neutrophils*. *The European respiratory journal*, 2011. **37**(2): p. 406-415.
279. Matsuzono, Y., et al., *Interleukin-6 in cerebrospinal fluid of patients with central nervous system infections*. *Acta Paediatr*, 1995. **84**(8): p. 879-83.
280. Gopalakrishnan, R.M., et al., *Increased IL-6 expression precedes reliable viral detection in the rhesus macaque brain during acute SIV infection*. *JCI insight*, 2021. **6**(20).
281. Hunter, C.A. and S.A. Jones, *IL-6 as a keystone cytokine in health and disease*. *Nature immunology*, 2015. **16**(5): p. 448-457.
282. Cenci, E., et al., *Impaired Antifungal Effector Activity but Not Inflammatory Cell Recruitment in Interleukin-6-Deficient Mice with Invasive Pulmonary Aspergillosis*. *The Journal of infectious diseases*, 2001. **184**(5): p. 610-617.
283. Mitani, H., et al., *Activity of interleukin 6 in the differentiation of monocytes to macrophages and dendritic cells*. *British journal of haematology*, 2000. **109**(2): p. 288-295.
284. Gao, J.-L., et al., *Impaired host defense, hematopoiesis, granulomatous inflammation and type 1-type 2 cytokine balance in mice lacking CC chemokine receptor 1*. *The Journal of experimental medicine*, 1997. **185**(11): p. 1959-1968.
285. Mehrad, B., T.A. Moore, and T.J. Standiford, *Macrophage inflammatory protein-1 α is a critical mediator of host defense against invasive pulmonary aspergillosis*

- in neutropenic hosts*. The Journal of immunology (1950), 2000. **165**(2): p. 962-968.
286. Mehrad, B., et al., *CXC Chemokine Receptor-2 Ligands Are Necessary Components of Neutrophil-Mediated Host Defense in Invasive Pulmonary Aspergillosis*. The Journal of immunology (1950), 1999. **163**(11): p. 6086-6094.
287. Werner, J.L., et al., *Requisite role for the dectin-1 beta-glucan receptor in pulmonary defense against Aspergillus fumigatus*. Journal of immunology (Baltimore, Md. : 1950), 2009. **182**(8): p. 4938.
288. Gessner, M.A., et al., *Dectin-1-Dependent Interleukin-22 Contributes to Early Innate Lung Defense against Aspergillus fumigatus*. Infection and Immunity, 2012. **80**(1): p. 410-417.
289. Gessner, M.A., et al., *Chlorine gas exposure increases susceptibility to invasive lung fungal infection*. American journal of physiology. Lung cellular and molecular physiology, 2013. **304**(11): p. L765-L773.
290. John, M., et al., *Inhaled corticosteroids increase interleukin-10 but reduce macrophage inflammatory protein-1 α , granulocyte-macrophage colony-stimulating factor, and interferon- γ release from alveolar macrophages in asthma*. American journal of respiratory and critical care medicine, 1998. **157**(1): p. 256-262.
291. Ito, K., et al., *Steroid-Resistant Neutrophilic Inflammation in a Mouse Model of an Acute Exacerbation of Asthma*. American journal of respiratory cell and molecular biology, 2008. **39**(5): p. 543-550.
292. Liu, R.R., et al., *Interleukin-17 Promotes Neutrophil-Mediated Immunity by Activating Microvascular Pericytes and Not Endothelium*. The Journal of immunology (1950), 2016. **197**(6): p. 2400-2408.
293. Flannigan, K.L., et al., *IL-17A-mediated neutrophil recruitment limits expansion of segmented filamentous bacteria*. Mucosal immunology, 2017. **10**(3): p. 673-684.
294. Happel, K.I., et al., *Cutting Edge: Roles of Toll-Like Receptor 4 and IL-23 in IL-17 Expression in Response to Klebsiella pneumoniae Infection*. The Journal of immunology (1950), 2003. **170**(9): p. 4432-4436.
295. Dixon, B.R.E.A., et al., *IL-17a and IL-22 Induce Expression of Antimicrobials in Gastrointestinal Epithelial Cells and May Contribute to Epithelial Cell Defense against Helicobacter pylori*. PloS one, 2016. **11**(2): p. e0148514-e0148514.
296. Taylor, P.R.P.R., et al., *Autocrine IL-17A-IL-17RC neutrophil activation in fungal infections is regulated by IL-6, IL-23, ROR γ t and Dectin-2*. Nature immunology, 2013. **15**(2): p. 143-151.
297. Song, X., et al., *The roles and functional mechanisms of interleukin-17 family cytokines in mucosal immunity*. Cellular & molecular immunology, 2016. **13**(4): p. 418-431.
298. Reeder, K.M., et al., *Role of common γ -Chain cytokines in lung interleukin-22 regulation after acute exposure to aspergillus fumigatus*. Infection and immunity, 2018. **86**(10).
299. Mackel, J.J., et al., *12/15-Lipoxygenase Deficiency Impairs Neutrophil Granulopoiesis and Lung Proinflammatory Responses to Aspergillus fumigatus*. The Journal of immunology (1950), 2020. **204**(7): p. 1849-1858.
300. Milovanovic, J., et al., *Interleukin-17 in Chronic Inflammatory Neurological Diseases*. Frontiers in immunology, 2020. **11**: p. 947-947.
301. Werner, J.L., et al., *Neutrophils Produce Interleukin 17A (IL-17A) in a Dectin-1- and IL-23-Dependent Manner during Invasive Fungal Infection*. Infection and Immunity, 2011. **79**(10): p. 3966-3977.

302. Kyrmizi, I., et al., *Corticosteroids block autophagy protein recruitment in Aspergillus fumigatus phagosomes via targeting dectin-1/Syk kinase signaling*. The Journal of immunology (1950), 2013. **191**(3): p. 1287-99.
303. Kotthoff, P., et al., *Dexamethasone induced inhibition of Dectin-1 activation of antigen presenting cells is mediated via STAT-3 and NF- κ B signaling pathways*. Scientific reports, 2017. **7**(1): p. 4522-11.
304. Ben-Ami, R., et al., *Aspergillus fumigatus inhibits angiogenesis through the production of gliotoxin and other secondary metabolites*. Blood, 2009. **114**(26): p. 5393-5399.
305. Johnson, D.H., et al., *Randomized phase II trial comparing bevacizumab plus carboplatin and paclitaxel with carboplatin and paclitaxel alone in previously untreated locally advanced or metastatic non-small-cell lung cancer*. J Clin Oncol, 2004. **22**(11): p. 2184-91.
306. Williams, J., R. Lim, and P. Tambyah, *Invasive aspergillosis associated with bevacizumab, a vascular endothelial growth factor inhibitor*. International journal of infectious diseases, 2007. **11**(6): p. 549-550.
307. Muzamil, J., et al., *Invasive pulmonary aspergillosis in oncological setting with use of newer vascular endothelial growth factor receptor inhibitor*. Community acquired infections, 2016. **3**(1): p. 16-23.
308. Li, J., et al., *Effect of VEGF on Inflammatory Regulation, Neural Survival, and Functional Improvement in Rats following a Complete Spinal Cord Transection*. Frontiers in cellular neuroscience, 2017. **11**: p. 381-381.
309. Jin, K., et al., *Vascular Endothelial Growth Factor (VEGF) Stimulates Neurogenesis in vitro and in vivo*. Proceedings of the National Academy of Sciences - PNAS, 2002. **99**(18): p. 11946-11950.
310. Froger, N., et al., *VEGF is an autocrine/paracrine neuroprotective factor for injured retinal ganglion neurons*. Scientific reports, 2020. **10**(1): p. 12409-12409.
311. Croll, S.D., et al., *VEGF-mediated inflammation precedes angiogenesis in adult brain*. Experimental neurology, 2004. **187**(2): p. 388-402.
312. Thurston, G., *Complementary actions of VEGF and Angiopoietin-1 on blood vessel growth and leakage*. Journal of anatomy, 2002. **200**(6): p. 575-580.
313. Chae, J.K., et al., *Coadministration of Angiopoietin-1 and Vascular Endothelial Growth Factor Enhances Collateral Vascularization*. Arteriosclerosis, thrombosis, and vascular biology, 2000. **20**(12): p. 2573-2578.
314. Wunderlich, M., et al., *AML cells are differentially sensitive to chemotherapy treatment in a human xenograft model*. Blood, 2013. **121**(12): p. e90-e97.
315. Wunderlich, M., et al., *Improved chemotherapy modeling with RAG-based immune deficient mice*. PloS one, 2019. **14**(11): p. e0225532-e0225532.
316. Daley, J.M., et al., *Use of Ly6G-specific monoclonal antibody to deplete neutrophils in mice*. Journal of leukocyte biology, 2008. **83**(1): p. 64-70.
317. Rowe, J.M., *The "7+3" regimen in acute myeloid leukemia*. Haematologica (Roma), 2022. **107**(1): p. 3-3.
318. Clemons, K.V., J.A. Schwartz, and D.A. Stevens, *Experimental central nervous system aspergillosis therapy: efficacy, drug levels and localization, immunohistopathology, and toxicity*. Antimicrobial agents and chemotherapy, 2012. **56**(8): p. 4439.
319. Warn, P.A., et al., *Comparative in vivo activity of BAL4815, the active component of the prodrug BAL8557, in a neutropenic murine model of disseminated Aspergillus flavus*. Journal of antimicrobial chemotherapy, 2006. **58**(6): p. 1198-1207.

320. Salas, V., et al., *Evaluation of the In Vitro Activity of Voriconazole As Predictive of In Vivo Outcome in a Murine Aspergillus fumigatus Infection Model*. Antimicrobial Agents and Chemotherapy, 2013. **57**(3): p. 1404-1408.
321. Wharton, R.E., et al., *Antibodies generated against streptococci protect in a mouse model of disseminated aspergillosis*. The Journal of immunology (1950), 2015. **194**(9): p. 4387-4396.
322. Clemons, K.V., et al., *Whole glucan particles as a vaccine against murine aspergillosis*. Journal of medical microbiology, 2014. **63**(12): p. 1750-1759.
323. Anand, R., et al., *Aspergillus flavus induces granulomatous cerebral aspergillosis in mice with display of distinct cytokine profile*. Cytokine (Philadelphia, Pa.), 2015. **72**(2): p. 166-172.
324. Rodriguez-de La Noval, C., et al., *Protective Efficacy of Lectin-Fc(IgG) Fusion Proteins In Vitro and in a Pulmonary Aspergillosis In Vivo Model*. Journal of fungi (Basel, Switzerland), 2020. **6**(4).
325. Siopi, M., et al., *A prospective multicenter cohort surveillance study of invasive aspergillosis in patients with hematologic malignancies in greece: impact of the revised eortc/msgerc 2020 criteria*. Journal of fungi (Basel), 2021. **7**(1): p. 1-11.
326. MÜHlemann, K., et al., *Risk factors for invasive aspergillosis in neutropenic patients with hematologic malignancies*. Leukemia, 2005. **19**(4): p. 545-550.
327. Buckley, S.A., et al., *Prediction of adverse events during intensive induction chemotherapy for acute myeloid leukemia or high-grade myelodysplastic syndromes*. American journal of hematology, 2014. **89**(4): p. 423-428.
328. Such, K.A., et al., *Environmental Monitoring for Aspergillus fumigatus in Association with an Immunosuppressed Rabbit Model of Pulmonary Aspergillosis*. Journal of the American Association for Laboratory Animal Science, 2013. **52**(5): p. 541-544.
329. Reilly, A., et al., *Immunologic consequences of chemotherapy for acute myeloid leukemia*. Journal of pediatric hematology/oncology, 2013. **35**(1): p. 46-53.
330. Carr, K.D., et al., *Specific depletion reveals a novel role for neutrophil-mediated protection in the liver during Listeria monocytogenes infection*. European journal of immunology, 2011. **41**(9): p. 2666-2676.
331. Walsh, T.J., et al., *Treatment of Aspergillosis: Clinical Practice Guidelines of the Infectious Diseases Society of America*. Clinical infectious diseases, 2008. **46**(3): p. 327-360.
332. Candoni, A., et al., *Fungal infections of the central nervous system and paranasal sinuses in onco-haematologic patients. Epidemiological study reporting the diagnostic-therapeutic approach and outcome in 89 cases*. Mycoses, 2019. **62**(3): p. 252-260.
333. Karakas, T., et al., *High expression of bcl-2 mRNA as a determinant of poor prognosis acute myeloid leukemia*. Annals of oncology, 1998. **9**(2): p. 159-165.
334. Kindler, T., D.B. Lipka, and T. Fischer, *FLT3 as a therapeutic target in AML: still challenging after all these years*. Blood, 2010. **116**(24): p. 5089-5102.
335. Stone, R.M., et al., *Midostaurin plus Chemotherapy for Acute Myeloid Leukemia with a FLT3 Mutation*. The New England journal of medicine, 2017. **377**(5): p. 454-464.
336. Samra, B., et al., *Venetoclax-Based Combinations in Acute Myeloid Leukemia: Current Evidence and Future Directions*. Frontiers in oncology, 2020. **10**: p. 562558-562558.
337. Cattaneo, C., et al., *High Incidence of Invasive Fungal Diseases in Patients with FLT3-Mutated AML Treated with Midostaurin: Results of a Multicenter Observational SEIFEM Study*. Journal of fungi (Basel), 2022. **8**(6): p. 583.

338. Ozga, M., et al., *The Incidence of Invasive Fungal Infections in Patients With AML Treated With a Hypomethylating Agent*. *Clinical lymphoma, myeloma and leukemia*, 2021. **21**(1): p. e76-e83.
339. Drosten, C., et al., *Identification of a novel coronavirus in patients with severe acute respiratory syndrome*. *N Engl J Med*, 2003. **348**(20): p. 1967-76.
340. Memish, Z.A., et al., *Family cluster of Middle East respiratory syndrome coronavirus infections*. *N Engl J Med*, 2013. **368**(26): p. 2487-94.
341. Huang, C., et al., *Clinical features of patients infected with 2019 novel coronavirus in Wuhan, China*. *Lancet*, 2020. **395**(10223): p. 497-506.
342. (WHO), W.H.O. *Weekly Operational Update on COVID-19, 10 May 2021, Issue No. 54*. 2021 [cited 2021 10 May]; Available from: <https://www.who.int/publications/m/item/weekly-operational-update-on-covid-19--10-may-2021>.
343. (CDC), C.f.D.C.a.P. *Symptoms of Coronavirus*. 2020; Available from: https://www.cdc.gov/coronavirus/2019-ncov/symptoms-testing/symptoms.html?CDC_AA_refVal=https%3A%2F%2Fwww.cdc.gov%2Fcoronavirus%2F2019-ncov%2Fsymptoms-testing%2Findex.html.
344. Mao, L., et al., *Neurologic Manifestations of Hospitalized Patients With Coronavirus Disease 2019 in Wuhan, China*. *JAMA Neurol*, 2020.
345. Chen, N., et al., *Epidemiological and clinical characteristics of 99 cases of 2019 novel coronavirus pneumonia in Wuhan, China: a descriptive study*. *Lancet*, 2020. **395**(10223): p. 507-513.
346. Yang, X., et al., *Clinical course and outcomes of critically ill patients with SARS-CoV-2 pneumonia in Wuhan, China: a single-centered, retrospective, observational study*. *Lancet Respir Med*, 2020.
347. Lodigiani, C., et al., *Venous and arterial thromboembolic complications in COVID-19 patients admitted to an academic hospital in Milan, Italy*. *Thrombosis research*, 2020. **191**.
348. TunÇ, A., et al., *Coexistence of COVID-19 and acute ischemic stroke report of four cases*. *Journal of clinical neuroscience : official journal of the Neurosurgical Society of Australasia*, 2020. **77**.
349. Al-Olama, M., A. Rashid, and D. Garozzo, *COVID-19-associated meningoencephalitis complicated with intracranial hemorrhage: a case report*. *Acta neurochirurgica*, 2020. **162**(7).
350. Scullen, T., et al., *Coronavirus 2019 (COVID-19)-Associated Encephalopathies and Cerebrovascular Disease: The New Orleans Experience*. *World neurosurgery*, 2020.
351. Farhadian, S., et al., *Acute encephalopathy with elevated CSF inflammatory markers as the initial presentation of COVID-19*. *BMC neurology*, 2020. **20**(1).
352. Lu, L., et al., *New-onset acute symptomatic seizure and risk factors in Corona Virus Disease 2019: A Retrospective Multicenter Study*. *Epilepsia*, 2020.
353. Moher, D., et al., *Preferred reporting items for systematic reviews and meta-analyses: the PRISMA statement*. *PLoS Med*, 2009. **6**(7): p. e1000097.
354. Williamson, P.O. and C.I.J. Minter, *Exploring PubMed as a reliable resource for scholarly communications services*. *J Med Libr Assoc*, 2019. **107**(1): p. 16-29.
355. Dugue, R., et al., *Neurologic manifestations in an infant with COVID-19*. *Neurology*, 2020. **94**(24): p. 1100-1102.
356. Xiong, W., et al., *New onset neurologic events in people with COVID-19 in 3 regions in China*. *Neurology*, 2020. **95**(11): p. e1479-e1487.

357. Anand, P., et al., *Posterior Reversible Encephalopathy Syndrome in Patients with Coronavirus Disease 2019: Two Cases and A Review of The Literature*. J Stroke Cerebrovasc Dis, 2020. **29**(11): p. 105212.
358. Cohen, J., *Set Correlation and Contingency Tables*: <http://dx.doi.org/10.1177/014662168801200410>, 1988.
359. Tiwari, L., et al., *COVID-19 associated arterial ischaemic stroke and multisystem inflammatory syndrome in children: a case report*. Lancet Child Adolesc Health, 2021. **5**(1): p. 88-90.
360. Gulko, E., et al., *Vessel Wall Enhancement and Focal Cerebral Arteriopathy in a Pediatric Patient with Acute Infarct and COVID-19 Infection*. AJNR Am J Neuroradiol, 2020. **41**(12): p. 2348-2350.
361. Dakay, K., et al., *Cerebral Venous Sinus Thrombosis in COVID-19 Infection: A Case Series and Review of The Literature*. J Stroke Cerebrovasc Dis, 2021. **30**(1): p. 105434.
362. Asif, R. and M.S. O' Mahony, *Rare complication of COVID-19 presenting as isolated headache*. BMJ Case Rep, 2020. **13**(10).
363. Cavalcanti, D.D., et al., *Cerebral Venous Thrombosis Associated with COVID-19*. AJNR Am J Neuroradiol, 2020. **41**(8): p. 1370-1376.
364. de Sousa, G.C., et al., *Vasculitis-related stroke in young as a presenting feature of novel coronavirus disease (COVID19) - Case report*. J Clin Neurosci, 2020. **79**: p. 169-171.
365. Vu, D., et al., *Three unsuspected CT diagnoses of COVID-19*. Emerg Radiol, 2020. **27**(3): p. 229-232.
366. Oxley, T.J., et al., *Large-Vessel Stroke as a Presenting Feature of Covid-19 in the Young*. N Engl J Med, 2020.
367. Chia, K.X., S. Polakhare, and S.D. Bruno, *Possible affective cognitive cerebellar syndrome in a young patient with COVID-19 CNS vasculopathy and stroke*. BMJ Case Rep, 2020. **13**(10).
368. Sabayan, B., et al., *COVID-19 Respiratory Illness and Subsequent Cerebrovascular Events, the Initial Iranian Experience*. J Stroke Cerebrovasc Dis, 2021. **30**(1): p. 105454.
369. Trifan, G., M. Hillmann, and F.D. Testai, *Acute Stroke as the Presenting Symptom of SARS-CoV-2 Infection in a Young Patient with Cerebral Autosomal Dominant Arteriopathy with Subcortical Infarcts and Leukoencephalopathy*. J Stroke Cerebrovasc Dis, 2020. **29**(10): p. 105167.
370. Diaz-Segarra, N., et al., *COVID-19 Ischemic Strokes as an Emerging Rehabilitation Population: A Case Series*. Am J Phys Med Rehabil, 2020. **99**(10): p. 876-879.
371. Cezar-Junior, A.B., et al., *Subarachnoid hemorrhage and COVID-19: Association or coincidence?* Medicine (Baltimore), 2020. **99**(51): p. e23862.
372. Shah, H., et al., *Case Report: Multiple Strokes and Digital Ischemia in a Young COVID-19 Patient*. Am J Trop Med Hyg, 2021. **104**(1): p. 60-62.
373. Pisano, T.J., I. Hakkinen, and I. Rybinnik, *Large Vessel Occlusion Secondary to COVID-19 Hypercoagulability in a Young Patient: A Case Report and Literature Review*. J Stroke Cerebrovasc Dis, 2020. **29**(12): p. 105307.
374. Fara, M.G., et al., *Macrothrombosis and stroke in patients with mild Covid-19 infection*. J Thromb Haemost, 2020. **18**(8): p. 2031-2033.
375. Al-Mufti, F., et al., *Acute Cerebrovascular Disorders and Vasculopathies Associated with Significant Mortality in SARS-CoV-2 Patients Admitted to The Intensive Care Unit in The New York Epicenter*. J Stroke Cerebrovasc Dis, 2021. **30**(2): p. 105429.

376. Al Saiegh, F., et al., *Status of SARS-CoV-2 in cerebrospinal fluid of patients with COVID-19 and stroke*. J Neurol Neurosurg Psychiatry, 2020. **91**(8): p. 846-848.
377. Wang, A., et al., *Stroke and mechanical thrombectomy in patients with COVID-19: technical observations and patient characteristics*. J Neurointerv Surg, 2020. **12**(7): p. 648-653.
378. Trifan, G., et al., *Characteristics of a Diverse Cohort of Stroke Patients with SARS-CoV-2 and Outcome by Sex*. J Stroke Cerebrovasc Dis, 2020. **29**(11): p. 105314.
379. Kantonen, J., et al., *Neuropathologic features of four autopsied COVID-19 patients*. Brain Pathol, 2020. **30**(6): p. 1012-1016.
380. Frisullo, G., et al., *Stroke and COVID19: Not only a large-vessel disease*. J Stroke Cerebrovasc Dis, 2020. **29**(10): p. 105074.
381. Patel, S.D., et al., *Malignant Cerebral Ischemia in A COVID-19 Infected Patient: Case Review and Histopathological Findings*. J Stroke Cerebrovasc Dis, 2020. **29**(11): p. 105231.
382. Yaghi, S., et al., *SARS-CoV-2 and Stroke in a New York Healthcare System*. Stroke, 2020. **51**(7): p. 2002-2011.
383. Anzalone, N., et al., *Multifocal laminar cortical brain lesions: a consistent MRI finding in neuro-COVID-19 patients*. J Neurol, 2020. **267**(10): p. 2806-2809.
384. Heman-Ackah, S.M., et al., *Neurologically Devastating Intraparenchymal Hemorrhage in COVID-19 Patients on Extracorporeal Membrane Oxygenation: A Case Series*. Neurosurgery, 2020. **87**(2): p. E147-E151.
385. de Almeida Lima, A.N., et al., *Images in Vascular Medicine: Acute peripheral artery occlusion and ischemic stroke in a patient with COVID-19*. Vasc Med, 2020. **25**(5): p. 482-483.
386. TunÇ, A., et al., *Coexistence of COVID-19 and acute ischemic stroke report of four cases*. J Clin Neurosci, 2020. **77**: p. 227-229.
387. Lapergue, B., et al., *Large vessel stroke in six patients following SARS-CoV-2 infection: a retrospective case study series of acute thrombotic complications on stable underlying atherosclerotic disease*. Eur J Neurol, 2020. **27**(11): p. 2308-2311.
388. Fu, B., Y. Chen, and P. Li, *2019 novel coronavirus disease with secondary ischemic stroke: two case reports*. BMC Neurol, 2021. **21**(1): p. 4.
389. Toledano-Massiah, S., et al., *Unusual Brain MRI Pattern in 2 Patients with COVID-19 Acute Respiratory Distress Syndrome*. AJNR Am J Neuroradiol, 2020. **41**(12): p. 2204-2205.
390. Nicholson, P., L. Alshafai, and T. Krings, *Neuroimaging Findings in Patients with COVID-19*. AJNR Am J Neuroradiol, 2020. **41**(8): p. 1380-1383.
391. Mullaguri, N., et al., *COVID-19 Disease and Hypercoagulability Leading to Acute Ischemic Stroke*. Neurohospitalist, 2021. **11**(2): p. 131-136.
392. Agarwal, A., et al., *Neurological emergencies associated with COVID-19: stroke and beyond*. Emerg Radiol, 2020. **27**(6): p. 747-754.
393. Fabbri, V.P., et al., *Brain ischemic injury in COVID-19-infected patients: a series of 10 post-mortem cases*. Brain Pathol, 2021. **31**(1): p. 205-210.
394. Gupta, N.A., C. Lien, and M. Iv, *Critical illness-associated cerebral microbleeds in severe COVID-19 infection*. Clin Imaging, 2020. **68**: p. 239-241.
395. Avci, A., et al., *Spontaneous subarachnoidal hemorrhage in patients with Covid-19: case report*. J Neurovirology, 2020. **26**(5): p. 802-804.
396. Sugiyama, Y., et al., *Cerebral venous thrombosis in COVID-19-associated coagulopathy: A case report*. J Clin Neurosci, 2020. **79**: p. 30-32.

397. Mousa-Ibrahim, F., et al., *Intracranial Hemorrhage in Hospitalized SARS-CoV-2 Patients: A Case Series*. J Stroke Cerebrovasc Dis, 2021. **30**(1): p. 105428.
398. Fayed, I., et al., *Intracranial hemorrhage in critically ill patients hospitalized for COVID-19*. J Clin Neurosci, 2020. **81**: p. 192-195.
399. Sangalli, D., et al., *A single-centre experience of intravenous thrombolysis for stroke in COVID-19 patients*. Neurol Sci, 2020. **41**(9): p. 2325-2329.
400. Kremer, S., et al., *Neurologic and neuroimaging findings in patients with COVID-19: A retrospective multicenter study*. Neurology, 2020. **95**(13): p. e1868-e1882.
401. Morassi, M., et al., *Stroke in patients with SARS-CoV-2 infection: case series*. J Neurol, 2020. **267**(8): p. 2185-2192.
402. Panico, F., et al., *Balint-Holmes syndrome due to stroke following SARS-CoV-2 infection: a single-case report*. Neurol Sci, 2020. **41**(12): p. 3487-3489.
403. D'Anna, L., et al., *Characteristics and clinical course of Covid-19 patients admitted with acute stroke*. J Neurol, 2020. **267**(11): p. 3161-3165.
404. Mansour, O.Y., A.M. Malik, and I. Linfante, *Mechanical Thrombectomy of COVID-19 positive acute ischemic stroke patient: a case report and call for preparedness*. BMC Neurol, 2020. **20**(1): p. 358.
405. Harrogate, S., et al., *Non-aneurysmal subarachnoid haemorrhage in COVID-19*. Neuroradiology, 2021. **63**(1): p. 149-152.
406. Beyrouiti, R., et al., *Characteristics of ischaemic stroke associated with COVID-19*. J Neurol Neurosurg Psychiatry, 2020. **91**(8): p. 889-891.
407. Prasad, A., et al., *Multiple embolic stroke on magnetic resonance imaging of the brain in a COVID-19 case with persistent encephalopathy*. Clin Imaging, 2021. **69**: p. 285-288.
408. Nepal, P., et al., *An unresponsive COVID-19 patient*. Emerg Radiol, 2020. **27**(6): p. 755-759.
409. Motoie, R., et al., *Coronavirus Disease 2019 Complicated by Multiple Simultaneous Intracerebral Hemorrhages*. Intern Med, 2020. **59**(20): p. 2597-2600.
410. Jaunmuktane, Z., et al., *Microvascular injury and hypoxic damage: emerging neuropathological signatures in COVID-19*. Acta Neuropathol, 2020. **140**(3): p. 397-400.
411. Saitta, L., et al., *Brain microvascular occlusive disorder in COVID-19: a case report*. Neurol Sci, 2020. **41**(12): p. 3401-3404.
412. Soldatelli, M.D., et al., *Neurovascular and perfusion imaging findings in coronavirus disease 2019: Case report and literature review*. Neuroradiol J, 2020. **33**(5): p. 368-373.
413. Shawkat, A., et al., *Multiple Thrombotic Events in a 67-Year-Old Man 2 Weeks After Testing Positive for SARS-CoV-2: A Case Report*. Am J Case Rep, 2020. **21**: p. e925786.
414. Guillan, M., et al., *Unusual simultaneous cerebral infarcts in multiple arterial territories in a COVID-19 patient*. Thromb Res, 2020. **193**: p. 107-109.
415. Siepmann, T., et al., *Increased risk of acute stroke among patients with severe COVID-19: a multicenter study and meta-analysis*. Eur J Neurol, 2021. **28**(1): p. 238-247.
416. Hemasian, H. and B. Ansari, *First case of Covid-19 presented with cerebral venous thrombosis: A rare and dreaded case*. Rev Neurol (Paris), 2020. **176**(6): p. 521-523.
417. Díaz-Pérez, C., et al., *Acutely altered mental status as the main clinical presentation of multiple strokes in critically ill patients with COVID-19*. Neurol Sci, 2020. **41**(10): p. 2681-2684.

418. Imoto, W., et al., *Coronavirus disease with multiple infarctions*. QJM, 2020. **113**(12): p. 907-908.
419. Roy-Gash, F., et al., *COVID-19-associated acute cerebral venous thrombosis: clinical, CT, MRI and EEG features*. Crit Care, 2020. **24**(1): p. 419.
420. Bolaji, P., et al., *Extensive cerebral venous sinus thrombosis: a potential complication in a patient with COVID-19 disease*. BMJ Case Rep, 2020. **13**(8).
421. Azpiazu Landa, N., et al., *Ischemic-hemorrhagic stroke in patients with Covid-19*. Rev Esp Anesthesiol Reanim, 2020. **67**(9): p. 516-520.
422. Co, C.O.C., et al., *Intravenous Thrombolysis for Stroke in a COVID-19 Positive Filipino Patient, a Case Report*. J Clin Neurosci, 2020. **77**: p. 234-236.
423. Bigliardi, G., et al., *Middle cerebral artery ischemic stroke and COVID-19: a case report*. J Neurovirol, 2020. **26**(6): p. 967-969.
424. Yong, M.H., et al., *A Rare Case of Acute Hemorrhagic Leukoencephalitis in a COVID-19 Patient*. J Neurol Sci, 2020. **416**: p. 117035.
425. Shoskes, A., et al., *Cerebral Microhemorrhage and Purpuric Rash in COVID-19: The Case for a Secondary Microangiopathy*. J Stroke Cerebrovasc Dis, 2020. **29**(10): p. 105111.
426. Garvı́ López, M., M. Tauler Redondo, and J. Tortajada Soler, *Intracranial hemorrhages in critical COVID-19 patients: report of three cases*. Medicina clinica (English ed.), 2021. **156**(1).
427. Khan, A.W., I. Ullah, and K.S. Khan, *Ischemic stroke leading to bilateral vision loss in COVID-19 patient-A rare case report*. J Med Virol, 2021. **93**(2): p. 683-685.
428. Cannac, O., L. Martinez-Almoyna, and S. Hraiech, *Critical illness-associated cerebral microbleeds in COVID-19 acute respiratory distress syndrome*. Neurology, 2020. **95**(11): p. 498-499.
429. Vattoth, S., et al., *Critical illness-associated cerebral microbleeds in COVID-19*. Neuroradiol J, 2020. **33**(5): p. 374-376.
430. Gonçalves, B., C. Righy, and P. Kurtz, *Thrombotic and Hemorrhagic Neurological Complications in Critically Ill COVID-19 Patients*. Neurocrit Care, 2020. **33**(2): p. 587-590.
431. Avula, A., et al., *COVID-19 presenting as stroke*. Brain Behav Immun, 2020. **87**: p. 115-119.
432. Papi, C., et al., *Unprotected stroke management in an undiagnosed case of Severe Acute Respiratory Syndrome Coronavirus 2 infection*. J Stroke Cerebrovasc Dis, 2020. **29**(9): p. 104981.
433. Zayet, S., et al., *Acute Cerebral Stroke with Multiple Infarctions and COVID-19, France, 2020*. Emerg Infect Dis, 2020. **26**(9).
434. Viguier, A., et al., *Acute ischemic stroke complicating common carotid artery thrombosis during a severe COVID-19 infection*. J Neuroradiol, 2020. **47**(5): p. 393-394.
435. Al-Dalahmah, O., et al., *Neuronophagia and microglial nodules in a SARS-CoV-2 patient with cerebellar hemorrhage*. Acta Neuropathol Commun, 2020. **8**(1): p. 147.
436. Burkert, J. and S. Patil, *Acute cerebrovascular event in a COVID-19 positive patient immediately after commencing non-invasive ventilation*. BMJ Case Rep, 2020. **13**(9).
437. Robles, L.A., *Bilateral Large Vessel Occlusion Causing Massive Ischemic Stroke in a COVID-19 Patient*. J Stroke Cerebrovasc Dis, 2021. **30**(3): p. 105609.
438. Mohamed, I.Z.B., L. Balson, and S. Madathil, *Massive bilateral stroke in a COVID-19 patient*. BMJ Case Rep, 2020. **13**(8).

439. Alay, H., F.K. Can, and E. Gözgeç, *Cerebral Infarction in an Elderly Patient with Coronavirus Disease*. Rev Soc Bras Med Trop, 2020. **53**: p. e20200307.
440. Khalifa, M., et al., *Guillain-Barré Syndrome Associated With Severe Acute Respiratory Syndrome Coronavirus 2 Detection and Coronavirus Disease 2019 in a Child*. J Pediatric Infect Dis Soc, 2020. **9**(4): p. 510-513.
441. Manji, H., et al., *Neurology in the time of covid-19*. J Neurol Neurosurg Psychiatry, 2020.
442. Hutchins, K.L., et al., *COVID-19-Associated Bifacial Weakness with Paresthesia Subtype of Guillain-Barré Syndrome*. AJNR Am J Neuroradiol, 2020. **41**(9): p. 1707-1711.
443. Toscano, G., et al., *Guillain-Barré Syndrome Associated with SARS-CoV-2*. N Engl J Med, 2020.
444. Ameer, N., K.M. Shekhda, and A. Cheesman, *Guillain-Barré syndrome presenting with COVID-19 infection*. BMJ Case Rep, 2020. **13**(9).
445. Lantos, J.E., S.B. Strauss, and E. Lin, *COVID-19-Associated Miller Fisher Syndrome: MRI Findings*. AJNR Am J Neuroradiol, 2020. **41**(7): p. 1184-1186.
446. Rajdev, K., et al., *A Case of Guillain-Barré Syndrome Associated With COVID-19*. J Investig Med High Impact Case Rep, 2020. **8**: p. 2324709620961198.
447. Gutiérrez-Ortiz, C., et al., *Miller Fisher syndrome and polyneuritis cranialis in COVID-19*. Neurology, 2020. **95**(5): p. e601-e605.
448. Dinkin, M., et al., *COVID-19 presenting with ophthalmoparesis from cranial nerve palsy*. Neurology, 2020. **95**(5): p. 221-223.
449. Homma, Y., et al., *Coronavirus Disease-19 Pneumonia with Facial Nerve Palsy and Olfactory Disturbance*. Intern Med, 2020. **59**(14): p. 1773-1775.
450. Tiet, M.Y. and N. AlShaikh, *Guillain-Barré syndrome associated with COVID-19 infection: a case from the UK*. BMJ Case Rep, 2020. **13**(7).
451. Nanda, S., et al., *Covid-19 associated Guillain-Barre Syndrome: Contrasting tale of four patients from a tertiary care centre in India*. Am J Emerg Med, 2021. **39**: p. 125-128.
452. Manganotti, P., et al., *Clinical neurophysiology and cerebrospinal liquor analysis to detect Guillain-Barré syndrome and polyneuritis cranialis in COVID-19 patients: A case series*. J Med Virol, 2021. **93**(2): p. 766-774.
453. Liberatore, G., et al., *Clinical Reasoning: A case of COVID-19-associated pharyngeal-cervical-brachial variant of Guillain-Barré syndrome*. Neurology, 2020. **95**(21): p. 978-983.
454. Abolmaali, M., et al., *Guillain-Barré syndrome as a parainfectious manifestation of SARS-CoV-2 infection: A case series*. J Clin Neurosci, 2021. **83**: p. 119-122.
455. Khaja, M., et al., *A 44-Year-Old Hispanic Man with Loss of Taste and Bilateral Facial Weakness Diagnosed with Guillain-Barré Syndrome and Bell's Palsy Associated with SARS-CoV-2 Infection Treated with Intravenous Immunoglobulin*. Am J Case Rep, 2020. **21**: p. e927956.
456. Velayos Galán, A., et al., *Guillain-Barré syndrome associated with SARS-CoV-2 infection*. Neurologia, 2020. **35**(4): p. 268-269.
457. Bigaut, K., et al., *Guillain-Barré syndrome related to SARS-CoV-2 infection*. Neurol Neuroimmunol Neuroinflamm, 2020. **7**(5).
458. Hirayama, T., et al., *Guillain-Barré syndrome after COVID-19 in Japan*. BMJ Case Rep, 2020. **13**(10).
459. Naddaf, E., et al., *Guillain-Barré Syndrome in a Patient With Evidence of Recent SARS-CoV-2 Infection*. Mayo Clin Proc, 2020. **95**(8): p. 1799-1801.
460. Korem, S., H. Gandhi, and D.B. Dayag, *Guillain-Barré syndrome associated with COVID-19 disease*. BMJ Case Rep, 2020. **13**(9).

461. Gale, A., S. Sabaretnam, and A. Lewinsohn, *Guillain-Barré syndrome and COVID-19: association or coincidence*. *BMJ Case Rep*, 2020. **13**(11).
462. Chan, J.L., H. Ebadi, and J.R. Sarna, *Guillain-Barré Syndrome with Facial Diplegia Related to SARS-CoV-2 Infection*. *Can J Neurol Sci*, 2020. **47**(6): p. 852-854.
463. Webb, S., et al., *Guillain-Barré syndrome following COVID-19: a newly emerging post-infectious complication*. *BMJ Case Rep*, 2020. **13**(6).
464. Petrelli, C., et al., *Acute Motor Axonal Neuropathy Related to COVID-19 Infection: A New Diagnostic Overview*. *J Clin Neuromuscul Dis*, 2020. **22**(2): p. 120-121.
465. Sancho-Saldaña, A., et al., *Guillain-Barré syndrome associated with leptomeningeal enhancement following SARS-CoV-2 infection*. *Clin Med (Lond)*, 2020. **20**(4): p. e93-e94.
466. Assini, A., et al., *New clinical manifestation of COVID-19 related Guillain-Barré syndrome highly responsive to intravenous immunoglobulins: two Italian cases*. *Neurol Sci*, 2020. **41**(7): p. 1657-1658.
467. Rana, S., et al., *Novel Coronavirus (COVID-19)-Associated Guillain-Barré Syndrome: Case Report*. *J Clin Neuromuscul Dis*, 2020. **21**(4): p. 240-242.
468. Barrachina-Esteve, O., et al., *[Guillain-Barré syndrome as the first manifestation of SARS-CoV-2 infection]*. *Neurologia*, 2020. **35**(9): p. 710-712.
469. Manganotti, P., et al., *Miller Fisher syndrome diagnosis and treatment in a patient with SARS-CoV-2*. *J Neurovirol*, 2020. **26**(4): p. 605-606.
470. Wada, S., et al., *Neurological Disorders Identified during Treatment of a SARS-CoV-2 Infection*. *Intern Med*, 2020. **59**(17): p. 2187-2189.
471. Abrams, R.M.C., et al., *Severe rapidly progressive Guillain-Barré syndrome in the setting of acute COVID-19 disease*. *J Neurovirol*, 2020. **26**(5): p. 797-799.
472. Bracaglia, M., et al., *Acute inflammatory demyelinating polyneuritis in association with an asymptomatic infection by SARS-CoV-2*. *J Neurol*, 2020. **267**(11): p. 3166-3168.
473. Sedaghat, Z. and N. Karimi, *Guillain Barre syndrome associated with COVID-19 infection: A case report*. *J Clin Neurosci*, 2020.
474. Juliao Caamaño, D.S. and R. Alonso Beato, *Facial diplegia, a possible atypical variant of Guillain-Barré Syndrome as a rare neurological complication of SARS-CoV-2*. *J Clin Neurosci*, 2020. **77**: p. 230-232.
475. Zhao, H., et al., *Guillain-Barré syndrome associated with SARS-CoV-2 infection: causality or coincidence?* *Lancet Neurol*, 2020. **19**(5): p. 383-384.
476. Senel, M., et al., *Miller-Fisher syndrome after COVID-19: neurochemical markers as an early sign of nervous system involvement*. *Eur J Neurol*, 2020. **27**(11): p. 2378-2380.
477. Bueso, T., et al., *Guillain-Barre Syndrome and COVID-19: A case report*. *Clin Neurol Neurosurg*, 2021. **200**: p. 106413.
478. Nasuelli, N.A., et al., *Critical illness neuro-myopathy (CINM) and focal amyotrophy in intensive care unit (ICU) patients with SARS-CoV-2: a case series*. *Neurol Sci*, 2021. **42**(3): p. 1119-1121.
479. Tankisi, H., et al., *Critical illness myopathy as a consequence of Covid-19 infection*. *Clin Neurophysiol*, 2020. **131**(8): p. 1931-1932.
480. Marta-Enguita, J., I. Rubio-Baines, and I. Gastón-Zubimendi, *Fatal Guillain-Barre syndrome after infection with SARS-CoV-2*. *Neurologia*, 2020. **35**(4): p. 265-267.
481. Fernández-Domínguez, J., et al., *Miller-Fisher-like syndrome related to SARS-CoV-2 infection (COVID 19)*. *J Neurol*, 2020. **267**(9): p. 2495-2496.

482. Su, X.W., et al., *SARS-CoV-2-associated Guillain-Barré syndrome with dysautonomia*. *Muscle Nerve*, 2020. **62**(2): p. E48-E49.
483. Alberti, P., et al., *Guillain-Barré syndrome related to COVID-19 infection*. *Neurol Neuroimmunol Neuroinflamm*, 2020. **7**(4).
484. Coen, M., et al., *Guillain-Barré syndrome as a complication of SARS-CoV-2 infection*. *Brain Behav Immun*, 2020. **87**: p. 111-112.
485. De Paulis, M., et al., *Multisystem Inflammatory Syndrome Associated With COVID-19 With Neurologic Manifestations in a Child: A Brief Report*. *Pediatr Infect Dis J*, 2020. **39**(10): p. e321-e324.
486. Abel, D., et al., *Encephalopathy and bilateral thalamic lesions in a child with MIS-C associated with COVID-19*. *Neurology*, 2020. **95**(16): p. 745-748.
487. Babar, A., et al., *SARS-CoV-2 Encephalitis in a 20-year old Healthy Female*. *Pediatr Infect Dis J*, 2020. **39**(10): p. e320-e321.
488. Kamal, Y.M., Y. Abdelmajid, and A.A.R. Al Madani, *Cerebrospinal fluid confirmed COVID-19-associated encephalitis treated successfully*. *BMJ Case Rep*, 2020. **13**(9).
489. Radnis, C., et al., *Radiographic and clinical neurologic manifestations of COVID-19 related hypoxemia*. *J Neurol Sci*, 2020. **418**: p. 117119.
490. Benameur, K., et al., *Encephalopathy and Encephalitis Associated with Cerebrospinal Fluid Cytokine Alterations and Coronavirus Disease, Atlanta, Georgia, USA, 2020*. *Emerg Infect Dis*, 2020. **26**(9): p. 2016-2021.
491. Pascual-Goñi, E., et al., *COVID-19-associated ophthalmoparesis and hypothalamic involvement*. *Neurol Neuroimmunol Neuroinflamm*, 2020. **7**(5).
492. Zayet, S., et al., *Encephalopathy in patients with COVID-19: "Causality or coincidence?"*. *J Med Virol*, 2021. **93**(2): p. 1193.
493. Dakay, K., et al., *Reversible cerebral vasoconstriction syndrome and dissection in the setting of COVID-19 infection*. *J Stroke Cerebrovasc Dis*, 2020. **29**(9): p. 105011.
494. Franceschi, A.M., et al., *Hemorrhagic Posterior Reversible Encephalopathy Syndrome as a Manifestation of COVID-19 Infection*. *AJNR Am J Neuroradiol*, 2020. **41**(7): p. 1173-1176.
495. Muccioli, L., et al., *COVID-19-related encephalopathy presenting with aphasia resolving following tocilizumab treatment*. *J Neuroimmunol*, 2020. **349**: p. 577400.
496. Fischer, D., et al., *Intact Brain Network Function in an Unresponsive Patient with COVID-19*. *Ann Neurol*, 2020. **88**(4): p. 851-854.
497. Ordoñez-Boschetti, L., C.M. Torres-Romero, and M.J. Ortiz de Leo, *[Associated posterior reversible encephalopathy syndrome (PRES) to SARS-CoV-2. Case report]*. *Neurologia*, 2020. **35**(9): p. 696-698.
498. Hosseini, A.A., et al., *Delirium as a presenting feature in COVID-19: Neuroinvasive infection or autoimmune encephalopathy?* *Brain Behav Immun*, 2020. **88**: p. 68-70.
499. Scullen, T., et al., *Coronavirus 2019 (COVID-19)-Associated Encephalopathies and Cerebrovascular Disease: The New Orleans Experience*. *World Neurosurg*, 2020. **141**: p. e437-e446.
500. Edén, A., et al., *CSF Biomarkers in Patients With COVID-19 and Neurologic Symptoms*. 2021.
501. Matos, A.R., et al., *COVID-19 Associated Central Nervous System Vasculopathy*. *Can J Neurol Sci*, 2021. **48**(1): p. 139-140.

502. Naaraayan, A., S. Pant, and S. Jesmajian, *Severe Hyponatremic Encephalopathy in a Patient With COVID-19*. Mayo Clin Proc, 2020. **95**(10): p. 2285-2286.
503. Abenza-Abildúa, M.J., et al., *Encephalopathy in severe SARS-CoV2 infection: Inflammatory or infectious?* Int J Infect Dis, 2020. **98**: p. 398-400.
504. Priftis, K., et al., *COVID-19 presenting with agraphia and conduction aphasia in a patient with left-hemisphere ischemic stroke*. Neurol Sci, 2020. **41**(12): p. 3381-3384.
505. Perrin, P., et al., *Cytokine release syndrome-associated encephalopathy in patients with COVID-19*. Eur J Neurol, 2021. **28**(1): p. 248-258.
506. Chaumont, H., et al., *Mixed central and peripheral nervous system disorders in severe SARS-CoV-2 infection*. J Neurol, 2020. **267**(11): p. 3121-3127.
507. Nicolas-Jilwan, M. and R.S. Almaghrabi, *Diffuse necrotising leukoencephalopathy with microhaemorrhages in a patient with severe COVID-19 disease*. Neuroradiol J, 2020. **33**(6): p. 528-531.
508. Dixon, L., et al., *COVID-19-related acute necrotizing encephalopathy with brain stem involvement in a patient with aplastic anemia*. Neurol Neuroimmunol Neuroinflamm, 2020. **7**(5).
509. Kakadia, B., et al., *Mild encephalopathy with reversible splenium lesion (MERS) in a patient with COVID-19*. J Clin Neurosci, 2020. **79**: p. 272-274.
510. Delorme, C., et al., *COVID-19-related encephalopathy: a case series with brain FDG-positron-emission tomography/computed tomography findings*. Eur J Neurol, 2020. **27**(12): p. 2651-2657.
511. Princiotta Cariddi, L., et al., *Reversible Encephalopathy Syndrome (PRES) in a COVID-19 patient*. J Neurol, 2020. **267**(11): p. 3157-3160.
512. Vaschetto, R., et al., *Cerebral nervous system vasculitis in a Covid-19 patient with pneumonia*. J Clin Neurosci, 2020. **79**: p. 71-73.
513. Farhadian, S., et al., *Acute encephalopathy with elevated CSF inflammatory markers as the initial presentation of COVID-19*. BMC Neurol, 2020. **20**(1): p. 248.
514. Butt, I., V. Sawlani, and T. Geberhiwot, *Prolonged confusional state as first manifestation of COVID-19*. Ann Clin Transl Neurol, 2020. **7**(8): p. 1450-1452.
515. Cebrián, J., et al., *Headache and impaired consciousness level associated with SARS-CoV-2 in CSF: A case report*. Neurology, 2020. **95**(6): p. 266-268.
516. Balestrino, R., et al., *Onset of Covid-19 with impaired consciousness and ataxia: a case report*. J Neurol, 2020. **267**(10): p. 2797-2798.
517. Alkeridy, W.A., et al., *A Unique Presentation of Delirium in a Patient with Otherwise Asymptomatic COVID-19*. J Am Geriatr Soc, 2020. **68**(7): p. 1382-1384.
518. Soysal, P. and O. Kara, *Delirium as the first clinical presentation of the coronavirus disease 2019 in an older adult*. Psychogeriatrics, 2020. **20**(5): p. 763-765.
519. de Miranda Henriques-Souza, A.M., et al., *Acute disseminated encephalomyelitis in a COVID-19 pediatric patient*. Neuroradiology, 2021. **63**(1): p. 141-145.
520. McCuddy, M., et al., *Acute Demyelinating Encephalomyelitis (ADEM) in COVID-19 Infection: A Case Series*. Neurol India, 2020. **68**(5): p. 1192-1195.
521. Pessoa Neto, A.D., et al., *Possible acute multifocal demyelinating lesions in a COVID-19 patient*. Arq Neuropsiquiatr, 2020. **78**(10): p. 666.
522. Lopes, C.C.B., et al., *Acute Disseminated Encephalomyelitis in COVID-19: presentation of two cases and review of the literature*. Arq Neuropsiquiatr, 2020. **78**(12): p. 805-810.

523. Chang, P., et al., *A Post-Infectious Steroid-Responsive Brainstem Lesion Associated With COVID-19*. *Neurohospitalist*, 2021. **11**(2): p. 152-155.
524. Brun, G., et al., *COVID-19-White matter and globus pallidum lesions: Demyelination or small-vessel vasculitis?* *Neurol Neuroimmunol Neuroinflamm*, 2020. **7**(4).
525. Abdi, S., A. Ghorbani, and F. Fatehi, *The association of SARS-CoV-2 infection and acute disseminated encephalomyelitis without prominent clinical pulmonary symptoms*. *J Neurol Sci*, 2020. **416**: p. 117001.
526. Langley, L., et al., *Acute disseminated encephalomyelitis (ADEM) associated with COVID-19*. *BMJ Case Rep*, 2020. **13**(12).
527. Parsons, T., et al., *COVID-19-associated acute disseminated encephalomyelitis (ADEM)*. *J Neurol*, 2020. **267**(10): p. 2799-2802.
528. Cani, I., et al., *Frontal encephalopathy related to hyperinflammation in COVID-19*. *J Neurol*, 2021. **268**(1): p. 16-19.
529. Reichard, R.R., et al., *Neuropathology of COVID-19: a spectrum of vascular and acute disseminated encephalomyelitis (ADEM)-like pathology*. *Acta Neuropathologica*, 2020. **140**(1): p. 1-6.
530. Erdede, O., et al., *An overview of smell and taste problems in paediatric COVID-19 patients*. *Acta Paediatr*, 2020. **109**(11): p. 2184-2186.
531. Hatipoglu, N., et al., *Olfactory bulb magnetic resonance imaging in SARS-CoV-2-induced anosmia in pediatric cases*. *Int J Pediatr Otorhinolaryngol*, 2020. **139**: p. 110469.
532. Mak, P.Q., et al., *Anosmia and Ageusia: Not an Uncommon Presentation of COVID-19 Infection in Children and Adolescents*. *Pediatr Infect Dis J*, 2020. **39**(8): p. e199-e200.
533. Chiu, S.S., et al., *Human coronavirus NL63 infection and other coronavirus infections in children hospitalized with acute respiratory disease in Hong Kong, China*. *Clin Infect Dis*, 2005. **40**(12): p. 1721-9.
534. Smith, L.T.A.C., et al., *Case Report: COVID-19 Patient With Chief Complaint of Anosmia and Ageusia; a Unique Perspective on Atypical Symptomatology and Management in the Military*. *Mil Med*, 2020. **185**(11-12): p. e2176-e2179.
535. Politi, L.S., E. Salsano, and M. Grimaldi, *Magnetic Resonance Imaging Alteration of the Brain in a Patient With Coronavirus Disease 2019 (COVID-19) and Anosmia*. *JAMA Neurol*, 2020. **77**(8): p. 1028-1029.
536. Laurendon, T., et al., *Bilateral transient olfactory bulb edema during COVID-19-related anosmia*. *Neurology*, 2020. **95**(5): p. 224-225.
537. Pissurno, N.S.C.A., et al., *Anosmia in the course of COVID-19: A case report*. *Medicine (Baltimore)*, 2020. **99**(31): p. e21280.
538. Vargas-Gandica, J., et al., *Ageusia and anosmia, a common sign of COVID-19? A case series from four countries*. *J Neurovirol*, 2020. **26**(5): p. 785-789.
539. Gilani, S., R. Roditi, and M. Naraghi, *COVID-19 and anosmia in Tehran, Iran*. *Med Hypotheses*, 2020. **141**: p. 109757.
540. Faber, I., et al., *Coronavirus Disease 2019 and Parkinsonism: A Non-post-encephalitic Case*. *Mov Disord*, 2020. **35**(10): p. 1721-1722.
541. Gane, S.B., C. Kelly, and C. Hopkins, *Isolated sudden onset anosmia in COVID-19 infection. A novel syndrome?* *Rhinology*, 2020. **58**(3): p. 299-301.
542. Sampaio Rocha-Filho, P.A. and L. Voss, *Persistent Headache and Persistent Anosmia Associated With COVID-19*. *Headache*, 2020. **60**(8): p. 1797-1799.
543. Melley, L.E., E. Bress, and E. Polan, *Hypogeusia as the initial presenting symptom of COVID-19*. *BMJ Case Rep*, 2020. **13**(5).

544. de Oliveira, F.A.A., D.C.C. Palmeira, and P.A.S. Rocha-Filho, *Headache and pleocytosis in CSF associated with COVID-19: case report*. *Neurol Sci*, 2020. **41**(11): p. 3021-3022.
545. Jacob, J., W. Flannery, and C. Mostert, *Novel ENT triad of anosmia, ageusia and hearing impairment in COVID-19*. *Intern Med J*, 2020. **50**(9): p. 1155.
546. Hjelmæsæth, J. and D. Skaare, *Loss of smell or taste as the only symptom of COVID-19*. *Tidsskr Nor Laegeforen*, 2020. **140**(7).
547. Chow, C.C.N., et al., *Acute transverse myelitis in COVID-19 infection*. *BMJ Case Rep*, 2020. **13**(8).
548. Raj, S.L., et al., *Neurological Manifestations of COVID-19 in Children*. *Indian Pediatr*, 2020. **57**(12): p. 1185-1186.
549. Kim, M.G., et al., *Fatal Cerebral Edema in a Child With COVID-19*. *Pediatr Neurol*, 2021. **114**: p. 77-78.
550. Kaur, H., et al., *Transverse Myelitis in a Child With COVID-19*. *Pediatr Neurol*, 2020. **112**: p. 5-6.
551. Natarajan, S., et al., *SARS-CoV-2 Encephalitis in an Adolescent Girl*. *Indian Pediatr*, 2020. **57**(12): p. 1186-1187.
552. Bektaş, G., et al., *Reversible splenic lesion syndrome associated with SARS-CoV-2 infection in two children*. *Brain Dev*, 2021. **43**(2): p. 230-233.
553. Lin, E., et al., *Brain Imaging of Patients with COVID-19: Findings at an Academic Institution during the Height of the Outbreak in New York City*. *AJNR. American journal of neuroradiology*, 2020. **41**(11).
554. Moriguchi, T., et al., *A first case of meningitis/encephalitis associated with SARS-Coronavirus-2*. *Int J Infect Dis*, 2020. **94**: p. 55-58.
555. Elkhalel, W., et al., *A 23-Year-Old Man with SARS-CoV-2 Infection Who Presented with Auditory Hallucinations and Imaging Findings of Cytotoxic Lesions of the Corpus Callosum (CLOCC)*. *Am J Case Rep*, 2020. **21**: p. e928798.
556. Álvarez Bravo, G. and L. Ramió I Torrentà, *[Anti-NMDA receptor encephalitis secondary to SARS-CoV-2 infection]*. *Neurologia*, 2020. **35**(9): p. 699-700.
557. Povlow, A. and A.J. Auerbach, *Acute Cerebellar Ataxia in COVID-19 Infection: A Case Report*. *J Emerg Med*, 2021. **60**(1): p. 73-76.
558. Efe, I.E., et al., *COVID-19-Associated Encephalitis Mimicking Glial Tumor*. *World Neurosurg*, 2020. **140**: p. 46-48.
559. Handa, R., et al., *Covid-19-associated acute haemorrhagic leukoencephalomyelitis*. *Neurol Sci*, 2020. **41**(11): p. 3023-3026.
560. Fumery, T., et al., *Longitudinally extensive transverse myelitis following acute COVID-19 infection*. *Mult Scler Relat Disord*, 2021. **48**: p. 102723.
561. Heller, H.M., et al., *Case 40-2020: A 24-Year-Old Man with Headache and Covid-19*. *N Engl J Med*, 2020. **383**(26): p. 2572-2580.
562. Ghosh, R., et al., *SARS-CoV-2-Associated Acute Hemorrhagic, Necrotizing Encephalitis (AHNE) Presenting with Cognitive Impairment in a 44-Year-Old Woman without Comorbidities: A Case Report*. *Am J Case Rep*, 2020. **21**: p. e925641.
563. Kadono, Y., et al., *A case of COVID-19 infection presenting with a seizure following severe brain edema*. *Seizure*, 2020. **80**: p. 53-55.
564. Poyiadji, N., et al., *COVID-19-associated Acute Hemorrhagic Necrotizing Encephalopathy: Imaging Features*. *Radiology*, 2020. **296**(2): p. E119-E120.
565. Picod, A., et al., *SARS-CoV-2-associated encephalitis: arguments for a post-infectious mechanism*. *Crit Care*, 2020. **24**(1): p. 658.

566. Monti, G., et al., *Anti-NMDA receptor encephalitis presenting as new onset refractory status epilepticus in COVID-19*. *Seizure*, 2020. **81**: p. 18-20.
567. Águila-Gordo, D., et al., *Acute myelitis and SARS-CoV-2 infection. A new etiology of myelitis?* *J Clin Neurosci*, 2020. **80**: p. 280-281.
568. Chaumont, H., et al., *Acute meningoencephalitis in a patient with COVID-19*. *Rev Neurol (Paris)*, 2020. **176**(6): p. 519-521.
569. Hanafi, R., et al., *COVID-19 Neurologic Complication with CNS Vasculitis-Like Pattern*. *AJNR Am J Neuroradiol*, 2020. **41**(8): p. 1384-1387.
570. Munz, M., et al., *Acute transverse myelitis after COVID-19 pneumonia*. *J Neurol*, 2020. **267**(8): p. 2196-2197.
571. Sotoca, J. and Y. Rodríguez-Álvarez, *COVID-19-associated acute necrotizing myelitis*. *Neurol Neuroimmunol Neuroinflamm*, 2020. **7**(5).
572. Seth, V. and S. Kushwaha, *Headache Due to COVID-19: A Disabling Combination*. *Headache*, 2020. **60**(10): p. 2618-2621.
573. Silva, M.T.T., et al., *Isolated intracranial hypertension associated with COVID-19*. *Cephalalgia*, 2020. **40**(13): p. 1452-1458.
574. Anand, P., et al., *Myoclonus in Patients With Coronavirus Disease 2019: A Multicenter Case Series*. *Crit Care Med*, 2020. **48**(11): p. 1664-1669.
575. Lyons, S., et al., *Seizure with CSF lymphocytosis as a presenting feature of COVID-19 in an otherwise healthy young man*. *Seizure*, 2020. **80**: p. 113-114.
576. Tu, T.M., et al., *Cerebral Venous Thrombosis in Patients with COVID-19 Infection: a Case Series and Systematic Review*. *J Stroke Cerebrovasc Dis*, 2020. **29**(12): p. 105379.
577. Noro, F., F.M. Cardoso, and E. Marchiori, *COVID-19 and benign intracranial hypertension: A case report*. *Rev Soc Bras Med Trop*, 2020. **53**: p. e20200325.
578. Ortiz-Seller, A., et al., *Ophthalmic and Neuro-ophthalmic Manifestations of Coronavirus Disease 2019 (COVID-19)*. *Ocul Immunol Inflamm*, 2020. **28**(8): p. 1285-1289.
579. Fasano, A., et al., *First motor seizure as presenting symptom of SARS-CoV-2 infection*. *Neurol Sci*, 2020. **41**(7): p. 1651-1653.
580. Ottaviani, D., et al., *Early Guillain-Barré syndrome in coronavirus disease 2019 (COVID-19): a case report from an Italian COVID-hospital*. *Neurol Sci*, 2020. **41**(6): p. 1351-1354.
581. Le Guennec, L., et al., *Orbitofrontal involvement in a neuroCOVID-19 patient*. *Epilepsia*, 2020. **61**(8): p. e90-e94.
582. Logmin, K., et al., *Non-epileptic seizures in autonomic dysfunction as the initial symptom of COVID-19*. *J Neurol*, 2020. **267**(9): p. 2490-2491.
583. Elgamasy, S., et al., *First case of focal epilepsy associated with SARS-coronavirus-2*. *J Med Virol*, 2020. **92**(10): p. 2238-2242.
584. Vollono, C., et al., *Focal status epilepticus as unique clinical feature of COVID-19: A case report*. *Seizure*, 2020. **78**: p. 109-112.
585. Kamal, Y., Y. Abdelmajid, and A. Al Madani, *Cerebrospinal fluid confirmed COVID-19-associated encephalitis treated successfully*. *BMJ case reports*, 2020. **13**(9).
586. Zhou, F., et al., *Clinical course and risk factors for mortality of adult inpatients with COVID-19 in Wuhan, China: a retrospective cohort study*. *Lancet*, 2020. **395**(10229): p. 1054-1062.
587. Gao, Y., et al., *Diagnostic utility of clinical laboratory data determinations for patients with the severe COVID-19*. *J Med Virol*, 2020.
588. Han, H., et al., *Prominent changes in blood coagulation of patients with SARS-CoV-2 infection*. *Clin Chem Lab Med*, 2020.

589. Hamming, I., et al., *Tissue distribution of ACE2 protein, the functional receptor for SARS coronavirus. A first step in understanding SARS pathogenesis*. J Pathol, 2004. **203**(2): p. 631-7.
590. To, K.F. and A.W. Lo, *Exploring the pathogenesis of severe acute respiratory syndrome (SARS): the tissue distribution of the coronavirus (SARS-CoV) and its putative receptor, angiotensin-converting enzyme 2 (ACE2)*. J Pathol, 2004. **203**(3): p. 740-3.
591. Varga, Z., et al., *Endothelial cell infection and endotheliitis in COVID-19*. Lancet, 2020. **395**(10234): p. 1417-1418.
592. Goshua, G., et al., *Endotheliopathy in COVID-19-associated coagulopathy: evidence from a single-centre, cross-sectional study*. The Lancet. Haematology, 2020. **7**(8).
593. Radmanesh, A., et al., *COVID-19-associated Diffuse Leukoencephalopathy and Microhemorrhages*. Radiology, 2020. **297**(1).
594. Fitsiori, A., et al., *COVID-19 is Associated with an Unusual Pattern of Brain Microbleeds in Critically Ill Patients*. Journal of neuroimaging : official journal of the American Society of Neuroimaging, 2020. **30**(5).
595. Kremer, S., et al., *Brain MRI Findings in Severe COVID-19: A Retrospective Observational Study*. Radiology, 2020. **297**(2).
596. Shoskes, A., et al., *Cerebral Microhemorrhage and Purpuric Rash in COVID-19: The Case for a Secondary Microangiopathy*. Journal of stroke and cerebrovascular diseases : the official journal of National Stroke Association, 2020. **29**(10).
597. Conklin, J., et al., *Cerebral Microvascular Injury in Severe COVID-19*. medRxiv : the preprint server for health sciences, 2020.
598. Lee, M.-H., et al., *Microvascular Injury in the Brains of Patients with Covid-19*. New England Journal of Medicine, 2020.
599. Pugin, D., et al., *COVID-19-related encephalopathy responsive to high-dose glucocorticoids*. Neurology, 2020. **95**(12).
600. Li, Y., et al., *Compromised Blood-Brain Barrier Integrity Is Associated With Total Magnetic Resonance Imaging Burden of Cerebral Small Vessel Disease*. Frontiers in neurology, 2018. **9**.
601. Franceschi, C., et al., *Inflamm-aging. An evolutionary perspective on immunosenescence*. Annals of the New York Academy of Sciences, 2000. **908**.
602. Yuki, N. and H.-P. Hartung, *Guillain-Barre syndrome.(Disease/Disorder overview)*. The New England Journal of Medicine, 2012. **366**(24): p. 2294.
603. Hughes, R.A.C., et al., *Immunotherapy for Guillain-Barré syndrome: a systematic review*. Brain, 2007. **130**(9): p. 2245-2257.
604. Guarneri, B., G. Bertolini, and N. Latronico, *Long-term outcome in patients with critical illness myopathy or neuropathy: the Italian multicentre CRIMYNE study*. J Neurol Neurosurg Psychiatry, 2008. **79**(7): p. 838-41.
605. Latronico, N., et al., *Simplified electrophysiological evaluation of peripheral nerves in critically ill patients: the Italian multi-centre CRIMYNE study*. Crit Care, 2007. **11**(1): p. R11.
606. Arbour, N., et al., *Neuroinvasion by human respiratory coronaviruses*. J Virol, 2000. **74**(19): p. 8913-21.
607. Schurink, B., et al., *Viral presence and immunopathology in patients with lethal COVID-19: a prospective autopsy cohort study*. The Lancet. Microbe, 2020. **1**(7).
608. Filatov, A., et al., *Neurological Complications of Coronavirus Disease (COVID-19): Encephalopathy*. Cureus, 2020. **12**(3): p. e7352.

609. Sungnak, W., et al., *SARS-CoV-2 entry factors are highly expressed in nasal epithelial cells together with innate immune genes*. Nat Med, 2020.
610. Perlman, S., G. Evans, and A. Afifi, *Effect of olfactory bulb ablation on spread of a neurotropic coronavirus into the mouse brain*. J Exp Med, 1990. **172**(4): p. 1127-32.
611. Cabirac, G.F., et al., *In vitro interaction of coronaviruses with primate and human brain microvascular endothelial cells*. Adv Exp Med Biol, 1995. **380**: p. 79-88.
612. Chen, T., et al., *Clinical characteristics of 113 deceased patients with coronavirus disease 2019: retrospective study*. BMJ, 2020. **368**: p. m1091.
613. Chien, J.Y., et al., *Temporal changes in cytokine/chemokine profiles and pulmonary involvement in severe acute respiratory syndrome*. Respirology, 2006. **11**(6): p. 715-22.
614. Kansagra, S.M. and W.B. Gallentine, *Cytokine Storm of Acute Necrotizing Encephalopathy*. Pediatric Neurology, 2011. **45**(6): p. 400-402.
615. Sun, T., et al., *Peripheral Blood and Cerebrospinal Fluid Cytokine Levels in Guillain Barré Syndrome: A Systematic Review and Meta-Analysis*. Front Neurosci, 2019. **13**: p. 717.
616. Yao, X.H., et al., *Pathological evidence for residual SARS-CoV-2 in pulmonary tissues of a ready-for-discharge patient*. Cell Res, 2020.
617. Hampshire, A., et al., *Cognitive deficits in people who have recovered from COVID-19 relative to controls: An N=84,285 online study*. 2020.
618. Huang, C., et al., *6-month consequences of COVID-19 in patients discharged from hospital: a cohort study*. Lancet (London, England), 2021.
619. Donegani, M., et al., *Brain Metabolic Correlates of Persistent Olfactory Dysfunction after SARS-Cov2 Infection*. Biomedicines, 2021. **9**(3).

BIOGRAPHY

Brianne Sullivan was born October 3, 1990, in Ventura, CA, to Robert and Lisa Sullivan. She grew up in Southern California with younger siblings Devin and Mikayla Sullivan. Brianne attended undergraduate college at California State University Channel Islands, receiving a B.A. in Communications with an emphasis in Business and Non-Profit Organizations and a B.S. in Chemistry with an emphasis in Biochemistry. While at CSUCI, Brianne conducted research under the direction of Drs. Brittnee Veldman and Ahmed Awad. After graduating in 2015, Brianne began working as a cosmetic chemist in R&D at Jafra International Cosmetics. In 2016, deciding to transition to life science, Brianne joined the Neuroscience Master's program at Tulane University. During her master's, Brianne conducted research under the guidance of Dr. Anne Robinson. Brianne joined the Neuroscience Ph.D. program at Tulane University in 2017 after completing her M.S. the same year. After joining the Ph.D. program, Brianne joined the lab of Dr. Bruce Bunnell, investigating the impact of biological sex on the therapeutic efficacy of adipose-derived stem cells in a murine model of multiple sclerosis, experimental autoimmune encephalomyelitis. Following Dr. Bunnell's departure from Tulane University for an appointment at the University of North Texas HSC at Fort Worth in 2020, Brianne joined the lab of Dr. Chad Steele. Under the guidance of Dr. Steele, Brianne developed a model of and investigated the neuroimmune during disseminated cerebral aspergillosis. During her Ph.D., Brianne has had the honor of being a High-Potential Entrepreneurs' Fellow with Celdara Medical. At the time of this writing, Brianne is planning to move to Boston, MA, with her boyfriend Sam Bliesner and dog Beauregard, where she will begin a career as a life science Consultant with Back Bay Life Science Advisors.